AEC-tr-3405

PROBLEMS OF HEAT TRANSFER DURING A CHANGE OF STATE

A COLLECTION OF ARTICLES

EDITED BY S. S. KUTATELADZE
Candidate of Engineering Sciences

STATE POWER PRESS

MOSCOW 1953 LENINGRAD

This collection includes articles reporting on several researches in the field of heat transfer during a change of state of the heat carrier.

The book is intended for those engaged in scientific work in the field of the theoretical foundations of heat engineering and for engineers calculating heat transfer in condensers, evaporators, high-pressure steam boilers, refrigeration machinery, the cooling of metals in liquid media, and the like.

Editor B. D. Katsnelson

Technical editor A. A. Zabrodina

PREFACE

The directives of the Nineteenth Party Congress on the Fifth Five-Year Plan for the development of the USSR during 1951-1955 laid down the assignment of insuring a further substantial increase in the quality of production in all branches of industry. This fully applies to newly installed thermal energy equipment. The greater efficiency of thermal processes and the greater degree of reliability of the computations involved, based on the latest theoretical and experimental data, are largely determining the solution of this assignment.

Research on heat transfer during a change of state of the heat carrier is a peculiar problem, the great complexity of which is due to the fact that in this case the substance exists simultaneously in at least two phases, at the boundaries of which the latent heat of phase transformation is either evolved or absorbed.

Up to the present time far from enough research has been done on the processes involved in the boiling of a liquid, the condensation of vapor, fusion, and solidification, which are the foundations of a number of major branches of industry. During the past 15 years substantial success has been achieved in the generalized analysis of processes of this nature. As a result, a number of problems of practical importance have been resolved, and the theory of heat transfer during a change of state has become an independent branch of the general science of heat transfer.

Soviet science has played a leading part in this branch of physical heat engineering. In particular, a large amount of new experimental data on extraction of heat during a change of state has been secured in recent years. Some of this material is published in the present symposium, based on work done in various scientific research organizations.

The first group of papers in the present symposium deals with problems of heat transfer in the condensers of steam prime movers and refrigeration machinery.

The second group of papers reports experimental data on the output of heat during boiling, especially in high-intensity processes.

The last two papers are devoted to the important problem of the rates of accumulation and melting of ice as functions of the conditions of heat transfer between the solid and liquid phases. Notwithstanding the fact that the papers in this symposium are based on research done in different scientific research institutes and institutions of higher learning, the nature of the problems considered is what they have in common, and they mutually complement one another.

To be sure, the present symposium makes no claim to full coverage of the topics considered. It must be assumed, however, that even in the present form it may be used in solving individual problems related to the technical progress of our thermal energy supply.

S. Kutateladze

TABLE OF CONTENTS

PART ONE

HEAT TRANSFER DURING CONDENSATION

PART TWO

HEAT EXCHANGE DURING CONDENSATION

PART THREE

HEAT EXCHANGE IN THE FREEZING AND MELTING OF ICE

PART ONE

HEAT TRANSFER DURING CONDENSATION

HEAT TRANSFER IN SURFACE CONDENSERS OF STEAM PRIME MOVERS

By L. D. Berman, Doctor of Engineering Sciences

The F. E. Dzerzhinsky Institute of Heat Engineering

Surface condensers have been widely adopted in practice in connection with the introduction of steam turbines, making the effective utilization of high vacuum possible. Up to the present time, however, our lack of sufficient knowledge of heat transfer during the condensation of steam in the presence of noncondensable gases has greatly hampered a rigorous analytical solution of the problems involved in the process of heat transfer in condensers. The theoretical and experimental research carried out during the last few years does enable us, however, to refine our concepts in this field and thus may aid substantially in securing a correct solution of practical problems that arise in the design and operation of condensers.

1. STEAM-CONDENSING CONDITIONS IN THE CONDENSERS OF STEAM PRIME MOVERS

The condensers of steam prime movers belong to the broad groups of heat exchangers in which steam is condensed by being cooled by a liquid at a lower temperature. Their principal difference from other apparatus in this group is the fact that the condensation of steam takes place in them at low absolute pressure (a vacuum). The practical impossibility of securing an absolutely hermetically sealed installation results in the entrance of a certain amount of air entering the condenser through the leaks.* As a result, the operation of the deaerating equipment has an important effect upon the operation of the condensing process. To avoid impairing the vacuum and expending unnecessary work in compressing to atmospheric pressure the vapor that is to be removed, the amount of vapor remaining uncondensed, which must be eliminated from the condenser together with the air, must be a negligible percentage of the vapor entering the condenser. In modern condensers for steam turbines as much as 99.97% of the total steam entering the condenser is condensed at absolute pressures of 0.02-0.10 atm absolute.

The percentage by weight of air in the steam when the latter enters a condenser is no more than 0.01-0.05%, though this percentage rises continuously as the steam condenses.

If we denote the initial quantity of air, expressed as a percentage of the weight of the mixture, by $\varepsilon_{\varkappa}$, and its current value by ε , we

* The percentage of noncondensable gases in the steam reaching the prime mover from the boiler is usually very small compared to the percentage of air entering the installation through leaks.

can write:

$$\varepsilon = \frac{G_2}{G_n + G_2} \cdot 100 = \frac{100\varepsilon_н}{100 - y + \frac{y\varepsilon_н}{100}} [\%], \quad (1)$$

where G , G = the consumption of air and steam respectively (the current value being used for steam) in kg per hour.

y = the ratio of the percentage of steam condensed to the percentage of steam entering the condenser, which we shall call "degree of condensation of steam."

The rise in , the proportion of air in the mixture, as y increases is especially high during the condensation of the last 10-15% of the steam entering the condenser (Fig. 1). At y = 99.97% and $\varepsilon_н$ = 0.01-0.05% the final percentage of air in the mixture, ε , reaches 25-60%, the value of ε rising as high as 80% for large values of y.

As the steam is condensed the volume of the steam-air mixture diminishes. If we assume that the total pressure and temperature of the mixture remain unchanged and if we regard the latter as a mixture of ideal gases, which is fully allowable under the conditions stated, we get:

$$\frac{V}{V_н} \cdot 100 = \frac{100 - y + 0{,}622\,\varepsilon_н}{1 + \frac{0{,}622\,\varepsilon_н}{100}} [\%], \quad (2)$$

where V, V = current and initial volumetric consumption of the mixture respectively, in m^3 per hour.

At $\varepsilon \ll 100$ the relationship between V and y is practically a straight line (Fig. 1), with the exception of the short section of the line near y = 100%. At y = 99.97% and $\varepsilon_н$ = 0.01-0.05%, the final volume of the mixture is no more than 0.01-0.008% of its initial volume.

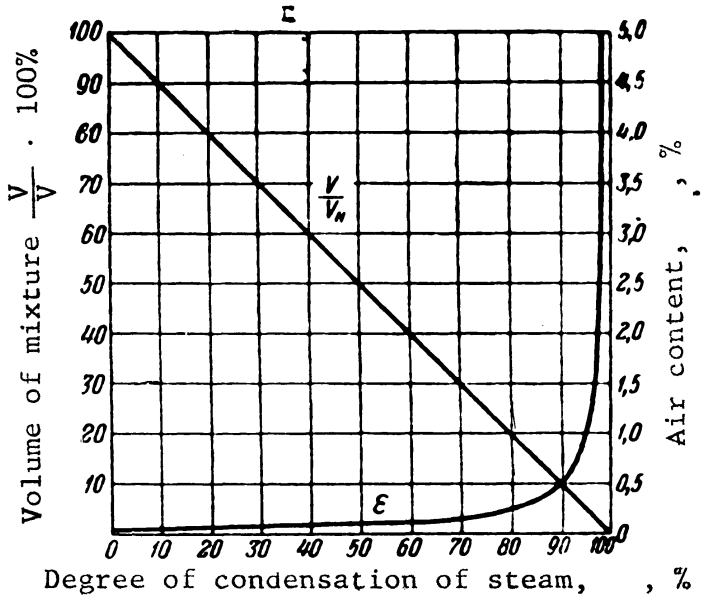

Fig. 1. Percentage of air and volumetric consumption of the steam-air mixture as functions of the degree of condensation of steam ($\varepsilon_н$ = 0.05%).

At the pressures that are ordinarily encountered in the condensers of steam prime movers and with the total pressure of the mixture unchanged, an increase in y results in a negligible drop in the temperature of the mixture within wide limits. If we regard the steam-air mixture as saturated, its temperature is governed by the partial pressure of the steam, or

$$p_n = \frac{p_{cm}}{1 + 0{,}622 \frac{\varepsilon_м}{100 - y}}, \qquad (3)$$

where p_{cm} = total pressure of the mixture.

Setting p_{cm} = 0.05 atm absolute and $\varepsilon_м$ = 0.05%, we find that the drop in the temperature of the mixture below its initial value is no more than 0.03° C at y = 90%, 0.5° C at y = 99%, and as much as 12° C at y = 99.97%. At lower values of $\varepsilon_м$ the temperature of the mixture drops more slowly, being 3.3° C at $\varepsilon_м$ = 0.01% and y = 99.97%, compared to 12° C at $\varepsilon_м$ = 0.05%. The drop in the temperature of the mixture in the region of high values of y results in a corresponding diminution in the volume of the mixture, compared to the value calculated from Eq. (2). This effect of temperature change is usually compensated and even overcompensated somewhat by the effect of the drop in the pressure p_{cm}, due to the steam resistance of the bundle of tubes, which operates in the opposite direction.

Thus, the condensation of steam in the case we are considering is characterized by the fact that it takes place in the presence of air, the percentage of the latter in the mixture changing from 0.005-0.05% at the inlet of the condenser's bundle of tubes to 25-80% at the outlet, or one to five thousand times. The volumetric consumption of the mixture diminishes to 0.01-0.08% of its initial value, or one to ten thousand times. Inasmuch as this is ordinarily not balanced out by a corresponding reduction in the cross section of the intertubular space, the velocity of flow of the mixture drops considerably during its passage.

As we know, the presence of air significantly changes the conditions of steam condensation, compared to those present when pure steam, i.e. steam containing no noncondensable gases, is condensed. The principal difference is the appearance of a substantial "external thermal resistance," related to the process of transporting the substance.

2. EXTERNAL THERMAL RESISTANCE IN THE CONDENSATION OF STEAM

In the condensers we are discussing the cooling surface is usually designed as a horizontal bundle of brass tubes. The cooling water passes through the tubes, whose outer surfaces are washed by a countercurrent of steam subject to condensation.

The surface of new tubes made of brass (or of other copper alloys, such as copper-nickel) is hydrophobic, so that we have dropwise condensation of the steam. As the tubes "age," due to the formation of a gradually thickening film of oxide on their surface, as well as to their fouling with greasy impurities, the surface's wettability with water increases, and condensation changes, first to mixed condensation (dropwise-filmwise), and then to pure filmwise condensation. It is the latter, as

a rule, that prevails in condensers, with the sole exception of the initial period after the installation of new tubes. Henceforth, we shall therefore consider only filmwise condensation of steam.

The intensity of steam condensation on a surface is governed by the rates of flow of two associated processes:

1) The flow of steam particles from the bulk of the steam to the surface at which condensation takes place.

2) The removal of the heat given off during condensation from this surface.

Accordingly, the thermal resistance on the steam side of the cooling surface, $R_n = \frac{1}{\alpha_n}$ (α_n— is the coefficient of heat transfer from the steam to the tube wall) may be represented in the general case as the sum of two terms:

$$R_n = \frac{t_n - t_{cm}}{q} = R_\delta + R_\beta, \tag{4}$$

where t_n, t_{cm} = temperatures of steam and wall, respectively, in ° C.
q = specific heat flow, kilocalories/m^2·hr.

The first term R_δ in Eq. (4) is the thermal resistance of the film of condensate formed at the surface of the solid wall. The second term R_β, which we call the "external thermal resistance," is determined by the rate of transfer of the substance (the flow of steam particles) to the surface of the condensate film and is not thermal resistance in the ordinary sense of the term, which presupposes the transfer of heat. Hence, the quantity R_n can be called a thermal resistance only conditionally, because of the purely external resemblance of the method of its determination with the determination of thermal resistance when there is no change of state of the cooling medium. Only in special cases, when $R_\beta \ll R_\delta$, does this restriction practically vanish. Then $t_n \approx t_{ж}$, and:

$$R_n \approx R_\delta = \frac{t_{ж} - t_{cm}}{q}, \tag{5}$$

where $t_{ж}$ is the temperature of the free surface of the film of condensate in degrees C.

The assumption involved in the statement that $R_\beta \ll R_\delta$, i.e. that the inflow velocity of steam particles does not limit the intensity of condensation, is usually a part of the foundation of the theory of film condensation of steam /Ref. 1/.

The magnitude of the external thermal resistance, R_β, can be determined for the case of the condensation of pure steam, starting out with the notions of the kinetic theory of matter, according to which visible condensation of steam must correspond to a temperature discontinuity at the boundary between the vapor and liquid phases. Because of this dis-

continuity the number of molecules of steam striking the surface of the liquid and being captured by the latter exceeds the number of molecules detached from the liquid surface as the result of thermal motion during the same interval of time.

The theoretical solution proposed by Silver results in the following expression for external thermal resistance in the condensation of pure saturated steam /Ref. 3, a/:

$$R_\beta = \frac{t_n - t_{ж}}{q} = \frac{v''\sqrt{T^3}}{280 \cdot 10^3 k r^2}, \qquad (6)$$

where v'' = specific volume of steam, m^3/kg.
T = saturation temperature of steam in degrees on the absolute scale.
k = coefficient of accomodation, indicating what proportion of the vapor molecules striking the surface of the liquid is captured by it.

According to Eq. (6), the magnitude of R_β depends upon the pressure of the condensing steam, and is independent of the specific thermal load on the surface, q. If we assume, in conformity with the figures given by several authors, that the coefficient of accomodation is independent of the pressure, we find that R_β rises sharply as the pressure drops. At pressures corresponding to the conditions prevailing in the condensers of steam prime movers and at low values of the coefficients of accomodation k, the external thermal resistance R_β, calculated from Eq. (6) attains values that are close to the order of magnitude of the values of R_δ (Fig. 2).

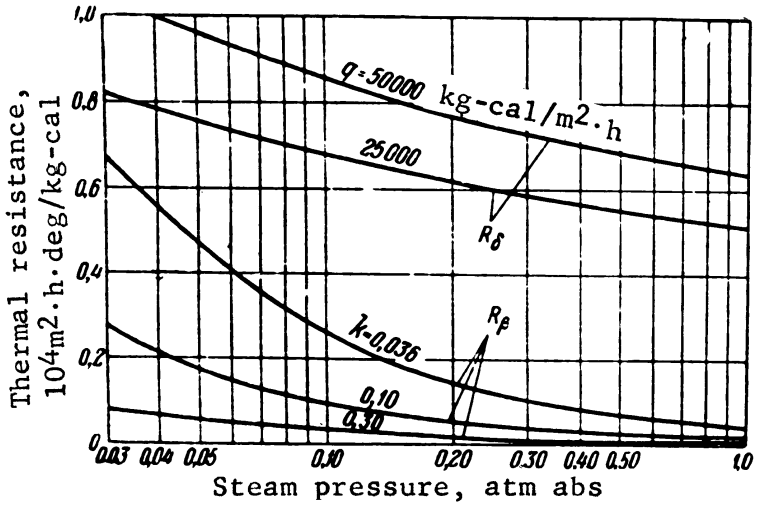

Fig. 2. External thermal resistance and thermal resistance of the condensate film in the condensation of pure steam as a function of pressure.

Precise quantitative evaluation of the thermal resistance R_β is ren-

dered difficult by the inconsistency of the data available for the magnitude of the coefficient of accomodation, though it is usually stated that the values of $\underline{k}$ should be low, of the order of 0.02-0.04 for liquids whose molecular structure is asymmetrical, including water /Ref. 3, a/.

We still do not have sufficient information on the problem of the influence of R_β on the rate of condensation of steam on a surface, which is of practical interest for a study of the conditions of heat exchange on the most heavily loaded inlet section of the condenser's bundle of tubes.

When even a comparatively minute proportion of air (or of other noncondensable gases) is present in the steam, the effect of the foregoing molecular processes at the phase boundary upon the rate of condensation of steam should drop substantially, if it is actually high for pure steam. The presence of an inert gas begins to have a predominant effect upon the rate at which steam flows to the surface.

When the steam-air mixture comes in contact with a surface that is at a lower temperature, and the steam begins to condense on the latter, the proportion of gas begins to rise in the layer of the mixture that is in immediate contact with the surface, and the partial pressure of the steam at the surface of the condensate film becomes lower than in the bulk of the steam-air mixture, while the partial pressure of the gas becomes higher. The inflow of steam particles to the surface takes place as the result of molecular or turbulent diffusion in this case. The mechanism of transfer of the substance (the steam) and the distribution of the partial pressures of the steam and the air in a direction normal to the surface then depend largely upon hydrodynamic conditions. Inasmuch as the fact that the partial pressure of the steam at the surface of the phase boundary is lower than the partial pressure of the steam in the bulk of the mixture is a necessary condition for the occurrence of the process of diffusion to this surface, the temperature at the surface of the condensate film must always be lower than the temperature of the mixture (even if we ignore the temperature discontinuity at the phase boundary referred to above).

The rise in the partial pressure of the air at the surface of the condensate film, compared to its partial pressure in the bulk of the mixture, must bring about diffusion of the air in a direction opposite to that of diffusion of the steam. When a restricted condensation surface is present, however, there can be no constant flow of air away from that surface, since it would have to bring about a continuous lowering of the total pressure of the mixture at the surface. According to present concepts, the diffusion of air is compensated by a flow of the steam-air mixture in the opposite direction, as a result of which the resultant flow of air in a direction normal to the surface is zero, while the flow of steam in the direction of the surface rises somewhat compared to that due to diffusion alone for the given difference in partial pressures of steam.

The total steam flowing to the condensation surface both as a result of diffusion and of this supplementary transverse flow of steam may be expressed by an empirical equation similar to the one employed to determine the heat flow when considering heat transfer*:

$$g_к = \beta_p (p_п - p_ж) \tag{7}$$

* Footnote appears on next page.

where p_n and $p_{ж}$ = the partial pressures of steam in the bulk of the mixture and at the surface of the liquid, respectively, in atm absolute.

β_p = coefficient of mass transfer, kg/m^2·hr·atm.

Similarly, we may write:

$$q = g_к \Delta i = \beta_p (p_n - p_{ж}) \Delta i \qquad (8)$$

for the quantity of heat liberated in the condensation of steam, where:

$\Delta i \approx i_n - i_{ж} \approx r$ is the difference between the heat content of the steam in the bulk of the mixture, i_n and that of the condensate $i_{ж}$ at the temperature $t_{ж}$, in kilocal/kg.

r = heat of condensation, kg-cal/kg.

Whence

$$R_\beta = \frac{t_n - t_{ж}}{q} = \frac{1}{\beta_p \Delta i} \frac{t_n - t_{ж}}{p_n - p_{ж}}. \qquad (9)$$

If we assume that the bulk of the steam-air mixture is saturated and that the steam pressure $p_{ж}$ at the boundary between the liquid and vapor phases is equal to the saturation pressure at the temperature $t_{ж}$, and if we employ an equation of the second degree to express the variation of the pressure of saturated steam with temperature in the narrow temperature range between t_n and $t_{ж}$:

$$p'' = a + bt + ct^2,$$

we obtain as an approximation from (9):

$$R_\beta = \frac{1}{\beta_p \Delta i (b + 2ct_{cp})}, \qquad (9a)$$

where $t_{cp} = \frac{t_n + t_{ж}}{2}$ is the arithmetical mean temperature of the steam-air mixture in the boundary layer in degrees C.

Moreover, bearing in mind that in the condensers of steam prime movers $\Delta i \approx$ constant and that $t_{ж}$ differs on slightly from t_n, we may conclude from (9a) that at the given t_n the external thermal resistance R_β is governed mainly by the magnitude of β_p, the coefficient of mass transfer. The latter, like the coefficient of heat transfer in convective heat exchange (without a change of state), depends largely upon the hydrodynamic conditions, i.e. upon the structure of the flow of the steam-air mixture.

---

* Some authors /Ref. 2/ employ the theoretical formula derived by Stefan, which makes allowance for the transverse flow of the mixture, in determining g_k. But this formula was derived for conditions of purely molecular diffusion of steam through a motionless layer of gas of finite thickness. It cannot be applied to the case of a moving steam-air mixture /Ref. 3, b, c/, inasmuch as this involves the necessity of introducing the fictitious quantity "diffusion height" (or "thickness of derived film"), which merely complicates the computational formulae without in any way making them approach the correct reflection of the physical picture of the phenomenon.

As is borne out by the experimental data cited below, the role of the external thermal resistance increases greatly with an increase in the percentage of steam in the steam-air mixture, and the magnitude of R_β may substantially exceed R_δ, the thermal resistance of the condensate film, at a comparatively low percentage of air. In the latter case, the factors that affect the rate of transfer of the substance prove to be decisice, both for the magnitude of R_n, the total thermal resistance, or, what amounts to the same thing, the magnitude of α_n, the coefficient of heat transfer from the steam to the wall.

Strictly speaking, in the case under consideration, when the rate of heat exchange depends upon the rate at which two processes of different physical nature take place, these latter should have been considered separately, Eq. (7) being used directly to evaluate the rate of transfer of the substance, employing the magnitude of β_p, referred to the difference in steam partial pressures, as the empirical coefficient. If we assume stationary conditions, the relationship between the rates at which these two processes take place can then be determined from the obvious equality:

$$q = \beta_p (p_n - p_{ж}) \Delta i = \frac{t_{ж} - t_{ст}}{R_\delta}.$$

This equality between the quantities of heat evolved and carried off is achieved in each individual case as a result of the fact that the corresponding parameters $t_{ж}$ and $p_{ж}$ are established at the phase boundary, both of these parameters being interrelated, i.e. $p_{ж} = f(t_{ж})$, inasmuch as it has been assumed that $p_{ж}$ is equal to the saturation pressure at the temperature $t_{ж}$.

Measuring the parameters $t_{ж}$ and $p_{ж}$ during experiments meets with considerable difficulty, however, and so far as we know no one has yet succeeded in doing so. That is why we still do not have sufficiently reliable data to evaluate the coefficient of mass transfer for the condensation of steam in the presence of air, especially for mixtures containing a comparatively small proportion of air. The values of R_n or α_n can be determined by using the available methods of measurement, both from laboratory experiments and from experiments on industrial units. Moreover, in considering heat exchange in a surface condenser, in particular, in determining the effect of various factors on the mean coefficient of heat transfer, it is found to be convenient and advisable to employ the quantities R_n and α_n. Equation (7) is employed below for the theoretical solution, enabling us to elucidate some qualitative features of the process of steam condensation in the presence of air under the conditions prevailing in a surface condenser, but refining the quantitative relationships requires our resorting to experiments on industrial units and, in particular, to the local and mean values of the coefficient of heat transfer α_n secured in these experiments.

3. LOCAL COEFFICIENTS OF HEAT TRANSFER AND MASS TRANSFER

Very little work has been done thus far on the influence of the parameters of the mixture, including its composition and the temperature and hydrodynamic conditions, upon heat transfer during the condensation of the steam in the presence of noncondensable gases, especially for the case where the steam-gas mixture flows across the tubes.

Experiments on heat transfer during the condensation of steam containing traces of air were once made by V. A. Gudemchuk in the All-Union Heat Engineering Institute /Ref. 4, 5/. In these experiments steam was condensed on the outer surface of a tube through which cooling water passed. The percentage of air in the steam-air mixture was varied from zero to 5%. The results of the experiments were worked up as a function showing the variation of α_n, the coefficient of heat transfer, with the percentage of air in the steam* $\varkappa = \frac{G_в}{G_п}$.

The data obtained (Fig. 3) confirmed the fact that the coefficient of heat transfer drops sharply even when a minute quantity of air is introduced into the steam. For example, when the air content in the steam was $\varkappa = 0.005$ (or 0.5%), the coefficient α_n for a horizontal tube was no more than about half of the value of the coefficient of heat transfer $\alpha_{n(o)}$ in the condensation of pure steam ($\varkappa = 0$).

Othmer /Ref. 11/ and Langen /Ref. 12/ ran analogous experiments on the condensation of steam on a horizontal tube. If the results of all these experiments are plotted as the equation $\frac{\alpha}{\alpha_{n(0)}} = f(\varkappa)$, as was done by S. S. Kutateladze /Ref. 1/, we find that though they agree satisfactorily, qualitatively speaking, Othmer's experimental points lie higher than the experimental points secured by other research workers, the discrepancies in the value of $\frac{\alpha_n}{\alpha_{n(0)}}$ being as much as 25-30%. An explanation for this may be found in the different conditions and methods of performing the experiments. Thus, the experiments by Gudemchuk and Langen were run with tubes 25-30 mm in diameter at low steam pressures (vacuum), the steam-air mixture being fed into the experimental condenser from below, the air together with the uncondensed steam being drawn out of the condenser with a vacuum pump. In Othmer's experiments, run at excess pressure, the experimental tube, of much larger diameter (77 mm), was run directly through the closed steam space of a steam generator above the level of the evaporating water. The partial pressure of the air (a definite amount of which was introduced into the steam space of the steam generator) was determined before and after the experimental run.

Even if we eliminate Othmer's experiments, where the methods employed enabled him to secure only a quite provisional value of $\varkappa$, the region of possible practical application of the experimental data referred to above remains quite limited. This is due not only to the fact that they cover narrow ranges of mixture pressures and air concentrations or refer only to single tubes, but even more so to the fact that the experiments were run with a sluggishly moving, practically motionless, steam-air mixture.

Before we turn to the problem of the influence of the velocity of the mixture, let us point out that Langen set himself the problem of determining the coefficient of mass transfer β_p, rather than α_n. He described the results of his experiments by means of the empirical formula:

$$\beta_p = \frac{14{,}5}{\varkappa^{0.6}\sqrt{p_п - p_ж}}. \qquad (10)$$

* It is not difficult to demonstrate that $\varkappa = \frac{\varepsilon}{1-\varepsilon}$

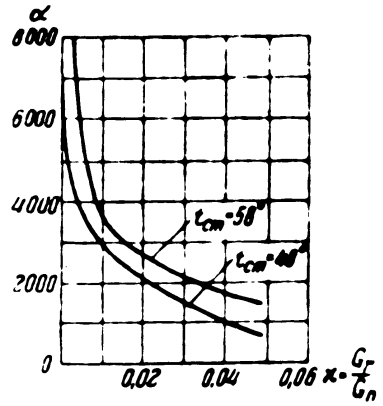

Fig. 3. Effect of a trace of air in steam on the coefficient of heat transfer during the condensation of steam on a horizontal tube (practically motionless steam).

The experimental points on which this formula is based, however, are scattered widely (± 35%) about the faired curves. Langen's assumption that this was due to the instability of film condensation is hardly convincing, inasmuch as the data secured in the experiments of the All-Union Heat Engineering Institute and in other researches indicate that the duration of Langen's experiments (several years), during which the tube was not replaced, greatly exceeded the period of time during which completely filmwise condensation of steam is achieved on a brass tube. We may assume that the scatter of points was largely due to the method employed for working up the experimental data, especially to the fact that in calculating the magnitude of β_p the parameters $t_{\text{ж}}$ and $p_{\text{ж}}$ at the phase boundary were determined by computation, several simplifying assumptions that resulted in substantial errors being introduced. As a result Langen was compelled to make the reservation, at the very outset of his paper /Ref. 12/, that his experiments did not aim at a precise determination of β_p because of the complexity of the problem.

The conditions prevailing during Langen's experiments (single tube, practically motionless mixture) and the low degree of accuracy of the data on which Eq. (10) is based do not permit us to employ this equation in calculating industrial equipment. Unfortunately, the faulty endeavor to employ this equation for a precise calculation of steam turbine condensers, already attempted in the past, has been repeated in V. P. Blyudov's text book on condensing equipment /Ref. 5/.

Colburn /Ref. 13/ endeavored to determine the influence of the velocity of the steam-gas mixture on the coefficient of mass transfer in external transverse flow across horizontal tubes and proposed a semiempirical equation for this. But as has already been demonstrated in detail /Ref. 3, d/, Colburn made a number of serious mixtakes in deriving this equation. Following the hydrodynamic theory of the transfer of heat and matter, and endeavoring to allow for the influence of the flow of substance normal to the surface that occurs during the condensation

of steam on a surface in the presence of a noncondensable gas, Colburn incorrectly (solving the internal problem) made allowance for the influence of this flow upon mass exchange between the core of the flow and the boundary layer and, in general, did not allow for its influence upon the transfer of momentum. Moreover, Colburn without any justification applied the result he secured for the conditions of the internal problem to external flow around tubes, so that he wrongly utilized the experimental data on heat transfer (in the absence of a change of state) pertaining to the latter case for determining the magnitude of the coefficient of mass transfer by analogy.

Moreover, in investigating the operation of industrial condensers we usually have to deal with a moving steam-gas mixture. That is why determining the influence of the velocity of the mixture on the rate of heat rejection during the condensation of steam that contains some air is very essential if we are to secure a correct idea of the operating process in condensers and if we are to solve the practical problems involved in the design and heat balance of apparatus of this sort.

The velocity of the steam-air mixture must have a substantial effect on the nature of the function $\frac{\alpha_n}{\alpha_{n(0)}} = f(x)$, i.e. on the relative change of the coefficient of heat transfer as the percentage of air in the steam-air mixture rises /Ref. 3, d, f/. The following considerations justify this conclusion. Of the two components of $R_n = \frac{1}{\alpha_n}$, the external thermal resistance R_β is largely determined, as we have seen, by the magnitude of the coefficient of mass transfer β_p, while the thermal resistance R_δ is determined by the thickness and nature of flow in the condensate film. That is why the magnitude of R_β must largely depend upon the hydrodynamic conditions, in particular, on the velocity of the mixture, whereas R_δ, unless we discuss the indirect influence of the magnitude of R_β upon it, depends upon the "external" hydrodynamic conditions only to the extent to which the thickness of the condensate film (provided the nature of its flow remains unchanged) depends upon the mechanical action of the moving steam-gas mixture upon the film. Inasmuch as the proportion of the overall thermal resistance due to R_β rises sharply with an increase in the percentage of air in the mixture, the richer the mixture is in air, the more will an increase in the velocity of the mixture result in an increase in α_n, all other process parameters remaining the same. Hence, the higher the velocity of the steam-air mixture, the smaller must be the relative drop in the coefficient of heat transfer as the percentage of air in the mixture increases.

It would follow that the higher the percentage of air in the steam-air mixture, the more effective would an increase in the velocity of the mixture be as a means of intensifying heat exchange during the condensation of steam.

The available experimental data, dealing with this only under conditions of the internal problem /Ref. 3, d/, did not permit a direct verification of this conclusion so important for practice, since the influence of the velocity of the steam-gas mixture was investigated experimentally only at very high percentages of noncondensable gas in it, where $R_\delta \ll R_\beta$. This led us to make the check of this conclusion one of the

problems to be handled during the research undertaken at the All-Union Heat Engineering Institute on the operating processes in condensing equipment. The experiments recently run at the All-Union Heat Engineering Institute fully confirmed the considerations set forth above. Some results of these experiments, run during the condensation of steam on the outer surface of a horizontal brass tube 19-16 mm in diameter, are given in Figs. 4 and 5. They show that the curves $\frac{\alpha_n}{\alpha_{n_0}} = f(x)$ are functions of the velocity of the steam-air mixture as well as of other parameters of the process. As w_g, the gravimetric velocity of the mixture, and its temperature, i.e. p_n, the partial pressure of steam, rise and as the temperature gradient $\theta = t_n - t_{cm}$ drops, the curves become flatter, rising upward from the curve previously secured for a sluggishly moving mixture as increases.

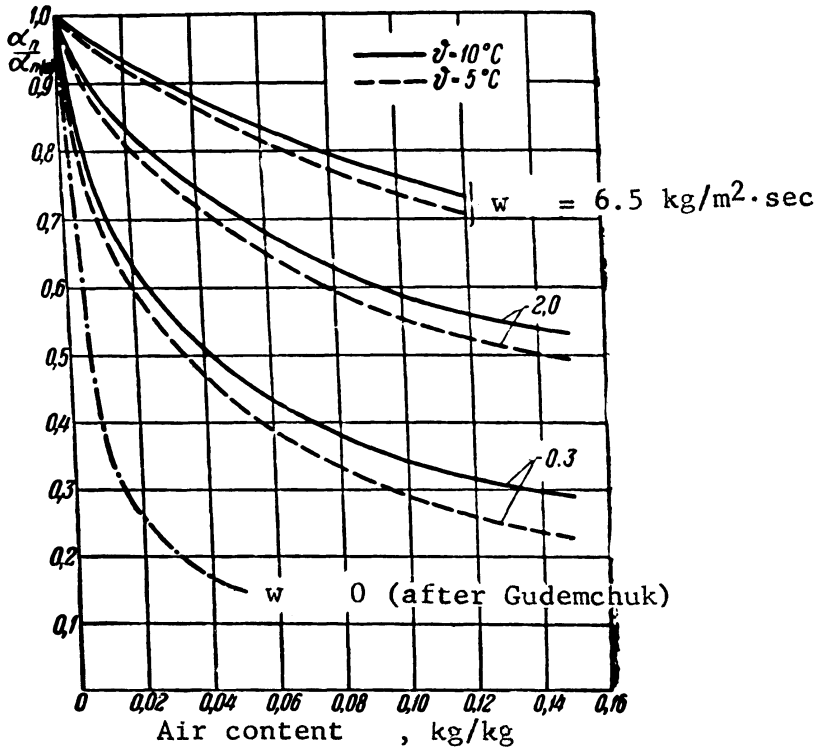

Fig. 4. Relative change in the coefficient of heat transfer as a function of the air content of the steam at different velocities of the steam-air mixture and temperature gradients (transverse flow accross a horizontal tube, steam pressure p_n = 0.81 atm absolute).

In plotting the curves of Figs. 4 and 5 we used for each curve the experimental value of the coefficient of heat transfer $\alpha_{n(0)}$ for the condensation of pure steam corresponding to the given conditions, which likewise depends on and other process parameters. If we take $\alpha_{n(0)} = \alpha_N$ (where α_N is the coefficient of heat transfer for the condensation of motionless pure steam, calculated from Nusselt's theoretical formula),

$\frac{\alpha_n}{\alpha_N}$ is found to be higher than unity for high mixture velocities (Fig. 6). This latter circumstance reflects the extent to which $\alpha_{n(o)}$ depends on the steam velocity observed in our experiments throughout the pressures employed therein (from 0.089 to 0.81 atm absolute).

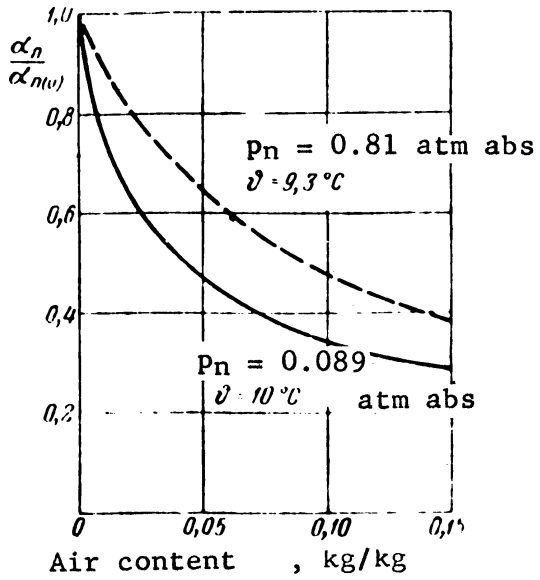

Fig. 5. Relative change in the coefficient of heat transfer as a function of the air content of the steam at various pressures ($\theta = 10^{\circ}$ C; ω_γ = 0.3 m/sec).

This shows that the widely accepted notion, based on the results of Nusselt's theoretical calculations for a single vertical wall, that the influence of steam velocity on the coefficient of heat transfer can be neglected in condensers that employ a vacuum, is completely wrong even for the case of the condensation of pure steam containing no admixture of air.

Obtaining more precise knowledge of the influence of various factors on heat rejection during the condensation of steam in the presence of noncondensable gases is a problem for further research, the securing of corresponding experimental data for bundles of tubes being important in that connection. The absence of these data leads to endeavors to employ the theoretical data available in the literature on the condensation of pure steam in horizontal tube banks.

4. HEAT TRANSFER IN THE CONDENSATION OF STEAM IN A HORIZONTAL TUBE BANK

It is a matter of coomon knowledge that when steam is condensed in a multiple bank of horizontal tubes, the value of the coefficient of heat transfer drops as we pass from the upper tubes to the lower ones. In the

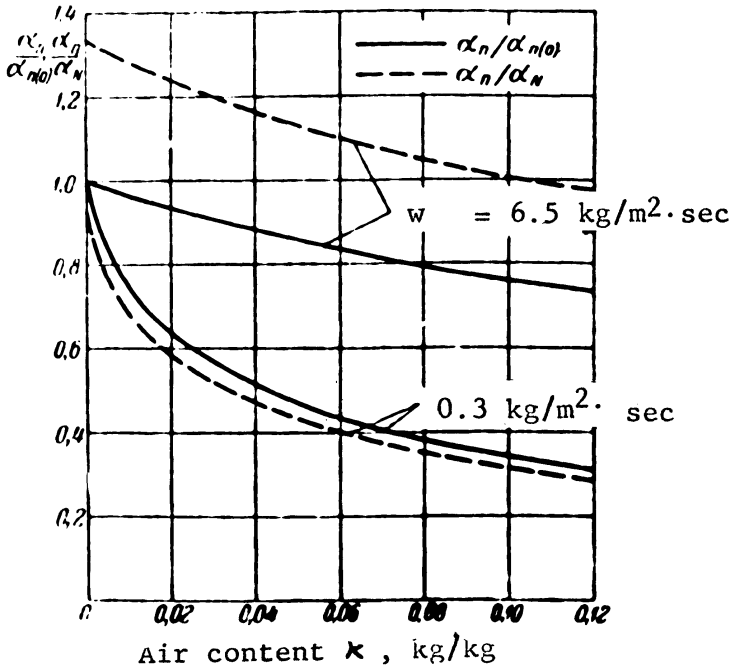

Fig. 6. The values of $\frac{\alpha_n}{\alpha_{n(0)}}$ and $\frac{\alpha_n}{\alpha_N}$.

special literature this is usually explained as due to the fact that the lower the tube in the bundle, the thicker the layer of condensate that washes it. Up to the present time, this explanation of the phenomenon, based on the paper by Nusselt published in 1916, has not been subjected to the adequate criticism it deserves, which is important for establishing a correct notion of the operation not only of heat-exchange apparatus, intended for the condensation of pure steam but for the operation of the condensers of steam prime movers we are considering.

In the condenser's bundle of tubes the most efficient peripheral tubes on the side of the steam inlet operate under conditions that are close to those obtaining in the condensation of pure steam. In modern so-called regenerative condensers, where much of the steam enters the bundle of tubes from the side rather than from above, a large numbe of these tubes is "drenched" with the condensate flowing down from the upper rows of tubes. It would seem that this ought to lower the coefficient of heat transfer substantially, though this is not found to be the case in experiments /Ref. 3, e/. Finding the reasons for this phenomenon and verifying the correctness of the conclusions drawn from existing theoretical notions of the condensation of pure steam in a horizontal bundle of tubes (with respect to the heat calculation and the design of the cooling surface of condensers) is of practical importance. Nusselt proceeded from the following assumptions in his paper:

a) Film flow is laminar, and the influence of friction between the vapor and the liquid film on the thickness of the latter can be neglected.

b) The temperature gradient θ is uniform for all tubes and around

the perimeter of each of them.

c) The condensate flows off the tube uniformly throughout the latter's length as a drawn-out, unbroken, narrow stream, falling on the top generatrix of the tube below.

On the basis of these assumptions, he calculated the coefficient of heat transfer for the horizontal tube in a vertical row that was second from the top.

M. I. Yanovsky /Ref. 9/, retaining the assumptions listed above, calculated the coefficients of heat transfer for twenty horizontal tubes arranged vertically one above another, as well as for tubes staggered with respect to one another so that the condensate flowing down from each tube strikes a lateral generatrix of the tube below rather than the top generatrix (Jinaba design). M. I. Yanovsky proposed to utilize the results of these calculations, frequently cited in our literature, in calculating the heat balance of condensers. On the basis of these calculations he also confirmed the substantial superiority of the tube bank built according to the Jinaba design for the condensers of steam prime movers. The error in the latter conclusion was correctly pointed out by S. S. Kutateladze /Ref. 1/. Comparing his own experimental data with the results of Yanovsky's calculations, Kutateladze concluded that the results of the theoretical calculations for the corridor (or more accurately, the "ordinary")* bank, though differing quantitatively somewhat from the experimental data, still yields a variation of the coefficient of heat transfer with the position of the tube in the vertical row that agrees satisfactorily with them, whereas calculations by the Nusselt-Yanovsky method do not yield satisfactory results for any other shape of bank, and, in particular, the advantage of the Jinaba bank is greatly exaggerated by these authors. S. S. Kutateladze attributes this to the fact that no allowance was made for the action of surface tension forces, which endeavor to even out the thickness of the condensate film around the perimeter of the tube, in calculating the Jinaba bank.

Observations of the flow of the liquid film as well as correlation and analysis of the available experimental data, however, justify the statement that the results of the theoretical calculations referred to above are useless even for ordinary banks, and that the Jinaba bank does not even possess the limited advantages mentioned by S. S. Kutateladze.

Data of several experiments, shown in the form of the function $\frac{\alpha_{n(i)}}{\alpha_{n(1)}} = f(i)$, and the theoretical curves based on M. I. Yanovsky's data are plotted in Fig. 7** The graph reveals extremely wide discrepancies between the experimental data and the theoretical figures for all forms of banks tested, as well as a substantial deviation of the experimental data among themselves for ordinary banks of identical form. These discrepancies cannot be attributed solely to experimental error; their cause must be sought in an essential difference between the actual conditions and the idealized conditions that were used as a basis for the

* By the term "ordinary" we mean a bank in which the horizontal tubes of one vertical row are arranged in parallel, with one strictly underneath the other, no matter whether the bank is of corridor or checkerwork form.

** Here $\alpha_{n(1)}$ is the coefficient of heat transfer for the top tube of the vertical row, while $\alpha_{n(i)}$ is the coefficient for the ith tube.

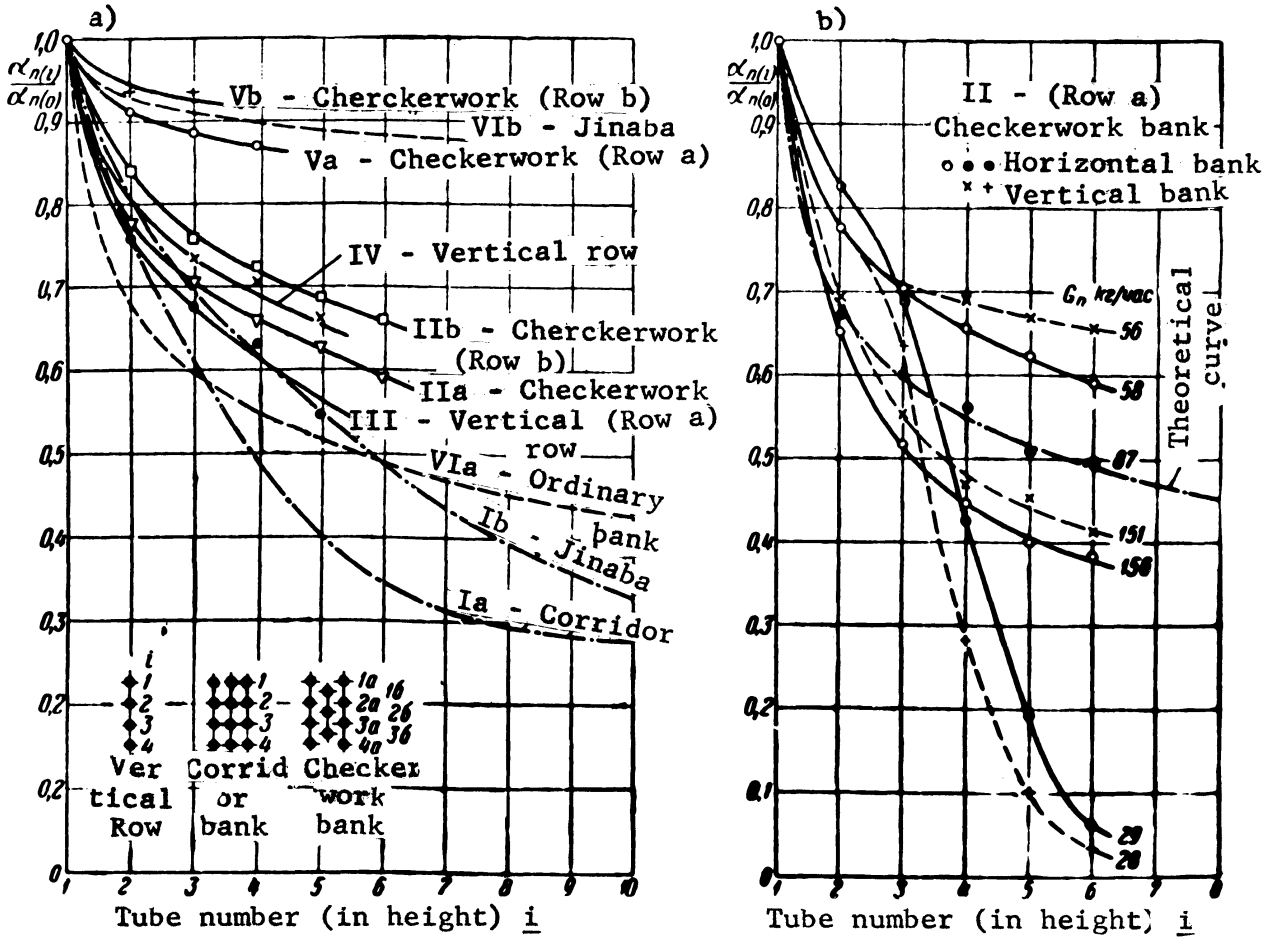

Fig. 7. Influence of the tube number according to its height in the vertical row on the coefficient of heat transfer in the condensation of pure steam.

I - Kutateladze experiments /Ref. 1/ at p $\geqslant$ 1 atm abs; II - Gudemchuk's experiments /Ref. 4, b/ at p = 1-1.5 atm abs (in Fig. 7a G_n = 58 kg/h); III - experiments of Ferguson and Oakden /Ref. 14/ at p = 0.12 atm abs; IV - ditto at p = 0.05 atm abs; V - ditto at p = 0.12 atm abs; VI - Yanovsky's theoretical calculations.

Without dealing with the problem of the variable θ, we may point out the following basic features of the actual conditions, which must have a major effect upon the results of laboratory experimental researches, as well as upon the operation of industrial installations:

1. The condensate runoff from each of the tubes in the bank is not uniform and continuous throughout the length of its lower generatrix, but is rather descrete, as individual drops.

2. The continuous decrease in the steam velocity as the steam condenses brings about a corresponding decrease in the rate of heat transfer in the bank of tubes, i.e. under real conditions heat transfer within the bank is found to depend largely on the interaction between the moving steam and the condensate film.

3. At a comparatively low inflow of steam, we find that the noncondensable gases that always enter with the steam, even though in minute quantity, has a very perceptible influence upon heat transfer in the final section of the path of the steam through the tube bank.

The fact that condensate runoff from the tubes occurs in the shape of individual drops was pointed out earlier, but the necessary conclusions were not drawn from this fact.

The author's observations indicate that the distance between the sites where drops are formed, which grows as the condensate runoff from the tube diminishes, may be as much as 80-100 mm and more, with the formation and detachment of drops occurring at different times. The condensate, falling as individual drops and striking the tube below, is unable to spread over any substantial length of this tube, despite the action of surface tension forces, but flows along it through a comparatively short section, producing underneath a site for the formation of a new drop (at approximately the same diametral plane in which the place where the drop fell on top of the tube is located).

That is why the thickening of the condensate film produced by the condensate dropping on the given tube from above proves to be no uniform throughout the length of the tube, but rather local, concentrated at the places where the drops fall. The nonuniform flow of condensate along the tube length (as well as with time) related to this must affect the flow of the film. Evidently the inflow of liquid from adjoining sections to places where the condensate velocity is higher can result in the formation of waves. Moreover, the falling of drops upon the tube and their detachment from the bottom of the tube (with the subsequent upward pull of the remaining portion of the neck of the drop) results in a periodic disturbance of the flow of the condensate film that may weaken the negative influence of its local thickening upon heat transfer.

This irregular runoff of condensate from the tube should result in a considerably smaller influence of the mean thickness of the condensate film upon heat transfer in a horizontal tube bank than would follow from the abstract scheme adopted by Nusselt. The influence of the condensate flowing downward on the rate of heat transfer is then determined for each individual tube not only by its serial number $\underline{i}$ (denoting its height in the vertical row) or by the ratio of the amount of condensate striking the tube $\sum_{1}^{i-1} G_{\kappa}$ to the amount of condensate produced at the tube G_k, but rather by factors that govern the spacing between the drops falling on the tube, their dimensions, and the frequency of fall, as well as by the intensity of the disturbances produced by the falling of drops on the tube. These factors include: the specific hydraulic load on the next tube bove, expressed in units of its length, $g_k = \frac{\sum_{1}^{i-1} G_{\kappa}}{L}$, the physical constants of the condensate, including its viscosity, the vertical spacing between the tubes, and so forth. In particular, the smaller g_k (i.e. the smaller the temperature gradient or the specific thermal load on the surface), the smaller must be the influence of the condensate flowing from above on the coefficient of heat transfer of the given tube for the same serial number $\underline{I}$ or for the same $\frac{\sum_{1}^{i-1} G_{\kappa}}{G_{\kappa}}$. The

variation of $\frac{\alpha_{n(i)}}{\alpha_{n(1)}}$ with $\frac{1}{i}$ or with $\frac{\sum_{1}^{i-1} G_k}{G_k}$ is not single-valued for a given bank, being determined by the combination of all the conditions under which steam is condensed at that bank.

This explains, for example, why experiments run at low thermal loads, approaching the loads in the condensers of steam prime movers, yielded a drop in α_n of no more than 12% for the fourth tube from the top (Fig. 7a - Curve Va) instead of the drop of 45% called for by Yanovsky's theoretical calculation (Curve VIa), despite the possible influence of a change in the steam velocity.

The effect of a change in steam velocity on heat rejection cannot be ignored, as a rule, when considering the condensation of steam in the tube bank. The diminution in the steam velocity as it condenses (provided the diminution in the volume of steam is not compensated for by a diminution in the cross section of passage through the bank) usually results in an appreciable lowering of the coefficient of heat transfer as well, which may result at times in an apparent coincidence of the experimental data with the results of theoretical calculations made on the assumption that α_n decreases only as the result of an increase in the thickness of the condensate film.

The less the steam velocity changes as it moves through the tube bank, the smaller should be the relative diminution of α_n along its path, due to a drop in the steam velocity. This explains the differences in the relative position of the curves for steam inputs ranging from 58 to 166 kg/h for the same tube bank in Fig. 7b. Owing to the influence of the decreasing steam velocity, the experimental curve $\frac{\alpha_{n(i)}}{\alpha_{n(1)}} = f(i)$ for the horizontal tube bank is appreciably below the theoretical curve for a steam inflow G_n = 166 kg/h and an initial velocity w_o = 26.3 m/sec. At a lower steam inflow (G_n = 87 kg/h and w_o = 19.4 m/sec) the experimental curve coincided with the theoretical one. A further diminution in the steam inflow (G_n = 58 kg/h, w_o = 13.6 m/sec) brought the experimental curve perceptibly above the theoretical one. It is apparent that if experiments had been run only at a steam inflow of 87 kg/h, we might reach the faulty conclusion that the experiments bore out the theoretical data satisfactorily, whereas the diminution in α_n was actually produced in this case mainly by a diminution in the steam velocity rather than by a thickening of the condensate film.

The correctness of this interpretation of the results of experiments run on the horizontal bank likewise follows from a comparison of these curves with the curves plotted as broken lines in Fig. 7b from the data on experiments on the same bank, which was turned, however, so that the tubes were vertical. After this change the values of $\frac{\alpha_{n(i)}}{\alpha_{n(1)}}$ for the individual rows by and large repeated the results secured for the horizontal tubes: As was noted by the researcher who performed these experiments, V. A. Gudemchuk, the reason for this was the basic cause of the diminution of α_n common to both cases, which proved to be the diminution in the steam velocity as the steam condensed (at the values of G_n given above).

The influence of the change in the steam velocity within the bank is reflected in the fact that the experimental data do not confirm the equivalence of the vertical rows a and b in the checkerwork tube bank which follows from the assumption made by Nusselt. According to Nusselt, the values of the coefficient of heat transfer for corresponding pairs of tubes (1a and 1b, 2a and 2b, etc.) ought to be identical, the change in α_n with the height of these two rows being described by a single common curve. In reality, however, the experimental curves $\frac{a_{n(i)}}{a_{n(1)}} = f(i)$ for the rows a and b does not agree (see Curves IIa and IIb, as well as Va and Vb in Fig. 7a), it being commonly observed that n decreases as we shift from Tube 1a to Tube 1b, then to Tube 2a, to Tube 2b, etc. in accordance with the change in the steam velocity (deviations from this are sometimes observed owing to the singular hydrodynamic conditions only for Tube 1b).

It follows from the foregoing that we can explain both the fact that the decrease in α_n as i increases, observed in experiments on the Jinaba bank (Curve Ib in Fig. 7a) and the fact that it proved to be somewhat lower than for a corridor bank (Curve Ia), whereas it considerably exceeded the diminution of α_n secured in a number of experiments with checkerwork banks (Curves II and V) and with a single vertical row of tubes (Curve IV). The location of these experimental curves we have compared was governed in actuality not by the form of the banks investigated, but mainly by the conditions under which the experiments were run (different initial parameters and steam velocities, different design dimensions of the installation and the like), resulting in a difference in the influence of the condensate runoff even for identical values of $\frac{\sum_1^{i-1} G_\kappa}{G_\kappa}$ and, chiefly, the steam velocity.

Hence, comparison of the experimental curves Ia and Ib gives us no reason to deduce any superiority, no matter how slight, of the Jinaba bank, nor can either of these curves be applied to conditions that differ from those at which the respective experiments were run.

The shape of the curve for the steam rate of 29 kg/h in Fig. 7b cannot, however, be explained as due to the change in the steam velocity. Here we are dealing with the influence of noncondensable gases, referred to above, which cannot be ignored when we analyze data on the condensation of steam in a multiple-row tube bank, inasmuch as practically all the entering steam is frequently condensed in experimental and industrial installations. If condensation of the bulk of the steam is completed by the time it leaves the tube bank, the extremely slight percentage of noncondensable gases present at the outset becomes so high during the final portion of the steam path as to produce an extremely sharp diminution of the coefficient of heat transfer at times. For example, the curve for G_n = 29 kg/h in Fig. 7b starts out less steeply than the curve for G_n = = 58 kg/h, as was to be expected, but then drops downward sharply owing to the rapidly rising concentration of noncondensable gases.

Thus, we may conclude that the theoretical data of Nusselt and Yanovsky prove useless for the real conditions of steam condensation in horizontal tube banks, no matter what the form of the latter may be. The fall of the coefficient of heat rejection observed in such banks is usually due, in the main, to a diminution in the steam velocity as it condenses and only to a comparatively small degree to the influence of the conden-

sate runoff, provided the influence of noncondensable gases does not make itself felt. The foregoing remarks referred to the condensation of pure steam. It is evident that if the calculations of Nusselt and Yanovsky do not yield satisfactory results for this case, we can make even less use of their results or, using them as a basis, draw any practical conclusions regarding the condensers of steam prime movers, where the presence of air in the steam greatly affects the distribution of the local values of the coefficient of heat transfer and the thermal loads within the tube bank.

5. DISTRIBUTION OF LOCAL THERMAL LOADS IN THE CONDENSATION OF STEAM IN THE PRESENCE OF AIR

It was shown above that as the steam-air mixture passes through the tube bank of the condenser, its composition changes, this being characterized by a substantial rise in its air content. The gravimetric and volumetric rates of flow of the mixture then drop, usually resulting in a drop in its velocity and producing a change in the rate of steam condensation as the mixture passes through the bank or, if we approach the problem from the standpoint of heat exchange, a change in the local specific thermal load.

In order to show the influence of a change in various parameters on the steam side of the cooling surface upon the distribution of local thermal loads we shall use an approximate analytical solution for the case where the condensation surface may be regarded as isothermal, i.e. where the temperature of the condensation surface or of an isolated part of it can be regarded as constant /Ref. 3, b/.

In this case we can write:

$$dG_n = -\beta_p (p_n - p_{ж})\, df. \tag{11}$$

for the quantity of steam condensing on an element of surface df in unit time.

The minus sign before the right-hand part of this equation indicates that the flow of steam G_n falls in the direction in which the steam-air mixture moves, which is here assumed to be positive.

Employing the equation of state of an ideal gas for the steam and the air and assuming that the total pressure of the mixture $p_{см}$ and its absolute temperature T are constant, we get:

$$dG_n = \frac{G_2 R_2 p_{см}}{R_n (p_{см} - p_n)}\, dp_n, \tag{12}$$

where R_n and R_2 are the gas constants for steam and air.

Let us denote the volume of air in the mixture* by $\varepsilon_0 = \frac{p_{см}}{p_2}$ and let us introduce an exponential expression:

$$\beta_p = C \frac{w^n}{\varepsilon_0^u}, \tag{13}$$

---

* ε_0 is related to the weight of air in the mixture by the following expression: $\varepsilon_0 = \frac{\varepsilon R_2}{R_n - \varepsilon (R_n - R_2)}$

for the coefficient of mass transfer, assuming as a first approximation that the coefficient C and the exponents n and u are constants for the steam-air mixture passing through the given apparatus. If the cross section of passage for the mixture remains constant throughout its path, we then have:

$$\beta_p = \beta_{p0}\left(\frac{p_{z0}}{p_z}\right)^m = \beta_{p0}\left(\frac{p_{c.m} - p_{n0}}{p_{c.m} - p_n}\right)^m, \tag{14}$$

where m = u + n, and the variables for the initial section are denoted by the subscript o.

Setting the right-hand sides of Eqs. (11) and (12) equal to each other and substituting the value of β_p from (14) we get:

$$-\frac{dp_n}{(p_{c.m} - p_n)^{2-m}(p_n - p_{ж})} = \frac{R_n \beta_{p0}(p_{c.m} - p_{n0})^m}{R_z G_z p_{c.m}} df. \tag{15}$$

Writing m as a simple fraction $m = \frac{a}{b}$, where a and b are integers, we can always convert the expression on the left-hand side of Eq. (15) into rational form by setting $(p_{cm} - p_n) = x^b$. This yields:

$$\frac{b\,dx}{x^{1+b-a}(p_{c.m} - p_{ж} - x^b)} = \frac{R_n \beta_{p0}(p_{c.m} - p_{n0})^m}{R_z G_z p_{c.m}} df. \tag{15a}$$

The solution of Eq. (15) can be written as follows: $\varepsilon_0 = \frac{\varepsilon R_z}{R_n - \varepsilon(R_n - R_z)}$.

$$f = \frac{R_z G_z p_{c.m}}{R_n \beta_{p0}(p_{c.m} - p_{ж})(p_{c.m} - p_{n0})} N, \tag{16}$$

where N is a function whose form depends on the value of m.

Resolving the expression at the left-hand side of Eq. (15a) into its simple elements and integrating from zero to f, we get the expressions for the function N listed in Table 1 for various values of m (from zero to 2.5). The value m = 0 corresponds to the case where β_p = constant.

When ω, the cross section of passage, is variable, Eqs. (14) and (15) must be replaced by the following:

$$\beta_p = \beta_{p0}\left(\frac{p_{z0}}{p_z}\right)^m \left(\frac{\omega_0}{\omega}\right)^n \tag{17}$$

and

$$-\frac{dp_n}{(p_{c.m} - p_n)^{2-m}(p_n - p_{ж})} = \frac{R_n \beta_{p0}\omega_0^2 (p_{c.m} - p_{n0})^m}{R_z G_z p_{c.m}} \frac{df}{\omega^n}. \tag{18}$$

It is evident from a comparison of Eqs. (15) and (18) that their left-hand parts are identical. This enables us to represent the results

of the solution of Eq. (18) as a function showing the variation of the surface f' of the bank with a variable cross section of passage with the surface f of the bank with a constant cross section of passage. For the bank illustrated in Fig. 8 we find that for any value of n, with the exception n = 2, on the assumption that flow is one-dimensional:

$$f' = \frac{2-n}{2\omega_0^2} \frac{\omega_0^2 - \omega^2}{\omega_0^{2-n} - \omega^{2-n}} f \tag{19}$$

and for n = 2:

$$f' = \frac{\omega_0^2 - \omega^2}{2\omega_0 \ln \frac{\omega_0}{\omega}} f, \tag{19a}$$

where f is determined from Eq. (16) by inserting the corresponding value of N therein.

To determine the distribution of thermal loads, we must know the change in p_n, the partial pressure of steam along the path of the steam-air mixture, i.e. the function $p_n = \Phi(f)$. Equation (16) cannot be solved for p_n in its general form, but inserting values of p_n in this equation that lie between its given initial value p_{no} and its final value p_{nk}, and finding the corresponding values of f, we can find how the partial steam pressure changes in the mixture along the cooling surface. We then can also determine the distribution of the amount of condensing steam and the local specific heat loads:

$$q = \beta_p (p_n - p_{ж}) \Delta i,$$

where Δi is the difference between the heat contents of the steam and the liquid in kg-cal/kg.

Let us take, for example the values $p_{см} = 0.05$ atm abs, $p_{ж} = 0.0374$ atm abs and $\varepsilon_{0(н)} = \frac{p_{см}}{p_{см} - p_{n0}} = 0{,}001$, and let us assume to begin with that β_p = constant (or m = 0). Then, using the equations given above, we secure the distribution of local thermal loads shown in Fig. 9. We see from the graph that a change in the partial pressure of steam in the bulk of the mixture is itself respondible for only a very slow decrease in q over most of the path of the mixture, provided the coefficient β_p does not change.

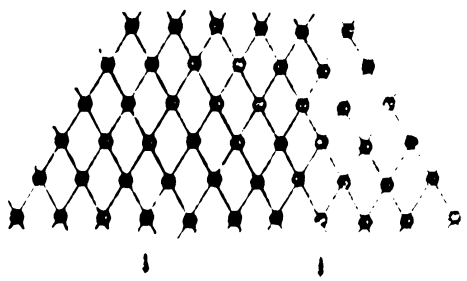

Fig. 8. Trapezoidal tube bank.

TABLE 1

$m = 0$	$N = 1 - \frac{\sigma_{z0}}{\sigma_z} + \sigma_{z0} \ln \frac{\sigma_z}{\sigma_{z0}} \frac{1 - \sigma_{z0}}{1 - \sigma_z}$
0,25	$N = \frac{4}{3}\left[1 - \left(\frac{\sigma_{z0}}{\sigma_z}\right)^{0,75}\right] + \sigma_{z0}^{0,75} (\ln X + 2 \operatorname{arc\,tg} Y)$
0,50	$N = 2\left(1 - \sqrt{\frac{\sigma_{z0}}{\sigma_z}}\right) + \sqrt{\sigma_{z0}} \ln \frac{\left(1 - \sqrt{\sigma_{z0}}\right)\left(1 + \sqrt{\sigma_z}\right)}{\left(1 + \sqrt{\sigma_{z0}}\right)\left(1 - \sqrt{\sigma_z}\right)}$
0,75	$N = 4\left(1 - \sqrt[4]{\frac{\sigma_{z0}}{\sigma_z}}\right) + \sqrt[4]{\sigma_{z0}} (\ln X - 2 \operatorname{arc\,tg} Y)$
1,00	$N = \ln \frac{\sigma_z}{\sigma_{z0}} \frac{1 - \sigma_{z0}}{1 - \sigma_z}$
1,50	$N = \frac{1}{\sqrt{\sigma_{z0}}} \ln \frac{\left(1 - \sqrt{\sigma_{z0}}\right)\left(1 + \sqrt{\sigma_z}\right)}{\left(1 + \sqrt{\sigma_{z0}}\right)\left(1 - \sqrt{\sigma_z}\right)}$
2,00	$N = \frac{1}{\sigma_{z0}} \ln \frac{1 - \sigma_{z0}}{1 - \sigma_z}$
2,50	$N = \frac{1}{\sigma_{z0}}\left[\frac{1}{\sqrt{\sigma_{z0}}} \ln \frac{\left(1 - \sqrt{\sigma_{z0}}\right)\left(1 + \sqrt{\sigma_z}\right)}{\left(1 + \sqrt{\sigma_{z0}}\right)\left(1 - \sqrt{\sigma_z}\right)} - 2\left(\sqrt{\frac{\sigma_z}{\sigma_{z0}}} - 1\right)\right]$

Notation:

$$\sigma_{z0} = \frac{p_{z0}}{p_{см} - p_{ж}}; \quad \sigma_z = \frac{p_z}{p_{см} - p_{ж}};$$

$$X = \frac{\left(1 - \sqrt[4]{\sigma_{z0}}\right)\left(1 + \sqrt[4]{\sigma_z}\right)}{\left(1 + \sqrt[4]{\sigma_{z0}}\right)\left(1 - \sqrt[4]{\sigma_z}\right)}; \quad Y = \frac{\sqrt[4]{\sigma_z} - \sqrt[4]{\sigma_{z0}}}{1 + \sqrt[4]{\sigma_{z0}\sigma_z}}$$

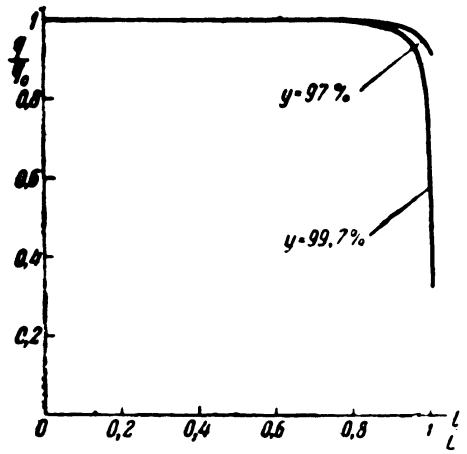

Fig. 9. Change in local thermal loads as the steam-air mixture passes through the condenser at β_p = constant.

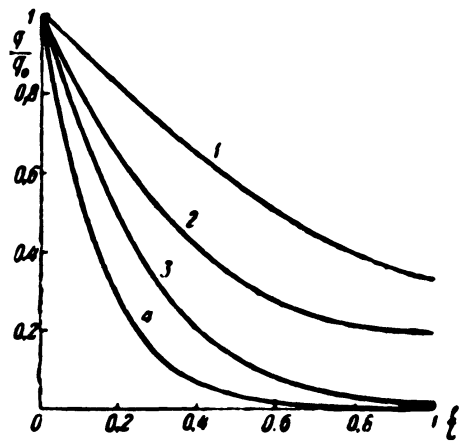

Fig. 10. Change in local thermal loads as the steam-air mixture passes through the condenser at β_p = variable.

Curve	m	s	y
1	0.5	0.25	97
2	0.75	0.25	97
3	0.75	0.25	99.7
4	1.0	1.0	99.7

The situation changes greatly, however, when we make allowance for the change in β_p, the coefficient of mass transfer, as a function of the composition and velocity of the mixture. Setting the same initial conditions as previously, and using different values of the exponent m, of the ratio of the final to the initial cross section $\frac{\omega_к}{\omega_0}$, and y, the degree of condensation of the steam, we get the curves for the distribution of local thermal loads shown in Fig. 10.

These curves show that the decrease in the coefficient of mass transfer (or, putting it otherwise, the increase of external thermal resistance) as the steam condenses results in an appreciable lowering of the specific thermal load on the cooling surface along the path of the steam-air mixture, and this nonuniformity of distribution of the thermal load cannot be eliminated, but can merely be somewhat reduced by grouping the heating surface appropriately.

This conclusion also applies to the industrial condenser, though the conditions for steam condensation in the latter are more complicated than those that were assumed above. To shed light on other important features of heat exchange in the condenser, let us turn to the experimental data.

6. EXPERIMENTAL DATA ON THE DISTRIBUTION OF THERMAL LOADS IN A CONDENSER

In a real condenser the influence of the thermal resistance on the

water side of the cooling surface decreases the nonuniformity of distribution of thermal load, compared to an isothermal condensation surface; moreover, the distribution of the thermal load prevailing in one condenser operating regime or another proves to be dependent upon the characteristics of the air-removal equipment, as will be shown in detail later. The local specific thermal load on the surface can be represented as:

$$q = \beta_p (p_n - p_ж) \Delta i = K \delta t. \tag{20}$$

In this equation K and δ t denote the local values of the coefficient of heat transfer (kg-cal/m^2·h·degree) and the temperature gradient (^{o} C)

$$\delta t = t_n - t_в$$

and

$$= R = R_n + R_{cm} + R_в,$$

where

t_n and t are the temperatures of the steam and cooling water, respectively, in ^{o} C.

R_n, R_{cm}, and R are the thermal resistances on the steam side, of the wall (including deposits on the latter), and on the water side, respectively, in m^2·h·degree/kg-cal.

When the cooling surface of the condenser is clean, the thermal resistance of the wall is small, as we know, compared to R_n and $R_в$, remaining constant over the entire surface. The thermal resistance on the water side likewise varies within comparatively narrow limits, and it is not so much the change in its absolute value that affects the distribution of local thermal loads as it is the change in the ratio of $R_в$ to the thermal resistance, R_n, which rises very rapidly along the path of the steam-air mixture.

$R_в$ is usually higher than R_p at the side where the steam (the mixture) enters the tube bank, and with clean tubes the thermal resistance on the steam side ranges from one-third to one-quarter of the total thermal resistance R, being an even smaller fraction if fouling is present. But R_n rises sharply as the steam-air mixture penetrates the tube bank and the steam condenses, beginning to constitute the predominant constituent of the overall resistance R, the other components undergoing practically no change. At the outlet side of the steam-air mixture R_n totals as much as 92-97% of R, as indicated by the experimental data. This should be borne in mind in considering the results of the experiments described below.

The distribution of thermal loads in industrial condensers is investigated by making measurements of individual tubes in the bank, isolated (on the water side) from the total flow. In the experiments run in the All-Union Heat Engineering Institute /Ref. 3, e/, on which most of our work is base, these measurements were made in the LMZ, Type OV, two-pass condenser with 32 tubes, located in one of the symmetrical halves of the condenser and selected so that they made it possible to cover the principal zones of the tube bank in the probable direction of motion of the flow of steam.

The curves of equal thermal load plotted from the data of these mea-

surements for one of the operating regimes of the condenser and the distribution of local thermal loads along the path of the steam-air mixture in different regimes are given in Figs. 11 and 12. The distribution of local coefficients of heat transfer is of the same nature, though they differ quantitatively owing to the differences in local temperature gradients.

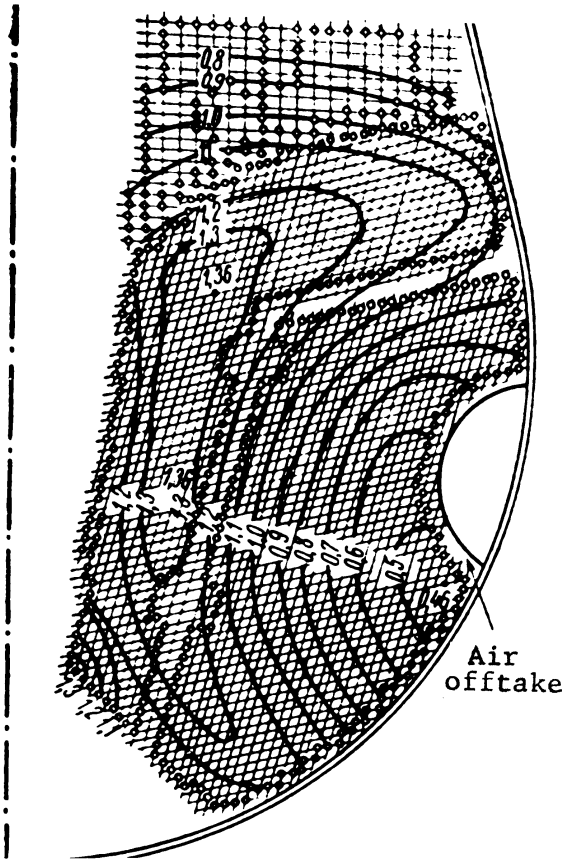

Fig. 11. Curves of equal thermal load in the condenser at $t_{1c} = 24^{\circ}$ C and $d_k \geq 35$ kg/m^2·h. (the numbers and lines denote the local thermal load, referred to the mean value).

The experiments confirm the substantial diminution of local thermal loads and of coefficients of heat transfer along the path of the steam-air mixture.* In these experiments the ratio of maximum load (at the in-

* A certain lowering of the thermal loads in the peripheral zone of the tube bank, observed in some operating regimes, are explainable as due to fouling of the surface of the peripheral tubes on the steam side, and to some extent possibly to the conditions of distribution of the entering steam along the length of the condenser.

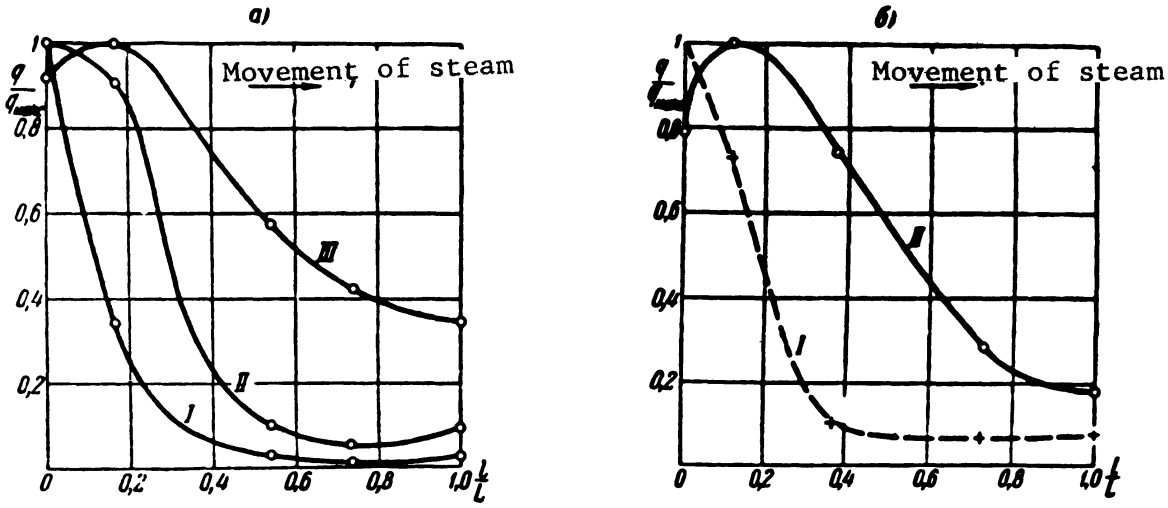

Fig. 12. Distribution of local thermal loads along the path of the steam-air mixture in the condenser:
a) as a function of the steam load and the temperature of the cooling water
I) d_k = 15 kg/m^2·h and $t_{1в}$ = 11° C; II) d_k = 26 kg/m^2·h and $t_{1в}$ = = 11° C; III) d_k 35 kg/m^2·h and $t_{1в}$ = 24° C.
b) as a function of the amount of air entering the condenser (d_k = = 36 kg/m^2·h and $t_{1в}$ = 17.3° C.
I) G_2 = 43.2 kg/h; II) G_2 = 15.9 kg/h.

let side of the bank) to the minimum load (at the outlet side of the bank) renged from 3 to 20, depending on the condenser's operating regime. The magnitude of the local coefficient of heat transfer on the steam side, α_n, dropped approximately from 13,000 kg-cal/m^2·h·degree at the inlet end to 500-1500 kg-cal/m^2·h·degree at the outlet end of the bank. The local values of K, the coefficient of heat transfer, ranged from 3600 kg-cal/m^2·h·degree at the inlet side of the bank to 400-1200 kg-cal/m^2·h·degree at the outlet side.

These measurements on selected tubes establish the following important fact for judging the operation of a condenser: the local coefficient of heat transfer at the steam inlet side of the bank does not change or changes comparatively little for various changes in the condenser's operating regime, whereas the local coefficients of heat transfer change more and more appreciably with a change in the condenser's operating regime as we penetrate into the interior of the bank. The maximum fluctuations in the value of the local coefficient of heat transfer are observed at the side where the steam-air mixture makes its exit from the tube bank. The fact that the local coefficient of heat transfer in the peripheral tubes remains practically constant as the steam load on the condenser and the quantity of air entering the condenser are changed (within limits ordinarily observed), notwithstanding the substan-

tial change in the steam velocity involved, is shown in Fig. 13.

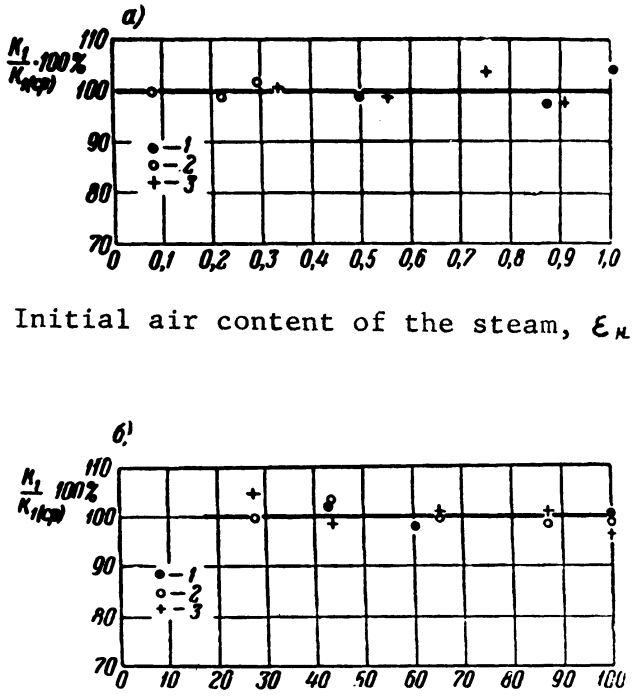

Fig. 13. Local coefficient of heat transfer for tubes in the first row as a function of the condenser's steam load and the initial air content of the steam.
a. 1) d_k = 23.9 kg/m^2·h; 2) d_k = = 64.3 kg/m^2·h; 3) d_k = 35.2 kg/m^2·h.
b. 1) Condenser 1; 2) Condenser 2; 3) Condenser 3.

The thermal loads on these tubes vary principally as a result of a change in the temperature gradient δ t (since a change in the condenser's operating regime also involves a change in the steam pressure and the steam temperature). The fact that K is practically constant for peripheral tubes may be explained by the fact that the thermal resistance on the water side, $R_в$, constitutes the major proportion of the overall thermal resistance R at the steam inlet side of the bank. As the temperature and the velocity of the cooling water decrease, the coefficient of heat transfer for the peripheral tubes drops somewhat owing to an increase in $R_в$, but in these cases the change in K for the peripheral tubes is extremely small compared to its change in the tubes located at the outlet side of the bank.

The ever greater change in the local values of K as we travel away from the entrance to the tube bank is related to the fact that a change in the conditions of condenser operation also involves a change in the distribution of all the basic process parameters along the path of the steam-air mixture.

Curves I and II in Fig. 12 first drop fairly sharply, after which they run nearly parallel to the axis of abscissas or even rise somewhat. We may conclude from the foregoing that the rapid drop of the curve at the outset, like the drop of the curves in Fig. 10, is a result of the lowering of the local values of the coefficient of heat transfer on the steam side. This part of the curve corresponds to the zone in which the bulk of the steam entering the condenser condenses.

The rate of steam condensation is low along the rest of the path of the steam-air mixture, and the coefficient of heat transfer changes comparatively little. This is also facilitated (with an appropriate configuration of the tube bank) by an increase in the velocity of the mixture owing to a pronounced diminution in cross-sectional area. Under certain conditions the latter even brings about some increase in the local values of the coefficient of heat transfer along this portion of the path.

In the initial zone the temperature of the steam-air mixture remains practically constant or drops only slightly, chiefly as a result of a drop in the total pressure of the mixture, caused by the "vapov resistance" of the tube bank. In the zone where the degree of steam condensation has already risen to a high value, the drop in temperature of the mixture becomes greater because of the rapid drop in the partial pressure of the steam.

In conformity with what has been said, the total cooling surface of the condenser can be conventionally divided into two zones:

1) The zone of condensation of the bulk of the steam (the zone of intense condensation), characterized by high local values of the coefficient of heat transfer and of specific thermal load at the steam inlet side, and a substantial drop in these values as the steam-air mixture propgresses through the bank (with a practically negligible drop in the temperature of the mixture).

2) The zone of cooling of the steam-air mixture, characterized by low local values of the coefficient of heat transfer and of thermal load changing comparatively little, and by an appreciable fall in the temperature of the mixture.

The boundary between these two zones is not a steady one, but moves in one direction or another as the operating regime of the condenser changes. In some regimes, for example, at high steam loads and a high temperature of the cooling water, the steam-air mixture's cooling zone nearly vanishes (see Curve III in Fig. 12).

The redistribution of the basic process parameters as the mixture passes through the tube bank that accompanies a change in the operating regime of the installation, producing a shift in the boundary between the zone of intensive condensation and the zone in which the steam-air is cooled, is governed not only by the operating conditions of the condenser itself, but by the effect of the air-removal equipment on heat exchange within the condenser as well.

7. INFLUENCE OF AIR-REMOVAL EQUIPMENT ON HEAT-EXCHANGE CONDITIONS IN THE CONDENSER

Maintenance of a vacuum within the condenser requires the constant

removal of the air that enters it and comes out of the tube bank together with the steam that has remained uncondensed.

The air-removal equipment mainly employed in modern condenser installations is the steam jet air ejector.

The suction pressure of the air-removal equipment is related to the pressure prevailing at the throat of the condenser by a simple equation when the installation is operating in a steady state:

$$p_к = p_э + \Delta p, \tag{21}$$

where p_k = pressure of the spent steam, atm absolute.
$p_э$ = suction pressure of the air-removal equipment (ejector), atm absolute.
Δp = vapor resistance of the condenser, atm.

We can write the following expression for the suction pressure of the air-removal equipment, no matter what its type:

$$p_э = p''_{см} + aG_в, \tag{22}$$

where p''_{cm} = pressure of saturated steam at the temperature of the steam-air mixture pumped out of the condenser, t_{cm}, atm absolute.
$G_в$ = weight of dry air in the mixture to be pumped out, kg/h.
a = a coefficient.

In a steam jet ejector operating without overload and with constant parameters of the live steam, the coefficient a proves to be practically constant, depending upon the individual properties of the ejector: its principal geometrical dimensions, the compression of the mixture in the first state, and the perfection of its design. Accordingly, at t_{cm} = = constant the operating section of the ejector's characteristic curve, representing the variation of the suction pressure $p_э$ with the weight of dry air $G_в$ in the pumped-out mixture, can be represented by a straight line whose slope is a for the given live steam parameters. The higher t_{cm}, the higher will be the corresponding straight line, though it retains practically the same slope (Fig. 14).

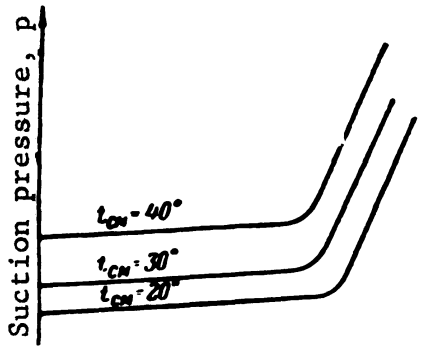

Weight of pumped-out air (in the mixture), G , kg/h

Fig. 14. Characteristic curve of a steam-air jet ejector.

The condition set forth in (21), together with the variation of $p_э$, the suction pressure of the air-removal equipment, with the temperature of the steam-air mixture entering it, leaves a considerable imprint on the conditions of heat exchange in the condenser. We shall demonstrate this in detail, using as an example the shift in the operating regime of the condenser as its steam load changes.

Let us assume that the steam load on the condenser, denoted by D_k, is reduced to D_k', and let us first consider the initial period of time during which the drop in the steam load has not yet affected the suction pressure of the ejector, and hence, has also not affected the pressure within the condenser p_k, (for the sake of simplicity we shall ignore Δp, the change in the condenser's resistance, assuming that Δp is small compared to p_k).

According to what has been said earlier, the coefficient of heat transfer remains practically constant within some small initial section of the cooling surface, ΔF_1, as the operating conditions of the condenser change. Inasmuch as the pressure p_k (on which the steam temperature t_n and the temperature gradient δt depend) likewise remains what it was in the period under consideration, there is no change in the quantity of steam condensing in the section ΔF_1. But when the absolute value of G, the amount of air entering the condenser remains unchanged, (this may even rise for the most part when the steam load on the condenser falls) the initial air content of the mixture, ε, proves to be higher, and the relative rise of ε above the initial regime will be still higher for the steam entering the following section ΔF_2 from the section ΔF_1. Let us assume, for example, that 1000 kg/h of steam with an air content = 0.05% enters the section ΔF_1 during the starting regime, 50 kg/h of steam condensing in this section. Then, if the steam load drops to 850 kg/h and both the entering air and the quantity of steam condensing in the section ΔF_1 remain unchanged, the proportion of air in the steam changes as follows:

	Initial regime	After lowering of D_k
Ahead of Section ΔF_1	0.0500	0.0575
Behind Section ΔF_1	0.0519	0.0610

In the next section of the surface, ΔF_2, within which α_n begins to affect K, the local coefficient of heat transfer proves to be lower than in the initial regime because of the lower velocity of the mixture and the higher percentage of air in it. Less steam condenses in the section ΔF_2 than before; however, the velocity of the mixture in this section will be lower and the concentration of air in it higher than in the initial regime. Let us assume, for example, that 40 kg/h of steam condensed in this section during the initial regime, while 30 kg/h condense during the regime we are considering. We then get the following values of ε, the air content, for the regime under consideration:

	Initial regime	After lowering of D_k
Ahead of Section ΔF_2	0.0519	0.0610
Behind Section ΔF_2	0.0540	0.0632

As a result of the lower velocity and the higher air content of the

steam the local coefficient of heat transfer in the third section ΔF_3 along the steam path likewise proves to be lower than during the initial regime. The same is found to be true in the remaining sections along the steam path, so that the curve showing the change in K as the steam flows through the tube bank will be lower for the regime we are considering than for the initial regime.

An example of the change in the values of ε, K and q as the steam passes through the condenser is given in Fig. 15. In the figure 1 denotes the curves for the initial regime, and 2 the curves referring to the initial period of time discussed above after the steam load had been lowered, when p_k, the pressure in the condenser, has not yet changed.

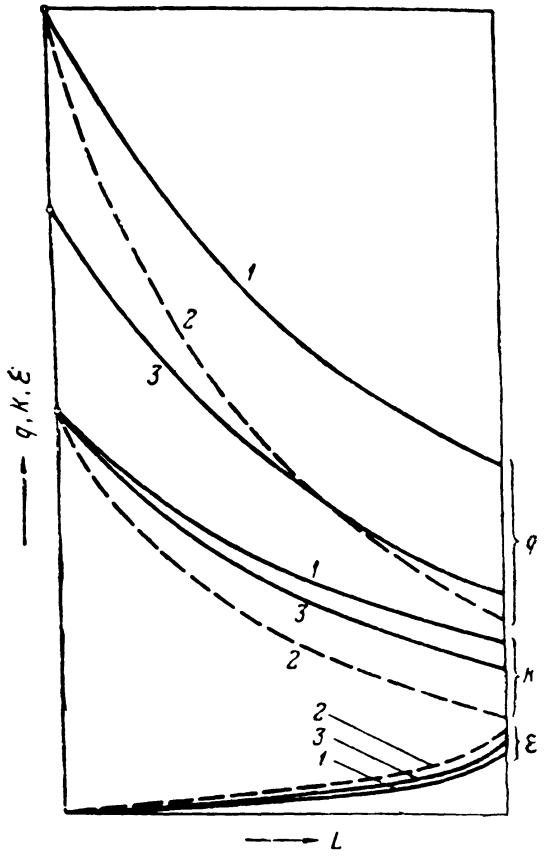

Fig. 15. Distribution of local values of air content in the mixture (ε), the coefficient of heat transfer (K), and the specific thermal load (q) as the steam passes through the condenser at various steam loads.
1 - Initial regime, load D_k;
2 - load $D'_k < D_k$ and p_k = constant; 3 - load D'_k, pressure $p'_k < p_k$.

If $p_э$, the suction pressure of the ejector, remained unchanged under all conditions, then (for a negligible change in Δp) the pressure within the condenser, p_k, would continue to remain practically unchanged, while the curves 2 in Fig. 15 would describe the conditions of heat exchange in the newly established state of the installation. In reality, however, a change in t_{cm}, the temperature of the steam-air mixture intering the ejector, caused by a change in the operating conditions of the condenser, results in a change in the ejector's suction pressure and, hence, in a change in the pressure within the condenser.

When the steam load of the condenser diminishes and p_k = constant, the zone of intense steam condensation grows shorter, while the zone in which the steam-air mixture is cooled grows wider. Correspondingly, the temperature t_{cm} becomes lower, causing $p_э$, the ejector suction pressure, to drop. The latter, in turn, lowers p_k, the pressure within the condenser, and as a result of the diminution of the temperature gradient (due to the fall of t_n) the local thermal loads in the condenser are again redistributed. The decrease in the temperature gradient results in a decrease in the quantity of steam that condenses in the section ΔF_1, i.e. in a decrease in the thermal load on the tubes at the steam inlet end of the tube bank, (even though the coefficient of heat transfer does not undergo any substantial change there). The local values of the coefficient of heat transfer rise in the following sections along the path of the steam, owing to an increase in the velocity of the mixture and a decrease in ε, compared to the regime considered earlier. The local thermal loads become lower in the initial section of the steam path, where it enters the tube bank, and higher along the rest of its path than during the regime described by Curves 2 in Fig. 15. The zone in which the mixture is cooled then grows shorter, compared to its dimensions corresponding to the diminished steam load, though the pressure p_k is still unchanged. The change in $p_э$, the suction pressure of the ejector, and p_k, the pressure in the condenser, will continue until the condition (21) is satisfied in some newly established state.

The distribution of the local values of $\underline{K}$ and $\underline{q}$ corresponding to the new regime (see the curves denoted by 3 in Fig. 15) will depend both upon the operation of the condenser, determining the temperature of the mixture pumped out by the ejector, and by the operation of the ejector, affecting the pressure in the condenser and thus the heat-exchange conditions within it.

It is obvious from the foregoing that when the air-removal equipment has no influence, i.e. when the pressure within the condenser remains unchanged, a drop in the latter's steam load would always result in a perceptible decrease in the local coefficients of heat transfer all along the path of the steam-air mixture within the tube bank, with the sole exception of the first few tubes at the entrance end of the bank. But in reality, owing to the influence of the ejector, a drop in whose suction lowers the pressure within the condenser, the change in the local coefficient of heat transfer proves to be less than when p_k = constant. As a result of the influence of the ejector we may also have conditons in which a change in the condenser steam load within fairly wide limits leaves the local values of the coefficient of heat transfer (though not of the thermal load) unchanged, i.e. Curves 1 and 3 for $\underline{K}$ coincide in Fig. 15.

The experimental data /Ref. 3, e/ bear this out, indicating that

under certain conditions, particularly when the amount of air entering remains almost constant as the steam load changes, the local values of the coefficient of heat transfer likewise change hardly at all with a change in D_k, while the local thermal loads vary about proportionally with the condenser steam load, whereas under other conditions we observe a perceptible change in the local coefficients of heat transfer, the farther the tubes considered being from the entrance to the tube bank, the greater the diminution in these local coefficients (as D_k decreases).

In some cases the influence of the ejector upon the conditions of heat exchange in the condenser occurring during any change in the operating conditions of the installation may result in a smaller change in the local values of K then when this influence is absent (as is the case, for example, in the case of a change in the steam load considered above), while in other cases it may result in a larger change in $\underline{K}$ (as, for example, when the amount of air entering the condenser increases).

The change in the local values of $\underline{K}$ brought about by the influence of the ejector also causes a change in the mean coefficient of heat transfer $\overline{K}$, which is thus found to depend both upon the operation of the condenser and the operation of the ejector /Ref. 3, d, e, g; 10/.

As a result of the correlation between the operation of the condenser and the operation of the ejector noted above the mean coefficient of heat transfer for a given condenser turns out to vary (all other conditions being the same), depending upon the characteristics of the ejector (or group of ejectors connected in parallel) serving it. However, as indicated by Eq. (22), the individual properties of a given ejector, determining the magnitude of $\underline{a}$, may have a great effect upon the value of the coefficient of heat transfer only when the installation operates with a large quantity of entering air G_{ε}, when the term aG_{ε} in Eq. (22) is significant compared to p''_{cm}. When G_{ε} is small, corresponding ordinarily to the normal air density of the installation, the influence of the individual properties of the ejector becomes much less, and the condition that the pressure $p_э$ cannot be lower than the saturation pressure at the temperature of the steam-air mixture removed from the condenser, which is independent of the type and properties of the air-removal equipment, proves to be decisive.

8. MEAN COEFFICIENT OF HEAT TRANSFER OF A CONDENSER

The complexity of the conditions under which the process of steam condensation takes place in condensers of steam prime movers makes the development of an analytical method for the thermal calculation of apparatus of this sort very difficult.

But in this case we can make use of an approximate method of calculating the cooling surface by sections (or by tube rows), employing the assumption that the parameters of the steam-air mixture and the coefficients of heat transfer remain constant in each of the sections of the surface. Reducing the size of the individual sections can increase the accuracy of the calculation.

Without considering some methodical difficulties arising in the use of this method for calculating condensers of steam prime movers, which

have not yet been eliminated, let us add that the principal obstacle to its practical use at the present time is the absence of adequate data for a dependable estimate of the local values of the experimental coefficients entering into the computational equations, as well as for determining the magnitude of steam resistance, which must necessarily be borne in mind in a calculation of this sort. For the present, we have to make use of an empirical method of calculation, based on the employment of an experimental value of the condenser's mean coefficient of heat transfer.

In the empirical calculation now employed the mean coefficient of heat transfer is determined from the usual expression:

$$\overline{K} = \frac{Q}{F \delta t_{cp}}, \tag{23}$$

where Q is the total amount of heat transferred from the condensing steam to the cooling water in kg/cal/h.

δt_{cp} is the mean temperature difference between the steam and the cooling water in ^{o}C.

F is the cooling surface of the condenser in m^2.

It is customary for the most part to determine the mean temperature difference from the logarithmic formula:

$$\delta t_{cp} = \frac{t_{2s} - t_{1s}}{\ln \frac{t_n - t_{1s}}{t_n - t_{2s}}}, \tag{24}$$

where t_n is the steam temperature, assumed to be equal to the saturation temperature at the pressure of the spent steam entering the condenser in ^{o}C.

t_{1s}, t_{2s} are the temperatures of the cooling water at the condenser inlet and outlet, respectively, in ^{o}C.

Determination of the mean coefficient of heat transfer and the mean temperature difference for condensers of steam prime movers by use of Eqs. (23) and (24) is a conventional method of calculation that is not related to the physical nature of the phenomena occurring within the condenser, which must not be lost sight of when employing these figures.

The suggestions to be found in the literature, which have been reflected in calculation practice, that the empirical method of calculating condensers be refined by changing the method used to determine the mean temperature gradient δt_{cp} to make allowance for the drop of temperature of the steam-air mixture are not well founded. These suggestions are based on the use of solutions referring to the conditions of heat exchange without any change of state of the medium being cooled, when the temperature drop of the latter is proportional to the amount of heat given off by it, which renders these solutions completely useless for the conditions prevailing in the condensers we are considering, in which the bulk of the heat given off by the steam represents the heat of change of state.

Alongside the mean coefficient of heat transfer $\bar{K}$ the mean coefficient of heat rejection from the steam side, $\bar{\alpha}_n$, referred to the entire surface and determined by the difference in thermal resistances, is frequently calculated when working up the results of tests of industrial condensers:

$$\bar{R}_n = \frac{1}{\bar{\alpha}_n} = \bar{R} - (R_{cm} + R_e), \tag{25}$$

where $\bar{R} = \frac{1}{\bar{K}}$.

As a conventional measure of the intensity of heat transfer from the steam to the water and of the heat rejection from the steam side, the experimental coefficients $\bar{K}$ and $\bar{\alpha}_n$ prove to be dependent upon all the factors that affect the conditions of heat exchange within the condenser. The latter, include, besides the design of the condenser and the characteristic curve of the air ejector, the temperature and the velocity of the cooling water, the steam loading of the cooling surface, the air density of the system, and the cleanliness of the cooling surface.

As was pointed out above, a change in the operating conditions of the condensing equipment results in a change in the local values of the coefficient of heat transfer and of the thermal load, with a corresponding shift to one side or the other of the boundary between the zones of intensive condensation of steam and cooling of the steam-air mixture. Inasmuch as the thermal resistance on the water side changes comparatively little in the various sections of the cooling surface, if it changes at all during this process, the redistribution of the local thermal load is related mainly to a change in the conditions of heat transfer on the steam side (local values of the coefficients β_p or α_n), as is likewise proved by the material influence of the operation of the air-removal equipment.

All these changes are also reflected in the "external" indexes of the operation of the condensing equipment, in particular, in the changes in the magnitude of the condenser's mean coefficient of heat transfer $\bar{K}$. But inasmuch as the distribution of α_n, K and q along the path of the steam-air mixture through the tube bank for any steady state is determined by the combined effect of all the factors influencing the operation of the installation, a change in any one of these factors that is of identical size may be reflected differently in the magnitude of $\bar{K}$, depending upon the other conditions under which this change took place.

Let us demonstrate this in somewhat more detail, using as an example the change in the quantity of cooling water used, which entails a corresponding change in the velocity of the water through the condenser tubes. All authors who have previously proposed empirical equations for $\bar{K}$ have assumed that when the water velocity w changes the coefficient $\bar{K}$ changes proportionally to the square root of w, independently of other conditions. In reality, however, this is not the case.

A decrease in the flow of cooling water results, on the one hand, in a decrease of α_β, the coefficient of heat transfer from the wall to the water, and, on the other hand, in an increase in Δt, the temperature rise of the water within the condenser. This results in a diminution of the local thermal loads and of the amount of steam condensing

along this section of its path. The decrease in the velocity of the mixture and the rise in the air content ε as the mixture passes through the tube bank then slow down, as a result of which the local values of α_n and, hence, the mean coefficient of heat rejection, $\bar{\alpha}_n$ rise, while the zone of intensive steam condensation widens at the expense of a shortening of the zone in which the steam-air mixture is cooled. The latter causes t_{cm} to rise and, as a result thereof, $p_э$, the ejector suction pressure, and p_k, the pressure within the condenser, likewise rise.

The pressure rise within the condenser produced by the efector decreases the "length" of the zone of intensive condensation, but once a new steady state has been reached, it still proves to be larger than its initial size, and the coefficient $\bar{\alpha}_n$ increases as the flow of water diminishes, as is borne out by experimental data (Fig. 16). It follows that a change in the mean coefficient of heat transfer $\bar{K}$ is governed by the influence of two opposite factors in the case under consideration: a decrease in the coefficient of heat transfer on the water side and an increase in the local values and in the mean value of the coefficient of heat transfer on the steam side.

Since the ratio between the local coefficients of heat transfer on the water and steam side changes greatly as the steam-air mixture passes through the tube bank, the influence of the diminution in the velocity $\bar{w}$ on the local values of $\bar{K}$ must also be different along different sections

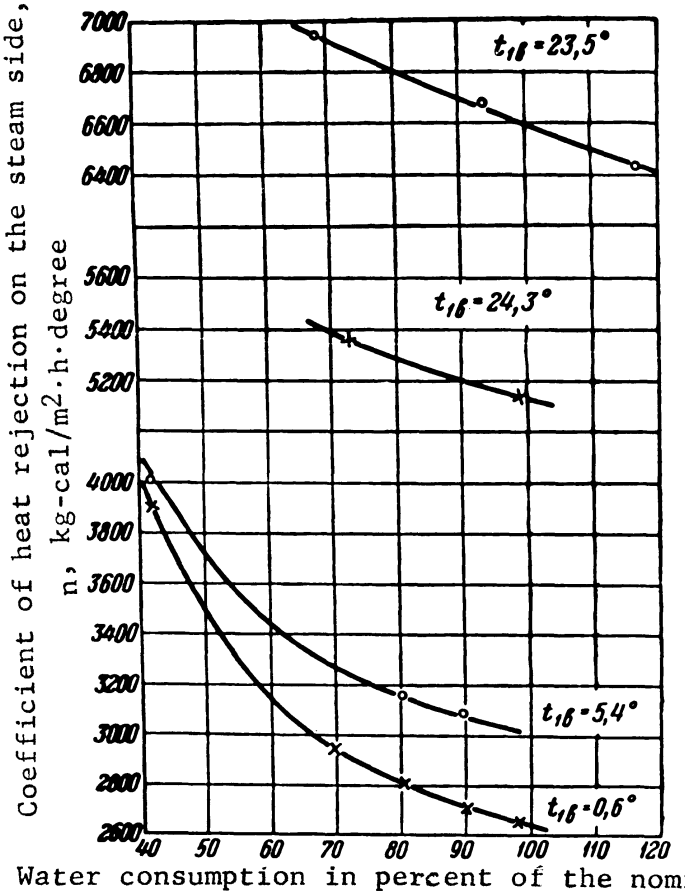

Fig. 16. Influence of the consumption of cooling water on the mean coefficient of heat transfer on the steam side.

of this path, and this is borne out by measurements of individual tubes of an industrial condenser /Ref. 3, e/. In that part of the path of the mixture where R_n, the thermal resistance on the steam side, is comparatively small (i.e. the coefficient α_n is still of significant size) and the thermal resistance $R_g = \frac{1}{\alpha_g}$ plays the predominant or fairly large role, the decrease in the water velocity results in a perceptibly larger decrease in $\underline{K}$ than in the section of the path where the thermal resistance on the water side is almost negligible under certain conditions, the rise in α_n may be of predominant importance compared to the diminution of α_g, and here the local values of $\underline{K}$ may not drop as they do in the rest of the cooling surface, but may even rise with a fall in $\underline{w}$. That is why the same decrease in the water velocity should result in a much smaller decrease in the mean coefficient of heat transfer under operating conditions where the cooling zone of the steam-air mixture is wider (for example, with low values of t_1 or D_k), than under operating conditions where the zone of intensive steam condensation predominates. This is borne out satisfactorily by the experimental data plotted in Fig. 17, showing that under certain conditions the mean coefficient of heat transfer $\bar{K}$ may even rise as $\underline{w}$ falls. The theoretical and experimental data likewise enable us to state that the effect of water velocity upon $\bar{K}$ is diminished when the cooling surface is fouled.

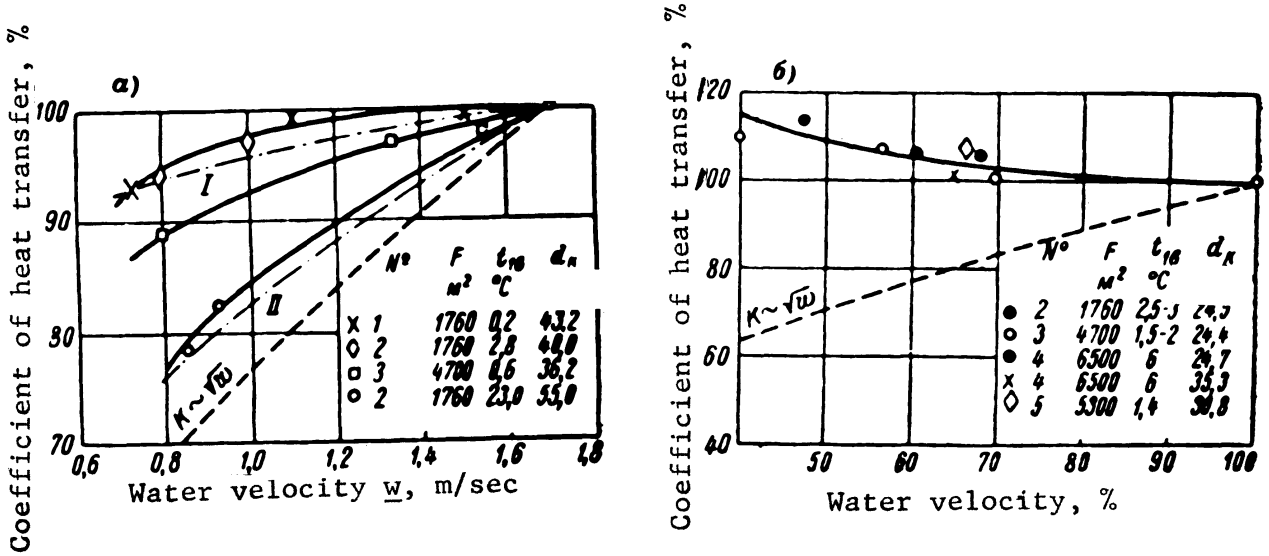

Fig. 17. Coefficient of heat transfer as a function of the velocity of cooling water in tubes.

I - From Eq. (26) at $t_{1в} = 0.6^{\circ}C$ and $a = 0.8$; II - the same at $t_{1в} = 23^{\circ}C$ and $a = 0.7$.

If the change in the water velocity is due to change in the number of times the water passes through the condenser rather than a change in its consumption, the change in $\bar{K}$, the mean coefficient of heat trans-

fer, should be different. This follows from the fact that when the number of water passes is changed, while its overall consumption remains the same, the rise in water temperature remains the same, and a different distribution of the local values of α_n, K, and q is established, which will then correspond to a different value of the mean coefficient of heat transfer. The influence of the number of water passes upon the magnitude of the mean coefficient of heat transfer is confirmed by experimental data (Fig. 18), though not one of the equations proposed for $\bar{K}$ makes allowance for it.

Major discrepancies are found in the estimates of the influence of the temperature of the cooling water and the condenser steam load upon the mean coefficient of heat transfer.

It therefore became practically necessary to review the variation of the mean coefficient of heat transfer with various factors determining the condenser operating conditions. In so doing we must be guided by the concepts set forth above concerning the condenser's operating process, which enable us to uncover errors made previously, which were subsequently borne out by an analysis of the available experimental data.

The equation given below, in the derivation of which we use the results of tests made in the All-Union Heat Engineering Institute and other organizations, is the first attempt to allow, even though partially, for the interrelationship of the effects of various parameters on the condenser's coefficient of heat transfer.

The formula proposed, applicable to contemporary condenser designs, is as follows:*

$$K=3500\left(\frac{1{,}1\ w}{\sqrt[4]{d_{вн}}}\right)^{x}\left[1-\frac{0{,}42\sqrt{a}}{1000}(35-t_{1в})^{2}\right]\Phi_z\Phi_\delta, \tag{26}$$

where

$$x=0.12\,a(1+0.15\,t_{1в}).$$

Here:

a = coefficient of cleanliness, allowing for the effect of fouling of the cooling surface.
w = velocity of water in the tubes, m/sec.
$d_{вн}$ = inside diameter of the tube, mm.
$t_{1в}$ = cooling water temperature at the inlet to the condenser, $^{\circ}$ C.
Φ_z = a factor allowing for the influence of the number of water passes through the condenser.
Φ_δ = factor allowing for the influence of the condenser's steam load.

Equation (26) is applicable to condensers with brass tubes at $t_{1в} \leqslant 35^{\circ}$ C, a cooling water velocity of 0.9 - 3 m/sec, and satisfactory airtightness of the equipment. The coefficient of heat transfer refers to the external (steam) surface of the tubes.

---

* For simplicity we shall henceforth omit the line above the letter used to denote the mean coefficient of heat transfer.

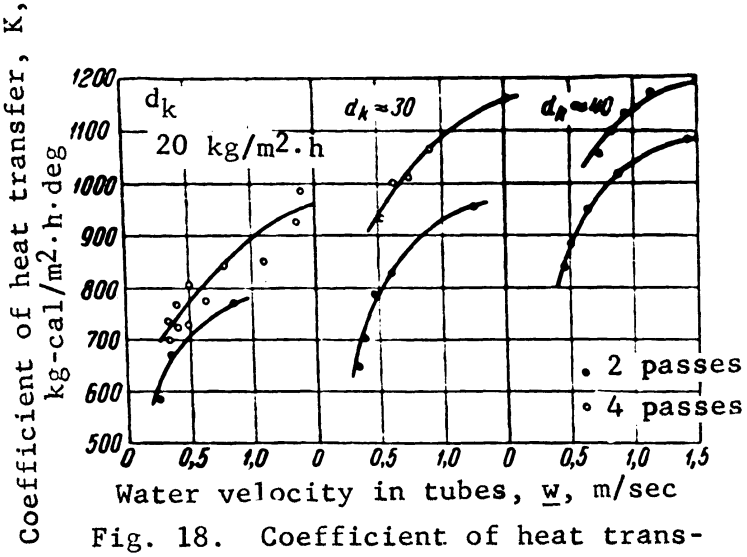

Fig. 18. Coefficient of heat transfer for different numbers of water passes through the condenser.

Strictly speaking, the equation for K is even more complicated and, in particular, if we consider an empirical equation such as Eq. (26), the steam load on the condenser also affects the magnitude of the exponent x and the term within brackets. However, it has been impossible to make allowance for this so far, because of the absence of adequate experimental data.

The value of the coefficient of heat transfer corresponding to $a = 1$ is observed in practice only in isolated cases, when testing new condensers shortly after the equipment has been placed in service. Under ordinary operating conditions the coefficient a is always less than unity and may have the following values, depending upon the local conditions:

For direct-flow water supply and pure water.... $a = 0.80\text{-}0.85$
For circulating water supply and adequate scavenging of the system or chemical treatment of the water..... $a = 0.75\text{-}0.80$
For dirty water and the possibility that mineral or organic deposits may be formed..... $a = 0.65\text{-}0.75$

In calculation, a may be taken equal to 0.80-0.85 as a rule, this value being lowered only when the operating conditions of the condenser are unfavorable.

The experimental data at our disposal are insufficient for an exact quantitative estimate of the influence of the number of water passes on the coefficient of heat transfer. As a first approximation, based on the available sparse experimental data, we may assume that:

$$\Phi_z = 1 + \frac{z-2}{10}\left(1 - \frac{t_{1в}}{35}\right), \qquad (27)$$

where $\underline{z}$ = number of water passes through the condenser.

A change in the condenser's steam load ordinarily has but little effect on the value of the coefficient of heat transfer, provided the amount of air passing through it is small and remains practically constant as the steam load changes /Ref. 3/. The steam load is found to have a more perceptible influence on $\underline{K}$ in these cases only at the lowest temperature of the cooling water. In the overwhelming majority of cases, however, a drop in the steam load of the given condenser is accompanied by an increase in the quantity of air entering, which causes a decrease in the coefficient of heat transfer that becomes more pronounced the lower the temperature of the cooling water then is. But an increase in G_{β}, the entering air, related to the extension of the vacuum zone within the turbine, is governed, as a matter of fact, not by the load on the condenser but by D_k, the amount of steam flowing through the low-pressure part of the turbine, as well as by the design features and the condition of the given equipment (the turbine itself and the part of the regenerative equipment connected to the vacuum zone). That is why the relationship $G_{\beta}=f(D_{\kappa})$, and hence $K=f(D_{\kappa})$ proves to be different for each installation.

On the basis of the results of experiments performed on installations whose condition may be evaluated as comparatively satisfactory, we may set forth the following instructions for a preliminary determination of the factor

Within the limits of the change of $d_{\kappa}=\frac{D_{\kappa}}{F}$, the condenser's specific steam load, from the nominal $d_{\kappa}^{ном}$ to $d_{\kappa}^{гр}=\delta_{гр}d_{\kappa}^{ном}$ where,

$$\delta_{гр}=0{,}9-0{,}012t_{1в}, \tag{28}$$

we may assume that $\Phi_{\delta}=1$.

When $d_k < d_k^{гр}$ we can determine Φ_{δ} from the equation:

$$\Phi_{\delta}=\delta(2-\delta), \tag{29}$$

where

$$\delta=\frac{d_{\kappa}}{d_{\kappa}^{гр}}.$$

The values of the coefficient of heat transfer obtained from Eq. (26) for a two-pass condenser at α = 0.80 and nominal steam load are given in Fig. 19. When $\underline{z}$, the number of water passes, is not equal to 2 and the condenser is only partially loaded, the values of $\underline{K}$ given in Fig. 19 must be multiplied by the correction coefficients Φ_z and Φ_{δ}, determined with the aid of Eqs. (27) and (29).

In the literature we find remarks concerning a possible change in the condenser's coefficient of heat transfer when steel tubes are used instead of brass ones. On the basis of several experiments involving the condensation of pure steam on single tubes made of carbon steel and yielding a diminution of the coefficient of heat transfer amounting to 30-35%, compared to brass tubes, the recommendation is sometimes made that a simi-

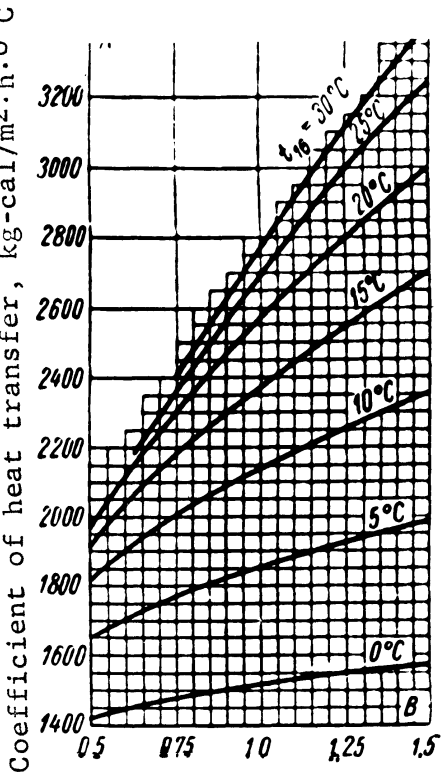

Fig. 19. Coefficient of heat transfer of a condenser as a function of $B = \frac{1{,}1w}{\sqrt[4]{d_{вн}}}$ and of the temperature of the cooling water for z = 2 (nominal load).

lar reduction in the mean coefficient of heat transfer be employed for industrial condensers. These recommendations, however, do not make allowance for the specific features of the heat-exchange conditions in condensers discussed above, as a result of which the indicated diminution in the coefficient of heat transfer, if it be considered correct, may be applied only to tubes located at the steam inlet end of the tube bank. For tubes located at the outlet end of the bank, where the supplementary thermal resistance due to the lower thermal conductivity of the walls, the presence of a layer of oxides, and, in part, the decrease in the local values of the coefficient of heat transfer will likewise be much less, about 5-6% on the average. The diminution in the mean coefficient of heat transfer then amounts to some 17-20%, varying with different operating conditions of the condenser.

The following must then also be borne in mind. This decrease in the coefficient of heat transfer is not the ultimate value for tubes made of ordinary carbon steel. As these tubes are progressively oxidized, the coefficient of heat transfer continues to fall. Partially

for that reason, but mainly because of their rapid destruction by corrosion, tubes made of carbon steel are not suitable for use in condensers. And when we speak of the use of tubes made of stainless steel, Type Ж-1 or Ж-2, assuming fresh cooling water, the results even of experiments run with new tubes made of carbon steel, which have an oxide film that perceptibly affects the rate of heat exchange even when they arrive from the warehouse, cannot be applied to these stainless steel tubes. The lower thermal conductivity of chrome steel (of the order of 23 kg-cal/m·h·degree) is counterbalanced in this case by the condition of its surface, which is better from the standpoint of heat-exchange condition, and this is important. Special experiments must then be run to determine the decrease in the coefficient of heat transfer of the condenser compared to the use of brass tubes.

In conclusion, let us also point out that the conditions of heat exchange within condensers of steam prime movers, the usual large dimensions of this equipment, dictated by the amount of steam to be condensed, and the conditions of their arrangement and operation present a series of specific requirements for the design of the cooling surface of condensers that do not arise in the design of other heat-exchange equipment. This aspect of the problem, which is likewise of considerable practical importance, has been discussed by the author in other papers /Ref. 3, h, i/.

9. CONCLUSIONS

The process of heat exchange in surface condensers of steam prime movers is characterized by several fundamental features, due mainly to the fact that the condensation of steam is effected in these condensers at low absolute pressures (vacuum) and in the presence of air. The rate of steam condensation as well as the rate of heat exchange between the steam and the cooling water then prove to be dependent, first of all, on the rate of transfer of the substance (steam) to the condensing surface and, second, to diminish sharply as the steam-air mixture passes through the tube bank of the condenser.

An extremely important fundamental feature of the conditions of heat exchange in the condensers of steam prime movers is the dependence of the distribution of the process parameters and of the local values of the coefficient of heat transfer along the path of the steam-air mixture upon the operation of the air-removal equipment. As a result, the characteristics of the air-removal equipment essentially influence the "external" indices of condenser operation, including the condenser's mean coefficient of heat transfer.

The theoretical and experimental research we have carried out have enabled us to define our concepts of the operating process in condensers and to infer several practical conclusions pertaining to their thermal calculation, design, and operation. This research must be continued, however, to secure a sufficiently rigorous method for the thermal calculation of condensers.

LITERATURE CITED

1. S. S. Kutateladze. Heat Transfer in Condensation and Boiling.

State Scientific and Technical Publishing House of Machinery Literature, 1949, 1952.

2. D. A. Frank-Kamenetsky. Heat Transfer and Diffusion in Chemical Kinetics. USSR Academy of Sciences Press, 1947.

3. L. D. Berman, a) Bull. All-Union Heat Engineeering Institute VTI, No. 7, 1947; b) ibid, No. 1, 1948; c) Oxygen, No. 3, 1948; d) Bull. VTI, No. 8, 1947; e) Bull. VTI, No. 5, 1947; f) For Fuel Economy, No. 12, 1947; g) Central Stations, No. 1, 1947; h) Bull. VTI, No. 6, 1948; i) For Fuel Economy, No. 3, 1952.

4. V. A. Gudemchuk, Vull. VTI, No. 12, 1935.

5. V. A. Gudemchuk, Thermal Power Economy, No. 4-5, 1938.

6. V. P. Blyudov, Condensing Equipment of Steam Turbines. State Power Engineering Press, 1951.

7. F. Merkel. Principles of Heat Transfer. State Publishing House, 1929.

8. A. M. Kazansky. Condensing Equipment. Power Engineering Press, 1939.

9. M. I. Yanovsky. Marine Condensing Installations. Navy Press, 1943.

10. G. A. Murin, For Fuel Economy, No. 9, 1950.

11. J. Othmer, Ind. Eng. Chem., No. 6, 1929.

12. E. Langen, Forschung, No. 10, 1931.

13. A. Colborn, Trans. Am. Inst. Chem. Eng., 29, 1933.

14. R. Ferguson and J. Oakden, Proceedings of the London Chemical Engineering Congress, No. 144, 1936.

INVESTIGATION OF HEAT EXCHANGE IN THE CONDENSATION OF THE VAPORS OF SOME REFRIGERANTS

I. V. Mazyukevich, Candidate of Engineering Sciences

Leningrad Institute of the Refrigeration and Dairy Industries

1. INTRODUCTION

The almost total absence of experimental material on heat exchange in the operation of refrigerating machinery made research into the processes involved in the condensation of refrigerants an urgent matter.

The conditions of condensation of refrigerant vapors in the condenser of a refrigerating machine often differ considerably from the ordinary. Thus, the vapor of the refrigerant may contain air and traces of lubricating oil in drop form upon leaving the compressor. The presence of oil drops, which cannot be eliminated completely in the oil separator, fourls the heat-transfer surface, facilitating the development of dropwise condensation. The presence of air in the condensing vapor of the refrigerant changes the process considerably, diminishing the magnitude of the coefficient of heat transfer.

In the present research we have investigated:

1) The process of condensation of saturated ammonia vapor on a clean, polished vertical surface, on a degreased corroded surface, and on a corroded surface covered with a film of oil.

2) The process of condensation of dichlorodifluoromethane (Freon-12) on a clean vertical surface.

3) The process of condensation of ammonia vapor mixed with inert impurities* on a clean vertical surface.

2. DESCRIPTION OF THE EXPERIMENTAL APPARATUS

The experimental apparatus is shown schematically in Fig. 1.

The vapor of the refrigerant, formed in the evaporator a, passed through the pipe line б to the condenser в via the inlet in the lower or upper flange. The valve д was closed when investigating the condensation of pure refrigerant vapor, as well as when investigating the condensation of ammonia vapor mixed with hydrogen. In these cases the vapor from the evaporator entered the top of the condenser, insuring satisfactory mixing with the vapor-hydrogen mixture there. When investigating the condensation of ammonia vapor mixed with water, the valve was closed. In that case the vapor entered the lower part of the condenser, thus preventing layering of the steam-air mixture in the steam zone of the condenser. The condensate produced in the condenser flowed down by gravity through the pipe line г to the bottom of the evaporator,

---

Henceforth the term "inert impurities" is understood to mean impurities of gas that do not condense in the given temperature range.

where it was mixed with the boiling liquid agent. Thus we insured continuous circulation of the working substance in the apparatus.

The pressure in the system remains constant as long as the amount of heat supplied to the evaporator equaled the amount of heat drawn off in the condenser.

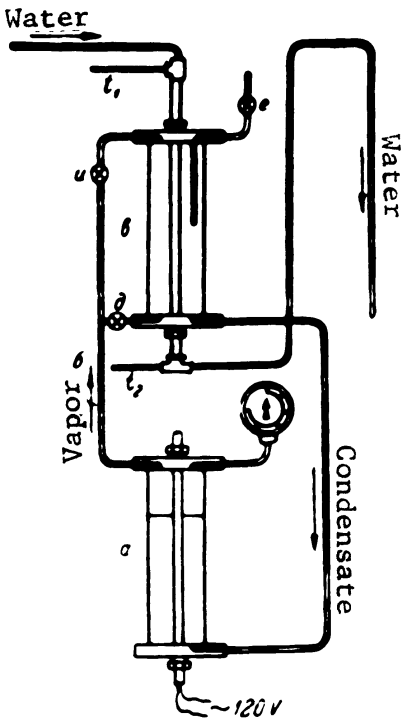

Fig. 1. Diagram of the experimental apparatus.

The vapor produced in the evaporator passed through a hole drilled in the top flange. A pressure gage graduated to 0.1 atmosphere was attached to another hole in the flange. The condensate entered the evaporator through a hole drilled in the bottom flange.

The heat flow was established by the output of the electric heater inserted in the evaporator and serving to evaporate the liquid agent. The flows in the evaporator and the condenser were made equal by keeping the condensation temperature equal to that of the air surrounding the experimental apparatus. The place where samples were taken from the condenser for chemical analysis of the vapor-gas mixture to determine the amount of gas it contained was located at the center of the vapor space, close to the hot junction of a thermocouple that measured the temperature of the vapor medium. The vapor-gas mixture was taken from the condenser for analysis by means of a fine-regulation valve e, attached to the top flange of the condenser. The condenser was cooled by running tap water, whose temperature before and after the condenser was measured by the thermometers t_1 and t_2 to within 0.1° C.

The temperature difference between the vapor and the wall was mea-

sured directly by means of thermocouples connected in a potentiometer circuit.

The thermocouple junctions were always soldered, so as to distort the surface of the tube by a negligible amount. The thermocouple junctions were located at the middle of the tube.

The temperature of the vapor medium was likewise determined by means of a thermocouple. The hot junction of this thermocouple was placed directly in the vapor space of the condenser opposite the point where the surface thermocouple was soldered.

3. INVESTIGATION OF HEAT EXCHANGE IN THE CONDENSATION OF PURE, DRY, SATURATED AMMONIA VAPOR

This research was done at condensation pressures of 9.0, 10.5, and 12.1 atmospheres absolute on a polished vertical surface with thermocouples sealed into the wall of the experimental tube. The temperature of the heat-transfer surface was measured, allowing for the thermal resistance of the layer of the tube wall from the place where the hot junction of the thermocouple was located to its outer surface.

In our research we found that the condensing ammonia vapor forms a continuous film of condensate on the cooling surface.

In view of the fact that condensation was filmwise, the temperature of the wall of the vertical tube varied with height, remaining constant around the perimeter at any given cross section.

Owing to the uniform change of thickness of the film of condensate, the temperature of the surface, measured halfway up the tube, may be regarded as the mean temperature over the entire length of the experimental tube.*

The following notation will be used:

t_k = condensation temperature, $^\circ$ C.

p_k = absolute condensation pressure, atmospheres absolute.

t_{cm} = temperature of cooling surface, $^\circ$ C.

$\Delta t = t_k - t_{cm}$ = temperature difference between vapor and wall, $^\circ$ C.

q = density of heat flow, kg-cal/$m^2 \cdot h$.

$$q = \frac{Q}{F}$$

Q = quantity of heat, kg-cal/h.

F = area of cooling surface according to the outside diameter, m^2.

* This assertion of the author's is not entirely correct, but it closely corresponds to actuality under the conditions of his experiments.-Editor's Note

α = coefficient of heat transfer from the condensing vapor to the surface, kg-cal/m^2·h·degree; $\alpha = \frac{q}{t}$.

A given temperature difference between the vapor and the wall corresponds to a fixed heat flow through the surface of the condenser. Rigorous correspondence between the temperature difference and the heat flow is independent of the cooling conditions of the heat-transfer surface. In fact, in running the experiments the same value of heat flow was achieved by varying the velocity and the initial temperature of the cooling water over a wide range.

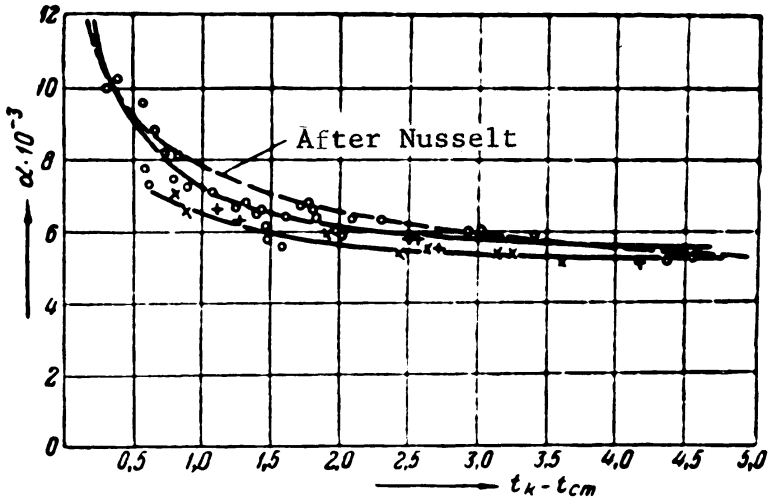

Fig. 2. Coefficient of heat transfer in the condensation of saturated ammonia vapor as a function of the temperature difference between the vapor and the wall for condensation pressures of 9.0 (denoted by o), 10.5 (denoted by X), and 12.1 (denoted by +) atmospheres absolute.

The variation of the coefficient of heat transfer in the condensation of saturated ammonia vapor with the temperature difference between the wall and the vapor is shown in Fig. 2 for condensation pressures of 9.0, 10.5, and 12.1 atmospheres absolute.

The figure indicates that the coefficient of heat transfer falls continuously from a value of approximately 11,000 to 5400 kg-cal/m^2·h·deg when the temperature difference is varied from 0.25° to 4.5° C.

The coefficient of heat transfer drops most sharply as the temperature difference is raised to 1.5° C, the coefficient of heat transfer diminishing comparatively little as the temperature difference is further increased to 4.5° C.

The experimental points obtained for pressures of 9.0, 10.5, and 12.1 atmospheres absolute lie very close to the curve plotted for the pressure 9.0 atmospheres absolute. But careful inspection will show that the coefficient of heat transfer diminishes somewhat as the condensation pressure increases.

The presence of a glass casing in the experimental condenser enabled us to observe the flow of the condensate film in all the experiments we ran. It was found that at low heat flows, up to 8500 kg-cal/$m^2 \cdot h$ inclusive, corresponding to a temperature difference of about 1.25° C, the film flows quite smoothly. The outer appearance of the experimental tube is then exactly as if it had been polished to a mirror finish throughout its length or covered with a coating of lacquer. As the heat flow is increased above 8500 kg-cal/$m^2 \cdot h$, the nature of film flow changes, as manifested in the appearance of minute waves on its surface. The waviness on the surface of the film during heat flows of the order of 9500-12,000 kg-cal/$m^2 \cdot h$ is observed along the lower section of the tube; as the heat flow is increased the starting point of a wave formation moves upward, and at a value of q above 14,500 kg-cal/$m^2 \cdot h$ waviness is found to exist along nearly the entire length of the tube.

In Fig. 2, we have also plotted a curve calculated from Nusselt's equation. The difference between the experimental results and the data calculated from Nusselt's equation is 5.4% throughout the range of temperature differences for the pressure of 9.0 atmospheres absolute.

At the same time as we investigated the condensation of ammonia vapor on a polished surface we ran a small number of tests on the condensation of ammonia vapor on a vertical tube whose surface was covered with a coat of rust. Some of the experiments were run on a corroded surface covered with a layer of oil. Our results are shown in Fig. 3. The values of the coefficients of heat transfer secured for a clean, polished surface are plotted in the same figure for the sake of comparing the effect of surface quality on the magnitude of the coefficient of heat transfer. As we see in the figure, the numerical values of the coefficients of heat transfer for a tube covered with a layer of rust are 22% below those for a clean, polished surface. It should be noted that the heat-insulating action of the layer of rust was ignored in calculating the temperature of the cooling surface. It was assumed that the entire thickness of the wall was homogeneous, with the same coefficient of thermal conductivity. The reason for the decrease in the values of the coefficients of heat transfer is that the rust layer possesses a high thermal resistance. Vapor condensation on the degreased corroded surface was always fimlwise.

These results agree with the observations of S. S. Kutateladze /Ref. 1/, on the condensation of steam.

The results of experiments on the condensation of ammonia vapor on a corroded surface with a layer of oil are plotted in Fig. 3.

The number of experiments run was unfortunately very limited, though the result is not without some interest. It was found that the presence of an oil layer on the heat-transfer surface produces dropwise condensation, which changes fairly rapidly into dropwise-filmwise condensation. Once the condensation process had reached the steady state, 50-70% of the heat-transfer surface was covered with a condensate film, with 30-40% co-

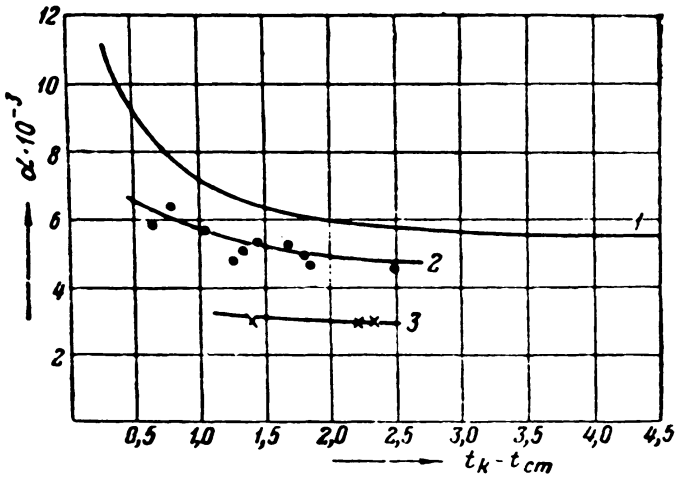

Fig. 3. The coefficient of heat transfer in the condensation of ammonia vapor as a function of the temperature difference between the vapor and the wall and of the state of the heat-transfer surface.
1 - Polished surface; 2 - degreased rusty surface; 3 - rusty surface covered with a coating of oil.

vered by areas of dropwise condensation.

The condensate drops formed were spaced very close together, while their mean diameter was of the order of 0.5-1.0 mm. The process as of drop formation, drop growth, and drop flow from the point of formation all took place very rapidly.

These experiments indicated a general decrease in the coefficients of heat transfer, compared to a degreased surface. Hence, notwithstanding the dropwise-filmwise nature of condensation, the rate of heat exchange does not increase, but, on the contrary, drops, due to the high thermal resistance of the oil layer.

Likewise of interest is the fact that the coefficient of heat transfer is practically independent of the temperature difference in these experiments. The reason for this is probably some slowing down of the rise in the temperature difference, produced by the break in the continuity of the condensate film.

4. INVESTIGATION OF HEAT EXCHANGE IN THE CONDENSATION OF DRY, SATURATED FREON-12 VAPOR

In the condensation of Freon-12 vapor, as in the condensation of ammonia vapor, we found that condensation was filmwise. Stable filmwise condensation was found in all the experiments we ran.

Observations of the flowing condensate film indicate a complete analogy with the movement of the film secured in the condensation of ammonia vapor.

The vapor-wall temperature gradient established in the condensation of Freon-12 vapor is about seven times as great as in the condensation of ammonia vapor under the same conditions.

The magnitude of the temperature difference is mainly due to the low coefficient of thermal conductivity of liquid Freon-12.

The variation of the coefficient of heat transfer in the condensation of saturated Freon-12 vapor with the vapor-wall temperature difference is shown in Fig. 4 for a condensation pressure of the order of 5 atmospheres absolute.

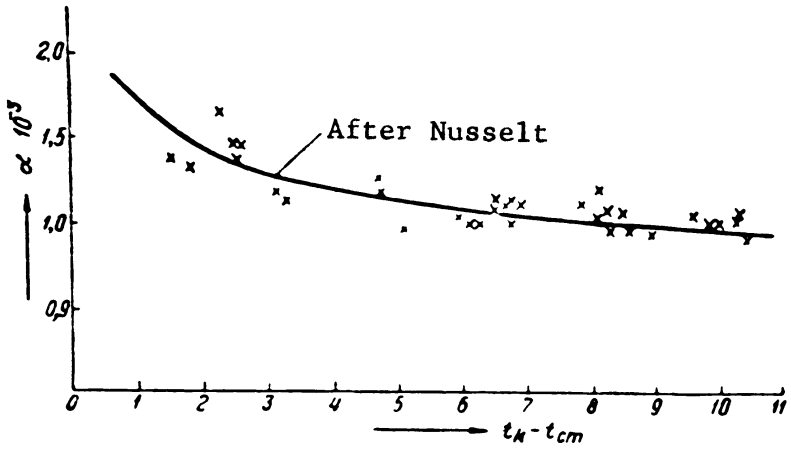

Fig. 4. Coefficient of heat transfer in the condensation of Freon-12 vapor as a function of the vapor-wall temperature difference for a condensation pressure of 5 atmospheres absolute.

The values of the coefficient of heat transfer in the condensation of Freon-12 vapor we obtained are not very accurate, since the thermocouples that measure the temperature of the surface were installed without inserting padding between the electrodes and the isothermal surface. As a result of the flow of heat through the thermocouple electrodes from the vapor to the hot junction, the vapor-wall temperature difference was found to be somewhat less than it actually was, and hence the value of the coefficients of heat transfer were somewhat higher.

5. INVESTIGATION OF HEAT EXCHANGE IN THE CONDENSATION OF AMMONIA VAPOR WITH AIR PRESENT

The problem of the condensation of vapor in the presence of noncondensable impurities is still unsolved today, notwithstanding the comparatively large number of investigations done in this field. The existing equations for calculating this process suggested by various authors are empirical ones and make no claim to wide applicability. The paper by L. D. Berman published in 1947 /Ref. 2/ furnishes an exhaustive analysis of the state of the problem.

The total absence of research papers on the condensation of the vapors of refrigerating agents in the presence of inert impurities makes this problem one of extremely great importance.

The operation of refrigerating machinery is usually accompanied by some suction of air into the compressor through leaks on the suction side. The compressed vapor of the refrigerant, together with an extremely minute amount of air, enters the condenser, where it condenses and then flows to the receiver. The air entering the condenser remains there and gradually accumulates, producing a vapor-air mixture with a high concentration of air. In practice it may be assumed that in the operation of the condenser the pure refrigerant vapor enters a vapor-air mixture, with which it is mixed, subsequently being condensed from the air mixture.

In our experiments a mixture of ammonia vapor and air was produced by feeding the latter into the experimental apparatus through the valve e (Fig. 1). After an air tank was connected to the apparatus, the valve e was opened, and enough air was admitted from the tank to the condenser, after which the valve was closed and the tank was disconnected. The quantity of air could be increased by repeating the operation described.

The quantity of air was diminished by opening the valve e, a certain quantity of the vapor-gas mixture leaving the condenser through the valve, thus reducing the concentration of air. During operation air accumulated in the condenser and, remaining there in a mixture with the ammonia vapor, produced a vapor-air mixture of constant concentration. There was no circulation of air through the system, which is borne out by the data of the chemical analysis of the vapor entering the condenser from the evaporator during operation.

During our investigation we observed the formation of fog in the vapor zone of the condenser under certain conditions, in the form of minute drops of liquid ammonia. The presence of these drops enabled us to see the movement of the medium filling the condenser. We noticed intense movement, accompanied by a displacement of particles throughout the volume of the condenser. This motion was caused by the stream of fresh vapor continuously entering through the inlet at the bottom of the condenser. The intensity of movement diminished with a decrease in the condenser's thermal load, though it remained appreciable even at the lowest loads employed during our experiments. The existence of such intense displacement enables us to assume that concentration and temperature of the vapor-air mixture were identical throughout the condenser.

The vapor-air mixture was analyzed by the volumetric method, the

ammonia vapor being absorbed by an acid solution.

All the investigations were conducted at as identical a temperature of the vapor-air medium, t_k, henceforth called the condensation temperature, as possible. It was found that the condensation temperature was always somewhat below the temperature of the surrounding medium. The difference between the temperature of the surrounding medium (i.e. the air in the laboratory) and the temperature of condensation attained a maximum of 2.5-2.0° C, as a result of which the inflow of heat was negligible and could be neglected without diminishing the accuracy of the experiment appreciably in any way.

The experimental data are presented as a function of the volumetric percentage of air in the vapor-air medium.

An increase in the vapor-wall temperature difference is found both when the thermal flow is increased while keeping the composition of the mixture constant and when the concentration of air is increased while keeping the magnitude of thermal flow constant. It is apparent that when the magnitude of thermal flow is the same, the temperature difference increases with an increase in the concentration of air as a result of the retarding effect of the air on the condensation process.

The variation of the coefficient of heat transfer in the condensation of ammonia vapor with the magnitude of heat flow is shown in Fig. 5 for different concentrations of air in the vapor-air mixture.

The function obtained proves to be nonuniform for different concentrations. When the mixture contains little air the usual function is obtained, the coefficient of heat transfer diminishing as the flow of heat increases. At high air concentrations, on the other hand, we find the coefficient of heat transfer rising as the flow of heat rises.

It also follows from the figure that the rate of change of the coefficient of heat transfer diminishes with an increase in the condenser's thermal load for the entire range of air concentrations investigated.

The vapor-wall temperature difference, from which the values of the coefficient of heat transfer were calculated, includes the temperature difference at the boundaries of the condensate film and the temperature difference between the outer surface of the film and the vapor-air mixture.

It is therefore more convenient to consider the experimental material by comparing the values of the coefficients of heat transfer secured at identical values of thermal flow but at different compositions of the vapor-gas mixture. It is evident that when the flow of heat remains constant the thickness of the condensate film ought to be the same. Hence, the temperature differences at the boundaries of the film likewise ought to be the same. Thus, the difference $\Delta t - \Delta t_0$ (where Δt_0 is the temperature difference at the boundaries of the film or the vapor-wall temperature difference for pure ammonia, while Δt is the vapor-wall temperature difference in the condensation of vapor from a vapor-air mixture) will be an index of the magnitude of the difference between the partial pressures governing the diffusion of vapor in the direction of the condensate film.

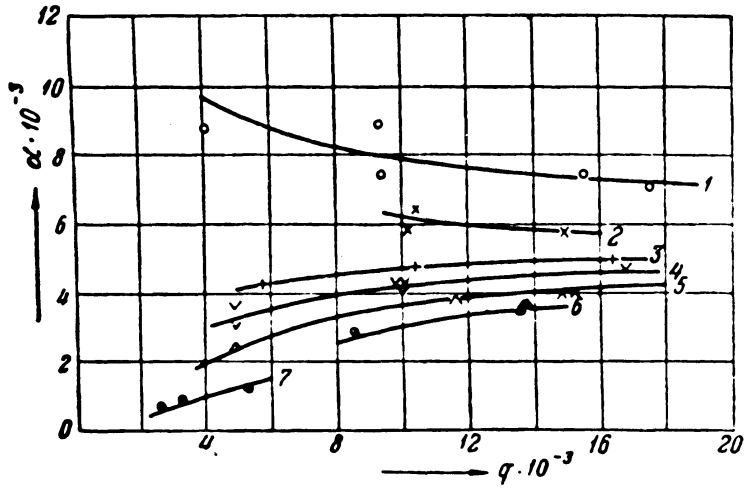

Fig. 5. Variation of the coefficient of heat transfer with the thermal load in the condensation of ammonia vapor from a mixture containing air.

1 - Pure vapor
2 - Mixture containing 1.75% air
3 - " " 5.5% "
4 - " " 7.2% "
5 - Mixture containing 11.7% air
6 - " " 17% "
7 - " " 34.1% "

The variation of the coefficient of heat transfer with the vapor-wall temperature difference for constant thermal flow and varying composition of the vapor-air mixture is given in Fig. 6.

The figure shows that an increasing temperature difference between the vapor and wall corresponds to a decrease in the coefficients of heat rejection for all the thermal flows investigated. At the same time we may point out that the rate at which the coefficient of heat transfer diminishes slows down as the thermal flow increases.

The results of these experiments can be employed for practical purposes under conditions similar to the experimental conditions. In the given case we have in mind vertical condensers of an ammonia refrigerating machine.

The results of the experiments are satisfactorily described by the following empirical formulas, which are applicable to an ammonia-air mixture containing up to 17 volume percent of air:

1) For q = 5000 kg-cal/m^2·h: $\alpha = \frac{\alpha_0}{1 + 0{,}4\varepsilon^{0{,}8}}$;

2) For q = 10,000 kg-cal/m^2· h: $\alpha = \frac{\alpha_0}{1 + 0{,}22\varepsilon^{0{,}7}}$;

3) For q = 15,000 kg-cal/m^2·h: $\alpha = \frac{\alpha_0}{1 + 0{,}15\varepsilon^{0{,}7}}$.

Here α = coefficient of heat transfer for condensation from a vapor-

air mixture.

α_0 = coefficient of heat transfer in the condensation of pure vapor.

ε = air content in volume percent.

The experimental curves should be used in determining the value of the coefficients of heat transfer for thermal flows that differ from those indicated.

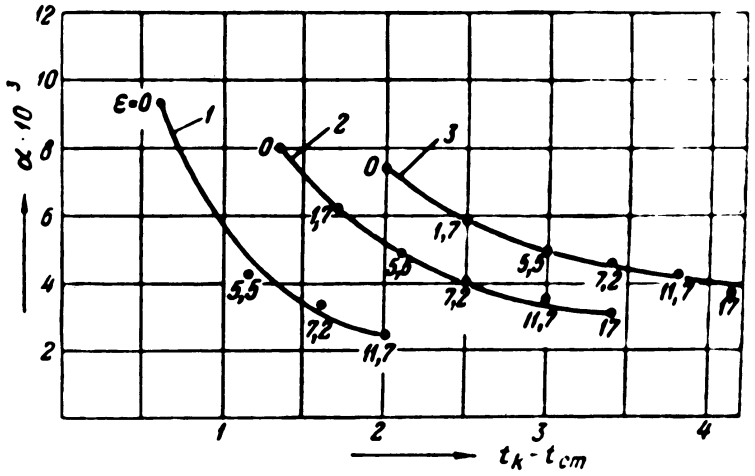

Fig. 6. Variation of the coefficient of heat transfer with the vapor-wall temperature difference for constant thermal loads and varying composition of the vapor-air mixture.
1 - For q = 5000 kg-cal/m^2·h; 2 - for q = = 10,000 kg-cal/m^2·h; 3 - for q = 15,000 kg-cal/m^2·h. The numbers at the dots represent the percentage of air.

6. INVESTIGATION OF HEAT EXCHANGE IN THE CONDENSATION OF AMMONIA VAPOR IN THE PRESENCE OF HYDROGEN

This investigation was conducted to determine the extent of the influence exerted by the physical properties of inert constituents upon the condensation process. In this respect hydrogen is the most suitable gas, especially since the condensation of ammonia vapor from an ammonia-hydrogen mixture does take place in some absorption refrigerating machinery.

The variation of the coefficient of heat transfer with the magnitude of thermal flow in the condensation of ammonia vapor at various concentrations of hydrogen in the vapor-gas mixture is shown in Fig. 7. It follows from the figure that an increase in the flow of heat corres-

ponds to a decrease in the numerical value of the coefficients of heat transfer throughout the range of concentrations investigated. Moreover, the rate of change of the coefficient of heat rejection diminishes as the percentage of hydrogen in the mixture increases.

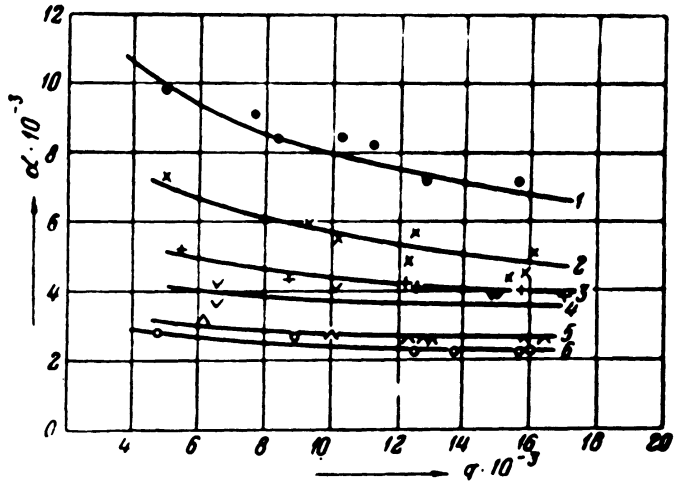

Fig. 7. Variation of the coefficient of heat transfer with thermal load in the condensation of ammonia vapor from a mixture containing hydrogen.

1 - Pure vapor
2 - Mixture containing 4.8% hydrogen
3 - " " 11% "
4 - Mixture containing 13% hydrogen
5 - " " 26.4% "
6 - " " 32.8% "

This phenomenon can be explained by considering the change of the corresponding temperature differences. It is found that when ammonia vapor is condensed from the vapor-hydrogen mixture, the resultant temperature difference between the vapor and the wall for a constant concentration changes with an increase in the thermal flow more intensively than when condensation is effected from a vapor-air mixture. What is more, the overall temperature gradient between the vapor and the wall consists approximately of two equal temperature differences in the condensate film and in the vapor-gas mixture

The variation of the coefficient of heat transfer with the temperature differences between vapor and wall is shown in Fig. 8 for thermal flows of 5000, 10,000, and 15,000 kg-cal/m^2·h and various composition of the vapor-hydrogen mixture. On the same curve we have plotted points corresponding to the condensation of ammonia vapor from a vapor-air mixture. As we see, the points fit the resultant curve satisfactorily. It is found, however, that the retarding effect of air on the condensation process is much greater than that of hydrogen at low thermal flows ($q = 5000$). Thus, at a temperature difference of 1.2° C the numerical value of the coefficient of heat transfer, 4000 kg-cal/m^2·h·degree, corresponds to an air concentration of 5.5% and a hydrogen concentration

of 13%.

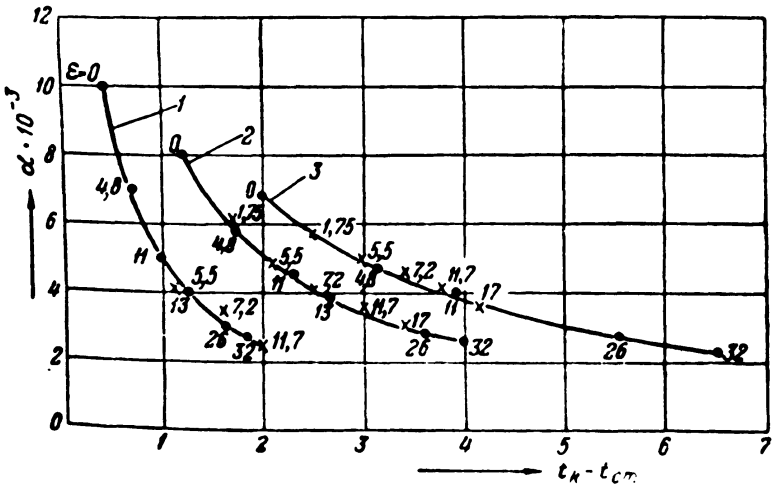

Fig. 8. Variation of the coefficient of heat transfer with the temperature differences between vapor and wall in the condensation of ammonia vapor for constant thermal loads and varying composition of the vapor-air and vapor-hydrogen mixtures. 1 - For q = 5000 kg-cal/m^2·h; 2 - for q = 10,000 kg-cal/m^2·h; 3 - for q = 15,000 kg-cal/m^2·h. The experimental data for the vapor-hydrogen mixture are indicated by dots, the experimental data for the vapor-air mixture by crosses.

As the thermal flow increases we find this difference diminishing. For example, at a temperature difference of 2.5° C and a thermal flow of 10,000 kg-cal/m^2·h the air concentration is 7.2% and the hydrogen concentration is 13% for a coefficient of heat transfer of 4000 kg-cal/m^2·h·degree. When the heat flow is 15,000 kg-cal/m^2·h, the experimental data indicates that hydrogen offers a greater obstacle to the condensation process than does air.

The empirical equations, which hold for concentrations of hydrogen in the mixture up to 33% by volume, may be employed in the practical use of the experimental results of the condensation of ammonia vapor from ammonia-hydrogen mixture:

For q = 5000 kg-cal/m^2·h: $\alpha = \frac{\alpha_0}{1 + 0{,}12z^{0.9}}$;

For q = 10,000 kg-cal/m^2·h: $\alpha = \frac{\alpha_0}{1 + 0{,}12\varepsilon^{0{,}83}}$;

For q = 15,000 kg-cal/m^2· h: $\alpha = \frac{\alpha_0}{1 + 0{,}2\varepsilon^{0{,}68}}$.

Here ε is the hydrogen content of the mixture, expressed in percent by volume.

7. INVESTIGATION OF HEAT EXCHANGE IN THE CONDENSATION OF AMMONIA VAPOR IN THE PRESENCE OF METHANE

The results of the experiments on the condensation of ammonia vapor from mixtures with air and with hydrogen have shown that the process of heat transfer proceeds differently in these two cases, namely: the coefficient of heat transfer rises with an increase in the thermal load in the condensation of ammonia from a vapor-air mixture and decreases in the condensation of ammonia from a vapor-air mixture and decreases in the condensation of ammonia from a vapor-hydrogen mixture.

After we discovered this phenomenon we investigated the process of heat transfer in the condensation of ammonia from a vapor-methane mixture, i.e. a mixture with approximately the same values of the molecular weights of the components of the mixture.

The variation of the coefficient of heat transfer with the specific thermal load for varying methane content in the mixture is shown in Fig. 9. The variation of the coefficient of heat transfer with the temperature difference between the vapor and the wall is shown in Fig. 10.

As we see, when the concentration of methane in the vapor-methane mixture is kept constant and not less than 4% by volume, the values of the coefficients of heat transfer remain practically constant and do not change as the thermal load or the vapor-wall temperature difference are varied.

The decrease in the coefficient of heat transfer becomes perceptible with an increase in load when the methane content of the mixture is less than 4%.

Thus, the nature of the variation of the coefficient of heat transfer with specific load in the condensation of ammonia vapor from a vapor-methane mixture differs from the corresponding functions secured for condensation from a vapor-air and a vapor-hydrogen mixture.

Further examination of the experimental material indicates that the addition of an admixture of air, hydrogen, or methane exerts the greatest influence on the process of ammonia condensation when their concentrations are below 12-15% by volume. The retardation of the condensation process is not as great for further increases in the percentage of inert admixtures. This is confirmed by the data reproduced in Figs. 11 and 12. It follows from this data that at low load (5000 kg-cal/m^2·h)

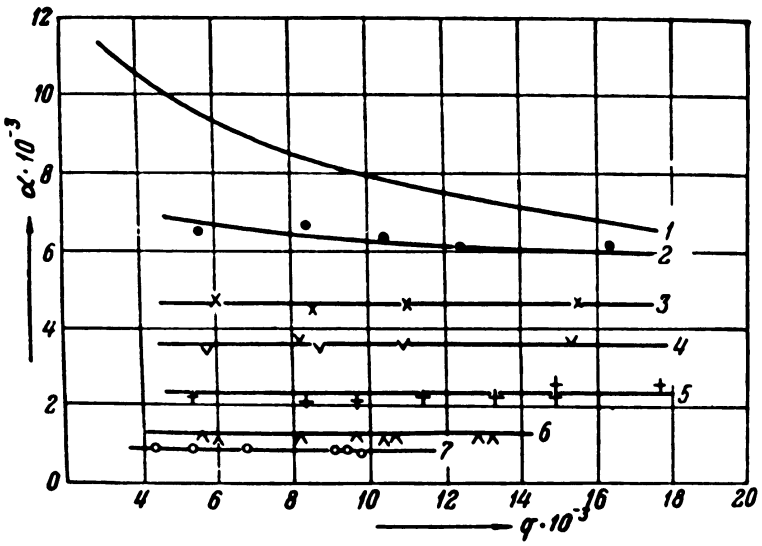

Fig. 9. Variation of the coefficient of heat transfer with thermal load in the condensation of ammonia vapor from a mixture containing methane.

1 - Pure vapor
2 - Mixture containing 2% methane
3 - " " 4.7% "
4 - " " 6.7% "
5 - Mixture containing 11.8% methane
6 - " " 20.5% "
7 - " " 31.1% "

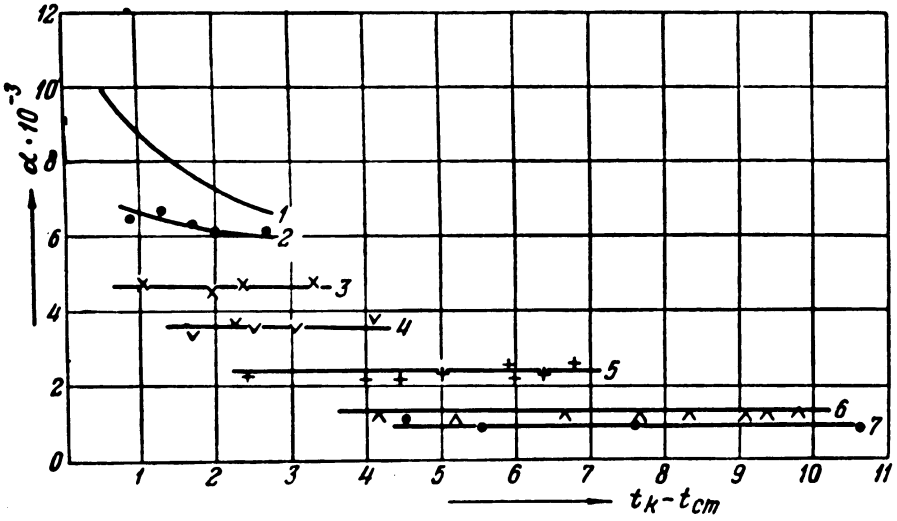

Fig. 10. Variation of the coefficient of heat transfer with the temperature difference between vapor and wall in the condensation of ammonia vapor from a mixture containing methane.

1 - Pure vapor
2 - Mixture containing 2% methane
3 - " " 4.7% "
4 - " " 6.7% "
5 - Mixture containing 11.8% methane
6 - " " 20.5% "
7 - " " 31.1% "

hydrogen has a much smaller effect in impairing heat exchange than air or methane.

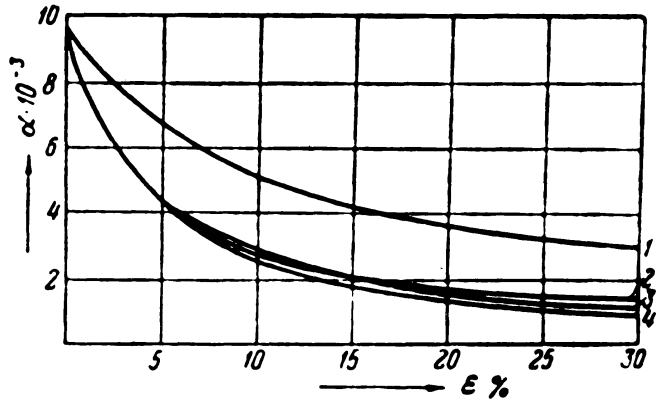

Fig. 11. Variation of the coefficient of heat transfer with the concentration of the vapor-gas mixture for a load of 5000 kg-cal/m^2·h.
1 - For a mixture containing hydrogen;
2 - for a mixture containing air;
3 - for a mixture containing ethylene;
4 - for a mixture containing methane.

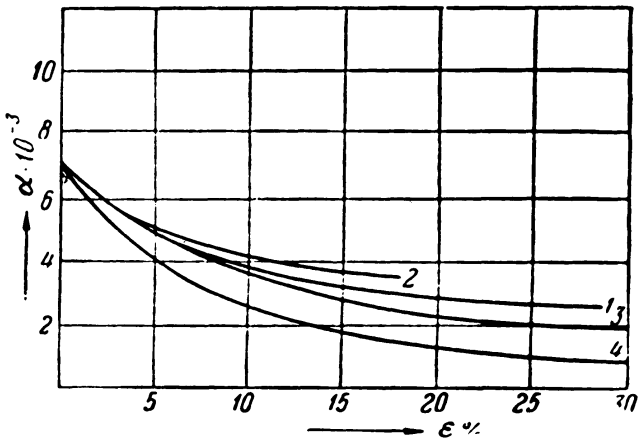

Fig. 12. Variation of the coefficient of heat transfer with the concentration of the vapor-gas mixture for a load of 15,000 kg-cal/m^2·h.
1 - For a mixture containing hydrogen;
2 - for a mixture containing air;
3 - for a mixture containing ethylene;
4 - for a mixture containing methane.

8. SOME CONSIDERATIONS ON THE MECHANISM OF THE PROCESS

Observations indicate that the vapor-gas mixture entering the condenser is in a state of fairly intense motion, which ceases in the immediate vicinity of the flowing film. Around the condensate film there is formed a vapor-gas layer, whose properties differ from those of the vapor-gas mixture in the rest of the condenser.

Because of the intensive motion of the vapor-gas mixture we may assume that the temperature and the concentration of this mixture remain constant throughout the volume of the condenser, both along the axis and radially, with the exception of the layer of mixture immediately surrounding the condensate film. The vapor-gas layer formed around the condensate film is characterized by motion in a definite direction, as well as by a change in the temperature and concentration of the mixture in cross section and along the length of the condenser.

The direction of motion and the thickness of the layer are governed by the interaction of the forces acting upon it. The principal forces acting on the layer will be: 1) an Archimedean force produced by the difference in the specific gravities of ammonia vapor and the noncondensable gas; 2) a frictional force arising at the boundary between the condensate film and the vapor-gas layer; 3) a frictional force within the vapor-gas layers; and 4) a force produced as the result of the radial motion of the particles of vapor and gas through the layer in the direction of the condensate film and of the motion, principally of gas particles, in an axial direction.

The composition of the vapor-gas mixture in this layer is characterized by a higher percentage of noncondensable gas than exists in the vapor-gas medium surrounding the layer.

The existence of the layer, the motion produced within it, and the increased percentage of noncondensable gas within the layer are all borne out by the experiments we ran. Thus, we observed a layering of the vapor-gas mixture during the process of condensation of ammonia vapor in the presence of air, when the vapor was introduced at the top of the condenser. In the lower portion of the condenser there collected a vapor-gas mixture, containing more air and having a lower temperature than the vapor-air mixture in the rest of the condenser. Furthermore, the condensation process is accompanied by the formation of a vapor-gas layer parallel to the condensate film. Within this vapor-gas layer there is set up a downward motion of the air particles. Layering of the vapor-gas mixture is likewise observed during the condensation of ammonia vapor in the presence of hydrogen, when the vapor is introduced at the bottom. A vapor-hydrogen mixture that contains a higher percentage of hydrogen than the rest of the mixture accumulates in the upper part of the condenser. Whereas the percentage of hydrogen in the principal part of the condenser (at the bottom) was 34%, the percentage of hydrogen in the sump (at the top) was 86%. The hydrogen particles in the vapor-gas layer moves upward, in a direction opposite to the motion of the condensate film.

It is probable that the direction of motion of the vapor-gas layer may be explained by the difference in the variation of the coefficients of heat transfer with thermal load during the condensation of ammonia vapor from a vapor-air, a vapor-hydrogen, and a vapor-methane mixture.

Inasmuch as the direction of motion is governed principally by the ratio of the specific gravities of the vapor and the noncondensable gas, it follows that the nature of this variation would be related to this ratio. As a matter of fact, if the molecular weight of the noncondensable gas is greater than the molecular weight of the vapor, as is the case with the ammonia-air mixture, we find the coefficients of heat transfer increasing with a rise in thermal load. If the molecular weight of the gas is lower than the molecular weight of the vapor, as is the case in the ammonia-hydrogen mixture, for example, the coefficient of heat transfer diminishes as the thermal load rises. If the molecular weight of the vapor and the gas are approximately the same (ammonia and methane), we find that the coefficients of heat transfer are practically independent of load.

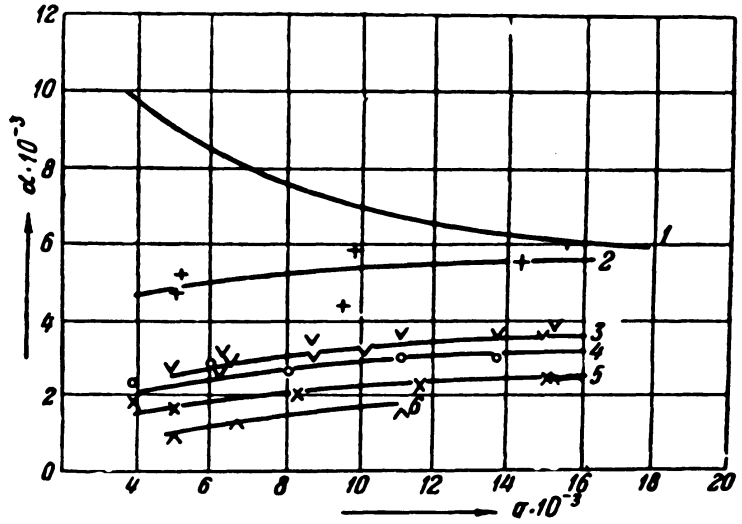

Fig. 13. Variation of the coefficient of heat rejection with thermal load in the condensation of ammonia vapor from a mixture containing ethylene.

1 - Pure vapor
2 - Mixture containing 3.95% ethylene
3 - " " 9.5% "
4 - Mixture containing 13.5% ethylene
5 - " " 20% "
6 - " " 30.5% "

This supposition is borne out by an investigation of heat exchange in the condensation of ammonia vapor in the presence of ethylene (C_2H_4), the results of which are given in Fig. 13. Ethylene has a molecular weight that is higher than that of ammonia and the variation of the coefficients of heat transfer with load is found to resemble that for a mixture of ammonia and air.

Heat transfer during condensation, in a process of this sort, is governed by the rate at which particles of vapor are supplied to the condensate film and the thermal resistance of that film. The rate at

which vapor particles are fed to the condensate film is governed by the thickness of the vapor-gas layer, their velocity of motion, the ability of the vapor particles to penetrate the layer, and the difference between the partial pressures of the vapor at the boundary of the condensate film and of the vapor-gas mixture in the principal zone of the condenser. The partial pressure at the boundary of the film is governed by the vapor tension at the temperature of the outer surface of the condensate film. When the composition of the vapor-gas mixture remains the same, and the load is varied, a change in the condensation process is governed mainly by the dynamics of the motion of the vapor-gas layer. At low loads, the velocity of motion of the outer surface of the condensate film is not high, so that the frictional force between the film and the vapor-gas layer is not great. The thickness of the vapor-gas layer is governed by the speed at which it moves, produced by the difference between the densities of vapor and gas in the layer.

As the load is increased, the speed at which the film moves rises, and the thickness of the vapor-gas layer is determined by the interaction of the functional forces at the interface, the forces produced by the differences between the densities, functional forces of a viscous nature, and the functional forces involved in the radial displacement of the vapor particles. It is possible that the thickness of the vapor-air layer ceases to grow in general, owing to its high velocity of movement downward under the action of film friction and difference of densities. The thickness of the vapor-hydrogen layer increases because its upward motion prevents an increase in the frictional forces at the interface and the frictional forces involved in the radial displacements of the vapor particles. The vapor-methane layer will be thickest of all because its movement is produced by the action of the frictional forces at the interface and extremely small difference of densities.

When the thermal load remains constant and the composition of the vapor-gas mixture varies, the condensation process will be governed by the forces produced by the difference of densities, the forces produced by radial displacement of the vapor particles, and forces of viscosity origin. The relationship between the active forces is such that the thickness of the vapor-gas layer increases with an increase of the percentage of noncondensable gas. The thickness of the layer rises rapidly as the gas content increases to 15% by volume. As the percentage of gas is raised further, the increase in the thickness of the layer slows down. It is probable that as the percentage of gas in the mixture increases the forces due to the difference in densities become the decisive factor.

9. SOME DATA ON THE COEFFICIENT OF MASS TRANSFER IN A VAPOR-GAS FILM

Using the measurement results obtained, we can determine the change in temperature at the boundaries of the vapor-gas layer with a certain degree of approximation, as well as the gradient of partial pressures. We know that in condensation of a pure vapor a given thermal load on the surface corresponds to a definite temperature difference between the vapor and the wall. Then, the resultant temperature difference is practically equal to the temperature difference at the boundary of the condensate film. The temperature difference between the vapor and wall that is established during the condensation of vapor from the vapor-gas mixture consists of two parts: 1) the temperature differences at the boundaries of the condensate film, and 2) the temperature differences

at the boundaries of the vapor-gas layer. The magnitude of the temperature difference in the vapor-gas layer may be found by deducting the temperature difference at the boundaries of the condensate film, known from the condensation of the pure vapor at the same thermal loads, from the total temperature difference between the vapor and the wall. In turn, the resultant temperature difference at the boundaries of the vapor-gas layer may be employed to determine the temperature at the outer surface of the condensate film by deducting the temperature difference at the boundaries of the vapor-gas layer from the temperature of the saturated core of flow. This is base on the assumption that the temperature at the outer boundary of the condensate film is the same as that at the inner boundary of the vapor-gas layer. The temperature found may be used to determine the partial pressure of the ammonia vapor at the boundary of the condensate film from the curve of vapor pressure and, consequently, the concentration of the vapor-gas mixture, using the measured total pressure for this purpose.

In Fig. 14 we have plotted the temperature differences in the vapor-gas layer ($t_{cond.} - t_{film}$) as a function of thermal load for vapor-air mixtures containing 5% and 15% of gas by volume, respectively.

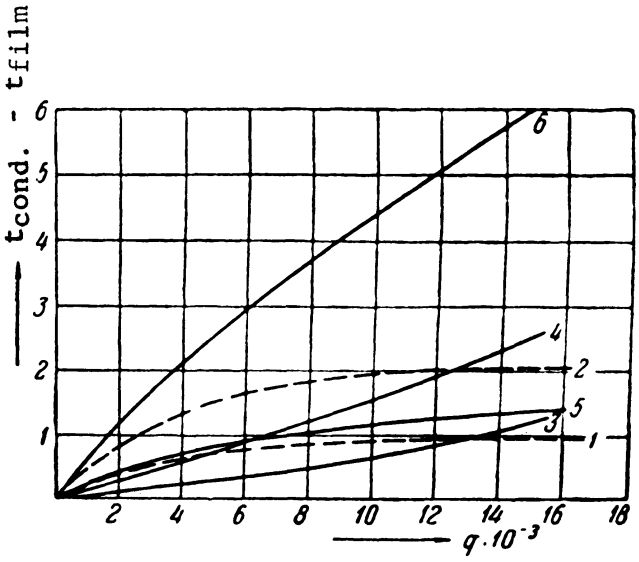

Fig. 14. Temperature difference in the vapor-gas layer as a function of thermal load with the mixture containing 5% and 15% of gas by volume.

1 - Ammonia plus air, ε = 5%
2 - " " ", ε = 15%
3 - " " hydrogen, ε = 5%
4 - Ammonia plus hydrogen, ε = 15%
5 - " " methane, ε = 5%
6 - " " " , ε = 15%

Examining the figure, we see that the results of calculation agree with the outline of the process set forth above.

The outline of the condensation process we have assumed enables us to process the experimental material in the form of an equation relating

the criteria of similitude.

The physical properties of substance in a diffusional process are characterized by the criterion:

$$Pr' = \frac{\nu}{D},$$

where ν = coefficient of kinematic viscosity for the vapor-gas mixture, m^2/sec.

D = diffusion coefficient, m^2/sec.

The motion in the vapor-gas layer, due mainly to the difference between the specific gravities of the vapor and the gas is characterized by the Archimedes number:

$$Ar = \frac{gl^3}{\nu^2} \frac{\gamma_г - \gamma_п}{\gamma_г},$$

where g = the acceleration dur to gravity, m/sec^2.

$\gamma_г$ = specific gravity of the gas, kg/m^3.

$\gamma_п$ = specific gravity of vapor, kg/m^3.

l = a characteristic dimension, m.

The interaction between the particles of the vapor diffusing toward the condensate film and the particles of gas moving along the condensate film must be characterized by an exchange of momentum.

The momentum of the flow of vapor per second equals MV, where we assume $M = \rho_п \frac{q}{r_s \gamma_п}$, the mass of vapor flowing per second, and

$V = \frac{q}{r_s \gamma_п} \cdot 2\pi Rl(1-\varepsilon_г)$, the nominal radial velocity of the vapor particles.

Here, $\varepsilon_г$ is the proportion of gas by volume.

In terms of unit area we have:

$$MV = \left(\frac{q}{r_s \gamma_п}\right)^2 \frac{\gamma_п}{g} \varepsilon_п, \qquad (1)$$

where $\varepsilon_п$ = proportion of steam by volume.

The momentum of the gas is mv, where, as before, $v\frac{\pi}{4}(D^2-d^2)\varepsilon_г$ is the nominal velocity of the gas particles along the condensate film.

Determining the approximate velocity of the gas without allowing for the interaction between the vapor-gas layer and the surface of the condensate film and setting the nominal thickness of the vapor-gas layer equal to y, we can set up the equation of equilibrium as follows:

$$ybl(\gamma_г - \gamma_п) = \mu_{см} \frac{v}{y} bl,$$

where b = length of the circumference.
l = height of the pipe.

Whence,

$$y = \sqrt{\frac{\mu_{см} v}{\gamma_г - \gamma_п}}.$$

If we take the volume of gas moving along the condensate film as equal to $\frac{q}{r_s \gamma_п}\left(\frac{\varepsilon_г}{\varepsilon_п}\right)$, the gas velocity will be defined by the expression:

$$v = \sqrt[3]{\frac{q^2 \varepsilon_г^2 (\gamma_г - \gamma_п)}{r_s^2 \gamma_п^2 \varepsilon_п^2 \mu_{см} b^2}}$$

or

$$v = \sqrt[3]{\left(\frac{q}{r_s \gamma_п}\right)^2 \left(\frac{\varepsilon_г}{\varepsilon_п}\right)^2 \frac{\gamma_г - \gamma_п}{\mu_{см}} l^2}.$$

In terms of unit annular cross-sectional area, we get the following expression for the momentum of the gas flow per second:

$$mv = \frac{\gamma_г}{g}\left[\left(\frac{q}{r_s \gamma_п}\right)^2 \left(\frac{\varepsilon_г}{\varepsilon_п}\right)^2 \frac{\gamma_г - \gamma_п}{\mu_{см}} l^2\right]^{\frac{2}{3}} \varepsilon_г. \qquad (2)$$

The ratio between the momenta, which characterizes the interaction between the diffusing vapor particles and the gas particles moving along the film, will be expressed by the following expression:

$$\frac{MV}{mv} = \left(\frac{q}{r_s \gamma_п}\right)^{0,66} \left(\frac{\varepsilon_п}{\varepsilon_г}\right)^{2,33} \left(\frac{\mu_{см}}{\gamma_г - \gamma_п}\right)^{0,66} \frac{\gamma_п}{\gamma_г} l^{-1,32}. \qquad (3)$$

The interaction between the flowing condensate film and the moving layer of vapor and gas can be allowed for, on the one hand, by the Reynolds number of the flowing condensate film and, on the other hand, by the relationship between the coefficients of kinematic viscosity of the vapor-gas layer and the flowing condensate. The Reynolds number can be determined from the ratio

$$Re_к = \frac{v_к \delta}{\nu_к} = 7{,}67 \cdot 10^{-3} \frac{q}{r_s \nu_к \gamma_к},$$

where q = thermal load.
r_s = latent heat of vaporization, kg-cal/kg.
ν_k and γ_k = coefficient of viscosity and specific gravity, respectively, of the condensate.

The process of heat exchange is characterized by the coefficient of mass transfer and can be expressed in dimensionless form by means of the

criterion:

$$Nu' = \frac{\beta y}{D'},$$

where β = coefficient of mass transfer, 1/hr.
D' = diffusion coefficient, m/h.
y = a characteristic dimension, in this case the nominal thickness of the vapor-gas layer.

The thickness of the vapor-gas layer can be determined from the considerations set forth in determining the ratio of momenta and is expressed by the relationship:

$$y = \sqrt[3]{\left(\frac{q}{r_s \gamma_n}\right)\left(\frac{\mu_{cm}}{\gamma_z - \gamma_n}\right)\left(\frac{\varepsilon_z}{\varepsilon_n}\right) l}. \qquad (4)$$

After the similitude criteria mentioned above have been determined, it becomes possible to plot a graph showing their interrelationship. The variation of the criterion Nu' with the expression $\left(Ar \cdot Pr' \frac{MV}{m v} \times Re_k \frac{\nu_{cm}}{\nu_k}\right)$. is plotted logarithmically in Fig. 15. In this figure we have plotted

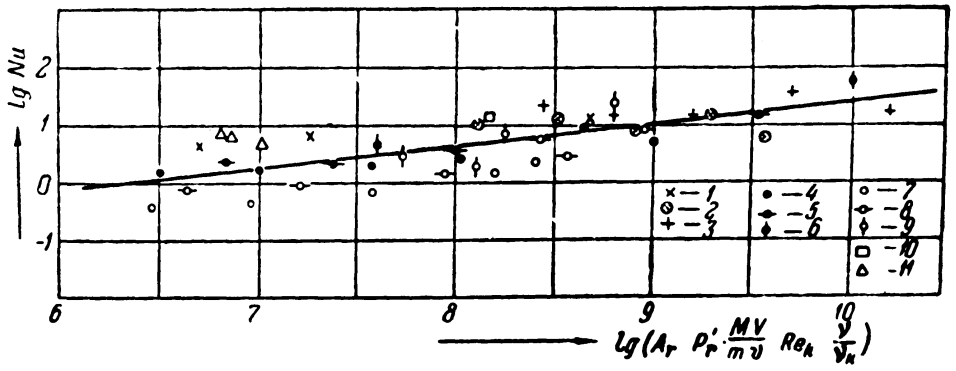

Fig. 15. Result of processing the experimental material as a relationship between the criteria of similitude.

1 - Ammonia plus air for q = 5,000
2 - " " " " q = 10,000
3 - " " " " q = 15,000
4 - " " ethylene, q = 5,000
5 - " " " , q = 10,000
6 - " " " , q = 15,000
7 - " " methane , q = 5,000
8 - Ammonia plus air for q = 10,000
9 - " " " " q = 15,000
10 - Water " " " q = 10,200
ε = 2.86%
11 - " plus air for q = 8.900 and 15.800
ε = 4.53%

the results secured in the condensation of ammonia vapor from mixtures containing air, ethylene, and methane with the thermal load varied from 5,000 to 15,000 kg-cal/m^2·h. The figure does not include the results of experiments on the condensation of ammonia vapor from a mixture containing

hydrogen, as the interaction of forces within the vapor-gas layer then results in upward movement within this layer.

The graph is satisfied by the following equation relating the criteria:

$$Nu' = 0.0158\left(Ar \cdot Pr' \frac{MV}{m_V} Re_K \frac{v_{cm}}{\nu_K}\right)^{0.31} \quad (5)$$

Having in mind the system of forces acting within the vapor-gas layer, we observe that when the Reynolds number of the vapor-gas mixture within the condenser is small, the intensity of the condensation process will be governed not only by the physical properties of the vapor and the gas but also by the arrangement of the heat-transfer surface. Thus, when vapor is condensed from a vapor-gas mixture, a vertical surface (vertical condenser) will be more efficient if the specific gravity of the vapor is lower than the specific gravity of the gas. On the other hand, a horizontal surface will be more efficient in condensing vapor from a vapor-gas mixture in which the specific gravity of the vapor is higher than the specific gravity of the gas. This comment holds good for those conditions of condenser operation where layering of the vapor-gas mixture is prevented by its motion, or by a special accessory.

We may conclude from these considerations that the place at which fresh vapor is introduced is far from immaterial in its condensation from a mixture with gas. Thus, admitting the vapor at the bottom will be advisable when vapor is condensed from a mixture in which its specific gravity is lower than the specific gravity of the gas, while an inlet at the top will be advisable, on the other hand, when the specific gravity of the vapor is higher than that of the gas.

These remarks on the process of vapor condensation from a vapor-gas mixture and on the interaction of forces within the vapor-gas layer are confirmed not only by the research results set forth above. Some of the results secured by Othmer in his investigation of the condensation of steam from a mixture containing hydrogen on a horizontal tube were utilized as a check. In particular, Othmer's figures on heat exchange during the condensation of steam from a mixture containing 2.86 and 4.53% of air with heat loads of 8000 to 15,600 kg-cal/m^2·h were recalculated, and the results plotted in Fig. 15. It should be borne in mind that the experimental data on the condensation of steam apply to a horizontal heat-transfer surface, while the data for the condensation of ammonia vapor apply to a vertical surface.

10. CONCLUSIONS

1. Condensing vapors of ammonia and Freon-12 on a polished surface follow the pattern of filmwise condensation.

2. The variation of the coefficient of heat transfer with the vapor-wall temperature difference in the condensation of ammonia and Freon-12 is in accordance with the theory of filmwise condensation for laminar flow of the condensate film.

3. The presence of a noncondensable gas in ammonia vapor impairs the condensation process. The degree of impairment of the process depends

upon the physical properties of the noncondensable gas and the thermal load of the heat-transfer surface.

4. The nature of the variation of the coefficient of heat transfer with the vapor-wall temperature difference in the condensation of ammonia vapor containing a gas is different for different mixtures. It is governed by the relationship between the molecular weights of the ammonia vapor and the noncondensable gas.

5. A method is recommended for processing experimental data to secure criteria of similitude. The temperature at the boundary between the vapor-gas layer and the condensate film can be determined by making use of the temperature difference within the condensate film, known from the condensation of pure vapor.

LITERATURE CITED

1. S. S. Kutateladze. Heat Transfer in Condensation and Boiling. State Scientific and Technical Publishing House of Machinery Literature, 1949, 1952.

2. L. D. Berman, Bull. All-Union Heat Engineering Institute, No. 8, 1947.

HEATING OF A JET OF WATER IN A VAPOR-FILLED SPACE

N. M. Zinger, Candidate of Engineering Sciences

The F. E. Dzerzhinsky All Union Heat Engineering Institute

In many industrial Heat-exchange apparatus of the mixing type (deaerators, jet heaters, condensers of the mixing type, and others) the water to be heated travels as jets issuing from orifices or nozzles. The theoretical and experimental data on the heat transfer from the steam to the water jet, required for calculating apparatus of this sort, is still sparse, however.

I. V. Vasiliev made an experimental investigation of the heating of a jet of water by steam as applied to the conditions of heat exchange at the top end of a deaerator in the Central Scientific Research Institute for Boilers and Turbines in 1938-1939. The experiments were run by letting water flow out of orifices with a diameter of d_1 = 3-7 mm, with the height of the jet H = 0.2-0.55 m. The initial velocity of the water was w_1 = 0.2-1.4 m/sec, and its initial temperature t_1 = 20-90° C. The water was heated by saturated steam at a pressure of approximately 1 atmosphere absolute. The coefficients of heat transfer obtained* were comparatively low, lying within the following limits:

$$K = 10\text{-}20 \cdot 10^3 \text{ kg-cal/m}^2 \cdot \text{h} \cdot \text{degree}.$$

On the basis of these experiments I. V. Vasiliev proposed an empirical formula for calculating the heating of the jet /Ref. 1/:

$$\lg \frac{t'' - t_1}{t'' - t_2} = 0{,}029 \left(\frac{g d_1}{w_1^2}\right)^{0{,}2} \left(\frac{H}{d_1}\right)^{0{,}7}, \qquad (1)$$

where t'' = saturation temperature of the heating steam, ° C.
t_2 = final water temperature, ° C.
d_1 = orifice diameter, meters.

This formula holds within the following limits:

$$Re > 1500;\ 1 < Fr < 40;\ 40 < \frac{H}{d_1} < 100.$$

S. S. Kutateladze and V. M. Borishansky (Central Scientific Research Institute for Boilers and Turbines) have recently proposed a theoretical formula for calculating the heating of a falling jet of liquid by vapor. The formula was derived on the assumption of a continuous cylindrical jet of liquid, in which there was no transverse velocity gradient. The hypothesis was accepted that the coefficient of turbulent thermal conductivity is proportional to the transverse dimension and to the absolute flow

---

* Although there was no solid wall between the steam and the liquid in this case, we are employing here and henceforth the term "coefficient of heat transfer," inasmuch as this coefficient refers to the average temperature difference between the steam and the bulk of the liquid along the length of the jet, rather than to the difference between the temperature of the steam and the temperature at the surface of the jet.

velocity. The formula is as follows:

$$\lg \frac{t'' - t_1}{t'' - t_2} = 0{,}162 + 10{,}08 \cdot \left\{ \frac{aH}{w_1 d_1^2} + \frac{\varepsilon_* w_1^2}{5\varphi^{2{,}5} g d_1} \left[\left(1 + \frac{2\varphi^2 gH}{w_1^2}\right)^{1{,}25} - 1 \right] \right\}. \quad (2)$$

Here $a = \frac{\lambda}{\gamma c}$, the coefficient of the thermal conductivity of the water, m^2/sec.

φ = contraction coefficient of the jet emerging from the orifice. The coefficient

$$\varepsilon_* = \frac{\varphi \mu_m}{\gamma r_1 \omega_1}$$

where μ_m is the coefficient of turbulent friction.

According to Nikuradze's experiments the value of ε_* is $5.0 \cdot 10^{-4}$ for the flow of liquids through pipes.

The results of calculations made by the authors, using Eq. (2), in which they took $\varepsilon_* = 5 \cdot 10^{-4}$ and $\varphi = 0.85$, agreed satisfactorily with the results of experiments made by A. A. Zakharov and R. G. Chernaya in the Central Scientific Research Institute for Boilers and Turbines, using $d_1 = 3.0$, 5.07, and 7.05 mm; H = 300-450 mm; and $w_1 = 0.5$-1.5 m/sec.

The values of the coefficient of heat transfer from the steam to the water jet in these experiments lie approximately in the range secured in the experiments by I. V. Vasiliev referred to. We also possess data on a much greater intensity of heat exchange between condensing steam and a water jet at larger diameters and higher flow velocities.

Extremely high values of the coefficient of heat transfer, exceeding 10^6 kg-cal/m^2·h·degree, were secured by N. G. Morozov in his laboratory investigation in the All-Union Heat Engineering Institute, as well as by E. Ya. Sokolov in an industrial test of a jet heater, in which the heating of the jet took place during a short initial section. In these experiments the rate of flow of the jet from the nozzle was 10-20 m/sec, the initial temperature of the water 20-80° C, and the steam pressure 1-5 atmospheres absolute.

The same order of magnitude of the coefficient of heat transfer is secured from the theoretical equation /Ref. 2/ proposed by G. N. Abramovich and A. P. Proskuryakov for the condensation of steam on the surface of an infinite plane turbulent jet. In deriving this formula they assumed that there is a core of undisturbed flow throughout the length of the jet, in which temperature and velocity remain constant, equal to the temperature and velocity at the initial stream cross section. The transfer of heat takes place in the turbulent boundary layer with a substantial transverse velocity gradient present. The principal experimental constant is a, the coefficient of jet structure, whose numerical value is taken to be 0.07-0.09, according to the research figures for a free air jet.

The formula advanced by G. N. Abramovich and A. P. Proskuryakov for

determining the coefficient of heat transfer from steam to the jet is as follows

$$K = 324{,}000\ \omega_1 \Phi(R)\ \text{kg-cal/m}^2\cdot\text{h}\cdot\text{degree},$$

where $\Phi(R)$ is a function of the parameter

$$R = \frac{c(t'' - t_1)}{r}$$

Here r = latent heat of condensation, kg-cal/kg.
c = specific heat of the liquid, kg-cal/kg·degree.

The following values of Φ (R) correspond to different values of R:

R	0.0020	0.0067	0.016	0.031	0.053	0.123	0.233
Φ (R)	0.100	0.149	0.198	0.246	0.288	0.370	0.432

At a steam temperature of 1.5 atmospheres absolute, a water temperature of 20° C, and a water discharge velocity of 20 m/sec, the coefficient of heat transfer from steam to water is $2.60 \cdot 10^6$ kg-cal/m^2·h·degree according to this formula.

The equations given above are usable within certain comparatively narrow limits for which they were derived and require further refinement. This is indicated, in particular, by the experiments described below, which were performed in the Dzerzhinsky All-Union Heat Engineering Institute.*

A general view of the apparatus in which the jet was heated is given in Fig. 1. The body of the apparatus was 250 mm in diameter and 1500 mm high. Through its top flange there was passed a branch pipe, to the lower end of which there were screwed the interchangeable water nozzles. Steam was admitted through the upper branch pipe. A perforated deflector plate was installed opposite the opening through which the steam entered the shell. The water level was determined by a water gage. Continuous scavenging was done through three branch pipes, arranged along the height of the shell, to remove the air separating out of the water.**

In some runs a special thermal probe was used to measure the temperature within the jet at various distances from the outlet cross section of the nozzle. The length of the jet was kept constant at 800 mm. The thermocouple junction (about 1 mm in diameter) was washed directly with water. The water consumption, the steam pressure within the shell, and the water level, which determine the length of the jet, were measured by appropriate valves in the water, steam, and discharge lines. During the experiments we measured the temperature of the inlet and heated water, and the temperature and pressure of the heating steam.

The distribution of temperature in various cross sections of the jet

* The engineer K. S. Andreev and the senior technician R. Kh. Kurmaev took part in these experiments.

** This circumstance should be borne in mind, inasmuch as the percentage of air in the steam may be increased considerably in industrial apparatus. In this case the rate of heating of the jet may be diminished, compared to the rate in the experiments described.

with a nozzle diameter of 15 mm and flow velocity of 14, 19, and 25 m/sec is shown in Fig. 2. The steam pressure within the shell was maintained at 1.7-2 atmospheres absolute. It should be noted that owing to some fluctuation of pressure within the apparatus the thermocouple did not always indicate the same steam temperature (which varied over a range of about 5° C).

As we see from the curves the deformation of the temperature field along the length of the jet is completely regular. The temperature along the axis rises as the distance from the jet increases, while the temperature gradient within the jet diminishes. The higher the velocity at which the jet emerges from the nozzle, the faster this process takes place.

Analogous data are reproduced in Fig. 3 for a jet emerging from a nozzle 10 mm in diameter at a velocity of about 10 m/sec. The steam pressure was 1.2-1.4 atmospheres absolute. This graph shows that the deformation of the temperature field slows down when the diameter of the nozzle is smaller and the velocity of flow is lower; even at a distance of 800 mm from the nozzle the difference between the temperatures at the surface and at the axis of the jet is about 30° C.

As shown in Fig. 4, the temperature rise along the axis of the jet is very rapid at the beginning, gradually slowing down later on. The rate at which water flows from the nozzle greatly affects this temperature rise: the temperature along the axis of the jet rises more rapidly as the velocity is increased, notwithstanding the corresponding increase in flow.

Visual observations through sight glasses showed that the jet is transparent for a considerable length when it flows into an air-filled space (w_1 = 10-20 m/sec), retaining its cylindrical form, with a diameter that is approximately the same as the diameter of the outlet cross section of the nozzle. When the jet emerges into a stea-filled space, the appearance of the jet changes perceptibly. It becomes white and opaque. The diameter of the jet increases the farther we get from the outlet cross section of the nozzle. The angle subtended by the jet, which can be estimated approximately from the temperature profiles obtained, lies within 3-6°, increasing as the velocity of flow rises.

The difference between the temperature to which the water is heated and the saturation temperature of the heating steam plotted in Fig. 5 as a function of the length of the jet, like the temperature field function, shows that at high flow velocities most of the heating takes place during the brief initial section of the jet, whereas at low flow velocities heating takes place throughout the length of the jet (800 mm).

The values of the coefficient of heat transfer from condensing steam to a jet of water were calculated from the results of our experiments. They were conventionally based on the surface of a cylinder whose diameter equaled the diameter of the outlet cross section of the nozzle and to a height equal to the length of the jet.

The mean values of K, the coefficient of heat transfer, are plotted in Fig. 6 as a function of the velocity at which the water flows from the nozzle for a jet 800 mm high (at d_1 = 10-15 mm).

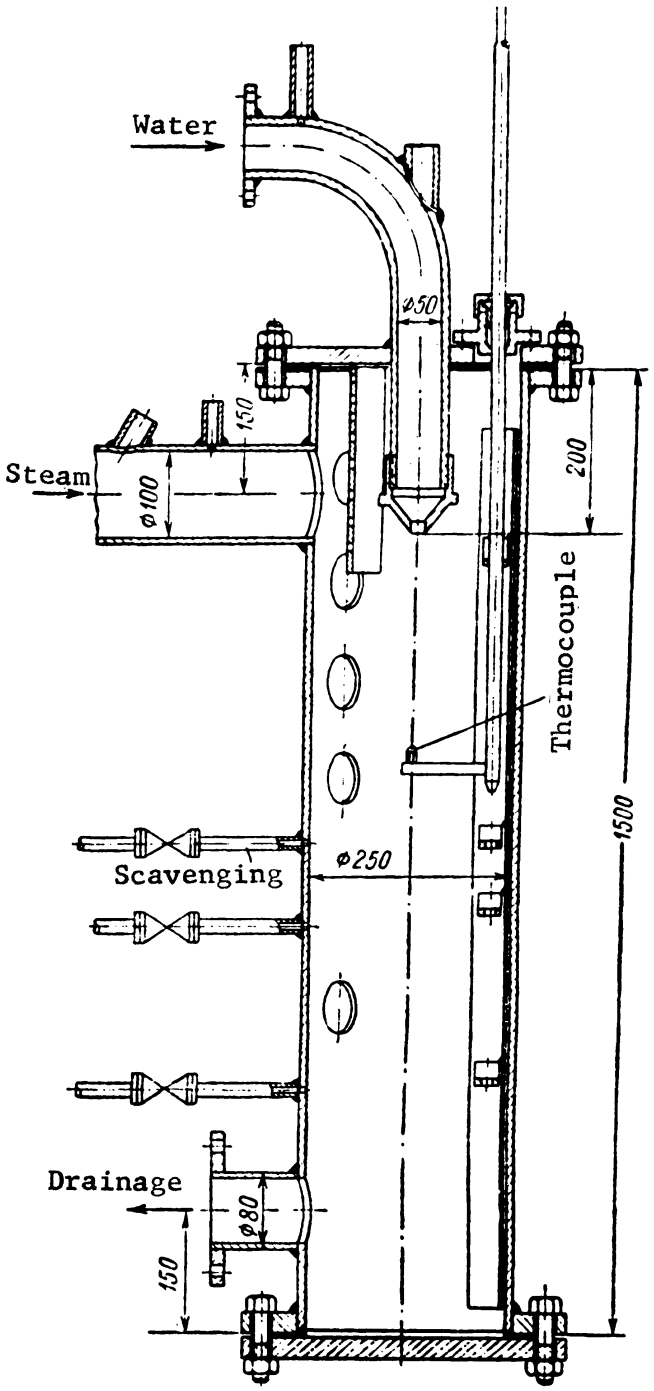

Fig. 1. Experimental setup for investigating heating of a jet.

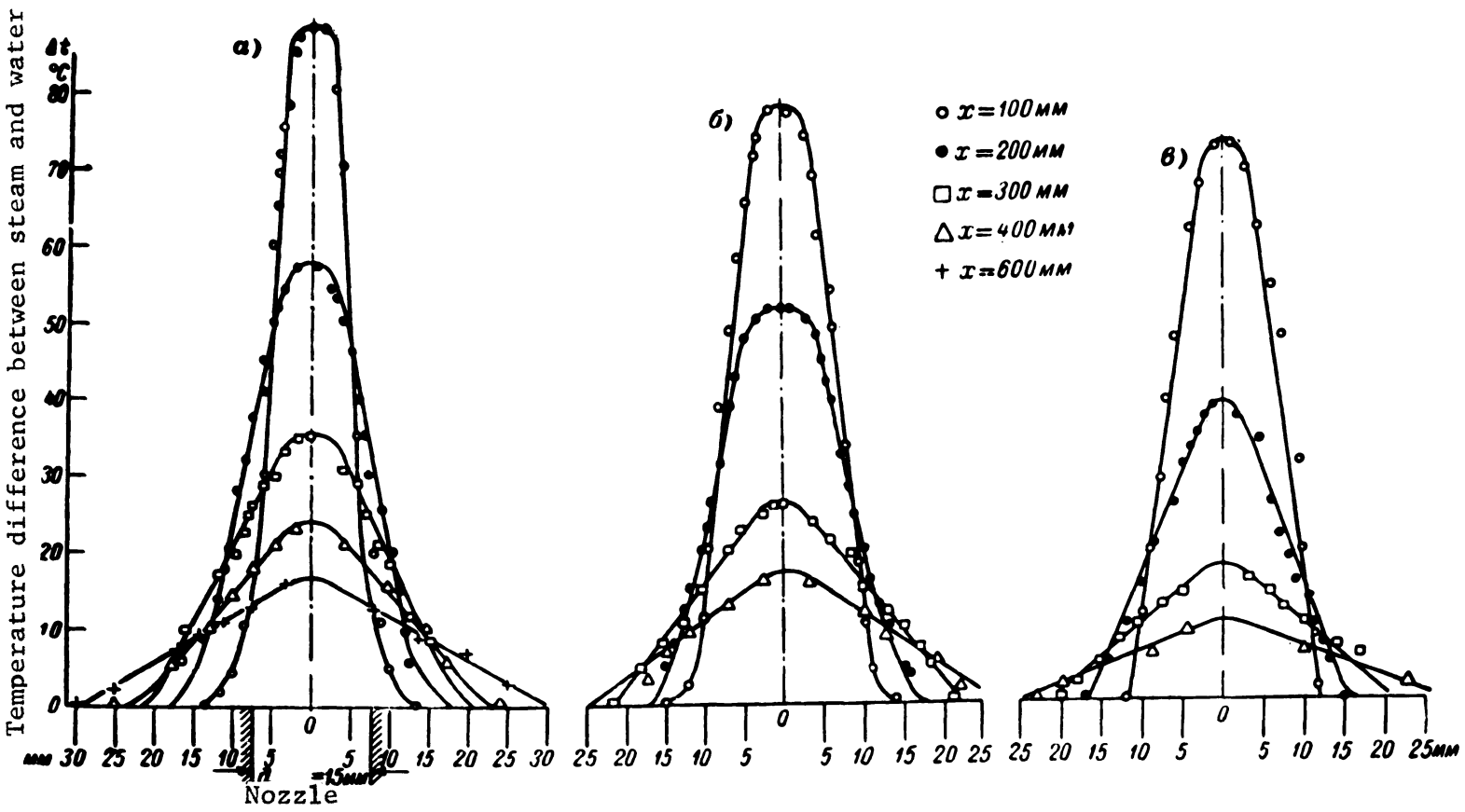

Fig. 2. Deformation of the temperature profile in a jet of water (d_1 = 15 mm; H = 800 mm; steam pressure $p_{\text{ат}}$ = 1.7-2 atmospheres absolute)

a) w_1 = 14 m/sec; b) w_1 = 19 m/sec; c) w_1 = 25 m/sec; x = distance between thermocouple and nozzle.

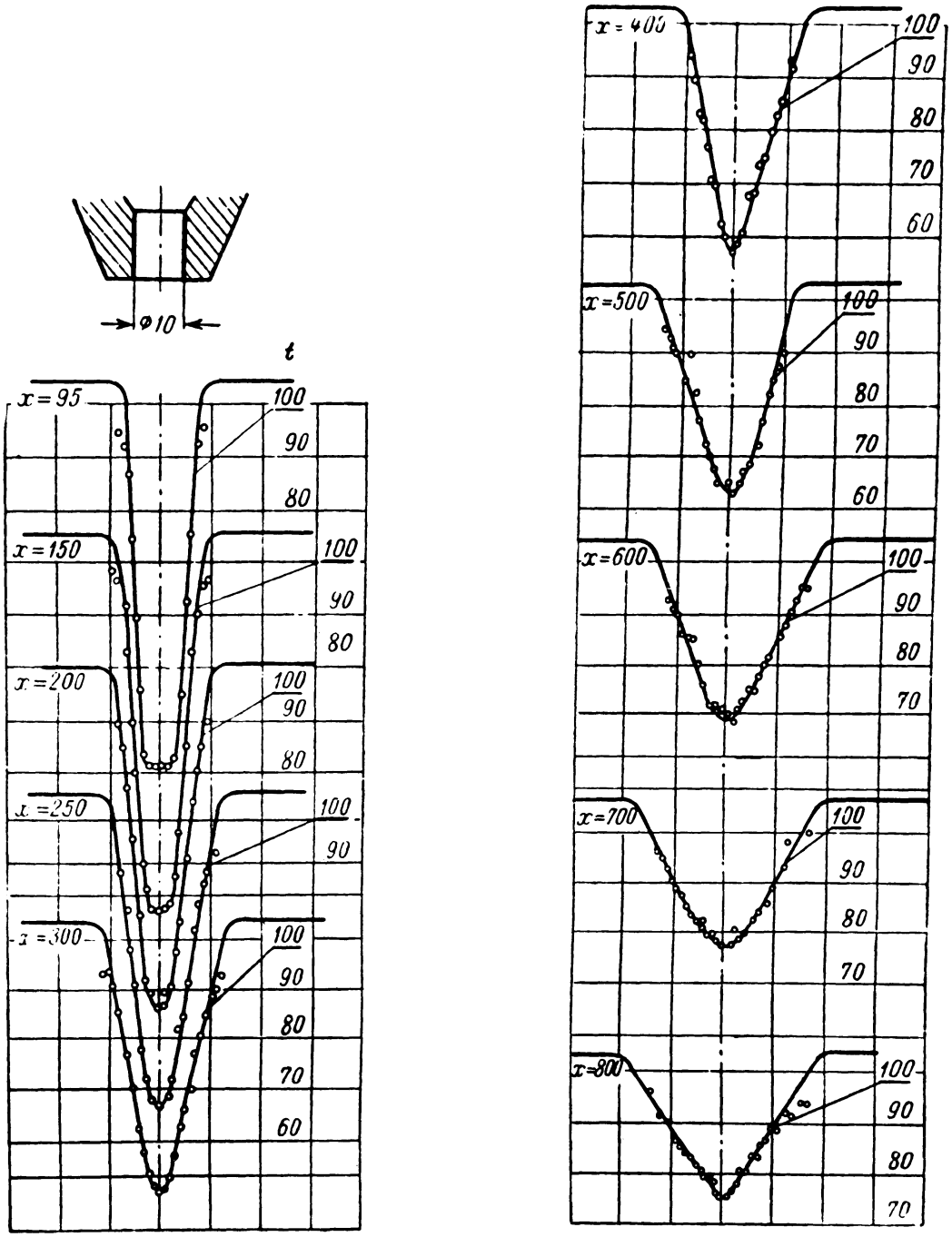

Fig. 3. Deformation of the temperature profile in a jet of water (d_1 = 10 mm; H = 800 mm; $p_м$ = = 1.2-1.4 atmospheres absolute; w_1 = 10 m/sec).

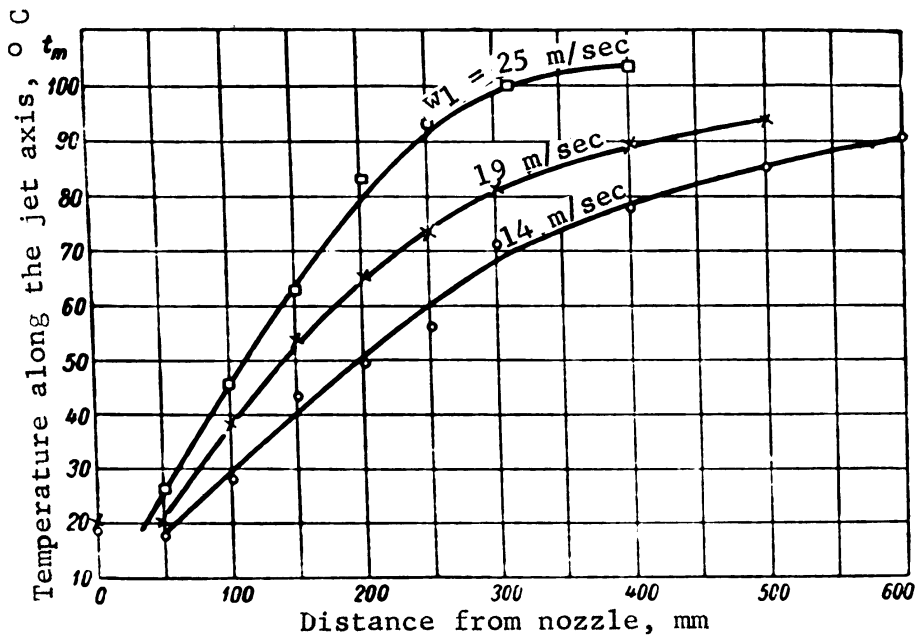

Fig. 4. Change of temperature along the axis of the jet (d_1 = 15 mm; H = 800 mm; p_{μ} = 1.2-1.4 atmospheres absolute).

The mean values of $\underline{K}$ are plotted in Fig. 7 as a function of the height of the jet (at d_1 = 15 mm and w_1 = 20 and 25 m/sec). The sharp rise in the coefficient of heat transfer with a decrease in the height of the jet is due to the fact that at high flow velocities most of the heating of the water takes place during the short initial section of the jet.

In Fig. 6 we have also plotted the values of the coefficient of heat transfer as calculated from the formula of S. S. Kutateladze and V. M. Borishansky and from the formula of G. N. Abramovich and A. P. Proskuryakov. It should be borne in mind that the values of the initial jet velocity and of the other parameters employed in these calculations greatly exceed the limits for which the first formula was derived.

As we see from Fig. 6, the values of $\underline{K}$ secured in experiments for a jet length of 800 mm and velocities of 10-25 m/sec considerably exceed those calculated from the formula of S. S. Kutateladze and V. M. Borishansky. As the rate of flow and the diameter of the nozzle are decreased, the values of $\underline{K}$ approach those calculated from these equations. Comparison with the formula of G. M. Abramovich and A. P. Proskuryakov indicates that the experimental values of $\underline{K}$ (the mean values for a length of 800 mm) are considerably below the calculated ones. When the length of the jet is shortened, i.e. when the conditions approach those for which the formula was derived, the experimental values of $\underline{K}$ we obtained approach the extremely theoretical calues.

It may be assumed that the continuity of the jet is broken because of its extremely high turbulence over a short path. This is indirectly confirmed by the temperature profiles given above, which reveal a percep-

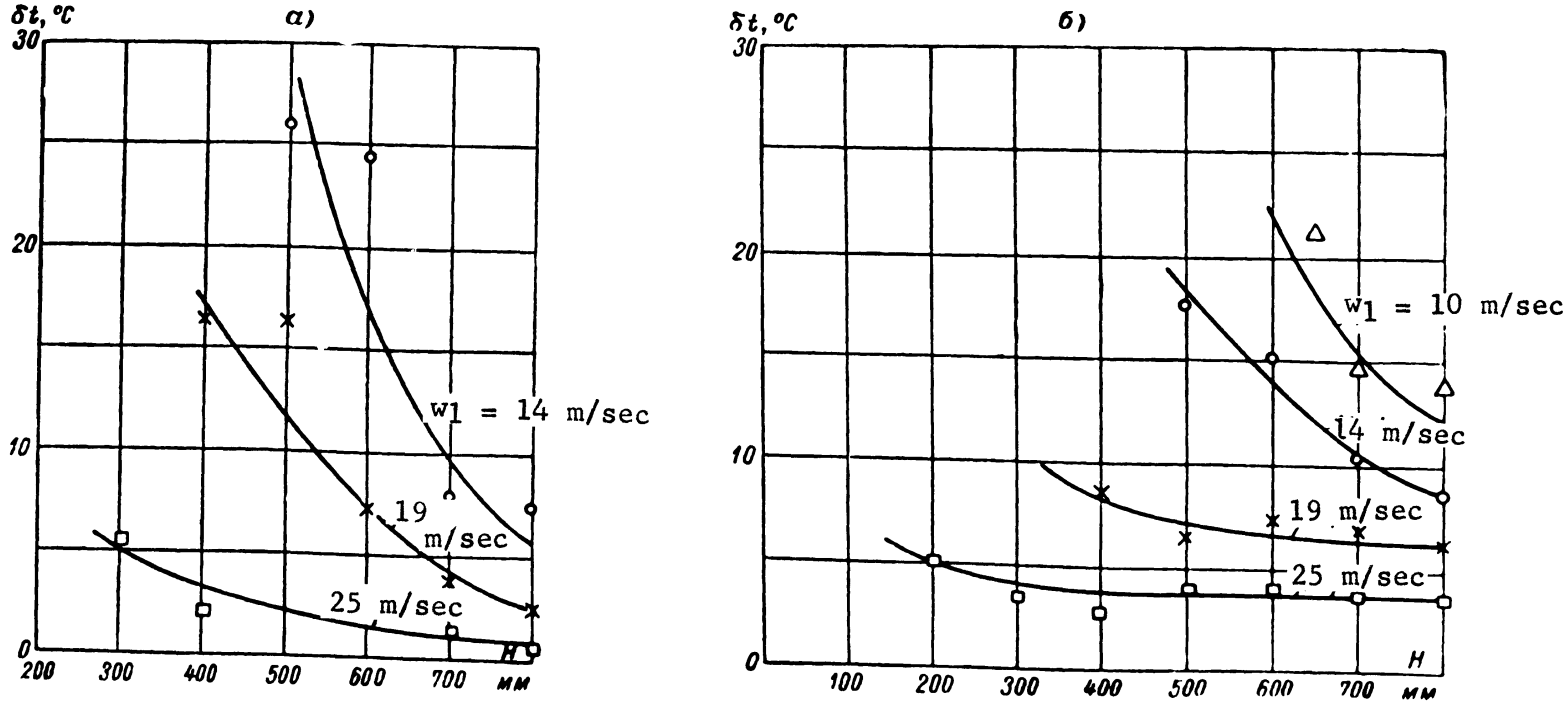

Fig. 5. Variation of δ t, the difference between the temperature to which the water is heated and the saturation temperature of the heating steam, with the height of the jet H:
a) d_1 = 10 mm; b) d_1 = 15 mm.

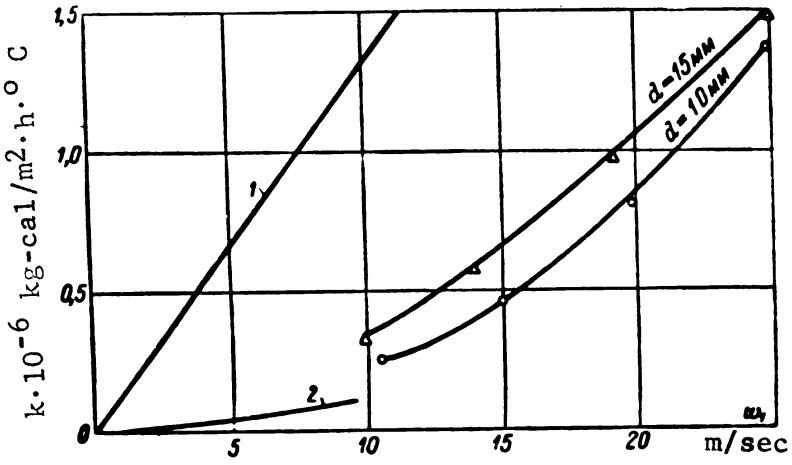

Fig. 6. Variation of the coefficient of heat transfer with the velocity of flow according to experimental and calculated data (H = 800 mm).
1 - From the formula of G. N. Abramovich and A. P. Proskuryakov; 2 - from the formula of S. S. Kutateladze and V. M. Borishansky.

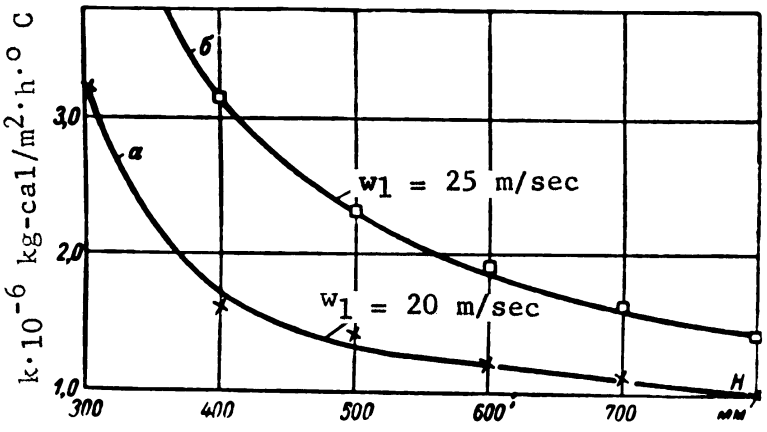

Fig. 7. Variation of K, the mean coefficient of heat transfer, with H, the height of the jet, according to experimental and calculated data (d_1 = 15 mm); a) w_1 = 20 m/sec; b) w_1 = 25 m/sec.

tible widening of the jet. The break in continuity results in a sharp difference between the actual conditions and the conditions assumed in deriving the theoretical formulas, and it explains the great discrepancy between the theoretical and experimental values of the coefficient of heat transfer from steam to a jet of water.

LITERATURE CITED

1. S. S. Kutateladze. Heat Transfer in Condensation and Boiling. State Scientific and Technical Publishing House of Machinery Literature, 1949, 1952.

2. G. N. Abramovich. Free Turbulent Jets of Liquids and Gases. State Power Engineering Press, 1948.

PART TWO

HEAT EXCHANGE DURING EVAPORATION

INFLUENCE OF PRESSURE ON THE PRODUCTION OF THE FIRST CRISIS IN THE BOILING OF WATER ON A HORIZONTAL PLATE

E. A. Kazakova, Candidate of Technical Sciences

The G. M. Krzhizhanovsky Power Institute of the USSR Academy of Sciences

In the previous research of the Power Institute of the USSR Academy of Sciences on the influence of pressure upon the magnitude of the initial critical thermal load q_{kpl} in the boiling of water at submerged heating plates /Ref. 1, 2/ we were unable to keep the condition of the surface of the heating element constant. At pressures above 80-90 atmospheres the material of the electrical insulators (porcelain, glass, quartz) dissolved strongly in the water, so that at high thermal loads a substantial layer of silicate and aluminosilicate compounds was deposited on the heating surface. With the appearance of these deposits the absolute values of q_{kpl} increased appreciably (by 50 to 100%) over the figure for the pure metallic surface, and a discontinuity appeared in the curve of $q_{kpl} = f(p)$.

Moreover, in the experiments run at atmospheric pressure we found that the geometric dimensions of the heating unit had an appreciable effect upon the magnitude of q_{kpl}, if a wire of small diameter, a thin-walled plate, or a thin-walled tube was used as the heating element. It was found in the researches of S. S. Kutateladze and G. M. Polyakov that the position of the heating surface likewise affected the magnitude of q_{kpl}.

In the experiments on the boiling of distilled water at pressures from 1 to 205 atmospheres, performed in 1950 in the Power Institute of the USSR Academy of Sciences, we succeeded in largely eliminating the deficiencies referred to above.

The heating surface used was a nichrome plate 5 mm wide, about 70-80 mm long, and 0.6 mm thick, which was heated by alternating current. The plate was set up horizontally on its narrow edge, which insured the unimpeded removal from the surface of the bubbles formed and eliminated the premature development of a vapor film as a result of local accumulation of steam. To insure the development of filmwise boiling at the middle of the plate, (where the hydrodynamic distortions due to the mountings had no effect), it was necessary to diminish the intensity of steam formation at the ends of the heating elements. To do this the ends of the plate were covered with a heavy layer of copper, as a result of which the electrical resistance was diminished in these areas, and hence the evolution of heat as well.

The electrical insulating material used was thin plates of mica, which covered the electric lead-ins. Tests indicated that mica is prac-

tically insoluble in water up to the critical pressure, which enabled us to get rid of the silicate and the aluminosilicate deposits.

A detailed description of the design of the high-pressure boiler is given by the author in a previously published paper /Ref. 2/.

A sketch of the plate heating element is shown in Fig. 1. The mechanical strength and rigidity of the nichrome plate made it possible to fasten it directly to the ends of the electric leads, without employing any special supporting frame (as was the case when thin wires were used as the heating element). A telescopic arrangement in one of the electric leads provided compensation for the temperature deformation of the entire apparatus. To avoid interfering with the constancy of the electrical resistance of the leads, as might have happened when the telescopic arrangement was moved, a short, heavy brass spiral of low resistance was welded to each end of the telescopic device. The magnitude of the critical thermal flow was calculated from the equation:

$$q_{кр} = \frac{0{,}860 I^2 R_{пл}}{F_{пл}}$$

where I = current (at the instant immediately preceding the develpment of filmwise boiling), amperes.
$R_{пл}$ = resistance of the nichrome plate, ohms.
$F_{пл}$ = plate area, m^2.

Measurements of the resistance of a sample of the nichrome plate at various temperatures indicated that the temperature coefficient of resistance is negligibly small and that $R_{пл}$ can be assumed to be constant. $R_{пл}$ was measured with an instrument of Class 0.1 precision. The current was measured with a Class 0.5 astatic ammeter, connected via Class 0.2 transformer.

Pressure was measured by a Class 0.2 master pressure gage with a range of 50 kg/cm^2 and 250 kg/cm^2, depending on the magnitude of the pressure to be measured. In experiments at pressures close to the atmospheric, measurement was made with a U-tube namoneter, filled with mercury, or with a spring-typemanometer with a range up to 4 kg/cm^2.

The temperature of the water within the boiler was measured by means of two nichrome-constantan thermocouples 0.1 mm in diameter. These measurements enabled us to judge the relationship between the temperature of the boiling water and the pressure. External heaters were installed to compensate for the heat loss to the surroundings, and at the same time they enabled us to maintain all the liquid in a state of simmering. The latter enabled us to eliminate any difference in temperature between the liquid and the boiling point, which would substantially affect the absolute value of q_{kpl}.

Owing to some corrosion of the walls of the apparatus, toward the end of the experiment the water, whose outer appearance remained clean and transparent, still contained a small percentage of ferric hydroxide. During vigorous boiling an extremely fine coating of ferric hydroxide settled on the surface of the nichrome plate. This coating was thinner or thicker,

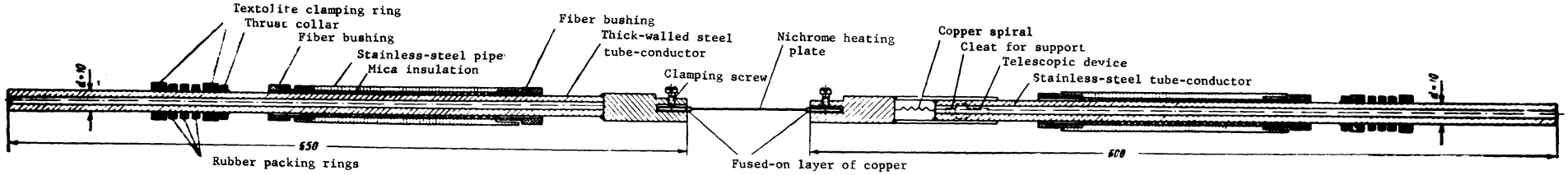

Fig. 1. Sketch of heater with lead-in arrangement.

depending upon the duration of the experiment. In some instances this coating could not be observed at all. Comparison of the results secured at identical pressures on the surface of the plate when completely clean and when covered with a coating disclosed no difference that exceeded the mean scattering of the experimental points.

The results of our experiments are given in Fig. 2 and in the table.

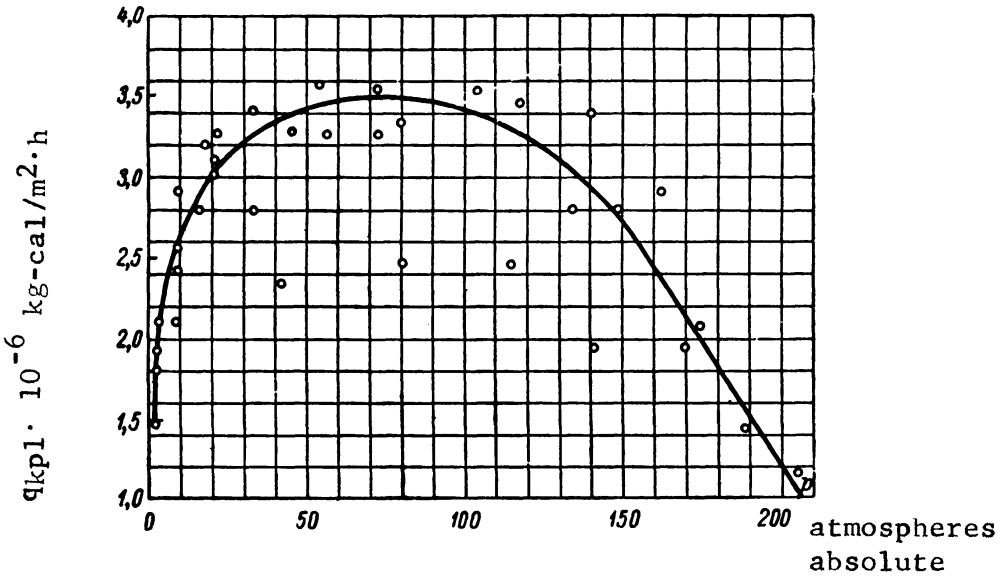

Fig. 2. Variation of q_{kpl} with p in the boiling of distilled water at a nichrome plate 5 mm wide and 0.6 thick, placed on its narrow edge.

The faired curve was plotted through 31 experimental points; 80% of the points lie along the curve with a despersion of ± 10%; 8% depart by ± 15-18%, and 12% (4 points) are 25-30% below the curve.

These results indicate that q_{kpl} rises with the pressure until about 1/3 of the p_{kp}. As the pressure continued to rise, the magnitude of q_{kpl} drops, becoming smaller than at atmospheric pressure in the region of high pressures (above 190 atmospheres absolute).

The curve is fairly flat at either side of the maximum, and we may assume:

$$q_{kpl} \approx 3{,}250{,}000 \pm 5\% \text{ kg-cal/m}^2\text{·h},$$

for all practical purposes within a pressure range of 25-125 atm (from 0.1 to 0.5 p_{kp}), which corresponds to the operating conditions in contemporary steam boilers.

The experimental data on q_{kpl} in the boiling of water in a large volume under pressure are plotted in Fig. 3. The data of Farber and Scorak /Ref. 3/ have not been plotted, since their experiments were run only up to 8 atm, and their results would not show up on the scale used for Fig. 3. What is more, analysis of the work of these authors indicates that their experimental data are definitely of poor quality.

The bulk of the experimental data indicates that the curve $q_{kpl} = f(p)$ for boiling water has a maximum in the neighborhood of $1/3\ p_{kp}$.

In the region where the curves ascend the discrepancies among them are as much as 30%. The highest absolute values of q_{kpl} were secured in the research done by S. S. Kutateladze on the surfaces of rough graphite plates and in the work done by the author on the surface of a corroded nichrome wire /Ref. 4/. The lowest values of q_{kpl} were secured when boiling was done at a clean platinum wire /Ref.1/.

The experimental curves converge in the region of high pressures, an indication of the relative decrease in the influence of differences in the condition of the heating surfaces on the magnitude of q_{kpl}.

The experimental data of American researchers /Ref. 5, Curve 7/ cut across all the other experimental material. Several difficulties in setting up their investigations and the substantial fouling of the heating surface as a result of the electrolytic deposition of copper led the authors of this paper to regard their results as preliminary and not completely dependable.

The experimental curve based on the 1950 data is plotted in Fig. 4 together with the curves plotted from the equations suggested by various authors.

Curve 1 gives the author's experimental data for 1950.

Curve 2 is plotted from the S. S. Kutateladze equation /Ref. 7/:

$$q_{kpl} = kr\sqrt{g\gamma'}\sqrt[4]{\sigma(\gamma-\gamma'')}, \tag{1}$$

for k = 0.16.

Curve 3 is plotted from the G. N. Kruzhilin equation /Ref. 6/:

$$q_{kpl} = B\frac{\lambda^{\frac{1}{2}}(\gamma-\gamma'')^{\frac{13}{24}}(\gamma_r' T_s)^{\frac{1}{3}}\sigma^{\frac{1}{24}}}{\gamma^{\frac{10}{24}} c^{\frac{1}{6}}}, \tag{2}$$

For B = 12,000.

Curve 4 is plotted from the S. M. Lukomsky equation:

$$q_{kpl} = \Phi r^{0,8}\gamma, \tag{3}$$

where Φ is a function of $\frac{p}{p_{kp}}$, which has the same sign for all substances.

When we examine these curves we find the following to be true:

1. The Kutateladze curve lies above the experimental curve throughout the pressure range, with the exception of the region in the vicinity of 1 atmosphere absolute, and yields results that average 10-12% higher than the experimental ones. The discrepancy is greatest at atmospheric pressure, for which Curve 2 yields a result that is 20% below the experimental value.

2. The Kruzhilin curve is shifted to the right of the experimental data, so that the calculated value of q_{kpl} is substantially higher than that for Curve 1 at pressures that are close to the critical value. In the region of moderate pressures, the curve computed from Eq. (2) is some 20% lower than the experimental curve on the average, the maximum discrepancy (33%) occurring at atmospheric pressure.

3. The Lukomsky curve gives a value for q_{kpl} that is 20% too low on the average. The maximum discrepancy occurs at atmospheric pressure (33%), as is the case for the other two equations.

The values of $\underline{k}$ calculated from the Kutateladze equation on the basis of our experimental values for q_{kpl} are plotted in Fig. 5 (with the exception of the four points that are far out of line). Where the value of $\frac{p}{p_{kp}}$ ranges from 0.1 to 1.0, the value of $\underline{k}$ is constant and about 0.13 with an accuracy of $\pm$ 10.15%. When $p \quad 0.1\ p_{kp}$, the value of $\underline{k}$ tends to rise, approximating 0.2 at a pressure close to the atmospheric.

An endeavor to change the values of the constant coefficient $\underline{B}$ and $\underline{k}$ in the Kruzhilin and Kutateladze equations in order to get the theoretical and experimental values of q_{kpl} to agree at atmospheric pressure results in a pronounced deviation of the calculated curves from the curve plotted from the experimental points throughout the pressure range (see Fig. 6).

Critical Thermal Loads in the Boiling of Water at the Surface of a Nichrome Plate (5 mm Wide, 0.6 mm Thick, and About 80 mm Long), Mounted Horizontally on Its Narrow Edge

Pressure, atm abs	q_{kpl} kg-cal/m^2·h	Remarks
8.7	2,550,000	Brownish coating on the plate
8.8	2,900,000	Extremely fine brownish coating on the plate
8.3	2,120,000	Brown coating on the plate
9.2	2,440,000	Light coating on the plate
18.7	3,200,000	" " " " "
20.0	3,010,000	" " " " "
15.3	2,780,000	" " " " "
21.0	3,100,000	" " " " "
32.5	3,380,000	" " " " "
32.5	2,780,000	" " " " "
54.0	3,550,000	Slight coating on the plate
56.0	3,260,000	Surface of the plate clean
104.0	3,510,000	Thin, solid brown deposit on the plate
79.5	3,320,000	Thin, slightly spalling deposit on the plate
134.0	2,780,000	Slight coating on the plate
115.0	2,440,000	Ditto
148.5	2,780,000	Coating on the plate
141.5	1,930,000	Coating only along a section 15-20 mm long, with the rest of the surface clean
162.0	2,890,000	Extremely fine, slightly spalling coating on the plate
41.5	2,330,000	Almost no perceiptible coating on the plate
45.0	3,260,000	Ditto
118.0	3,450,000	Extremely fine, slightly spalling coating on the plate
140.0	3,380,000	Clean plate
72.0	3,520,000	Barely perceiptible coating on the plate
80.0	2,440,000	Plate absolutely clean
73.0	3,250,000	Extremely fine coating on the plate
170.0	1,930,000	Thin coating on the plate
22.0	3,260,000	Plate clean
174.0	2,030,000	Barely perceptible coating on the plate
189.5	1,415,000	Coating on the plate
205.0	1,150,000	Ditto
2.0	1,785,000	Barely perceptible coating on the plate
1.4	1,475,000	Plate clean
2.85	2,130,000	Ditto
2.0	1,920,000	Coating on the plate

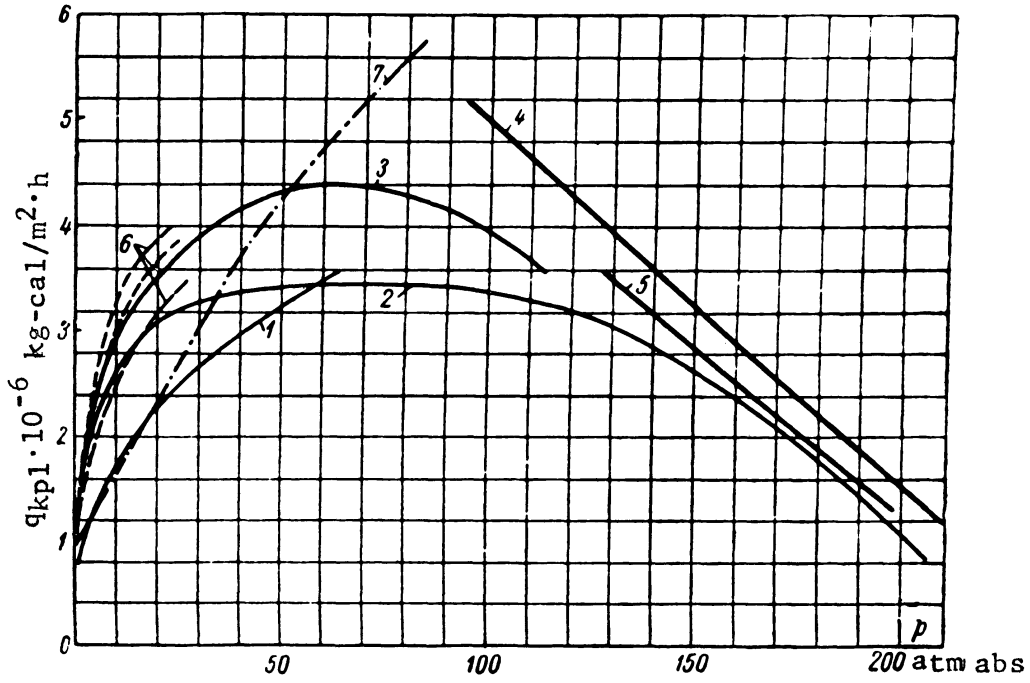

Fig. 3. Comparison of experimental data on q_{kpl} for water.

The author's experiments: 1 - clean platinum wire 0.15 mm diameter; 2 - nichrome plate 5 X 0.6 mm; 3 - highly corroded nichrome wire 0.3 mm diameter; 4 - platinum wire 0.15 mm diameter, covered with deposits of aluminosilicate compounds; 5 - the same wire covered with silicate deposits; 6 - graphite plates of varying roughness (Kutateladze's experiments); 7 - platinum wire 0.3 mm diameter, covered with a coating of copper (Day's experiments).

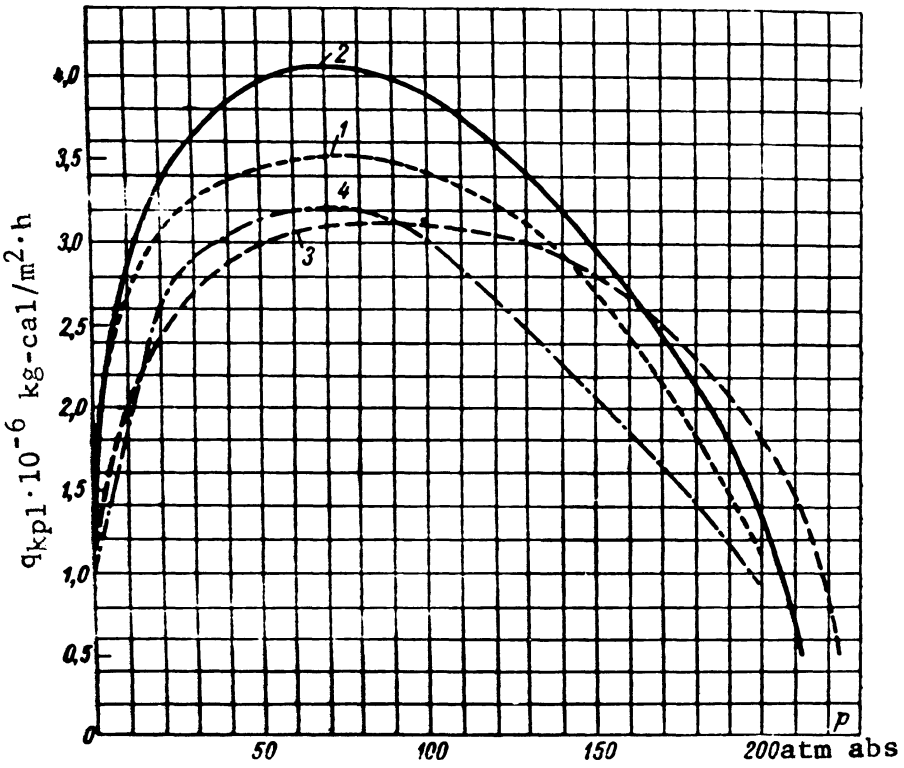

Fig. 4. Comparison of experimental data with the Kutateladze, Kruzhilin, and Lukomsky equations.

1 - Experimental curve for nichrome plates; 2 - Kutateladze equation for k = 0.16; 3 - Kruzhilin equation for B = 12,000; 4 - Lukomsky equation.

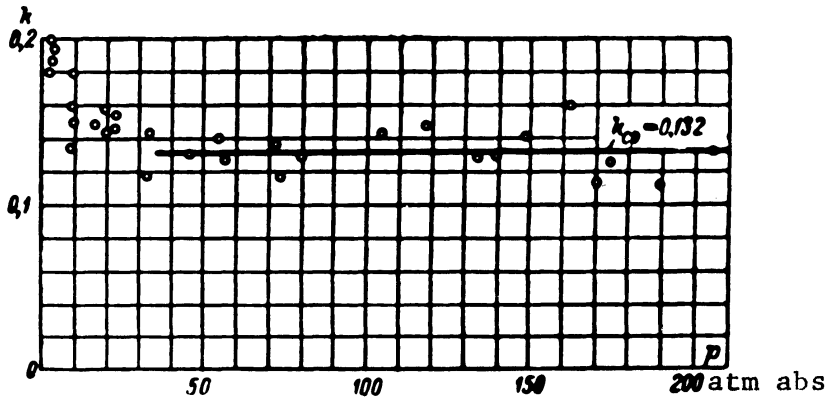

Fig. 5. Values of $\frac{q_{kpl}}{r\sqrt{g\gamma''}\sqrt[4]{\sigma(\gamma-\gamma'')}}$ according to experiments with a nichrome plate.

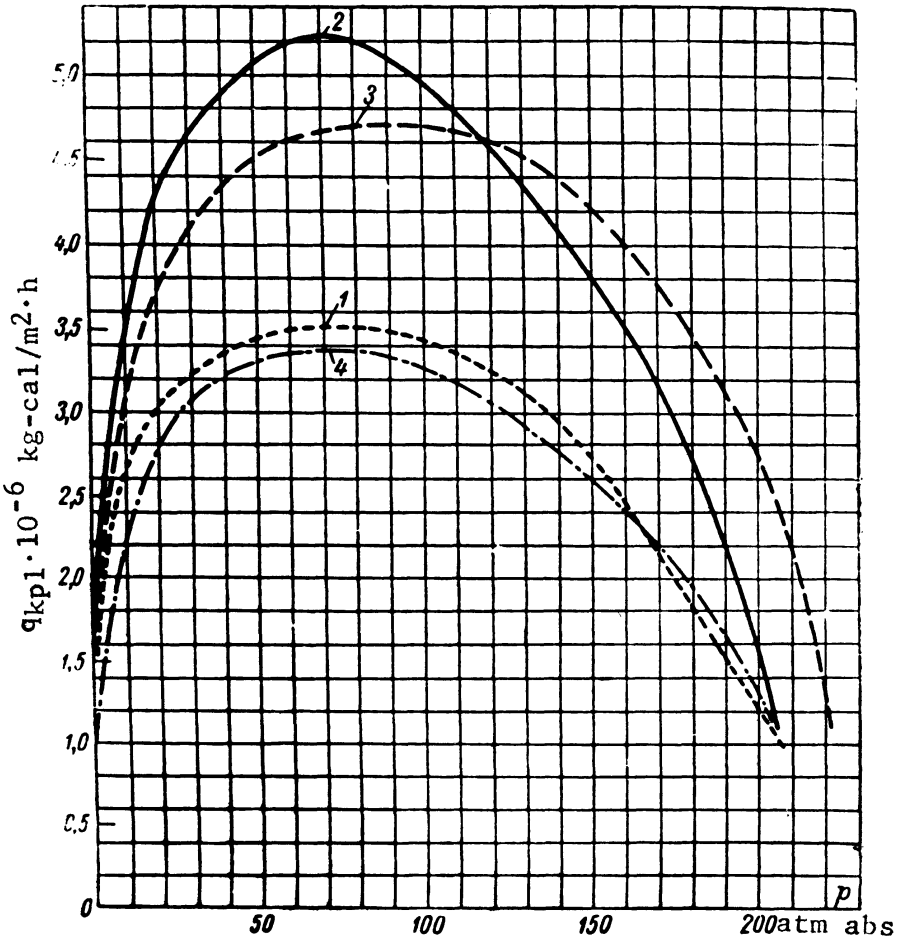

Fig. 6. Comparison of the calculated and experimental function $q_{kpl} = f(p)$ for water when boiled in a large space.
1 - Experimental curve; 2 - Kutateladze equation for k = 0.2; 3 - Kruzhilin equation for B = 18,000; 4 - Kutateladze equation for k = 0.13.

At low pressures and, in particular, for water in the neighborhood of 1 atmosphere absolute, the influence of several additional factors (condition of the heating surface, material and thickness of the heating wall, underheating of the liquid), not allowed for in the equations cited above, have a very pronounced effect upon the mechanism of steam generation. It therefore seems to us advisable that the values of the constant coefficients in the generalized equations available at the present time be selected on the basis of the experimental results secured at comparatively high pressures.

Curve 4 in Fig. 6 is plotted from the S. S. Kutateladze equation for $k = 0.13$, corresponding to the experimental data secured in the pressure range of 0.1-0.9 p_{kp}.

As we see from the graph, this curve corresponds to the experimental one within $\pm$ 5-7% throughout the pressure range, with the exceiption of pressures close to the atmospheric.

CONCLUSIONS

1. Most of the experimental data indicate that the magnitude of the initial critical density of thermal flow (q_{kp1}) for boiling water rises to a figure several times larger than that for atmospheric pressure when pressures are increased to 1/3 of the critical, after which it drops with a further rise of pressure, becoming lower than the q_{kp1} for atmospheric pressure at $p > 190$ atmospheres.

2. On the basis of the 1950 data, it may be assumed for practical purposes in the boiling of water in the pressure range 25-125 atmospheres that:

$$q_{kp1} \approx 3{,}250{,}000 \pm 5\% \text{ kg-cal/m}^2\cdot\text{h}.$$

3. The S. S. Kutateladze equation satisfies the experimental data best. Optimum mean agreement is had when the coefficient k is taken as 0.13.

LITERATURE CITED

1. E. A. Kazakova, Reports USSR Acad. Sci. 71, No. 1, 1950.
2. E. A. Kazakova, Bull. USSR Acad. Sci., Div. Tech. Sci., No. 9, 1950.
3. Farber and Skorak, Trans. ASME, No. 5, 1948.
4. E. A. Kazakova, Bull. USSR Acad. Sci., Div. Tech. Sci., No. 1, 1949.
5. McAdams, Addom, Rinaldo, and Day, Chem. Eng. Progress 44, No. 8, 1948.
6. G. N. Kruzhilin, Bull. USSR Acad. Sci., Dept. Tech. Sci., No. 5, 1949.
7. S. S. Dutateladze, J. Tech. Phys. 20, No. 11, 1950.

EXPERIMENTAL STUDY OF THE INFLUENCE OF THE TEMPERATURE OF A LIQUID ON A CHANGE IN THE RATE OF BOILING

S. S. Kutateladze, Candidate of Engineering Sciences, and
L. L. Shneiderman, Engineer

The I. I. Polzunov Central Scientific Research Institute for Boilers and Turbines

The hydrodynamic theory of crises in boiling has led to the conclusion that the relative effect of the temperature of the core of the flow of liquid on the critical density of thermal flow in the boiling boundary layer ought to decrease substantially as the pressure is increased. /Ref. 1/.

This conclusion, which is important both from the practical and the theoretical standpoint, could not be checked against published experimental data. The latter were confined to a few experiments by Miscicki and Broder /Ref. 2/, made by boiling water at thin wires at atmospheric pressure and with free convection, and the experiments of McAdams /Ref. 3/, made by boiling water in a constrained stream, flowing through a slit channel at a pressure of 2-6 atmospheres absolute. Thus, these data are not only limited in number but also not comparable with one another owing to the great difference between the ways in which the experiments were set up. We therefore made an experimental investigation of the influence of the liquid temperature upon the critical density of thermal flow in order to make a many-sided check of the theory and to secure numerical coefficients based on experiment.

The basic outline of the experimental setup is shown in Fig. 1, with a general view shown in Fig. 2.

The experimental heater 2 was mounted between special contacts within the drum 1. A heater served to compensate for the heat losses through the body of the drum and to maintain the given liwuid temperature in accordance with the readings of the thermocouple 4. Two windows of pyrex glass served for visual observation. The thermocouple 5 embedded in the experimental heater, made it possible to use the readings of the galvanometer 8 to fix the sharp change in the temperature of the heating service at the moment the boiling process changed.

When using a liquid, the bulk of which was not heated to the saturation temperature, pressure was maintained by using an inert gas (air, nitrogen), supplied via a reducing valve 11 from the tank 12.

Current was supplied to the experimental heater through a stepdown transformer 9, which had a regulating theostat 7 in its primary circuit. The voltage across the heater terminals and the current to the heater were measured by a Class .05 voltmeter and a Class 0.2 transformer with a Class 0.2 or 0.5 ammeter, respectively. The power taken by the compensating heater was regulated by the theostat 6.

It was found in calibrating tests that the ratio of the contact resistance to that of the heater remained constant to within 1-3% at all loads. We therefore ran the tests so that we found the relative of q_{kp}

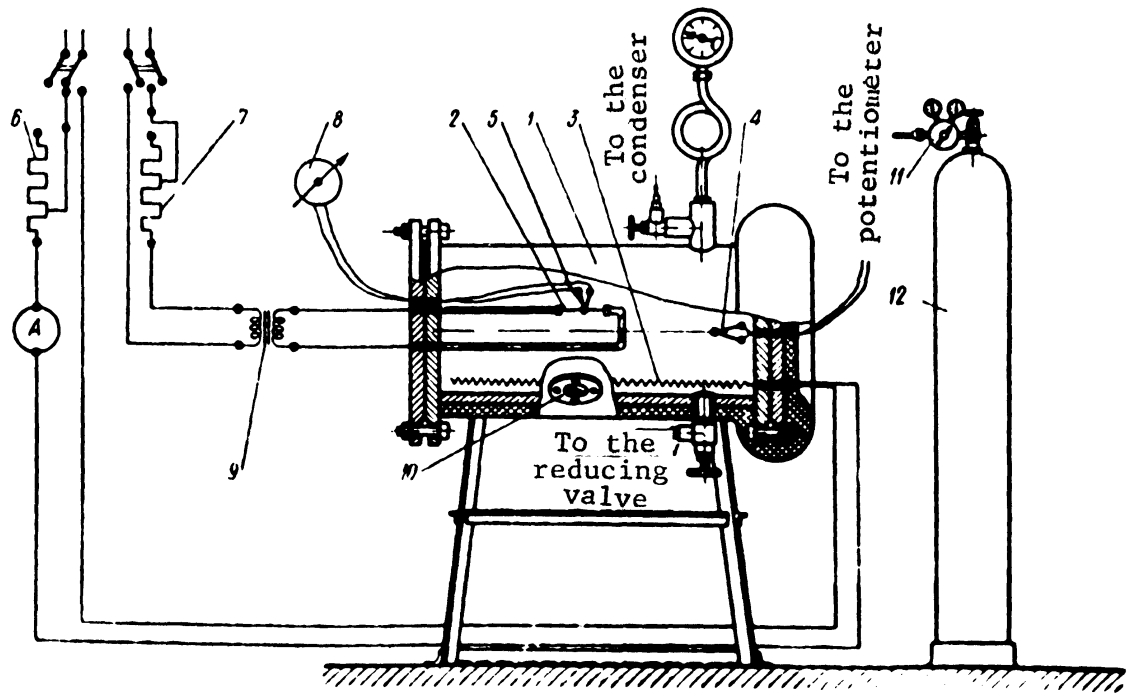

Fig. 1. Diagram of the experimental setup.
1 - Drum; 2 - experimental heater; 3 - compensating heater; 4 - thermocouple to measure the temperature of the liquid; 5 - thermocouple to measure the temperature of the experimental heater; 6 - rheostat for the compensating heater; 7 - rheostat in the transformer of primary winding; 8 - galvanometer; 9 - step-down transformer; 10 - sighthole; 11 - reducing valve; 12 - tank of gas.

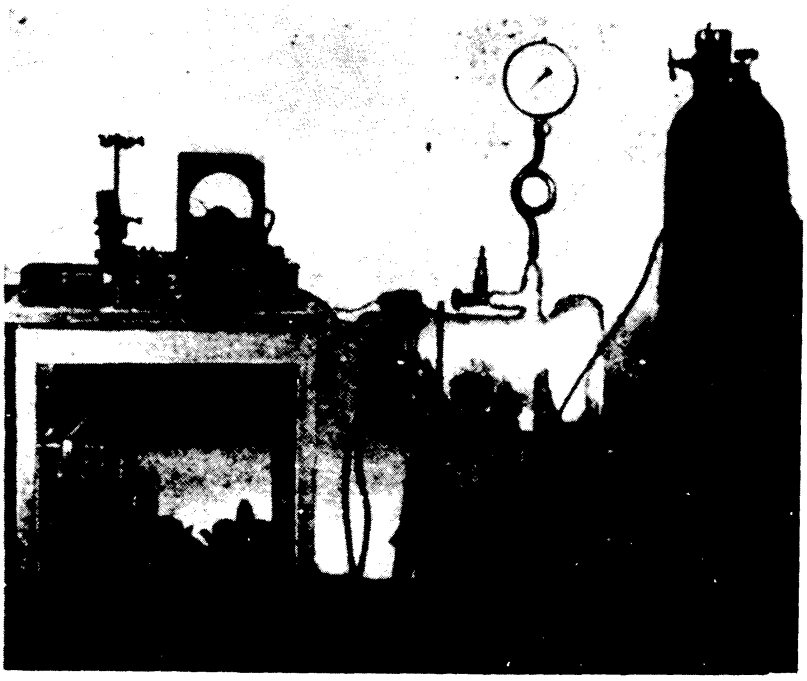

Fig. 2. General view of the setup.

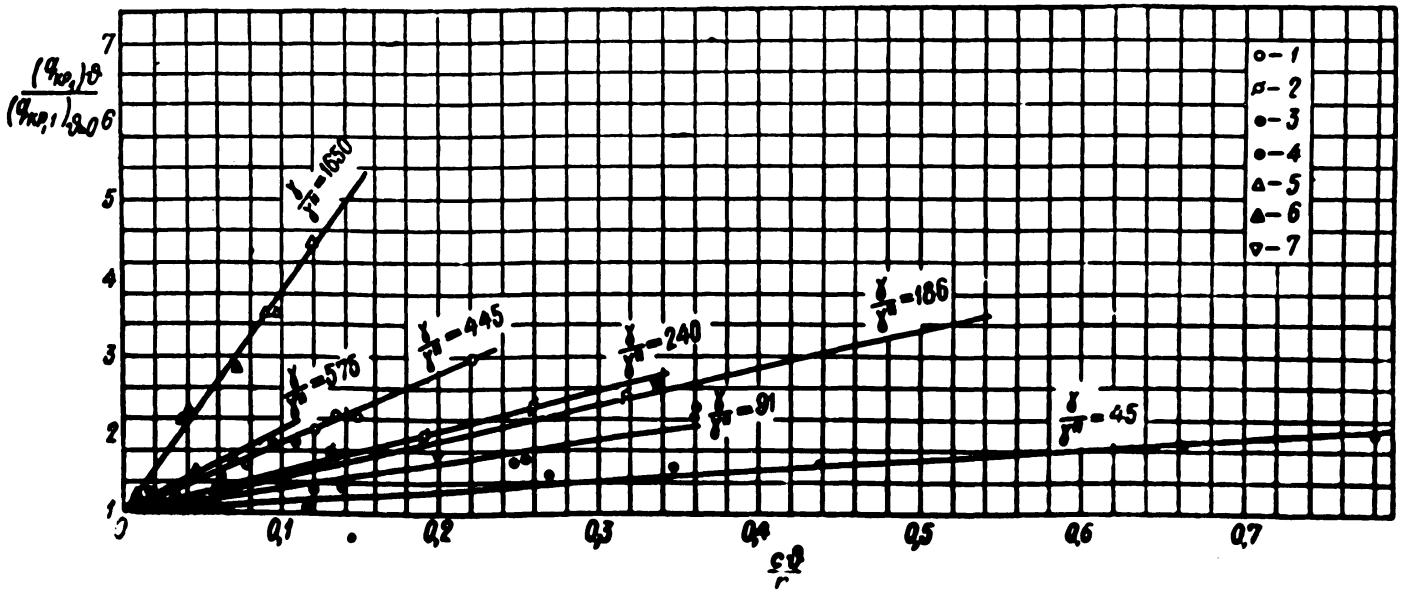

Fig. 3. Variation of $\frac{(q_{кр})_\theta}{(q_{кр})_{\theta=0}}$ with $\frac{c\theta}{r}$ and $\frac{T'}{T''}$ for the first critical density of thermal flow with free convection.

Alcohol: 1) p = 1 atm abs; 2) p = 2 atm abs; 3) p = 5 atm abs; 4) p = 10 atm abs. Water: 5) p = 1 atm abs; 6) p = 3 atm abs. Iso-octane: 7) p = 1 atm abs.

at various liquid temperatures without regard to the absolute value of the voltage drop at the contacts. This was done by running all the tests on the same heating surface, which was made of high-quality graphite to insure stability at high temperatures.

The liquid was heated by the compensation heater to the required temperature at a given pressure within the drum, established by admitting compressed gas. Then the main heater was turned on and its output was gradually raised by means of theostat 7. The instant when a vapor film was formed was fixed by the galvanometer (the onset of a sharp rise in the emf of thermocouple 5) and visually - by the shimmer of a graphite rod, whose reflection was observed in a mirror set at an angle to the sight-hole.

To prevent the high temperature from affecting the heating surface for any length of time, the current in the heater circuit was disconnected as soon as the development of film boiling had been detected.

In one series of experiments q_{kp} was measured at the same liquid temperature and different pressures. In some cases the pressure was kept constant and the liquid temperature was varied. At all pressures employed in the test we measured the expenditure of electric energy with the entire mass of liquid heated to the saturation temperature ($\vartheta = 0$).

Thus, without making corrections for losses at the contact, we determined the relationship:

$$\frac{(q_{\kappa p})_{\vartheta}}{(q_{\kappa p})_{\vartheta=0}} = \frac{(IV)_{\vartheta}}{(IV)_{\vartheta=0}}.$$

The experiments were run with water, alcohol, and iso-octane at various temperatures. The results of the tests are given in the table below and in Fig. 3. The tabulated data confirmed the correctness of the principal conclusions of the theory and made it possible for the first time to calculate the influence of the temperature of the liquid core on a change in the rate of boiling within the boundary layer /Ref. 1/.

Table of Experimental Data

Substance	Pressure, atm abs	Temperature of the liquid core °C	Difference between liquid temperature and saturation temperature, °C	Ratio
Ethyl alcohol	1.00	78.3	0	1.00
" "	1.00	74.2	41.1	1.10
" "	1.00	73.7	4.6	1.31
" "	1.00	70.0	8.3	1.33
" "	1.00	66.4	11.7	1.46
" "	1.00	61.5	16.8	1.48
" "	1.00	57.4	20.9	1.64
" "	1.00	52.8	25.5	1.91
" "	1.00	48.8	29.5	1.92
" "	1.00	45.7	32.6	2.10
" "	1.00	42.0	36.3	2.24
" "	1.00	38.5	39.8	2.21

Table Continued

Substance	Pressure	Temperature of the liquid core °C	Difference between liquid temperature and saturation temperature, °C	Ratio
Ethyl alcohol	1.00	18.6	59.8	2.98
" "	2.00	95.0	0	1.00
" "	2.00	94.2	0.8	1.10
" "	2.00	87.5	7.5	1.14
" "	2.00	81.4	13.6	1.27
" "	2.00	81.4	13.6	1.24
" "	2.00	63.5	31.5	1.79
" "	2.00	50.2	44.8	2.02
" "	2.00	33.2	61.8	2.36
" "	2.00	19.0	76.0	2.50
" "	5.00	123.6	0	1.00
" "	5.00	118.0	5.6	1.05
" "	5.00	116.6	7.0	1.05
" "	5.00	118.0	5.6	1.02
" "	5.00	97.5	26.1	1.34
" "	5.00	100.2	23.4	1.33
" "	5.00	75.6	48.0	1.74
" "	5.00	77.0	46.6	1.67
" "	5.00	55.4	68.2	2.23
" "	5.00	55.4	68.2	1.98
" "	5.00	55.4	68.2	2.32
" "	9.90	147.0	0	1.00
" "	9.90	129.0	18.0	1.04
" "	9.90	105.5	41.5	1.51
" "	9.90	93.5	53.5	1.58
" "	9.90	79.6	67.4	1.61
" "	9.90	45.0	102.0	1.87
" "	9.90	27.0	120.0	2.00
Iso-octane	1.00	9.7	0	1.00
" "	1.00	68.4	28.6	1.76
" "	1.00	48.6	48.4	2.62
" "	1.00	20.7	76.3	3.60
Water	1.00	100.0	0	1.00
"	1.00	80.2	19.8	2.20
"	1.00	77.5	22.5	2.29
"	1.00	60.7	39.3	2.82
"	1.00	51.1	48.9	3.55
"	1.00	48.8	51.2	3.55
"	1.00	36.4	63.6	4.45
"	2.05	132.0	0	1.00
"	2.05	126.8	5.2	1.23
"	2.05	121.5	10.5	1.24
"	2.05	103.5	28.5	1.54
"	2.05	96.0	36.0	1.71

LITERATURE CITED

1. S. S. Kutateladze, Bull USSR Acad. Sci, Div. Tech. Sci, No. 4, 1951.

2. Moscicki and Broder, Rocznicki chem., No. 6, 1926.

3. McAdams and others, Industrial and Eng. Chem., No. 9, 1949.

INFLUENCE OF PRESSURE AND PROPERTIES OF THE LIQUID ON THE CESSATION OF FILM BOILING WITH FREE CONVECTION IN A LARGE SPACE

V. M. Borishansky, Candidate of Engineering Sciences

The I. I. Polzunov Central Scientific Research Institute of Boilers and Turbines

It has been established experimentally that film boiling replaces nuclear boiling at definite thermal loads at the heating surface, q_{kp1}. The continuous vapor film observed in this case results in a sharp decrease of the rate of heat transfer and in overheating of the heating surface. The experiments described below were devoted to an investigation of the reverse transition from film to nuclear boiling. This phenomenon is manifested in a destruction of the vapor layer at a certain thermal load on the heating surface, q_{kp2}, which depends on the properties of the liquid and the saturation pressure.

1. EXPERIMENTAL METHOD

The experimental setup consisted of a steel drum filled with the liquid under test. A horizontal cylindrical heating surface, made of carbon, about 50 mm long and about 2.2 mm in diameter, and heated by electric current, was installed along the axis of the drum. The details of the setup are to be found in Fig. 1 of the preceding paper, where we show a diagram of the setup, slightly changed, compared to that used in running the present experiments.* Neva tap water, benzene (commercial), iso-octane, and carbon tetrachloride (commercial) were used as the working liquids.

After the experimental rod was mounted between the contacts, the drum was filled with liquid, which was then heated to the saturation temperature by connecting the compensating heater. Then the stopcock was closed, and the pressure was raised. When the desired pressure had been reached, the operating circuit was energized and nuclear boiling was established at the heating surface. The thermal load on the heating surface was raised to the critical value q_{kp1} by regulating the current flowing in the operating circuit, nuclear boiling was stopped, and film boiling was set up over the entire surface. The latter was determined (by direct observation through sightholed) by the disappearance of vapor bubbles and the formation of a vapor jacket over the heating surface, this being checked by the sharp deflection of the needle of a galvanometer inserted in the circuit of a thermocouple embedded in the experimental heating surface. Then the thermal load was gradually lowered while maintaining film boiling. The cessation of film boiling was determined visually by the disappearance of the vapor layer at the surface and by the establishment on the surface of the state of affairs that is characteristic for the development of nuclear boiling. It was checked by the galvanometer reading, the needle of the latter sharply dropping at

* The diagram does not show the condenser, which was connected to the upper valve when organic liquids were used. No gas tanks were required, as the experiments were run along the saturation line. For details see "Boiler and Turbine Construction," 3, 1951.

the instant of the second crisis owing to the rapid drop of the temperature of the surface during the change from film to nuclear boiling. The thermal load on the heating surface corresponding to this change of boiling rates was recorded as q_{kp2}. It should be borne in mind that the onset of the second crisis cannot be identified with the incandescence of the heating surface, inasmuch as the darkening of the surface occurs long before cessation of boiling when organic liquids are used.

The method described above for determining q_{kp2} was employed in our work with benzene, iso-octane, and carbon tetrachloride. In the case of water at pressures above the atmospheric, the establishement of film boiling was accompanied by intensive heating of the heating surface, which sometimes resulted in damage to it. We therefore changed the procedure soemwhat in our water experiments.

At first, film boiling was set up at atmospheric pressure over the entire heating surface. Then the thermal load was lowered somewhat to approximately 400,000 kg-cal/m^2·h. Then the stopcock was closed and the pressure within the apparatus was raised with the compensation heater turned on. As the temperature rose it was found necessary to raise the thermal load somewhat to maintain steady film boiling over the heating surface. Once the desired pressure had been reached, q_{kp2} was determined as in the experiments with the organic liquids. In so doing the compensating heater was cut out almost completely.

The main experiments with benzene, as well as the experiments with iso-octane and carbon tetrachloride, were made with the same heating surface, made of the same material and processed as in the water experiment, this being necessary to secure comparable data.

2. EXPERIMENTAL RESULTS

The data of our experiments with water, benzene, iso-octane, and carbon tetrachloride to determine the variation of q_{kp2}, the second critical density of thermal flow, with the saturation pressure are shown in Fig. 1 and in Tables 1, 2, 3, and 4. The pressure was raised to 16 kg/cm^2 in the water experiments. The points plotted on the graph were secured with 17 rods. The reproducibility of the experiments, which indicate that the second critical density of thermal flow, q_{kp2}, depends rather substantially on the pressure, rising as the latter is raised.

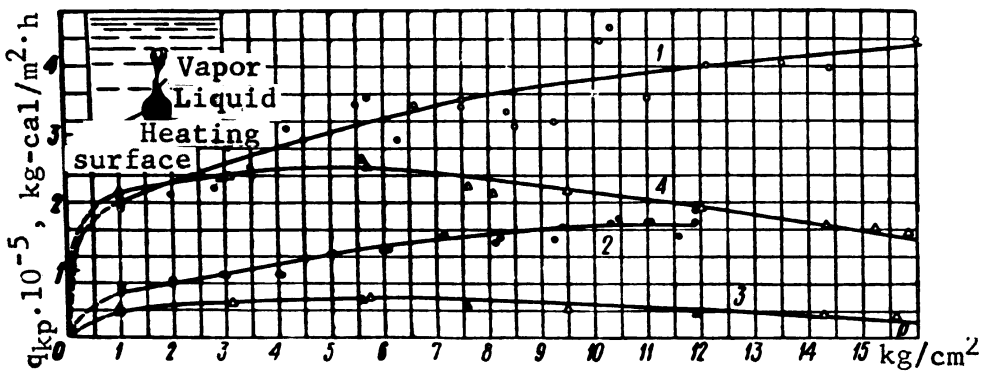

Fig. 1. Influence of saturation pressure on a change in boiling. q_{kp2}: 1 - water; 2 - benzene; 3 - iso-octane; q_{kp1}: 4 - iso-octane.

In our experiments with benzene the pressure was raised to 12 kg/cm^2. The value of q_{kp2} was determined twice for each pressure for the sake of greater dependability.

TABLE 1

Influence of Pressure on Cessation of Film Boiling of Water, q_{kp2}

Saturation pressure p kg/cm^2	Diameter of experimental heater d mm	Critical thermal load q_{kp2} kg-cal/m^2·h	Saturation pressure p kg/cm^2	Diameter of experimental heater d mm	Critical thermal load q_{kp2} kg-cal/m^2·h
4.2	2.15	310,000	3.5	2.195	250,000
4.5	2.155	292,000	2.0	2.195	213,000
5.7	2.197	355,000	9.25	2.196	319,000
11.0	2.194	355,000	6.3	2.197	288,000
5.5	2.24	343,000	6.6	2.197	340,000
10.3	1.192	457,000	1.03	2.197	206,000
13.5	2.195	406,000	7.5	2.194	340,000
14.4	2.193	393,000	1.03	2.194	201,000
12.1	2.193	401,000	10.1	2.198	435,000
16.0	2.199	440,000	7.5	2.181	352,000
8.5	2.174	308,000	1.03	2.181	187,000
2.8	2.174	222,000	1.03*	2.195	188,000
8.3	2.195	331,000	1.03*	2.195	209,000

NOTE: The diameters of the rods were determined as the mean value of ten measurements with a micrometer along the length of the rod.

After the experiments with benzene had been made, the apparatus was not opened, but was thoroughly washed out with boiling water for a long time (about 30 hours). Then the value of q_{kp2} was twice determined for water at atmospheric pressure, using the same heating surface. The values secured agreed with the values obtained in the water experiments (last two columns in Table 1). We were thus able to compare the results secured for different liquids.

It is seen in Fig. 1 that the value of q_{kp2} for benzene in the pressure range investigated rose with pressure exactly as was the case with water. In the case of benzene, however, the curve becomes practically horizontal at a pressure of as little as 12 kg/cm^2, i.e., the rate of change of q_{kp2} is more abrupt than for water.

In the experiments with iso-octane the pressure was varied from 1 to 16 kg/cm^2. The latter pressure corresponds to $\frac{p}{p_{kp}} \approx 0.6$. This made it possible to secure the maximum on the curve $q_{kp2} = f(p)$, already noted in benzene experiments, and to investigate the nature of the change of the curve as it approached the critical pressure p_{kp}. In addition to the se-

* After experiments with benzene.

TABLE 2

Influence of Pressure on Cessation of the Film Boiling of Benzene
(Graphite, d = 2.2 mm)

Saturation pressure p kg/cm^2	Critical thermal load q_{kp2} kg-cal/m^2·h	Critical surface temperature t_{kp2} °C	$\Delta t_{kp2} = t_{kp2} - t''$ °C	$\alpha = \frac{q_{kp2}}{\Delta t_{kp2}}$ kg-cal/m^2·h·deg
1.03	68,000	192	112	609
1.03	68,000	192	112	609
2.0	84,200	218	115	728
2.0	81,200	211	109	745
3.0	91,600	248	130	705
2.95	91,600	246	129	711
4.05	94,000	266	135	695
4.0	95,000	268	137	690
5.05	126,000	290	149	848
5.0	126,000	307	167	756
6.06	132,000	331	179	740
6.0	128,000	309	158	810
7.15	154,000	338	178	865
1.03	72,500	--	--	--
7.05	149,000	336	175	851
8.2	149,000	339	172	869
8.1	141,000	350	185	761
9.4	161,000	356	181	890
9.2	146,000	365	192	761
10.45	175,000	380	201	873
10.3	168,000	369	179	939
11.05	171,000	383	200	855
11.0	173,000	383	205	862
11.95	190,000	--	--	--
11.9	171,000	--	--	--
11.6	150,000	336	149	1005
1.03	68,600	--	--	--
1.03	67,500	--	--	--

cond critical density of thermal flow, in these experiments we also measured the first critical density of thermal flow, q_{kp1}. Our results indicate that the curve of $q_{kp2} = f(p)$ passes through a maximum approaching zero at the critical point $\left(\frac{p}{p_{kp}} = 1\right)$. Thus we find an analogy in the shape of the pressure function for both crises. The ratio $\frac{q_{kp2}}{q_{kp1}}$ remains approximately constant throughout the pressure range, being approximately 0.2 The ratio $\frac{q_{kp2}}{q_{kp1}}$ is 0.17 in the experiments with water and 0.22 in the experiments with benezene. This ratio is 0.17 according to Kazakova's experiments on water at atmospheric pressure. These figures obviously bear out the view that the value of $\frac{q_{kp2}}{q_{kp1}}$ practically varies but little

throughout the pressure range when liwuid is boiled in a large space

In the experiments using carbon tetrachloride the values of q_{kp2} were determined only for two pressures and are shown only in Table 4. Comparing the values of q_{kp2} at a pressure of 3 kg/cm^2, we see that that they differ considerably for different liquids. Whereas q_{kp2} = 250,000 for water, 100.000 for benzene, and 48,000 for iso-octane, it is only 43,000 kg-cal/m^2·h for carbon tetrachloride.

The experiments with benzene on heating surfaces made of various grades of lead-pencil graphite indicated that the condition of the heating surface likewise affects the value of q_{kp2} to a certain extent. The nature of the influence of the saturation pressure remains the same, however (the pressure was varied from 1 to 16 kg/cm^2)

TABLE 3

Influence of Pressure on the Cessation of Nuclear (q_{kp1}) and Film (q_{kp2})

Boiling of Iso-octane
(Graphite, d = 2.2 mm)

Saturation pressure p kg/cm^2	Cessation of nuclear boiling q_{kp1} kg-cal/m^2·h	Cessation of film boiling q_{kp2} kg-cal/m^2·h
1.03	219,000	38,800
1.03	--	43,000
2.9	239,000	--
3.1	239,000	48,900
5.7	251,000	53,000
5.6	265,000	51,000
7.6	224,000	41,500
8.1	215,000	--
9.5	219,000	42,700
11.9	190,000	38,200
14.3	167,000	36,900
15.2	164,000	--
15.6	--	34,900
15.8	159,000	--

TABLE 4

Influence of Pressure on the Cessation of Film Boiling of Carbon Tetrachloride, q_{kp2}

Saturation of pressure p kg/cm^2	Critical thermal load q_{kp2} kg-cal/m^2·h	Remarks
3.0	43,500	)
5.6	62,500	) Diameter 2.2 mm

At high thermal loads the flow of the vapor layer along the heating surface is steady during film boiling, and the interphase boundary is clearly outlined and smooth. But as the thermal load is reduced the behavior of the vapor film changes. The interface between liquid and vapor begins to pulsate vigorously. When we approach thermal loads close to the values of q_{kp2}, the vapor film is irregular and undergoes pronounced fluctuations; we observe that the steadiness of flow of the vapor layer diminishes considerably. The second crisis and the subsequent transition to nuclear boiling is marked by the final breakdown of steady flow of the vapor film, resulting in its destruction. The latter begins with the disappearance of a continuous vapor layer at some place or other on the heating surface and the establishment in this area of the state of affairs that is characteristic of nuclear boiling. Then, the boundary between the zones of film and nuclear boiling gradually shifts, with the thermal load on the heating surface remaining unchanged, and nuclear boiling is set up over the entire surface.

The behavior of the vapor layer during film boiling as the thermal load is reduced differs somewhat for different liquids. Thus for water the instability of flow of the vapor film becomes directly noticeable only in the vicinity of the second crisis. On the other hand, in the boiling of benzene and, especially, of carbon tetrachloride the breakdown of flow stability is observed long before the crisis, the mobility of the vapor film being quite high and the film exhibiting a completely irregular form at times.

The experiments and observations described above justify the assumption that the breakdown of the vapor film, i.e. the cessation of film boiling, occurs as the result of a disturbance in the flow of the vapor layer due to an inadequate supply of vapor to it at some thermal load that is defined as q_{kp2}. This assumption enables us to relate the problem of the disturbance of stability of the free flow of the vapor layer at the heating surface during the boiling of a liquid in a large space with the thermal parameters of the process. In this case q_{kp2} should be regarded as the minimum thermal load on the heating surface that is required to barely insure the stable existence of a vapor layer over the heating surface.

The measured values of the heating-surface temperature at the instant film boiling ceases in benzene are shown in Fig. 2. These measurements were made at the same time as the measurements of q_{kp2} (see Table 2). The latter made it possible to calculate the coefficient of heat transfer in film boiling at the instant immediately preceding the breakdown of the vapor layer. As is seen in Fig. 2, the values of the coefficient of heat transfer rise with a rise in the saturation pressure.

Analysis of the boiling process from the standpoint of the theory of similitude has been discussed in fairly great detail in the literature /Ref. 1/. We may write the following system of criteria for the state in which film boiling breaks down:

$$\frac{q_{кр}}{r(g\gamma'')^{0,5}[\sigma(\gamma-\gamma'')]^{0,25}};\quad \frac{gl^2}{\nu^2};\quad \frac{\sigma}{(\gamma-\gamma'')l^2};\quad \frac{\gamma-\gamma''}{\gamma};\quad \frac{\nu}{a};$$
$$\frac{p}{l(\gamma-\gamma'')};\quad \frac{cT''\gamma^{\frac{3}{2}}\sigma^{0,5}}{(r\gamma'')^2A}. \qquad (1)$$

On the assumption that the process involved in the breakdown of the

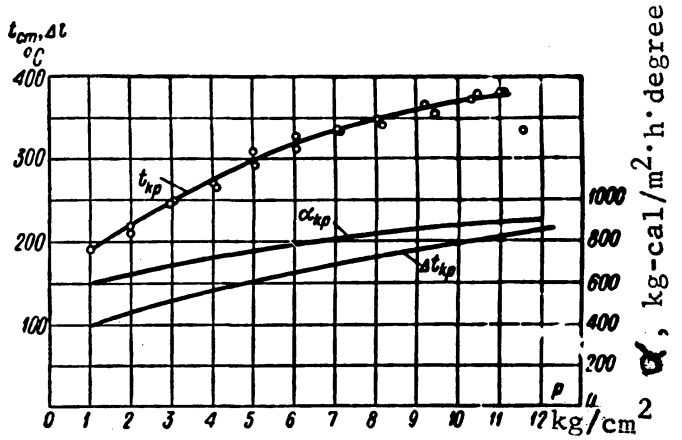

Fig. 2. Variation of t_{kp2}, Δt_{kp2}, and α_{kp2} with pressure in experiments using benzene.

t_{kp2} = temperature of heating surface at which the vapor layer breaks down;
$\Delta t_{kp2} = t_{kp2} - t''$, where t" = saturation temperature.

vapor layer is independent of the dimensions of the heating surface and, in view of the sparseness of the experimental material, and ignoring the last three system criteria (1) as a first approximation, we can confine ourselves to the following criterial relationship:

$$\frac{q_{kp2}}{r(g\gamma'')^{0,5}[\sigma(\gamma-\gamma'')]^{0,25}} = f\left[\frac{\gamma\sigma^{\frac{3}{2}}}{\mu^2 g(\gamma-\gamma'')^{0,5}}\right]. \qquad (2)$$

In these equations:

r = latent heat of vaporization.
γ, γ'' = specific gravities of the liquid and the vapor, respectively.
μ = dynamic viscosity of the liquid.
σ = surface tension.
g = acceleration due to gravity.
a = temperature conductivity.
T" = saturation temperature, °K.
p = saturation pressure.
l = dimensional factor.
A = mechanical equivalent of heat.

The results of our working-up* of the water experiments, using the

* Subsequent experiments are planned to shed light on the problem of the influence of the linear dimension of the heating surface on the value of q_{kp2}. If it is found that such influence does exist in the system (2), the criterion $\frac{\sigma}{(\gamma-\gamma'')l^2}$ must be introduced independently.

coordinates of Eq. (2) are shown in Fig. 3. As we see in the graph the criteria, including viscosity, have no perceptible effect, the experimental points lying close to a horizontal at 0.023.

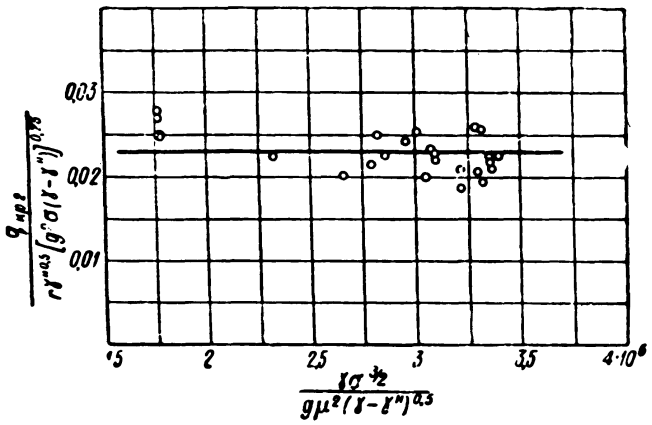

Fig. 3. Experimental data for water plotted in coordinates of Eq. (2).

3. CONCLUSIONS

1. A method has been developed for investigating the cessation of film boiling of a liquid in a large space.

2. The cessation of film boiling may be described by a definite value of thermal load on the heating surface, q_{kp2} (the second critical density of thermal flow).

3. It follows from the experiments that cessation of film boilinb is apparently related to a disturbance of steady flow of the vapor layer along the heating surface.

4. The experiments have shed light on the nature of the influence exerted by the saturation pressure on the value of q_{kp2}. It has been found that the curve $q_{kp2} = f(p)$ has a maximum at $\frac{p}{p_{kp}} < 0.5$, approaching zeto at the critical point $\frac{p}{p_{kp}} = 1$. It has been found that the values of q_{kp2} are greatly influenced by the physical properties of the liquid.

5. In the first approximation the curves q_{kp2} and $q_{kp1} = f(p)$ are similar. Practically speaking, they both have a maximum at the same pressure, the ratio $\frac{q_{kp2}}{q_{kp1}}$ remaining approximately constant throughout the pressure range.

LITERATURE CITED

1. S. S. Kutateladze. Heat Transfer in Condensation and Boiling. State Scientific and Technical Publishing House of Machinery Literature, 1949, 1952.

HEAT TRANSFER TO A LIQUID FREELY FLOWING OVER A SURFACE HEATED TO A TEMPERATURE ABOVE THE BOILING POINT

V. M. Borishansky, Candidate of Engineering Sciences

The I. I. Polzunov Central Scientific-Research Institute

Metal heated to a high temperature is cooled by a liquid in several technological processes (for example, hardening, metal cutting, continuous casting, setting up water curtains in heating furnaces, and the like).

A characteristic feature of heat transfer in the free flow of a liquid over a surface heated to a high temperature is the existence of a vapor in-between that impairs heat exchange considerably, compared to ordinary nuclear boiling. In some case, the heating surface may also be a liquid, whose boiling point and density are higher than those of the cooling liquid /Ref. 1/.

Several papers have been written on the problem of the so-called "spheroidal state" of a liquid. Of greatest interst is the research done by N. A. Gezekhus /Ref. 2/, who demonstrated as far back as 1876 that a liquid is separated from the heating surface by a layer of vapor, the thickness of which depends upon the volume of the liquid being vaporized (the dimension of the spheroid) and the temperature of the heating surface. N. A. Pleteneva and P. A. Rebinder /Ref. 3/ found that when small drops are vaporized at a fixed temperature of the heating surface, the ratio $\frac{\tau}{D_o}$, where τ is the total time required for vaporization of the drop, and D_o is its initial diameter, remains constant. They also investigated the effect of adding surface-acting substances and of changing the hydrodynamic conditions of liquid flow upon vaporization. These papers were confined to an investigation of a comparatively narrow range of dimensions of the vaporizing volumes of the liquid and did not yield a generalized method for calculating the cooling of the heating surface.

The present paper presents material stemming from an experimental investigation of the vaporization of a liquid flowing freely along the heating surface over a comparatively wide range of volumes of the vaporized liquids and of the heating-surface temperature.

1. EXPERIMENTAL SETUP

The experimental apparatus was used in investigating the vaporization of various liquids on open horizontal plates made of brass, copper, and steel heated to temperatures in the neighborhood of 600° C.

The apparatus consisted of a ceramic furnace with interchangeable covers, which served as the heating surfaces. The dimensions of the latter were varied both in thickness (2-8 mm) and in diameter (70-200 mm). To avoid edge losses the heater heated a much larger area than the working portion of the heating surface. The furnace was placed in a glass-walled thermostat (Fig. 1).

The temperature of the liquid and of the air within the thermostat

was measured by thermometers, thermocouples being used to measure the temperatures of the heating surface. The initial volumes of liquid to be vaporized ranged from 0.00742 to 34 cm^3.

Pipettes were used to secure minute drops. The pipettes were graduated by counting the drops, whose volume was determined as the mean of several thousand readings. Larger quantities of liquid (0.5-5 cm^3) were poured on the heating surface directly from burettes and graduated cylinders (for quantities in excess of 5 cm^3).

The geometric dimensions of the spheroids were determined by means of a coordinate grating whose scale was graduated to 0.02 mm. The diameter of the large bubblelike spheroids was determined by pouring the liquid into previously measured metal rings. We had available for this purpose a set of rings with diameters of 30, 60, 80, and 100 mm, which were successively placed on the heated surface.* Then enough liquid was poured out for the resultant spheroid to take up the entire area bounded by the ring. By making several tests in succession we managed to measure the quantity of liquid corresponding to a ring of given diameter with a fair degree of accuracy. By way of check we also photographed the bubblelike spheroids of measured volume without the bounding rings. In this case, the diameter of the spheroid was determined by using a planimeter to measure the areas on the photographs. The working liquids used were water (distilled), alcohol (rectified), benzene (commercial), and carbon tetrachloride.

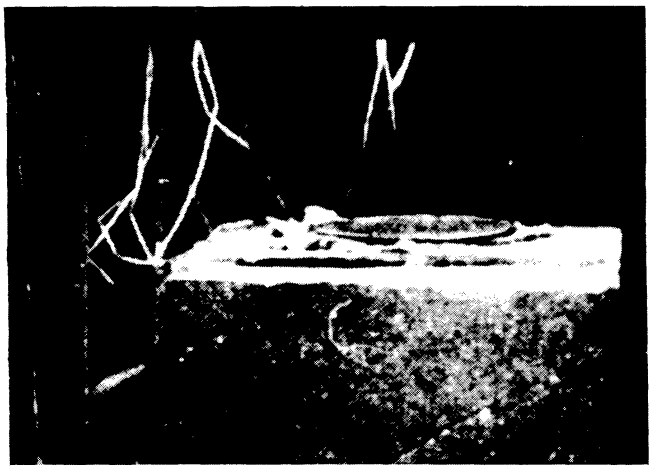

Fig. 1. General view of the apparatus.

2. EXPERIMENTS WITH SMALL DROPS

At the beginning of the experiment we established the definite temperature of the heating surface, t_{cm}, which was maintained constant throughout the vaporization of the given quantity of liquid. A drop of the liquid was placed on the heating surface by means of a pipette, and a stopwatch was used to measure the elapsed time for its vaporization, τ.

* When this was done the temperature of the ring was practically the same as that of the heating surface.

The results of our measurements of the total vaporization time for a drop of water on brass surface 2 and 8 mm thick are shown in Fig. 2 and Table 1.

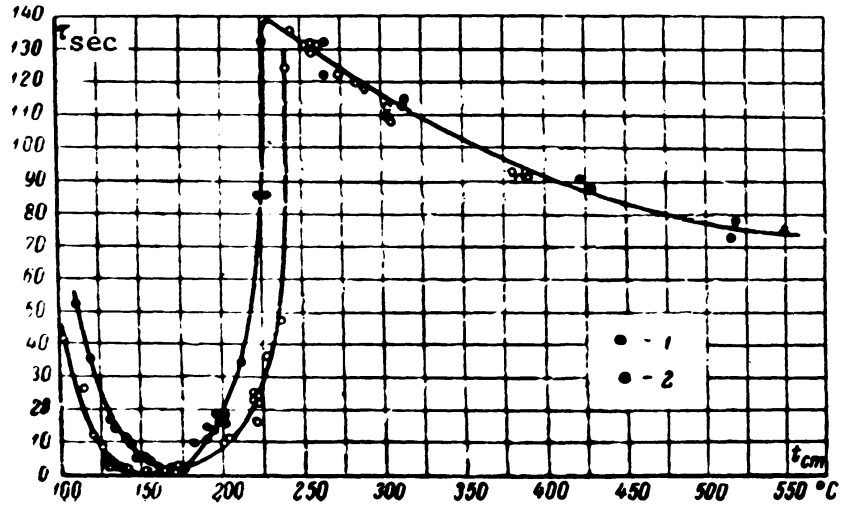

Fig. 2. Total vaporization time of a drop of water as a function of the temperature of the heating surface:
1) $v_o = 0.0465$ cm^3; brass 2 mm thick.
2) $v_o = 0.0458$ cm^3; brass 8 mm thick.

The curves plotted in Fig. 2 show that there are two characteristic temperatures of the heating surface, t_{kp1} and t_{kp2}, at which the curve $\tau = f(t_{cm})$ undergoes abrupt changes during the course of vaporization.

TABLE 1

Total Vaporization Time for a Drop, , as a Function of the temperature of the Heating Surface, t_{cm}

t_{cm} °C	τ sec	t_{cm} °C	τ sec	t_{cm} °C	τ sec	t_{cm} °C	τ sec
Water (distilled); $v_o = 0.0465$ cm^3; first test series							
118	35.0	141	9.0	222	85.0	422	91.0
110	52.0	152	2.0	225	132.0	430	88.4
197	15.0	165	1.8	229	85.0	514	73.0
138	11.0	170	1.2	261	129.0	518	78.0
146	4.6	175	1.2	265	122.0	550	75.0
149	4.6	193	13.0	265	132.0	181	9.6
153	3.0	194	17.6	314	115.0	189	13.6
130	16.6	199	17.0	314	112.5	187	10.0
133	13.6	210	34.0	--	--	--	--
Water (distilled); $v_o = 0.0458$ cm^3; second test series							
114	26.8	142	0.8	236	47.2	159	0.6

Table 1 continued

t_{cm} °C	τ sec	t_{cm} °C	τ sec	t_{cm} °C	τ sec	t_{cm} °C	τ sec
119	12.2	142	0.8	219	23.6	101	41.4
118	11.8	142	1.0	219	24.2	128	1.6
124	8.0	145	1.0	220	15.8	132	1.2
128	4.2	150	0.6	220	21.8	136	1.0
127	3.6	286	119.6	221	22.4	136	1.0
128	3.0	289	118.4	219	22.0	138	0.8
133	3.0	276	112.2	258	131.0	140	0.6
133	2.8	274	112.0	259	131.0	169	1.6
136	1.8	255	131.0	259	131.6	200	15
136	1.8	244	135.4	259	131.2	170	2.6
137	1.8	256	131.6	202	10	227	35.6
140	1.6	257	128.8	200	9	306	108.6
140	1.2	257	131.0	199	9	304	112.8
142	0.8	242	124.0	199	9	304	110.0
389	90.6	388	92.6	388	92.0	381	93.6
--	--	--	--	--	--	386	90.4
		Alcohol (C_2H_5OH); v_o = 0.01362 cm^3					
260	30	132	1.8	167	34.8	245	33.0
260	30.6	135	2.2	168	35.2	252	29.6
260	31.2	136	4.4	168	36.2	259	30.8
260	29.6	138	6.0	168	36.8	260	31.2
262	30.2	139	6.8	168	37.2	261	30.2
342	22.2	142	7.4	168	36.0	291	26.0
343	22.0	146	9.6	168	39.6	292	27.0
343	22.2	148	11.8	168	38.0	293	26.2
343	22.0	150	11.8	168	35.6	293	27.6
343	20.6	153	20.6	188	36.4	305	24.2
343	21.8	152	17.2	188	36.6	305	25.2
184	36.4	153	26.2	198	37.0	305	25.6
113	0.4	158	26.6	198	37.2	353	21.6
81.0	2.0	159	30.6	198	37.4	365	20.2
111	0.4	162	28.6	197	35.8	369	20.8
123	0.2	165	33.8	197	37.0	371	20.2
118	0.2	166	33.2	197	36.4	373	20.6
132	1.6	166	35.8	241	33.6	403	20.6
--	--	--	--	--	--	405	18.8
		Carbon Tetrachloride (CCl_4); v_o = 0.00913 cm^3					
460	10	535	7.2	464	10.6	304	15.8
460	10	535	9.4	394	10.8	304	16.4
463	8.6	535	9.2	394	12.6	304	14.0
465	9.0	544	8.8	394	11.6	304	14.0
465	10.2	544	8.6	386	11.0	235	16.0
465	10.6	544	8.6	386	12.4	235	17.0
532	7.6	544	8.4	380	11.2	235	16.0
532	7.0	464	10.0	380	12.2	235	17.8
535	8.4	464	9.8	380	12.2	235	16.2
535	8.4	464	10.8	310	15.0	235	17.0
535	8.4	--	--	--	--	--	--

Table 1 continued

t_{cm} °C	τ sec	t_{cm} °C	τ sec	t_{cm} °C	τ sec	t_{cm} °C	τ sec
			CCl_4; v_o = 0.00742 cm^3				
373	11.8	376	12.2	383	11.0	381	12.4
386	12.0	386	11.0	390	11.2	--	--

NOTES. 1. Heating surface in these tests: water, 1st series - brass 2 mm thick; water, 2nd series - brass 8 mm thick; alcohol (rectified) - brass 8 mm thick; carbon tetrachloride (commercial) - steel 5 mm thick for v_o = 0.00913 and brass 8 mm thick for v_o = 0.00742.

2. Initial temperature of the liquid: water, 1st series, and carbon tetrachloride: t = 20° C; water, 2nd series, and alcohol: t = 38° C.

3. The drop diameters were computed from the formula:

$$D = \sqrt[3]{\frac{6v_0}{\pi}},$$

where v_o is the initial volume of the drop.

4. In calculations using Eq. (11) the physical properties were based on the saturation temperature (Table 8).

The visual observations indicate that at $t_{cm} < t''$, where t" is the temperature of the saturated vapor, the drop of liquid spreads over the heating surface after falling on it and then vaporizes comparatively slowly. After the temperature of the heating surface rises above the saturation temperature, nuclear boiling is observed in the drop after it spreads. The process of nuclear boiling becomes more vigorous as the surface temperature is raised. The vaporizing time of the spreading drop of liquid then decreases, which is an indication of the increase in the coefficient of heat transfer.

When the temperature of the heating surface reaches t_{kp1}, the liquid no longer spreads after it strikes the surface, but collects into a spherical drop, and the time required for its complete vaporization begins to increase, notwithstanding a further rise in the temperature of the heating surface, which is an indication of a decrease in the rate of heat transfer.

When this form of vaporization first sets in, we frequently observe discontinuous contact between the spherical drop of liquid and the surface. As the temperature of the heating surface is raised contact is made less frequently, which lowers the rate of heat transfer and prolongs the time required for complete vaporization. At the instant of contact with the surface we observe the liquid boiling away, forming minute bubbles of vapor at the lower edge of the spheroid. As the temperature of the heating surface is raised still further the time required for the spheroid to vaporize continues to increase, reaching its maximum value at $t_{cm} = t_{kp2}$. It is of interest to replot these data in the following coordinates:

$$\frac{1}{\tau(t_{cm} - t'')} = f(t_{cm}),$$

inasmuch as the magnitude of $\frac{1}{\tau \Delta t}$ is proportional to the coefficient of heat transfer α.

We see in Fig. 3, where this replotting is shown for the test series at $v_0 = 0.0465$ cm^3, that the nature of the change in the curve is qualitatively analogous to the corresponding equation for the boiling of a liquid in a large space.

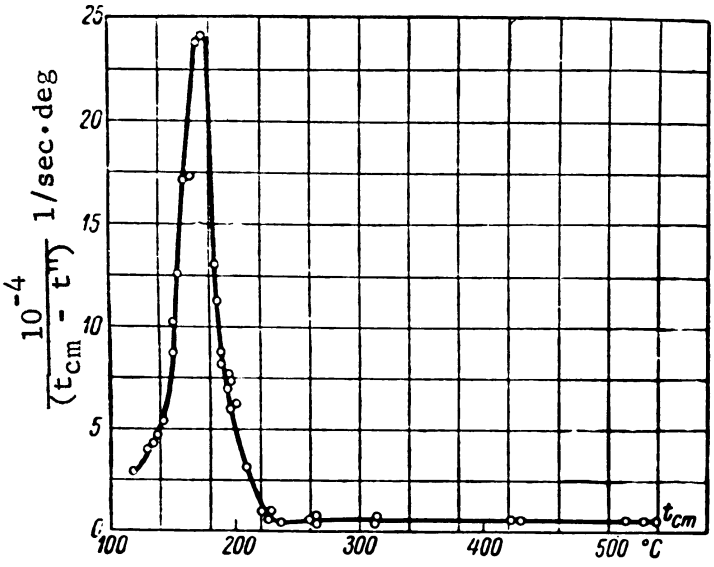

Fig. 3. Replot of the data in Fig. 2 in the coordinates:

$$\frac{1}{\tau (t_{cm} - t'')} = f(t_{cm})$$

The ordinates of the points to the left of the maximum have been reduced by a factor of 5, since the drop of liquid spreads in nuclear boiling, and its area is about 5 times as large as the projected area of the drop, referred to the right-hand branch of the curve.

Comparison of the data of the two series of tests run on surfaces of different thickness (Fig. 2) indicates that the points agree satisfactorily in the region of pure spheroidal state $(t_{cm} > t_{кр2})$. In the intermediate region $(t_{кр1} < t_{cm} < t_{кр2})$, and especially in the zone of nuclear boiling $(t_{cm} < t_{кр1})$, we observe a considerable difference between the curves. This is due, evidently, to the effect of some difference in the state of the heating surface between the two series of tests, which cannot manifest itself in the region of the pure spheroidal state, where the liquid is separated from the heating surface by a layer of vapor. Comparison of the values of t_{kp1} for the two series of tests indicates that

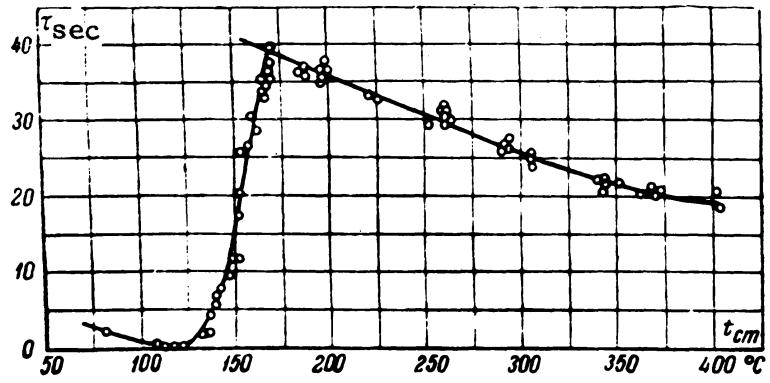

Fig. 4. The function $\tau = f(t_{cm})$ for alcohol.

this value is lower for the thicker plate (8 mm) than for the thin one (2 mm), being approximately 150° C and 175° C, respectively. The latter is apparently due to the deeper local cooling of the heating surface. As the experiments show, the thickness of the metal of the surface has a still smaller effect on the magnitude of t_{kp2}.

The data of our experiments on alcohol and carbon tetrachloride* are given in Fig.s 4 and 5 and in Table 1. Though the shape of the curve remains the same, the numerical values of the parameters vary, depending upon the physical properties of the liquid. Thus in tests run on the same surface (Figs. 2 and 4) t_{kp2} = 240° for water, 170° C for alcohol, while t_{kp1} = 150° and 120° C, respectively.

The results of our tests enable us to state that there are two critical temperatures in the vaporization of a liquid on an open heating surface. The first one is t_{kp1}, at which nuclear boiling ceases in the spreading liquid; this is the temperature that corresponds to the minimum vaporization time for the drop and the maximum rate of heat transfer from the heating surface to the vaporizing liquid. The second is t_{kp2}, at which the pure spheroidal state of the liquid is established. This is the temperature of the heating surface at which vaporization of the drop takes the longest time.

Special tests were run in which the initial water temperature was varied from 20 to 90° C in order to shed light on the effect of the initial temperature of the liquid on the critical temperatures. A brass plate 2 mm thick and a copper plate 5 mm thick were used as the heating surfaces.

The experiments (Fig. 6, Table 2) show that both the initial water temperature and the material of the heating surface do affect the values of t_{kp1} and t_{kp2}, even though the effect is not very great. An approximate estimate of the effect of the initial water temperature may be se-

* For CCl_4 all we got was the right-hand branch of the curve for

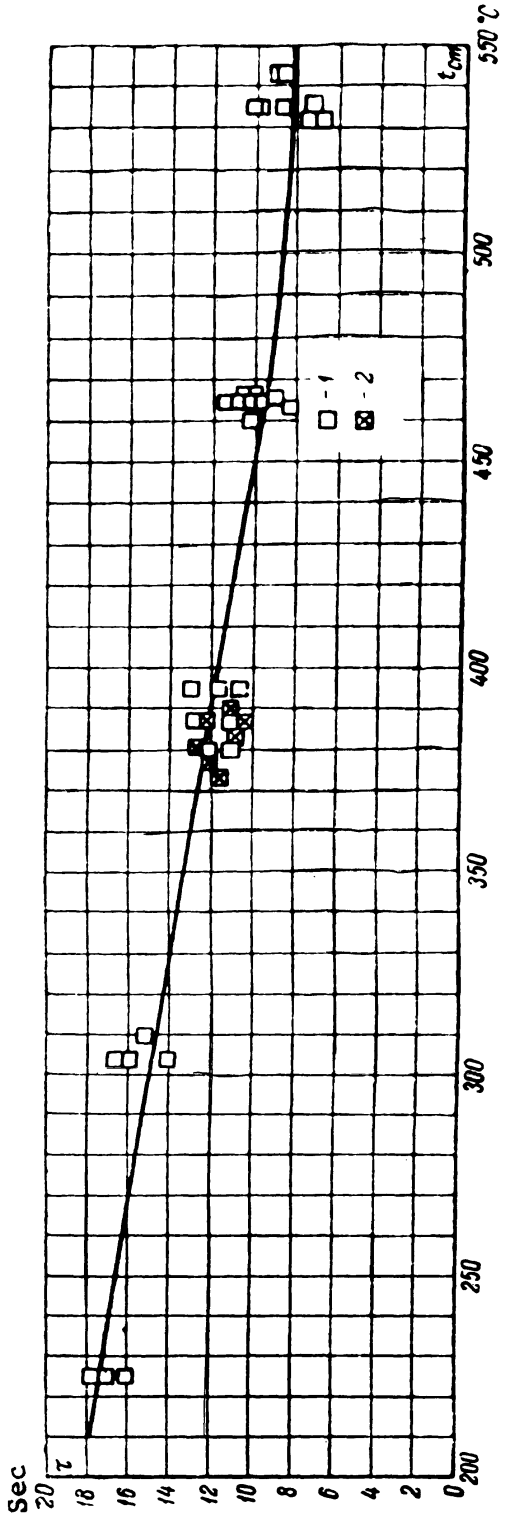

Fig. 5. The function $\tau = f(t_{cm})$ for carbon tetrachloride
1) v_o = 0.00913 cm^3; 2) v_o = 0.00742 cm^3.

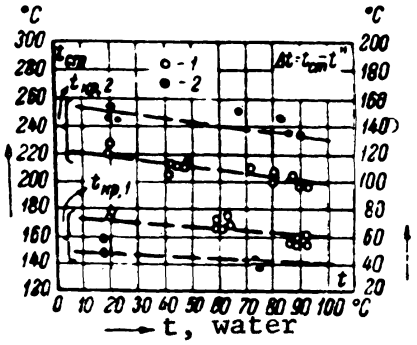

Fig. 6. Influence of the initial water temperature on the critical temperatures of the heating surface.
1 - brass, 2 - copper.

curd from the following considerations.

When the liquid is initially underheated, a certain quantity of heat must be expended to warm up the boundary layer of liquid in the drop to the saturation temperature at the instant it touches the heating surface. Hence, the ratio between the quantities of heat used in the two cases to vaporize the same quantity of liquid from a drop of the same size may be written as follows:

$$\frac{q}{q_{нед}} = \frac{r}{r + c\,(t'' - t_{ж})}. \qquad (1)$$

On the other hand, on the assumption that the coefficients of heat transfer are the same for underheating and when no underheating is present, we can write:

$$\frac{q}{q_{нед}} = \frac{t_{кр} - t''}{t_{кр.\,нед} - t''}, \qquad (2)$$

where $q_{нед}$ is the quantity of heat when the liquid is not heated to the saturation temperature, and q is the same quantity of heat when no underheating is present.

Combining these expressions, we get:

$$\frac{t_{кр} - t''}{t_{кр.\,нед} - t''} = \frac{r}{r + c\,(t'' - t_{ж})}. \qquad (3)$$

In this equation:

t'' = saturation temperature.

$t_{ж}$ = temperature of the liquid not heated to the saturation temperature.

r = latent heat of evaporization.

c = specific heat of the liquid.

TABLE 2

Effect of Initial Water Temperature on the Critical Temperatures of the Heating Surface

Water temperature t, °C	Surface temperature t_{kp}, °C	Water temperature t, °C	Surface temperature t_{kp}, °C	Water temperature t, °C	Surface temperature t_{kp}, °C	Water temperature t, °C	Surface temperature t_{kp}, °C
		I. Cessation of nuclear boiling, t_{kp1}					
			Brass, 2 mm thick				
20.0	174	58.0	170	63.0	166	89.5	152
20.0	177	63.0	172	91.5	152	91.0	155
59.0	168	61.0	165	88.0	158	86.0	156
--	--	--	--	--	--	91.0	160
			Copper, 5 mm thick				
18.0	155	18.5	147	21.0	151	74.0	137
19.0	152	73.0	144	--	--	--	--
		II. Establishment of the pure spheroidal state, t_{kp2}					
			Brass				
18.0	219	42.0	211	71.5	210	88.5	202.5
19.0	225	43.0	210	79.5	206	94.5	193.5
19.0	220	47.0	210	80.0	201	89.0	194.5
41.5	206	47.0	212	88.0	204	--	--
			Copper				
21.0	242	20.0	244	89.0	232	85.0	237
20.0	251	68.5	251	82.0	245	--	--
20.0	245	70.0	243	83.0	238	--	--

t_{kp} = critical temperature of the surface in the experiment using a saturated liquid.

t_{kp} = the same when the liquid is underheated below the saturation temperature.

In deriving the expression (3) we assumed that the drops are of identical size and have the same area of contact between the liquid and the heating surface.

The broken lines in Fig. 6 are plotted on the basis of calculations using Eq. (3). Their position agrees fairly satisfactorily with the experimental points.

Thus the method suggested may be regarded as practically adequate to account for the effect of liquid underheating on the values of the

critical temperatures of the heating surface.

3. EXPERIMENTS WITH LARGE QUANTITIES OF LIQUID

These experiments were generally run using the method employed for investigating the vaporization of small drops. In addition, we measured the dimensions of the spheroids directly and by photography. The heating surfaces were made of brass and steel. Only evaporation in the purely spheroidal state was investigated systematically.

Whereas the shape of small drops is close to that of a sphere during their vaporization, the shape of the sample changes as the initial quantity of liquid to be vaporized is increased, the spheroid becoming flatter and flatter.

As the size of the spheroid is further increased the vapor formed on its surface is unable to flow off to the periphery (see Fig. 7), beginning to break through the thickness of the liquid as systematically formed bubbles of vapor. The process of nuclear vapor formation sets in.*

As the initial volume of liquid is increased the number of vapor bubbles in the spheroid likewise increases. The frequency of their formation is affected by the temperature of the heating surface. After the vapor bubble breaks through the liquid a hole is formed, which is subsequently closed.

When electric current was passed in series through the bubbly spheroid and heating surface, we found that the circuit was briefly closed at the instant the vapor bubble broke through. When a flat spheroid was inserted in the circuit the circuit did not close.

Lowering the temperature of the heating surface to a level below the critical resulted in an explosive destruction of the vaporizing spheroid owing to the marked increase in vapor evolution, due to the onset of nuclear boiling. The temperature of the heating surface then begins to drop sharply.

The thickness of the spheroid δ and its diameter $\underline{D}$ are shown in Figs. 8 and 9 and Table 3 as functions of its volume $\underline{v}$. In these experiments the volume was varied up to 3 cm^3. As we see from the graph, the spheroid thickness remains practically unchanged after a certain volume has been attained, and the curve $\delta = f(v)$ approaches the horizontal. In experiments using water the appearance of a vapor bubble was observed as a rule in spheroids whose volume was 3 cm^3 or more. The results of experiments with large bubbly spheroids are given in Fig. 10 in coordinates of $D^2 = f(v)$ and in Table 4. The experimental points lie along straight lines with different slopes, depending upon the properties of the liquid. Hence, the thickness of the developed bubbly spheroid does not depend upon its volume, but is a constant for the given liquid.

The thickness δ of a bubbly spheroid, determined from the graph (Fig. 10), is lower than it should be, since the volume of the liquid is based on the entire area of the spheroid, although a substantial portion

---

* Detailed photographs of various forms of spheroids have been published previously /Ref. 8/.

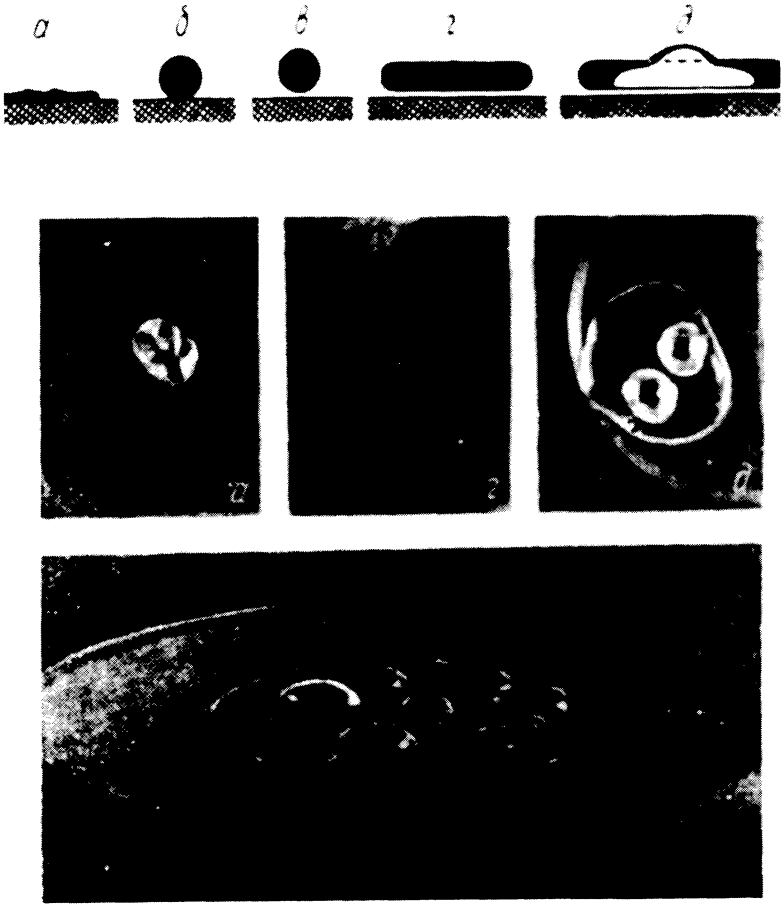

Fig. 7. Various stages of the spheroidal state: а - liquid spreading over the surface: nuclear boiling; б - cessation of nuclear boiling: liquid forms a sphere that makes intermittent contact with the heating surface; в - establishment of the purely spheroidal state: liquid separated from the heating surface by a continuous layer of vapor; г - flat spheroid; д - bubbly spheroid, with two large vapor bubbles clearly visible on its surface; е - large multibubble spheroid 100 mm in diameter.

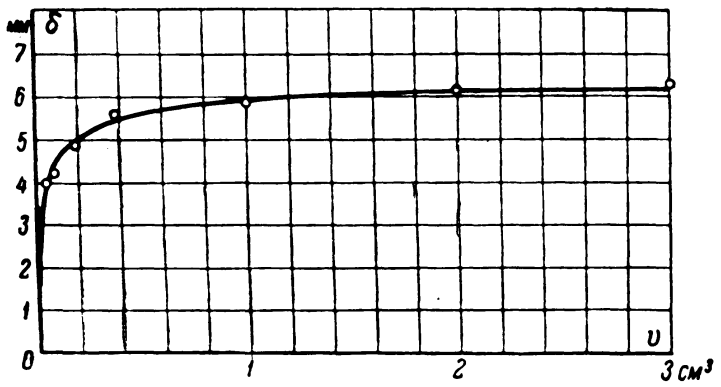

Fig. 8. Thickness of a water spheroid as a function of its volume.

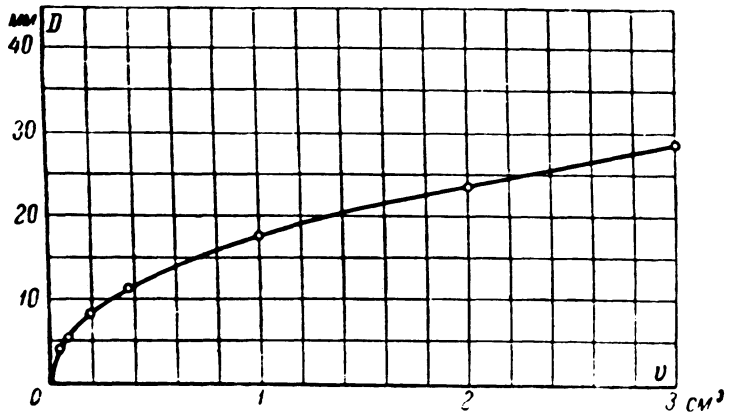

Fig. 9. Diameter of a water spheroid as a function of its volume.

TABLE 3

Correlation of Dimensions of Small Water Spheroids

Volume of liquid in the spheroid, V cm^3	Thickness of spheroid at its center, δ mm	Diameter of spheroid, D mm	Number of measurements
0.0465	4.0	4.04	18
0.093	4.2	5.32	15
0.086	4.86	8.4	27
0.372	5.58	11.1	17
1	5.86	17.7	79
2	6.14	23.7	107
3	6.28	28/9	59

of the volume is occupied by vapor bubbles. The overall area occupied by the latter may amount to as much as 50% of the total area of the spheroid in some cases. Direct measurements of the thickness of bubbly water spheroids with a micrometer yielded a value for $\delta \approx$ 7.5-8 mm.*

In our subsequent calculations we took the value of δ for water as 8 mm.

The fact that the volume of the spheroid has no effect upon its thickness enables us to consider a large bubbly spheroid as a system of single-bubble spheroids, each vaporizing independently of the other. We may therefore conclude that the coefficient of heat transfer is independent of volume for a fully developed multibubble spheroid.

* These measurements refer to the thickness of the liquid outside the zone of vapor bubbles.

TABLE 4

Correlation of Dimensions of Bubbly Spheroids

Volume, v cm^3	Diameter, D mm	Volume, v cm^3	Diameter, D mm	Volume, v cm^3	Diameter, D mm
		Water			
2.9	30	12.2	60.0	21.5	80.0
3.0	30	12.4	60.0	33.5	100.0
4.0	34.4*	13.2	60.0	34.0	100.0
5.0	37.6*	20.0	80.0	20.8	80.0
--	--	25.0	87.2**	25.0	87.4**
		Alcohol			
2.0	30.0	7.8	60.0	12.6	80.0
--	--	--	--	22.0	100.0
		Benzene			
2.05	30.0	2.0	30.0	9.0	60.0
2.1	30.0	2.2	30.0	15.5	80.0
--	--	16.3	80.0	25.0	100.0
		Carbon Tetrachloride			
1.9	30.0	6.5	60.0	11.8	80.0
2.0	30.0	7.0	60.0	11.9	80.0
1.5	30.0	7.0	60.0	18.6	100.0

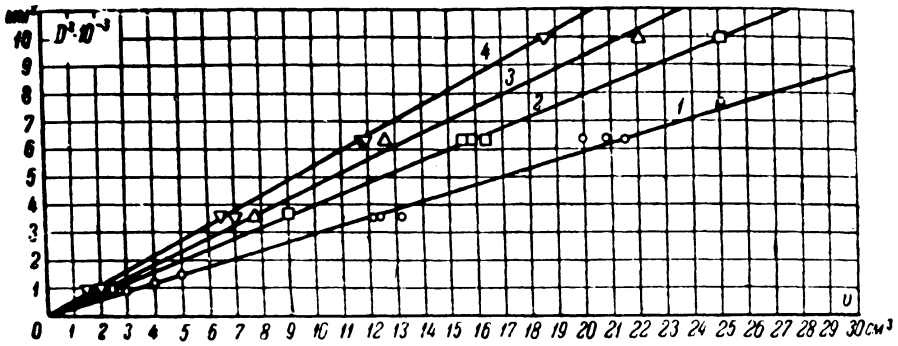

Fig. 10. The function $D^2 = f(v)$ for bubbly spheroids.

1 - Water, 2 - benzene, 3 - alcohol, 4 - carbon tetrachloride.

* These measurements were not made with rings but by the use of micrometers. The figure 34.4 is the arithmetical mean of 65 measurements, while 37.6 is the mean of three measurements.

** Obtained by planimetric measurement of photographs of the spheroid taken from above.

The other figures in the table were obtained by the use of measuring rings.

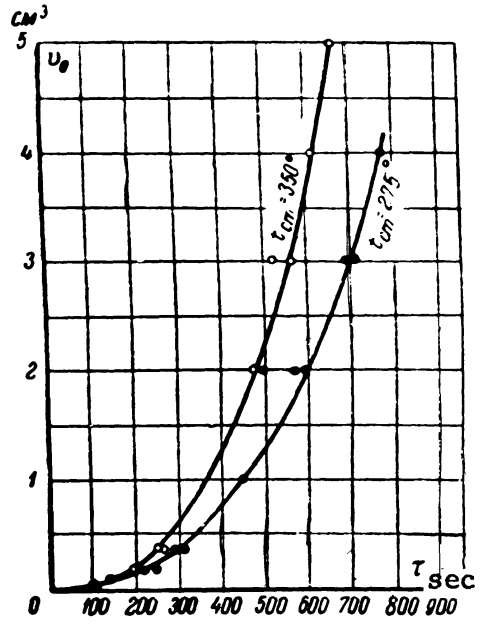

Fig. 11 The function $\tau = f(v)$.

TABLE 5

Total vaporization Time for Spheroids of water as a Function of Their Initial Volume and the Temperature of the Heating Surface*

Spheroid volume, $\frac{v}{cm^3}$	Total vaporization time, τ t_{cm} = 350°C sec	t_{cm} = 275°C sec	Spheroid volume, $\frac{v}{cm^3}$	Total vaporization time, τ t_{cm} = 350°C sec	t_{cm} = 275°C sec
0.0465	100	125	1	--	442
0.093	134	145	2	472	585
0.186	190	214	2	492	564
0.186	--	245	3	520	685
0.372	260	287	3	560	704
0.372	247	306	4	614	770
--	--	--	5	666	--

The variation of the total time required for the vaporization of water spheroids with their dimensions is shown in Fig. 11 and in Table 5 for two different temperatures of the heating surface. Special experiments were run to determine the rate of heat transfer solely in the pe-

* Brass heating surface. Initial water temperature: 20° C.

TABLE 6

Variation of the Vaporization Time of Bubbly Spheroids with the Temperature of the Heating Surface and the Properties of the Liquid

Vaporization time τ, sec	Initial volume of spheroid v_o, cm^3	Final volume of spheroid v_k, cm^3	Vaporization time τ, sec	Initial volume of spheroid v_o, cm^3	Final volume of spheroid v_k, cm^3
		I. Water (distilled)			
		Temperature of heating surface = 350° C			
84.0	25.0	17.0	118.0	25.0	15.2
85.0	25.0	18.2	138.0	25.0	14.0
82.0	25.0	18.0	126.0	25.0	14.1
120.0	25.0	15.2	67.0	25.0	18.8
83.0	25.0	17.0	145.0	25.0	13.4
59.0	25.0	19.7	150.0	25.0	13.1
117.0	25.0	16.0	133.0	25.0	14.0
110.0	25.0	15.9	--	--	--
97.0	25.0	17.0	--	--	--
		Temperature of heating surface = 405° C			
68.0	25.0	18.2	110.0	25.0	15.2
69.0	25.0	18.0	131.5	25.0	12.5
68.0	25.0	17.6	141.0	25.0	11.5
70.0	25.0	18.0	85.0	25.0	16.6
124.0	25.0	13.6	99.0	25.0	15.7
98	25.0	16.0	64.5	25.0	18.7
82.6	25.0	16.0	153.5	25.0	10.0
73.5	25.0	18.0			
		Temperature of heating surface = 500° C			
89.0	25.0	15.2	69.0	25.0	16.5
72.0	25.0	16.1	--	--	--
87.0	25.0	14.4	54.0	25.0	18.2
--	--	--	97.5	25.0	13.7
63.0	25.0	17.2	75.0	25.0	15.9
50.0	25.0	17.3	87.5	25.0	14.7
		II. Alcohol (rectified), C_2H_5OH			
		Temperature of heating surface = 260° C			
37.5	25.0	16.4	78.6	25.0	10.0
49.0	25.0	14.0	33.4	25.0	18.6
43.2	25.0	16.4	41	25.0	16.3
27.0	25.0	19.5	41.2	25.0	16.2
48.2	25.0	15.0	34.2	25.0	18.5
57.2	25.0	13.6	39.6	25.0	16.9
64.5	25.0	12.2	--	--	--
70.0	25.0	11.1			

Vaporization time τ, sec	Initial volume of spheroid v_o, cm^3	Final volume of spheroid v_k, cm^3	Vaporization time τ, sec	Initial volume of spheroid v_o, cm^3	Final volume of spheroid v_k, cm^3
	Temperature of heating surface = 345° C				
64.0	25.0	9.7	36.6	25.0	14.3
45.0	25.0	12.0	36.8	25.0	14.6
48.0	25.0	11.1	33.0	25.0	16.5
46.5	25.0	14.0	23.0	25.0	18.5
39.0	25.0	13.3	18.2	25.0	19.7
33.4	25.0	15.4	--	--	--
	Temperature of heating surface = 485° C				
40.0	25.0	9.1	31.0	25.0	12.6
34.0	25.0	11.7	23.2	25.0	15.9
30.0	25.0	12.3	20.8	25.0	17.0
31.0	25.0	12.4	19.2	25.0	16.8
30.8	25.0	12.1	19.8	25.0	16.8
23.0	25.0	15.3	17.0	25.0	17.9
	III. Carbon Tetrachloride, CCl_4				
	Temperature of heating surface = 320° C				
30.5	19.7	9.0	26.2	19.6	11.3
29.8	19.7	9.9	27.8	19.6	10.6
31.6	19.7	9.3	30.2	19.7	9.4
27.4	19.6	11.0	29.8	19.6	9.0
26.0	19.6	11.4	32.5	19.6	9.9
24.0	19.6	12.0	27.8	19.6	11.3
25.4	19.6	10.9	27.2	19.6	11.3
25.2	19.6	11.5			
	Temperature of heating surface = 410° C				
25.5	19.6	8.0	20.0	19.6	10.6
25.8	19.6	8.2	27.5	19.6	8.0
25.3	19.6	8.0	31.2	19.6	6.5
25.3	19.6	8.0	18.0	19.6	11.5
25.3	19.6	8.4			
	Temperature of heating surface = 590° C				
25.0	18.5	6.9	22.2	19.6	7.9
28.0	19.4	8.3	18.2	19.6	9.4
20.0	19.6	8.0	19.0	19.6	8.7
25.0	19.5	7.5	24.2	19.5	7.2
21.2	19.6	7.7			
	IV. Benzene, C_6H_6				
	Temperature of heating surface = 285° C				

Vaporization time, sec	Initial volume of spheroid v_o, cm^3	Final volume of spheroid v_k, cm^3	Vaporization time, sec	Initial volume of spheroid v_o, cm^3	Final volume of spheroid v_k, cm^3
38.6	25.0	12.7	41.2	25.0	11.5
29.0	25.0	14.7	31.2	25.0	14.0
25.0	25.0	16.9	20.4	25.0	19.0
49.4	25.0	9.5	26.4	25.0	15.7
34.8	25.0	13.2			
	Temperature of heating surface = 340° C				
33.6	25.0	11.7	19.8	25.0	16.4
24.2	25.0	15.0	29.2	25.0	12.2
25.8	25.0	15.0	--	--	--
24.4	25.0	15.0	32.2	25.0	11.5
--	--	--	34.0	25.0	10.9
22.0	25.0	16.0	25.3	25.0	14.7
21.6	25.0	16.0	25.8	25.0	14.5
			34.4	25.0	10.3
	Temperature of heating surface = 420° C				
24.4	25.0	13.3	20.0	25.0	14.5
25.8	25.0	11.5	26.8	25.0	10.8
26.4	25.0	12.0	29.8	25.0	9.5
20.8	25.0	14.5	26.8	25.0	10.5
26.8	25.0	12.0	30.0	25.0	9.5
23.4	25.0	13.0	26.0	25.0	11
21.2	25.0	14.4	--	--	--
21.0	25.0	14.0			
	Temperature of heating surface = 530° C				
24.8	25.0	9.5	19.8	25.0	12.5
25.0	25.0	9.8	18.2	25.0	13.0
24.3	25.0	10.0	19.8	25.0	11.2
--	--	--	18.4	25.0	12.5
23.5	25.0	10.5	24.2	25.0	10.0
22.2	25.0	11.5	20.8	25.0	12.3

NOTE. Steel heating surface: initial liwuid temperature = 20° C.

riod when the dimensions of the spheroid are so large that the appearance of vapor bubbles is equiprobable over the entire surface of the liquid. In these experiments the heating surface was made of steel. We did not measure the total vaporizing time, but rather that part of it corresponding to the period when several vapor bubbles were observed to appear steadily and simultaneously in the spheroid. This was done by producing a spheroid on the heating surface with an initial volume v_o = 20-25 cm^3 After a certain interval of time had elapsed a specially designed pipette was used to collect the remaining liquid rapidly, after which its volume v_k was measured. This made it possible to determine the quantity of li-

quid vaporized, $\Delta v = v_0 - v_k$, during the time $\Delta\tau$ from the instant the spheroid was formed to the instant the remaining liquid was removed from the heating surface. The final volume v_k bore out the existence of a fully developed bubbly spheroid. The results of these experiments are given in Table 6.

4. WORKING UP EXPERIMENTAL DATA ON VAPORIZATION OF LIQUID IN THE PURELY SPHEROIDAL STATE

Let us consider the case of the purely spheroidal state, where the liquid is separated from the heating surface by a layer of vapor. This problem is a special case of heat exchange during a change of state /Ref. 9/.

Consideration of the conditions of heat exchange at the phase interface is of specific interest. In the general case heat is transmitted to the spheroid by thermal conduction through the layer of vapor separating the liquid from the heating surface as well as by radiation from this surface. Bu not all the liquid in the spheroid may be heated to the saturation temperature. On these assumption we can write the following equation for the phase interface:

$$q_p F + \lambda'' (-\operatorname{grad} t)_{+0} F = (r + c\Delta t') \frac{dG}{d\tau} - \lambda (\operatorname{grad} t)_{-0} F. \tag{4}$$

On the other hand, the heat balance for the evaporating spheroid may be written as follows:

$$(\alpha + \alpha_p)\, \Delta t\, F d\tau = r\gamma dv + c\gamma d(v\bar{t}_{ж}). \tag{5}$$

In these equations:

α and α_p = convective and radiant heat transfer coefficients, respectively.
q_p = heat transferred to the liquid by radiation.
G = weight of the spheroid.
v = volume of the spheroid.
F = area of the projection of the spheroid on the heating surface.
λ, c, γ = thermal conductivity, specific heat, and specific gravity of the liquid, respectively.
λ'', c'', γ'' = thermal conductivity, specific heat, and specific gravity of the vapor, respectively.
r = latent heat.
τ = time.
l = dimensional factor, identical for the vapor and liquid phases (because of the interconnection of phase flow).

Treating Eq. (4) and (5) by the methods of the theory of models yields the following criteria:

$$\left.\begin{aligned} &\mathrm{Nu} = \frac{\alpha l}{\lambda''};\ \frac{\lambda}{\lambda''} K = \frac{\lambda}{\lambda''} \frac{r}{c\Delta t};\\ &\mathrm{Fo}_\kappa = \frac{\lambda}{c\gamma} \frac{\tau}{l^2};\ \frac{\lambda \Delta t'}{\lambda'' \Delta t};\ \mathrm{Bi} = \frac{q_r l}{\lambda'' \Delta t}. \end{aligned}\right\} \tag{6}$$

Here

$$\Delta t = t_{cm} - t'', \quad \Delta t' = t'' - \bar{t}_{ж},$$

where t_{cm}, t'', and $t_{ж}$ = temperatures of the heating surface, of saturation, and of the liquid, respectively.*

To these criteria we must add the criterion $We = \frac{l^2(\gamma - \gamma'')}{\sigma}$, determined by the shape of the spheroid in the gravitational field /Ref. 4/. Here σ is the surface tension of the liquid.

The equations for the movement and distribution of heat for the vapor and the liquid and the equation for the conservation of mass yield two defining criteria:**

$$\frac{\gamma''}{\gamma}; \quad \frac{c\lambda''}{c''\lambda}. \tag{7}$$

Calculation shows that radiation may be ignored under the conditions of our experiments and the Bi number can be left out of consideration. We thus get the following system:

$$\left\{\mathrm{Nu};\ \mathrm{Fo}_{\kappa};\ \frac{\lambda \Delta t'}{\lambda'' \Delta t};\ \mathrm{We};\ \frac{\lambda}{\lambda''} K;\ \frac{\gamma''}{\gamma};\ \frac{c\lambda''}{c''\lambda}\right\}. \tag{8}$$

In this system the last four criteria are the controlling factors.

Small drops. In the vaporization of small drops we are usually interested in determining the total time required for their vaporization. Calculation of the mean coefficient of heat transfer is of conventional nature, since the dimensions of the drops and the heat transfer coefficient both change as vaporization proceeds. In the first approximation, omitting the criteria (7), we represent the general functional relationship that follows from the system (8) as:

$$\mathrm{Fo}_{\kappa} = f\left(\frac{\lambda}{\lambda''} K;\ \mathrm{We}\right). \tag{9}$$

If dependence on the criterion $\frac{l^2(\gamma - \gamma'')}{\sigma}$ is expressed as an exponential relationship, the experimental data enable us to determine the exponent n.

In fact, we rewrite (9) in this form:

$$\frac{\lambda \tau}{c_l l^2}\left[\frac{l^2}{\sigma}(\gamma - \gamma'')\right]^n = \varphi\left(\frac{c\Delta t}{r}\frac{\lambda''}{\lambda}\right). \tag{10}$$

* It is assumed that the liquid is at the saturation temperature at the phase interface toward the heating surface

** The criterion $\frac{c\lambda''}{c''\lambda}$ was secured by combining the Fo numbers for the liquid and the vapor, allowing for the general nature of the characteristic geometrical dimension.

As has been stated above, Pleteneva and Rebinder /Ref. 3/ found that the relationship between , the total time required for vaporization of the drop, and D_0, the drop's initial dimension, is constant for a given liquid with a fixed temperature of the heating surface. The right-hand side of Eq. (1) does not depend upon the linear dimension; hence, the only value of n-that can satisfy the condition $\frac{\tau}{D_0}$ = constant is 0.5

The relationship between the criteria then becomes:

$$\frac{\lambda}{c\gamma}\frac{\tau}{D_0^2}\left[\frac{D_0^2}{\tau}(\gamma-\gamma'')\right]^{0.5}=\varphi\left(\frac{c\,\Delta t}{r}\frac{\lambda''}{\lambda}\right). \qquad (11)$$

The initial experimental data on the evaporation of small drops of various liquids are shown in Fig. 12 (see Table 1). As we see, the discrepancies between the individual series of experiments for various substances and drop dimensions is as much as 300-400%

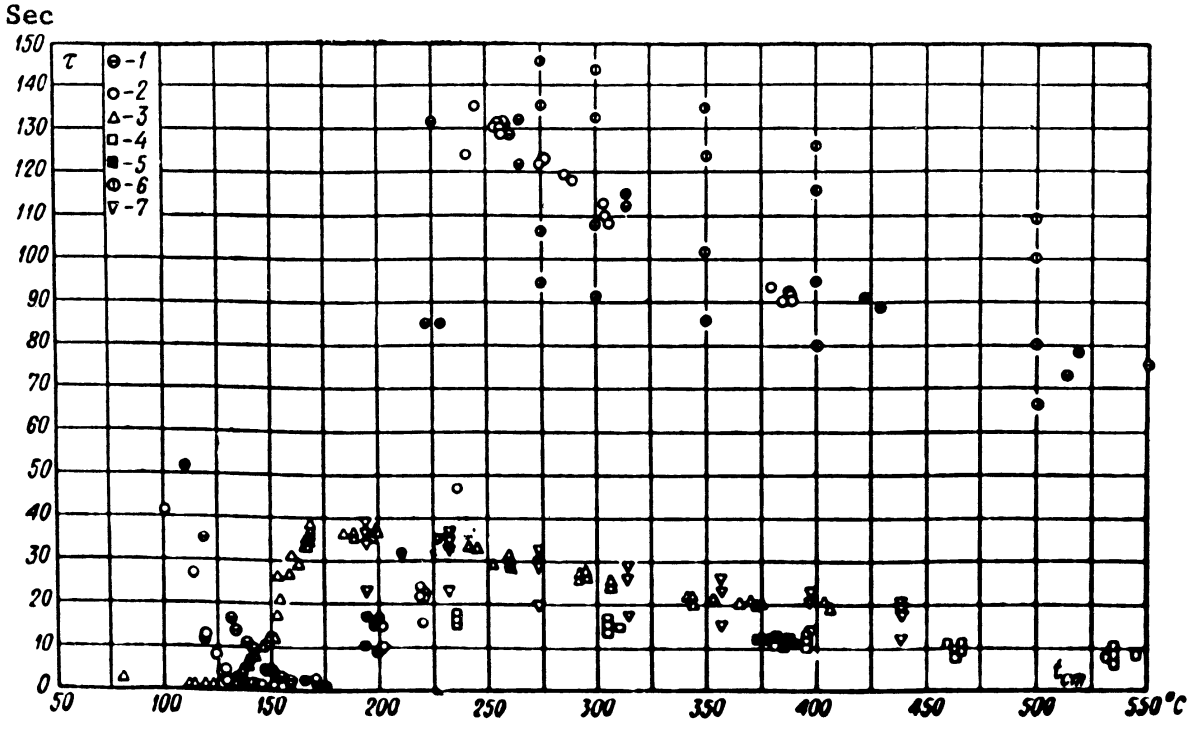

Fig. 12. The function $\tau = f(t_{cm})$ for small drops.
The author's experiments: 1 - water, v_0 = 0.0465 cm^3; 2 - water, v_0 = = 0.0458 cm^3; 3 - alcohol, v_0 = 0.0136 cm^3; 4 - CCl_4, v_0 = 0.00913 cm^3; 5 - CCl_4, v_0 = 0.00742 cm^3.
Pleteneva and Rebinder's experiments /Ref. 3/: 6 - water, v_0 = 0.029; 0.04; 0.026; 0.1 cm^3; 7 - benzene, v_0 = 0.1; 0.035; 0.04; 0.05 cm^3.

The experimental data* were processed using Eq. (11), and are shown in Fig. 13. Only the points referring to the purely spheroidal state,

* In calculating the criteria for Eq. (11), the physical constants referred to the saturation time.

i.e. the experiments in which $t_{cm} > t_{kp2}$, were used in computation. Inspection of the graph shows that the proposed system of criteria (11) satisfactorily generalizes, in a first approximation, the known experimental data on the vaporization of small drops of various liquids in the purely spheroidal state, when there is no contact between the liquid and the heating surface. There is not enough experimental material available at the present time to ascertain the influence of the other controlling criteria of the system (8).

Flat Spheroids. As was stated above, the thickness of the spheroid, δ, undergoes little change with further increase in its volume, beginning with a spheroid volume of $v \approx 1$ cm^3, and approaches a constant value. This circumstance enables us to plan a computational method for determining the coefficient of heat transfer from the heating surface to the liquid.

The volume of a flat spheroid may be written as $v = F\delta$ in the first approximation (see Fig. 17), where F is the area of the projection of the spheroid on the heating surface, and δ is its thickness. Then, neglecting radiation and the fact that the liquid is not heated to the saturation temperature, Eq. (5) can be transformed as follows:

$$r\gamma dv = \alpha \Delta t \frac{v}{\delta} d\tau. \tag{12}$$

Whence we get:

$$\alpha = \frac{r\gamma}{\Delta t} \frac{\delta}{v} \frac{dv}{d\tau}. \tag{13}$$

This formula was used in computing the mean coefficients of heat transfer based on the initial dimensions of the spheroid, δ_0 and v_0, where δ_0 is the thickness at the center of the spheroid. The values of δ_0 and v_0 are taken from Fig. 8.

The numerical values of $\frac{dv}{d\tau}$ for the given initial value v_0 were determined graphically from the curves of complete vaporization reproduced in Fig. 11. The results of calculating the coefficient of heat transfer for flat spheroids at v_0 = 1-3 cm^3 and δ_0 = 6 mm are shown in Fig. 14.

We see from the figure that the coefficient of heat transfer is a function of the initial dimensions of the spheroids and of the temperature of the heating surface. The calculation gives mean values of α for

* Assuming $F = \pi \frac{D^2}{4}$, we have:

$$dv = \frac{1}{2} \pi \delta D \, dD, \tag{14}$$

as the thickness δ undergoes practically no change in the range v = 1-3 cm^3, and Eq. (13) is transformed into:

$$\alpha = 2 \frac{r\gamma}{\Delta t} \frac{\delta}{D} \frac{dD}{d\tau}, \tag{15}$$

where D is the diameter of the projection of the spheroid on the heating surface.

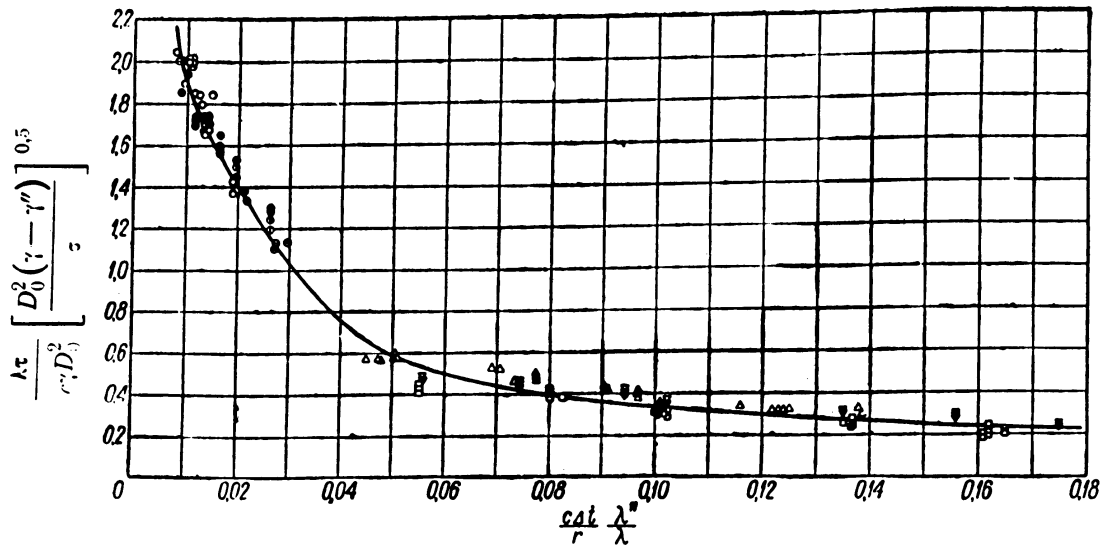

Fig. 13. Generalized processing of the experimental data shown in Fig. 12 in the following coordinates:

$$\left(\frac{\lambda}{c\gamma}\frac{\tau}{D_0^2}\right)\left[\frac{D_0^2}{\tau}(\gamma-\gamma'')\right]^{0,5}=f\left(\frac{c\,\Delta t}{r}\frac{\lambda''}{\lambda}\right)$$

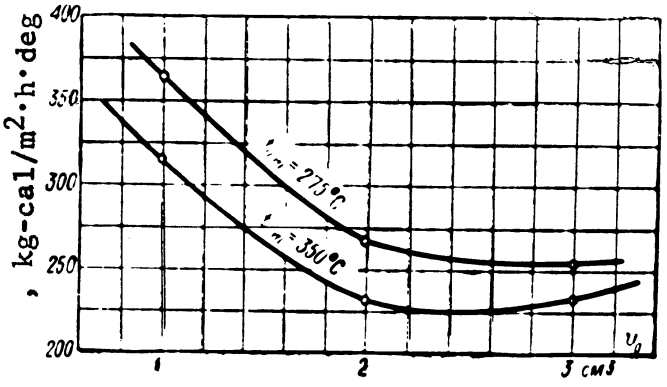

Fig. 14. Mean coefficient of heat transfer to a flat spheroid of water, calculated from Eq. (13).

the total vaporiztion time. This signifies that the terminal period of vaporization, when δ, the thickness of the spheroid, undergoes pronounced change compared to its gradual vaporization, also affects the magnitude of the coefficient of heat transfer.

The experimental material, however, also enables us to calculate instantaneous (local) coefficients of heat transfer, corresponding to vaporization of a flat spheroid in the volume range of 3-1 cm^3. Let us assume that the spheroid is in an atmosphereof saturated vapor and all the

heat is transmitted by thermal conductivity ($\alpha\delta'' = \lambda''$) through a layer of vapor (δ'') that separates the liquid from the heating surface. The pressure within the vapor layer exceeds that in the surrounding medium by $\delta\gamma$. Practically speaking, the bottom surface of the spheroid is convex. The vapor evolved at this surface flows out through the annular peripheral gap $\pi\beta\delta''$. The excess pressure is counterbalanced by frinction and the reactive force of the escaping vapor, due to the separation of the vapor from the liquid at the surface of the spheroid. Ignoring the reactive force* and the sphericity of the liquid surface, we may write:

$$\zeta \frac{\gamma''}{2g} w''^2 = \delta\gamma, \tag{16}$$

where ζ is the coefficient of resistance and w'' is the vapor velocity.

Further, setting up the vapor flow balance underneath the spheroid, we can show /Ref. 8/ that the coefficient of heat transfer is given by the equation:**

$$\alpha = 2{,}38\,\zeta^{-0{,}25}\left(\frac{r\lambda''}{\Delta t}\right)^{0{,}5}(g\gamma''\gamma)^{0{,}25}\frac{\delta^{0{,}25}}{D^{0{,}5}}. \tag{17}$$

In this equation $\Delta t = t_{cm} - t''$, where t_{cm} is the temperature of the heating surface and t'' is the saturation temperature.

Proceeding to the expression that includes the volume of the spheroid,*** we finally obtain:

$$\alpha = 2{,}24\,\zeta^{-0{,}25}\left(\frac{r\lambda''}{\Delta t}\right)^{0{,}5}(g\gamma\gamma'')^{0{,}25}\frac{\delta^{0{,}5}}{v^{0{,}25}}. \tag{18}$$

The coefficient $\zeta^{-0.25}$ can be found by processing the experiments cited above on the vaporization of flat spheroids. The expression for the flow of substance through the peripheral slit may be written as follows /Ref. 8/:

$$dv = \pi D\delta''\frac{1}{\sqrt{\zeta}}\sqrt{\frac{\gamma''}{\gamma}2g\delta''}\,d\tau. \tag{19}$$

Combining (19) with (16) and remembering that $\delta'' = \frac{\lambda''}{\alpha}$, we get:

$$\frac{dD}{d\tau} = \frac{\delta''}{\delta}\frac{1}{\sqrt{\zeta}}\sqrt{\frac{\gamma''}{\gamma}8g\delta} = \frac{\lambda''}{\alpha}\frac{1}{\sqrt{\zeta}}\sqrt{8\frac{g}{\delta}\frac{\gamma''}{\gamma}}. \tag{20}$$

Eliminating α from Eqs. (15) and (20) yields:

$$\frac{dD}{d\tau} = \frac{D^{0{,}5}}{\delta^{0{,}75}}\left(\frac{\lambda''\Delta t}{r\gamma}\right)^{0{,}5}\left(2g\frac{\gamma''}{\gamma}\right)^{0{,}25}A = A\frac{D^{0{,}5}}{\delta^{0{,}75}}f(t^\circ) = c_1 D^{0{,}5}, \tag{21}$$

---

* For water at q $\approx$ 500,000 kg-cal/m^2·h the reactive pressure on the spheroid is only 0.23% of the force of gravity acting on a spheroid 5 mm thick.

** The expression $\frac{\eta^2}{4}$ is given in the paper cited instead of the coefficient ζ .

*** See the footnote to page 130.

where $A = \zeta^{-0.25}$, while the constant c is independent of the dimensions of the spheroid, since δ = constant in the given volume range. Integrating the last equation from D to D_k, and from 0 to $\Delta\tau$, where $\Delta\tau$ is the interval of time elapsed from the beginning of vaporization, we get:

$$D_0^{0,5} - D_к^{0,5} = -0{,}5c_1\Delta\tau. \tag{22}$$

Proceeding to v, the volume of the spheroid, and omitting the algebraic sign, which merely indicates the direction in which the process is developing, we get:

$$v_0^{0,25} - v_к^{0,25} = 0{,}5\Delta\tau\left(\frac{\pi\delta}{4}\right)^{0,25} = c_2\Delta\tau. \tag{23}$$

The constant c_2 must be determined experimentally, bearing in mind that it depends on the temperature of the heating surface inasmuch as the physical constants of the vapor enter into it.

The experimental data were worked up as follows. The intermediate values of v_k and the corresponding values of $\Delta\tau$ from the beginning of vaporization were determined from the curve $v = f(\tau)$ (Fig. 11); the calculation was made for two ranges of volumes v: 3-2 cm^3 and 2-1 cm^3. These calculations were used in plotting the function

$$v_0^{0,25} - v_к^{0,25} = f(\Delta\tau),$$

shown in Fig. 15.

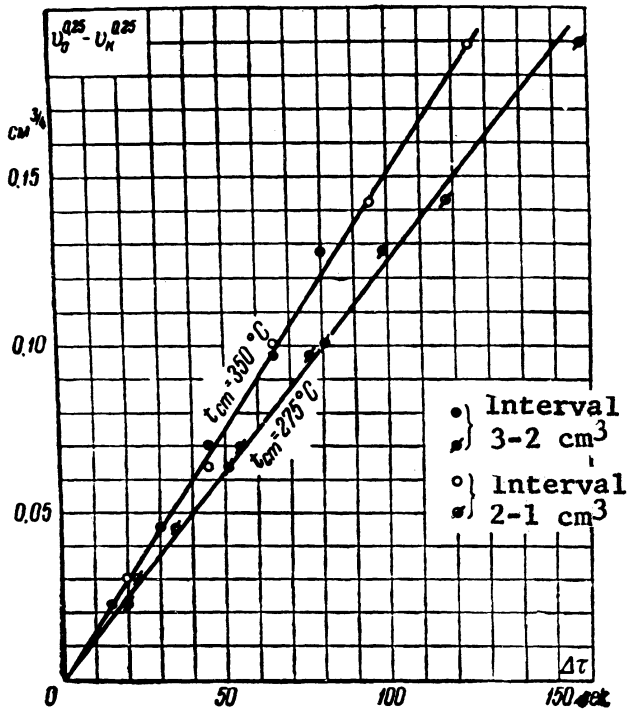

Fig. 15. The function $v_0^{0,25} - v_к^{0,25} = f(\Delta\tau)$ for plane spheroids of water.

We see from the graph that the points for different ranges of spheroid volumes lie on a single straight line. On the other hand, lines of different slopes are secured for different temperatures of the heating surface. It is well to bear this difference, due to the influence of

temperature on the value of the physical constants, in mind. Combining Eqs. (21), (22), and (23), we get:

$$A = 1{,}79\,\delta^{0{,}5}\left(\frac{\lambda''\,\Delta t}{r\gamma}\right)^{-0{,}5}\left(\frac{g\gamma''}{\gamma}\right)^{-0{,}25}\frac{v_0^{0{,}25} - v_\kappa^{0{,}25}}{\Delta\tau}. \qquad (24)$$

If we select the dimensionless expressions:

$$Y = \frac{v_0^{0{,}25} - v_\kappa^{0{,}25}}{\delta^{0{,}75}}; \quad X = \frac{\Delta\tau}{\delta^{1{,}25}}\left(\frac{\lambda''\,\Delta t}{r\gamma}\right)^{0{,}5}\left(g\frac{\gamma''}{\gamma}\right)^{0{,}25},$$

as ordinates, all the experimental points should lie on one line if the influence of temperature on the physical constants has been allowed for correctly. For this purpose the data of Fig. 15 were plotted in the coordinates X, Y. The physical properties of water were referred to the saturation temperature, while that of the vapor (λ'', γ'') to the arithmetical mean of the heating-surface temperature and the saturation temperature. The results are shown in Fig. 16.

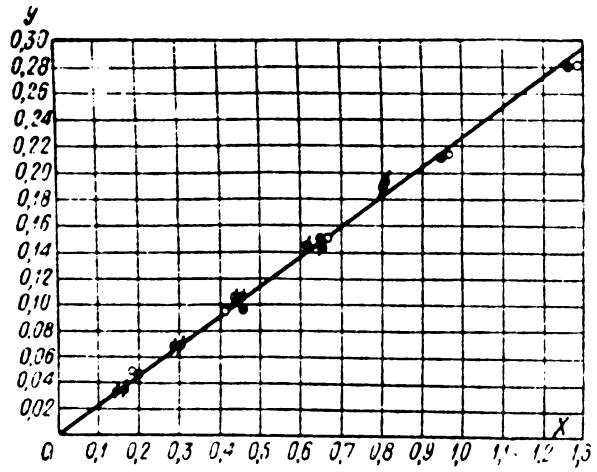

Fig. 16. The function for determining A.

Hence, A can be determined from the equation:

$$A = 1{,}79\,\frac{Y}{X}.$$

We see that (in the range of 1-3 cm^3) A is practically independent of the dimensions of the spheroid and the temperature of the heating surface. The foregoing enables us to calculate the local values of the coefficient of heat transfer in the vaporization of flat spheroids from Eq. (18). The results of this calculation* are shown in Fig. 17.

The observed variation of the coefficient of heat transfer with the temperature of the heating surface and the dimensions of the spheroid agree with the qualitative picture previously described by N. A. Gezekhus /Ref. 2/.

* It is assumed that δ = 6 mm; in using Eq. (18) for calculation, the thermal conductivity λ'' and the specific gravity γ'' of the vapor were referred to the arithmetical mean of the heating-surface temperature and the saturation temperature /as was done for Eq. (17)/.

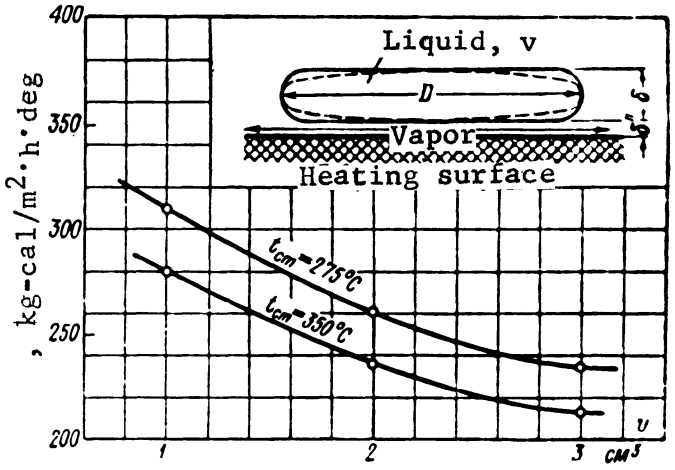

Fig. 17. Coefficient of heat transfer to flat spheroids, calculated from Eq. (18).
(The broken line in the diagram for the flat spheroid corresponds to the actual form of the surface.)

Large Bubbly Spheroids. In Figs. 8, 9, and 10 and in Tables 3 and 4 above we cited data of experiments run to determine the dimensions of the spheroids. The criterion $\frac{l^2(\gamma-\gamma'')}{\sigma}$ may be employed to generalize the experimental material. The feasibility of employing this criterion for bubbly spheroids is not immediately evident, inasmuch as the vapor is observed to move in it through the mass of liquid.

To clear up this problem the experimental data on large bubbly spheroids were plotted in the following coordinates:

$$D^2\left(\frac{\gamma-\gamma''}{\sigma}\right)=\left\{v\left(\frac{\gamma-\gamma''}{\sigma}\right)^{\frac{3}{2}}\right\}$$

and reproduced in Fig. 18.

As we see from the graph, the points for various liquids and spheroids of different dimensions are located about a straight line.

On the assumption that the coefficient of heat transfer is independent of the volume of the spheroid for fully developed bubbly spheroids and bearing in mind that the thickness of the latter is independent of volume, we may write Eq. (13) as follows:

$$d\ln v=-\frac{\alpha\Delta t}{r\gamma\delta}d\tau. \qquad (13a)$$

Integration of this expression yields:

$$\ln v=-\frac{\alpha\Delta t}{r\gamma\delta}\tau+\ln c.$$

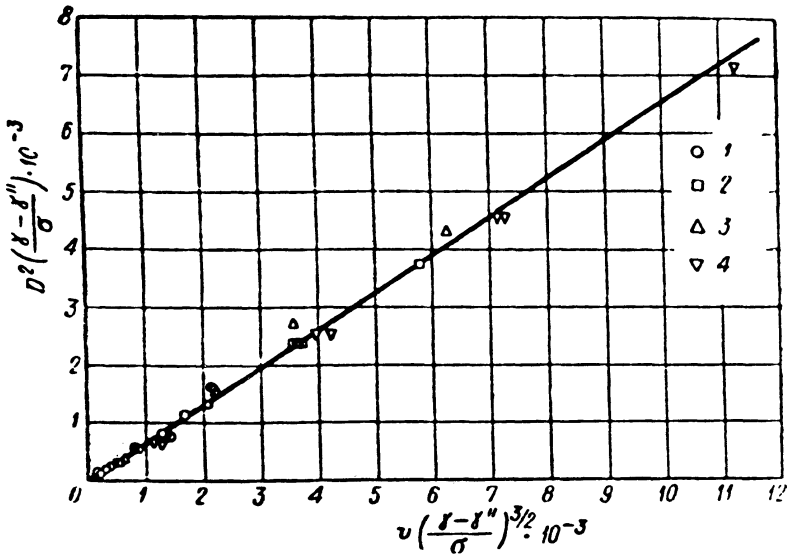

Fig. 18. Plotting data on measurement of bubbly spheroids:

$$D^2\left(\frac{\gamma-\gamma''}{\sigma}\right)=f\left[v\left(\frac{\gamma-\gamma''}{\sigma}\right)^{\frac{3}{2}}\right]$$

1 - Water, 2 - benzene, 3 - alcohol, 4 - CCl_4

The constant of integration is determined from the condition that $v = v_0$ at $\tau = 0$, where v_0 is the initial volume of the spheroid. Then we get in its final form:

$$v_k = v_0 e^{-\frac{\alpha \Delta t}{r_1 \delta}\tau}$$

where v_k is the volume of the spheroid at the instant of time τ.

Hence, if our assumption that the coefficient of heat transfer α is constant corresponds to reality, plotting the data in the coordinates $\ln\frac{v}{v_0}, \tau$ ought to yield straight lines.

The plot of the available experimental data for four liquids (Table 6) in the coordinates $\lg \frac{v_k}{v_0} = f(\tau)$ is shown in Fig. 19. We see from the graphs of Fig. 19 that the experimental points are located about straight lines for each liquid, the slopes of these lines varying with the temperature of the heating surface. Some scattering of the points is observed only for comparatively low terminal dimensions of the spheroids. The foregoing justified the assumption that the coefficient of heat transfer is independent of the dimension of the bubbly spheroid and that the following computational formula can be used to compute it:

$$\alpha = \frac{r_1 \delta}{\Delta t}\frac{1}{\tau}\ln\frac{v_k}{v_0} = k\frac{r_1\delta}{\Delta t} \qquad (25)$$

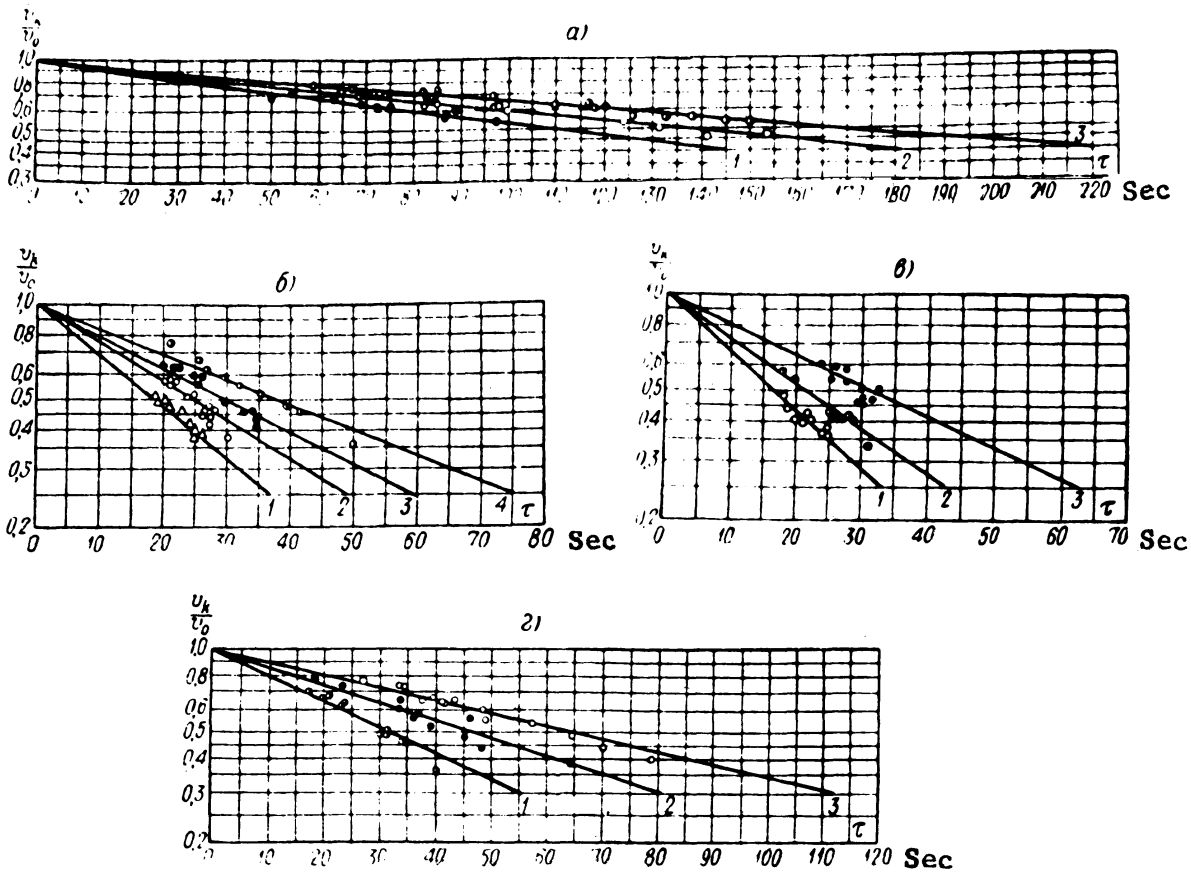

Fig. 19. The function $\lg \frac{v_k}{v_0} = f(\tau)$ for bubbly spheroids:

Line	Temperature of heating surface t_{cm}, °C			
	а) Water	б) Benzene	в) Carbon tetrachloride	г) Alcohol
1	500	530	590	485
2	405	420	410	345
3	350	340	320	260
4	--	285	--	--

The value of $k = \frac{2{,}3 \lg \frac{v_к}{v_0}}{\tau}$ was determined from the graphs of Fig. 19 for the given temperature of the heating surface. The thermal load on the heating surface was determined from the formula:

$$q = kr\gamma\delta \ [ккал/м^2 \cdot ч]. \qquad (25a)$$

Using these formulas for calculation requires that we know δ, the thickness of the bubbly spheroid.

The plot of data for bubbly spheroids reproduced in Fig. 18 justifies the assumption that the criterion $\delta\left(\frac{\gamma-\gamma''}{\sigma}\right)^{0.5}$ is a constant that is independent of the nature of the liquid. Taking δ = 8 mm for water, we find this criterion to be equal to 3.2 Hence, the thickness of bubbly spheroids for other liquids can be determined from the formula:

$$\delta = 3{,}2\left(\frac{\sigma}{\gamma-\gamma''}\right)^{0.5}. \qquad (26)$$

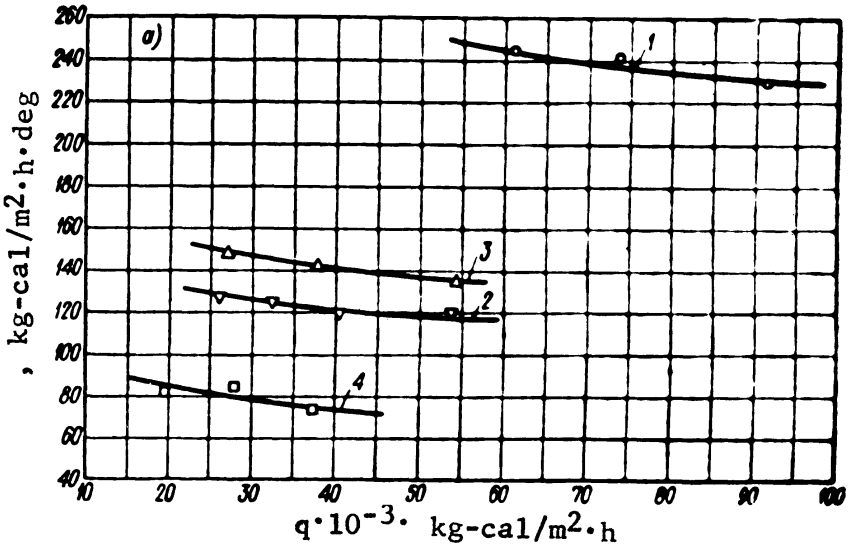

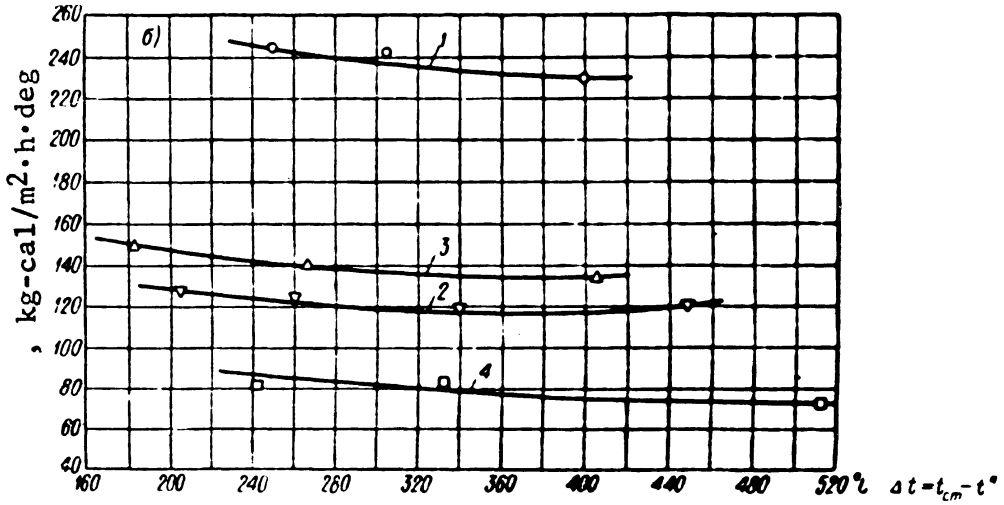

Fig. 20. Heat transfer to bubbly spheroids.
a) $\alpha = f(q)$; б) $\alpha = f(t_{cm} - t'')$.
1 - Water; 2 - benzene ; 3 - alcohol; 4 - CCl_4.

The values of δ calculated from Eq. (26) for all the liquids tested in the experiments are listed in Table 7. The results of plotting the experimental data on heat transfer* in the coordinates $\alpha = f(\Delta t)$ and

* The curve $\alpha = f(q)$ for water reproduced in our paper /Ref. 8/ was plotted from our initial experiments, which apparently yielded results that were somewhat high.

TABLE 7

Data on the Vaporization of Bubbly Spheroids

Substance	t_{cm}, °C	$\Delta t = t_{cm} - t''$, °C	δ, mm	α, kg-cal/m^2·h·deg	q, kg-cal/m^2·h	$\frac{c'_n \Delta t}{r}$	$\frac{\alpha}{\lambda'_n}\sqrt{\frac{\sigma}{\gamma - \gamma'_n}}$
Water	350	250	8	245	61,200	0.216	20.1
"	405	305	8	242	73,900	0.27	18.3
"	500	400	8	229	91,500	0.357	15.4
Alcohol	260	182	4.86	149	27,100	0.42	10.35
"	345	267	4.86	142	37,800	0.615	8.50
"	485	407	4.86	134	54,400	1.02	6.66
Carbon tetrachloride	320	242	3.78	82	19,800	0.755	10.4
"	410	332	3.78	84.5	28,100	1.03	9.40
"	590	512	3.78	73.1	37,400	1.59	6.86
Benzene	285	205	5.2	127	26,000	0.831	10.0
"	340	260	5.2	125	32,400	1.11	8.56
"	420	340	5.2	119	40,500	1.56	7.01
"	530	450	5.2	120	54,000	2.26	5.75

NOTES. 1. Initial temperature of the liquid: 20° C.

2. The thermal conductivity λ''_n, the specific heat c''_n, and the specific gravity γ''_n of the vapor are based on the arithmetical mean of the temperature heating surface and the saturation temperature. See Table 8 for extrapolated data.

$\alpha = f(q)$ are shown in Figs. 20$_4$ and 20, σ. In this case, owing to the fact that the vaporization process is independent of the volume of the liquid, it is advisable to employ a criterial function that includes the coefficients of heat transfer rather than the time of vaporization. We therefore use the following functional relationship between the criteria* that follow from the system (8) as a first approximation:

$$\left(\frac{\alpha l}{\lambda''}\right)\left(\frac{l^2(\gamma - \gamma'')}{\sigma}\right)^n = f\left(\frac{c''\Delta t}{r}\right). \tag{27}$$

In the vaporization of bubbly spheroids the freely evolving geometrical dimensions are indeterminate quantities that depend only upon the process of vapor formation. Hence, the linear dimension l must be eliminated from Eq. (27).

We then finally get:

$$\frac{\alpha}{\lambda'_n}\left(\frac{\sigma}{\gamma - \gamma'_n}\right)^{0,5} = f\left(\frac{c'_n \Delta t}{r}\right). \tag{28}$$

---

* $\frac{c''\Delta t}{r} = \frac{c\Delta t}{r}\frac{\lambda''}{\lambda}\frac{c''\lambda}{c\lambda''}$

In plotting the experimental data difficulties arose in selecting the physical constants and in the necessity of extrapolating them. This was especially true of carbon tetrachloride. The available data in the literature /Ref. 5, 6, 7/ are listed in Table 8.

In calculating the criteria, the coefficients of thermal conductivity, the specific heats, and specific gravities of the vapors were based on the mean of the heating-surface temperature and the saturation temperature.* The physical properties of the liquid are based on the saturation temperature.

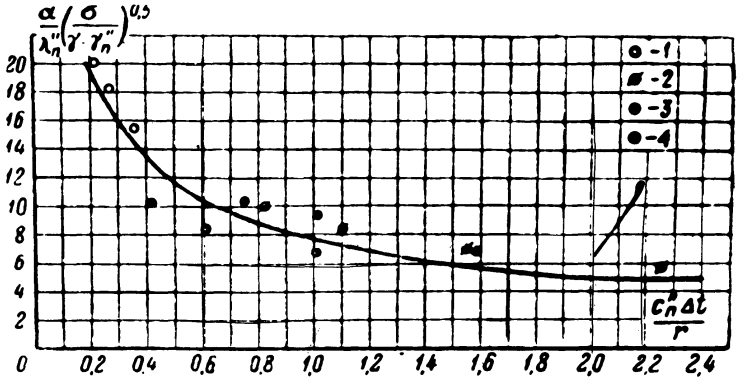

Fig. 21. Generalized plot of data on heat transfer to bubbly spheroids.

Nomenclature is the same as in Fig. 21.

The results of plotting the experimental data in accordance with Eq. (28) are shown in Fig. 21. The faired curve is described by the equation:

$$\frac{\alpha}{\lambda''_n}\left(\frac{\sigma}{\gamma-\gamma''_n}\right)^{0,5}=7{,}9\left(\frac{c''_n \Delta t}{r}\right)^{-0.6}. \qquad (29)$$

Using this formula to extrapolate for values of $\frac{c''_n \Delta t}{r} > 2.4$ is not recommended because of the absence of experimental data.

Further analysis indicates that the ratio $\frac{\gamma}{\gamma''}$ has some effect (very slight) upon heat transfer, though the available experimental material is insufficient to determine the quantitative relationships.

5. CONCLUSIONS

1. A single vaporization curve (water, alcohol) has been secured, which has enabled us to establish the fact that there are two characteristic (critical) temperatures of the heating surface, t_{kp1} and t_{kp2} for the vaporization of a liquid on an open heating surface. The first temperature corresponds to the cessation of nuclear boiling in a liquid spreading over the heating surface, while the second corresponds to the

* This is indicated by the notation $\lambda''_n, \gamma''_n, c''_n$.

establishment of the purely spheroidal state. The properties of the liquid and of the heating surface fundamentally affect the values of both critical temperatures.

2. It has been found that the initial temperature of the liquid influences both critical temperatures of the heating surface. A method of calculation is suggested for computing this influence, yielding satisfactory agreement in the first approximation with the experimental data.

3. The liquid takes on different geometrical forms, depending upon the quantity of liquid spreading over the heating surface; almost true spheres for small drops and spheroids that are flattened out to a different extent, depending upon their size. When the spheroids are sufficiently large, vapor is evolved as large vapor bubbles, breaking through the mass of the liquid from time to time.

4. The rate of vaporization depends upon the properties of the liquid, the dimensions of the spheroid, and the temperature of the heating surface.

5. Experiments were run on the vaporization of small drops of water, alcohol, and carbon tetrachloride, with the temperature of the heating surface ranging up to 600° C. Analysis of this experimental material and of the data of other authors, employing the theory of similitude, made it possible to proposed a generalized treatment that enables us to calculate the time required for complete vaporization of the drops to a certain degree of approximation.

6. The rate of heat transfer to a normal flat spheroid diminishes with an increase in size of the spheroid and a rise in the temperature of the heating surface. The thickness of the vapor layer increases correspondingly. It may be stated, as a first approximation, that heat transfer is governed by the balance between the outflow of vapor evolved and the rate of heat transfer through the vapor layer that separates the liquid from the heating surface.

7. Experiments using flat spheroids of water with a volume v = 1-3 cm^3 have yielded a calculating method for determining the mean coefficients of heat transfer for the total vaporization time, based on the initial dimensions of the spheroids. A semiempirical formula is given for calculating the (dimensionally) local coefficient of heat transfer, allowing for the effect of the physical properties of the liquid and of the temperature of the heating surface.

8. Experiments with large bubbly spheroids (water, alcohol, benzene, and carbon tetrachloride) indicated the data on the measurement of the freely developing geometrical dimensions of the spheroids, notwithstanding the appearance of vapor bubbles in the mass of liquid, can be successfully generalized in similitude criteria derived on the assumption of equilibrium of the liquid volume subjected to gravitational and surface-tension forces. It was found that the thickness of the developed bubbly spheroid is independent of its volume.

9. Investigation of the vaporization of large bubbly spheroids indicated that in this case the coefficient of heat transfer α is independent of the quantity of liquid and is controlled by the density $\underline{q}$ of the

TABLE 8

Physical Properties of Liquids and Vapors

I. Physical properties of substances along the saturation line at atmospheric pressure

Substance	Latent heat of vaporization r, kg-cal/kg	Specific heat of liquid c, kg-cal/kg·deg	Density of liquid, γ kg/m^3	Density of vapor, γ'' kg/m^3	Coefficient of thermal conductivity of liquid, λ kg-cal/m·h·deg	Coefficient of thermal conductivity of vapor, λ'' kg-cal/m·h·deg	Surface tension, σ kg/m	Boiling point t'', °C
Water	539	1.0	958	0.598	0.587	0.0208	$60 \cdot 10^{-4}$	100
Benzene, C_6H_6	93.6	0.464	817	2.76	0.1235	0.0122	$21.6 \cdot 10^{-4}$	80.6
Carbon tetrachloride, CCl_4	45	0.209	1433	5.5	0.087	0.00662	$20.6 \cdot 10^{-4}$	78.0
Alcohol, C_2H_5OH	197	0.731	737	1.655	0.137	0.0157	$17.1 \cdot 10^{-4}$	78.4

II. Specific heats of vapors of various substance

Benzene, C_6H_6

Temperature, °C	20	27	74	77	100	107	127	167	177	227	327	350
Specific heat, c_p'', kg-cal/kg·deg	0.256	0.257	0.298	0.303	0.331	0.350	0.342	0.375	0.380	0.418	0.480	0.498

Alcohol, C_2H_5OH

Temperature, °C	100-223	350
Specific heat, c''_p, kg-cal/kg·deg	0.454	0.612

Carbon Tetrachloride, CCl_4

Temperature, °C	0	30	70
Specific heat, c''_p, kg-cal/kg·deg	0.140	0.132	0.115

III. Thermal conductivity of vapors of various substances

Substance	Alcohol, C_2H_5OH			Benzene, C_6H_6				Carbon tetrachloride, CCl_4		
Temperature, °C	7.5	20	100	0	46	100	184	212	46	100	184
Thermal conductivity ", kg-cal/m·h·deg	0.01065	0.0121	0.01685	0.0071	0.01	0.014	0.207	0.024	0.00565	0.00695	0.00877

NOTE. Data taken from the literature /Ref. 5, 6, 7/.

thermal flow supplied.

10. Working up the experimental data on heat transfer to bubbly spheroids, on the basis of the theory of similitude, made it possible to secure an approximate criterial relationship that may be employed with an accuracy of $\pm$ 15% for values of the complex:

LITERATURE CITED

1. O. D. Khvolson, Treatise of Physics, Vol. 3, 514, 1923.

2. N. A. Gezekhus, Russ. Phys.-Chem. Soc., Phys. Sect., 310, 356, 1876.

3. N. A. Pleteneva and P. A. Rebinder, Phys. Chem., 961, 973, 1946; Bull. USSR Acad. Sci., Div. Tech. Sci., 12, 1946.

4. A. N. Krylov, Lectures on approximate calculations. USSR Acad Sci. Press, 1935.

5. Physico-chemical properties of individual hydrocarbons, No. I, 1945; No. II, 1947. All-Union Scientific, Engineering, and Technical Society of Oil Workers.

6. Handbook of physical constants. Appendix to the Technical Encyclopedia.

7. Handbook of physical constants. Edited by Dorfman and Frish, 1933.

8. V. M. Borishansky and S. S. Kutateladze, J. Tech. Phys., No. 8, 1947.

9. S. S. Kutateladze. Heat Transfer in Condensation and Boiling. State Scientific and Technical Publishing House of Machinery Literature, 1949, 1952.

HEAT EXCHANGE IN THE QUENCHING OF METAL PARTS IN LIQUID MEDIA

V. M. Borishansky, Candidate of Engineering Sciences, M. M. Zamyatnin, Candidate of Engineering Sciences, S. S. Kutateladze, Candidate of Engineering Sciences, and A. L. Nemchinsky, Candidated of Engineering Sciences

The I. I. Polzunov Central Scientific Research Institute for Boilers and Turbines and
The M. I. Kalinin Institute of Technology, Leningrad

1. STATEMENT OF THE PROBLEM

Wuenching in liquids, most often in water or oil, plays an important part in the heat treatment of steel parts. Steel is quenched to establish a definite structure (martensite), which is secured at high cooling rates that are unattainable when cooling is done in a furnace or in air. The required cooling rate of the surface of the parts may differ considerably, depending upon the dimensions of the part and the composition of the steel. In small parts a few millimeters thick the use of oil yields cooling rates that are adequate to produce martensite in practically all quenchable grades of steel.

Large parts can be quenched in oil only when they are made of steels containing special components that retard the transformation processes. Faster cooling in water makes it possible to quench large parts or parts made of steel containing low percentages of alloys right through.

A study of the austenite transformation has shown that rapid cooling from the quenching temperature (usually 800-900°) to temperatures of 300-150° is required to insure quenching, i.e. the production of martensite. High cooling velocities are particularly necessary in the range 700-500° for carbon steel and low-alloy steels and in the range 450-350° for high-alloy steel. From the standpoint of structural transformation the cooling velocities may be substantially lower at higher and lower temperatures. It should be borne in mind, however, if massive parts are to be quenched all the way through, that there is a considerable difference (amounting to several hundred degrees) between the temperature of the surface and the core of the parts, due to thermal inertia. As a result the cooling velocity of the core of large parts at 400-350° may depend upon the cooling of their surface at much lower temperatures.

In addition to insuring definite cooling velocities, the production of quench cracks must be avoided in quenching; moreover, distortion must be held down to a minimum.

Practice indicates that quenching in oil does not produce cracks in the part in the overwhelming majority of cases and produces less deformation than quenching in water. Therefore, oil is widely used for quenching notwithstanding its lower cooling ability. The reason for these favorable results of quenching in oil is the slower cooling of the surface, compared to cold water, at low temperatures (which is important for small parts) and at comparatively high temperatures (which is important for large parts. In some instances the use of expensive special steel instead of ordinary carbon steel is dictated solely by the danger of the occurrence of cracks or deformation in the latter when quenched in water.

Owing to the use of parts of various dimensions and steels of various dimensions and steels of various grades the two ordinary quenching media often prove to be inadequate, and heat treaters employ special measures to change their cooling properties.

A change in the cooling ability of water and oil is attainable within certain limits by using forced circulation (including air blast) and additives that accelerate (salt and alkalis for water) or retard (water glass and soap) cooling. Temperature appreciably affects the cooling ability of water and, to a lesser degree, of oil. This factor is utilized in production. It has also been noted that the condition of the surface (scale, a thin layer of grease) has some effect on the cooling process, and this is likewise employed at times in practice to regulate the rate at which the process takes place.

It should be borne in mind that the position of the surfaces of the part to be cooled greatly affects its cooling. Thus, for example, the bottom flat surfaces are cooled by water much more slowly than the top surfaces.

2. CHARACTERISTIC CURVES

Direct visual observation of the process of quenching in liquid media and special investigations made by heat-treatment specialists have indicated that there are always three stages of cooling in quenching in water, in mediums with an aqueous base, and in oil: "the period of a stable vapor blanket," "the period of boiling," and "the period of convective heat transfer."

From the standpoint of contemporary theory it would be more correct to call these stages: first - the stage of film boiling; second - the stage of nuclear boiling; and third - the stage of convective heat transfer without boiling.

In the first stage the vapor blanket, which is a poor heat conductor, is comparatively stable, thus reducing the rate of heat transfer.

Heat transfer is at a maximum in the second stage, nuclear boiling, and slowest in the third stage.

So-called "characteristic curves" of quenching media have been widely adopted of late in literature on heat treatment.

A characteristic curve is a graph showing the cooling capacity of the medium as a function of the temperature of the surface to be cooled. Some authors use the cooling velocity of a standard sample, i.e. a quantiry that is directly proportional to the thermal flow, as the quantitative characteristic of cooling power.

Conceptually, characteristic curves should represent the physical characteristic of the quenching liquid at a given temperature and for given circulation conditions, independent of the shape and dimensions of the part, the initial temperature to which the part has been heated, and the absolute of the surface cooling rate.

The section of characteristic curves that is most important in

practice lies within the first and second stages, the last stage (convective heat transfer) being of much less importance in most cases.

Besides the three stages mentioned above, there is another characteristic initial period on temperature curves, related apparently to the establishment of the cooling process (see the broken-line section of the curve in Fig. 1). This initial section is short, both on a temperature

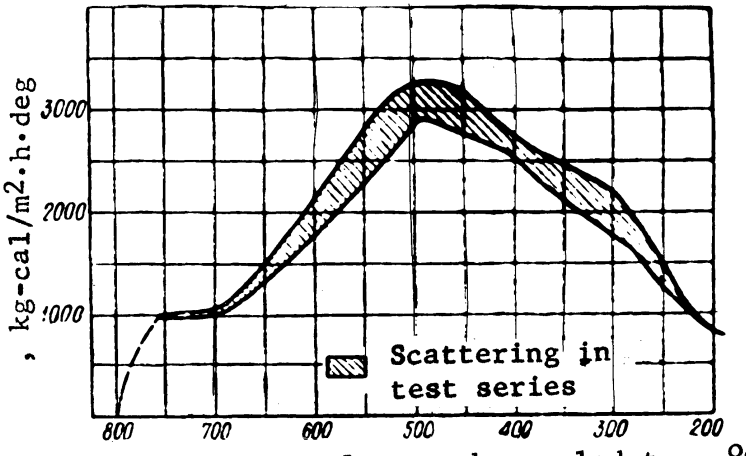

Fig. 1. Variation of α, coefficient of heat transfer, in linseed oil with the temperature of the surface to be cooled.

scale and on a time scale. This stage of the process shifts along the temperature scale with a change in the initial temperature of the sample and depends upon the latter's dimensions, and no allowance should be made for it in calculation when evaluating the cooling power of the medium or plotting its characteristic curve.

All the characteristic curves published up to the present time were secured by cooling a sample of small size and recording the cooling curves for the center on a low-inertia instrument. The sample should be small enough to make the temperature difference across its section negligible.

If, for example, we set the maximum allowable temperature difference across the section of the sample as $\Delta t = 20^\circ$ C, and the coefficient of heat transfer α = 10,000 kg/cal/m^2·h·deg (with a surface temperature of 300° for the sample), the maximum allowable radius of a spherical sample is 0.04 cm for steel and 1 cm for silver.

In practice, most research workers have used a sample in the shape of a silver sphere with a radius of 1 cm. The advantage of a silver sample over a steel one is that the area of its surface is about 100 times as great for the same thermal inertia.

As experiment has shown, a silver sample with a radius of 1 cm yields sufficiently stable (averaged) results in determining characteristic curves (see the curve in Fig. 1, plotted from Khozan's data /Ref. 1), whereas an iron sample with a radius of 0.5 mm yields very great scattering of the experimental points.

The characteristic curves for still water at 20°, 60°, and 100°, as well as for mineral oil, are given in Figs. 1 and 2. The curve shown for cold water differs from the well-known curves of Rose by the position of the maximum of the coefficient of heat transfer: 250-300° instead of 500° given by Rose. The reason for this discrepancy is that Rose's experiments were inaccurate because of poor contact between the sample and the thermocouple inserted in it.

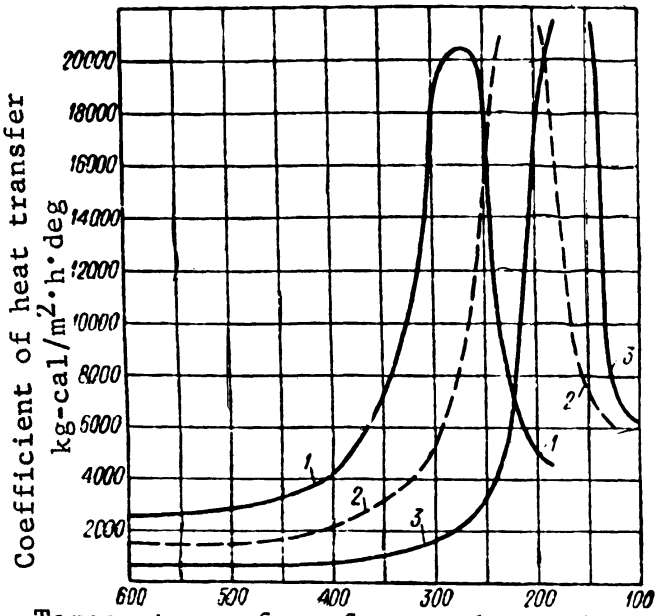

Temperature of surface to be cooled $\underline{t}$, °C

Fig. 2. Cooling power of water as a function of the temperature of the surface to be cooled.
1 - Mean water temperature, $\overline{t}$ = 20° C; 2 - the same, $\overline{t}$ = 60° C; 3 - the same, $\overline{t}$ = 100° C.

The literature likewise contains characteristic curves for water at a few circulation velocities and for aqueous solutions of salts, alkalis, and acids.

All these curves differ from those shown in Fig. 2 in exhibiting a higher rate of heat exchange during the initial period - at surface temperatures of 350-400° and higher. This increase may be quite appreciable under certain circumstances (100-200° and even more).

The presence of emulsified particles of oil in the water has an opposite effect on the characteristic curve. In this case, the cooling rate diminishes during the initial period, apparently due to the high stability of the vapor blanket.

A diagram showing the influence of dissolved salts and alkalis and of emulsified oils on the characteristic curve is shown in Fig. 3.

These data indicate that heat-treatment specialists are able to change the cooling power of water at comparatively high temperatures of the surface to be cooled. Unfortunately, we still have no means of substantially diminishing the cooling power of water below about 350°.

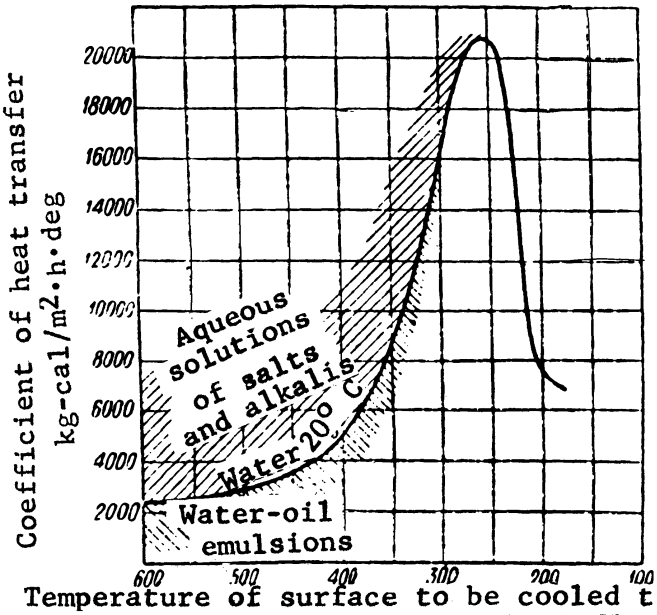

Fig. 3. Diagram showing the influence of additives on the cooling power of water.

What is more, solution of this problem would make it possible to replace oil completely as a quanching medium in the heat treatment of thin parts by some other medium that would provide deeper hardening and at the same time would be safe as far as the appearance of quench cracks is conerned.

3. DETERMINING CHARACTERISTIC CURVES BY THE METHOD OF STATIONARY HEAT FLOW

The difficulties involved in plotting "characteristic curves" by the method of cooling a silver ball and a certain degree of uncertainty introduced by the fact that the experiment is not run in a stationary state make it desirable to secure similar data for stationary thermal flow, which requires the establishment of steady conditions of heat transfer from the solid surface, at a temperature ranging from 800-900° to 100°, to the quenching medium and to determine the variation of the coefficient of heat transfer with temperature. An important factor in this is insuring accurate measurement of the temperature of the heating surface.

In this investigation we employ the method of heating wires or cylinders by electric current. The diameters of the conductors used were 0.1-0.5 mm for metals and somewhat more for graphite. Temperature was measured by the change in the resistance of the conductor, since all external methods of measurement do not yield reliable results with heaters of such small diameter.

The experiments indicated that the ordinary quenching media - cold water (20-40°) and cold oil - do not allow any of the numerous materials tested as conductors: copper, platinum, tungsten, molybdenum, nickel, and, nichrome, constantan, copel, graphite, etc., to be heated to high temperatures (800-900°).

As the current was increased the conductors were gradually heated to a temperature that was 20-40° higher than the boiling point of water and then were burned out. Burning out was not preceded by any external effect (sparking or warming-up). The reason for this burning out is the appearance of film boiling along a small section of the conductor, heating it up to the melting point, owing to the exceptionally high thermal flow (as much as 4,000,000 kg-cal/$m^2 \cdot h$).

Oil permits graphite to be overheated, but damages it by reacting with the graphite at high temperature.

Some of the materials listed can be heated to high temperature in boiling water. In particular, we were able to heat graphite, platinum, and the copper-nickel alloy copel (55% Cu, 45% Ni) to 1000°.

The best results were secured by copel with a conductor 0.2 mm in diameter. This alloy, however, has a negligible temperature coefficient of resistance and is thus not well adapted for measuring temperature. Nonetheless, we were able to run experiments in boiling water with it in the 700-1000° range (the temperature was measured by an optical pyrometer). The coefficients of heat transfer agreed with the data secured by other methods.

It is worthy of note that the visual effect of boiling was observed at currents that produced a mean conductor temperature of no more than 60-70°, which may be explained as due to the local nature of overheating and boiling.

In the case of transformer oil (temperature 35°) thermal flow and the coefficient of heat transfer both rise sharply when the wire temperature is 300-400°. The thermal flow rises to about 2,000,000 kg-cal/$m^2 \cdot h$, and the coefficient of heat transfer to 5000 kg-cal/$m^2 \cdot h \cdot deg$, the wires burning out when the thermal flow grows above this level.

4. PHYSICAL NATURE OF THE CHARACTERISTIC CURVES

The curves of the change in the coefficient of heat transfer from the surface of the part to be quenched to the quenching liquid as a function of the surface temperature of the part, shown in Figs. 1-3, are inverse functions of α with respect to Δt, secured in the investigation of heat transfer to boiling liquids under stationary conditions, with the sole difference, however, that in the latter case heat transfer is a maximum at the first critical density of thermal flow q_{kp1}, whereas on the "characteristic curve" the region of transition to maximum heat transfer starts at the second critical density of thermal flow q_{kp2}.

As we know, nuclear boiling, which is characterized by contact of the liquid with the heating surface and the resultant high rate of heat transfer, is replaced at thermal flow densities of the order of q_{kp1} by film boiling. At thermal flow densities of the order of q_{kp2} the poor heat-conducting vapor film breaks down, and nuclear boiling sets in.

As $q_{kp2} < q_{kp1}$ and $\frac{q_{kp2}}{q_{kp1}} \approx$ constant for free convection, the maximum of the coefficient of heat transfer on the characteristic curve may be lower than the maximum for the corresponding curve plotted under statio-

nary conditions by gradually raising the thermal load on the heating surface. The course of the "characteristic curve" during quenching is shown in Fig. 4 on the general curve of $\alpha = f(t_{cm})$.

The hydrodynamic theory of crises in the mechanism of boiling and the theory of heat transfer in a continuous vapor film /Ref. 2/ make it possible to elucidate in greater detail the effect of the dimensions of the body and of the mean temperature of the liquid on the shape of its "characteristic curve."

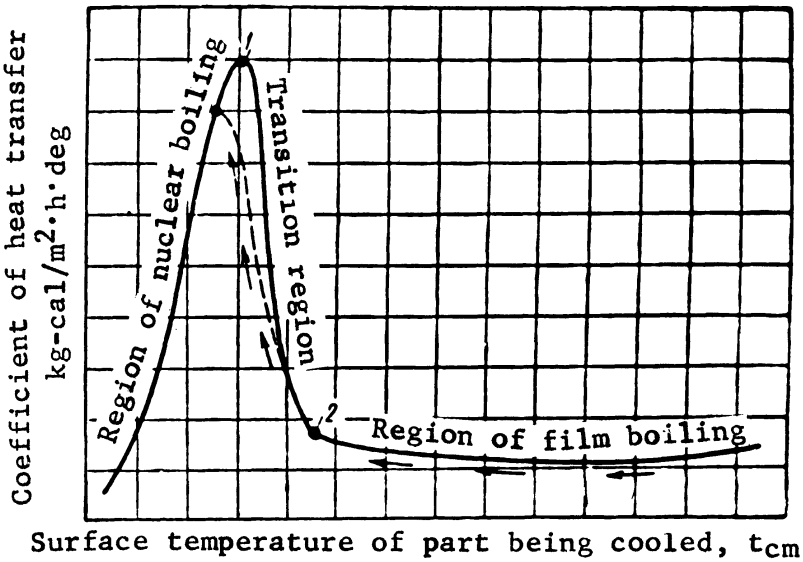

Fig. 4. "Characteristic curve" of the quenching liquid on the usual graph of $\alpha = f(\Delta t)$ during boiling.
1 - First critical point (Δt_{kp1}; q_{kp1}); 2 - second critical point (Δt_{kp2}; q_{kp2}; 3 - "characteristic curve" departing from the curve of normal nuclear boiling ($\Delta t < \Delta t_{kp1}$); $\rightarrow\rightarrow$ denotes the change in surface temperature during cooling of the part to be quenched.

During the period of film boiling at bodies of small size (diameter, height) the coefficient of heat transfer is given by the equation:

$$\alpha = \beta \sqrt[4]{\frac{\lambda''^3 \gamma'' (\gamma - \gamma'')}{\mu'' D (t_{cm} - t'')} \left[r + c'' \frac{t_{cm} - t''}{2} + c(t'' - \bar{t})(1 - n)\frac{\gamma}{\gamma''} \right]}. \qquad (1)$$

Here β = coefficient depending upon the circulation conditions of the fluid.
n = coefficient of recirculation of hot liquid near the vapor layer.
t_{cm} = surface temperature of the body.
t'' = boiling point of the liquid.
$\bar{t}$ = mean liquid temperature.
λ'' = coefficient of thermal conductivity of vapor.
μ'' = coefficient of dynamic viscosity of the vapor.

c'' = specific heat of the vapor.
γ'' and γ = densities of the vapor and the liquid, respectively.
c = specific heat of the liquid.
r = latent heat of vaporization.
D = diameter of the body.

According to the available experimental data:

$$(1-n)=0{,}065\left(\frac{\gamma''}{\gamma}\right)^{0,-} \tag{2}$$

The coefficient of heat transfer in Eq. (1) refers to the basic temperature difference $\Delta t = t_{cm} - t''$, i.e. the thermal flow is calculated from the formula:

$$q=\alpha\left(t_{cm}-t''\right) \tag{3}$$

both for the boiling and for the cooled liquid (but with a boiling boundary layer).

If the coefficient of heat transfer is based on the temperature difference $\Delta t = t_{cm} - \bar{t}$, i.e. the thermal flow is calculated from the formula:

$$q=\alpha\left(t_{cm}-\bar{t}\right), \tag{4}$$

Eq. (1) then becomes:

$$\alpha=\frac{\alpha_1}{1-\frac{t_{cm}-t''}{t_{cm}-\bar{t}}}, \tag{5}$$

where the value of α_1, the coefficient of heat transfer, is calculated from Eq. (1).

The critical density of thermal flow is related to the temperature of the liquid by the equation:

$$\frac{(q_{кр})_\theta}{(q_{кр})_{\theta-0}}=1+(1-n)\frac{c\gamma\theta}{r\gamma''}, \tag{6}$$

where $\theta = t'' - \bar{t}$ is the difference in temperature between the mass of the liquid and the boiling point.

The critical temperature at which the vapor film breaks down is:

$$t_{cm.кр}=t''+\frac{q_{кр2}}{\alpha_{кр2}}, \tag{7}$$

where $\alpha_{кр2}$ is the value of the coefficient of heat transfer from Eq. (1) at $q = q_{кр2}$.

Converting from Δt to q, we get Eq. (1) in the following form:

$$\alpha = \beta\lambda'' \sqrt[3]{\frac{\gamma''(\gamma-\gamma'')}{\mu''qD}\left[r + c''\frac{t_{cm}-t''}{2} + c(t''-\bar{t})(1-n)\frac{\gamma}{\gamma''}\right]}.$$

Inserting in this equation the value of qkp2 calculated from Eq. (6), we get:

$$\alpha_{кр2} = \beta\lambda'' \sqrt[3]{\frac{r\gamma''(\gamma-\gamma'')}{\mu''D(q_{кр2})_{\theta=0}}\left[1 + \frac{\frac{c''(t_{cm}-t'')}{2r}}{1+(1-n)\frac{c\gamma\theta}{r\gamma''}}\right]}, \qquad (9)$$

where θ = t" - $\bar{t}$ is the difference in temperature between the mass of the liquid and the boiling point.

$(qkp2)_{\theta=0}$ is the second critical density of thermal flow in a liquid boiling completely.

Hence, from (7):

$$t_{кр2} = t'' + \frac{(q_{кр2})_{\theta=0}\left[1+(1-n)\frac{c\gamma\theta}{r\gamma''}\right]}{\alpha_{кр2}}. \qquad (10)$$

If we neglect the superheat of the vapor $c(t_{cm} - t'')$ in Eq. (9), Eq. (10) then becomes

$$t_{кр2} = t'' + (\Delta t_{кр2})_{\theta=0}\left[1+(1-n)\frac{c\gamma\theta}{r\gamma''}\right], \qquad (11)$$

where $(\Delta t_{кр2})_{\theta=0} = \frac{(q_{кр2})_{\theta=0}}{(\alpha_{кр2})_{\theta=0}}$ is the critical temperature difference in a liquid that is boiling completely.

Hence, the theory yields the conclusion that the maximum of the "characteristic curve" should shift to the region of higher temperatures when the mean temperature of the cooling liquid is lowered. This conclusion is borne out by experiment, as seen in Fig. 2.

As for the variation of the coefficient of heat transfer with the dimensions of the part, the modern theory of heat exchange yields the following conclusions. In the region of film boiling the coefficient of heat transfer is either slightly dependent upon the dimensions of the surface, as seen in Eq. (1) or, for bodies of fairly large size, where the stability of the vapor film is disturbed, is completely independent of the dimensions of the body (self-modeling with respect to D).

In the region of nuclear boiling the coefficient of heat transfer is self-modeling with respect to the dimensions of the body. In the region of ordinary free convection α changes qualitatively with the dimensions of the body exactly as it does during film boiling.

CONCLUSION

Because of the widespread use of so-called "characteristic curves" in the heat treatment of steel it was important in evaluating quenching media to determine the extent to which these curves, secured by cooling a silver ball, are objective.

The investigation, based on the hydrodynamic theory of crises during boiling and on a series of special experiments, indicates that:

1. Characteristic curves can be plotted both by using the method of a nonstationary process (cooling of balls), and by the method of stationary heating of wires and rods.

2. The most objective characteristic of the cooling power of a liquid is the variation of the coefficient of heat transfer with the surface temperature of the body to be cooled and with the mean temperature of the cooling liquid.

3. The characteristic curves secured by the method of cooling a ball correctly reflect in general the principal qualitative features of the function $\alpha = f(t_{cm}\bar{t})$.

4. The region in which the characteristic curve departs from the maximum heat transfer corresponds to the so-called second critical density of thermal flow q_{kp2}, at which film boiling breaks down and nuclear boiling with a high rate of heat transfer sets in.

5. The absolute value of the coefficient of heat transfer depends upon the dimensions of the body only in the region of film boiling and of convection without boiling. This dependence is fairly slight. The dimensions of the standard sample should not be made very small, however, to avoid any appreciable influence of this factor on the absolute value of the ordinates of the characteristic curve.

6. The larger the latent heat of vaporization and the densities of the cooling liquid and vapor, the higher the thermal conductivity, and the lower the viscosity of the vapor, the higher the coefficient of heat transfer in the region of film boiling.

7. Lowering the mean temperature of the liquid compared to the boiling point increases the intensity of heat transfer in the regions of high wall temperatures.

8. The higher the latent heat of evaporation and the density of the cooling liquid, the greater the temperature at which maximum heat transfer occurs on the characteristic curve.

9. For any given liquid the position of maximum heat transfer on the characteristic curve shifts to the region of higher temperatures as the temperature of the cooling liquid drops. The reason for this is the increase in q_{kp2}, the critical density of thermal flow.

The second important problem posed in connection with the problem under discussion is a substantial decrease in the cooling power of water at temperatures of the cooling surface that lie below 350-300°.

LITERATURE CITED

1. Plant Laboratory, No. 2, 1948.

2. S. S. Kutateladze, Bull. USSR Acad. Sci., Div. Tech. Sci., No. 4, 1951.

SOME DATA ON THE NUMBER OF CENTERS OF VAPORIZATION IN BOILING ON INDUSTRIAL HEATING SURFACES

L. M. Zysina-Molozhen, Candidate of Engineering Sciences

The I. I. Polzunov Central Scientific Research Institute for Boilers and Turbines

In nuclear boiling the rate of heat transfer from the solid surface to the liquid depends largely on the number of active centers of vaporization.

Slow-motion moving pictures were used in investigatin the mechanism of vaporization in nuclear boiling, several determinations being made of the number of centers of vaporization on some heating surfaces.

In the foolowing we present material only on determination of the variation of the number of vaporization centers with different factors. The heating surfaces in these experiments were designed as horizontal plates. We investigated the boiling of water and of aqueous solutions of sodium chloride and glycerol. The pressures employed in the test ranged from 1 to 5 atmospheres absolute. The experimental plate was placed in a glass vessel filled with water, so that the vaporization process was accessible to visual and cinematographic observation.

The number of vaporization centers in the boiling of water are plotted in Fig. 1 as a function of the pressure and of the thermal loads on the heating surface. As the pressure is raised, with the density of thermal flow constant, the number of vaporization centers increases.

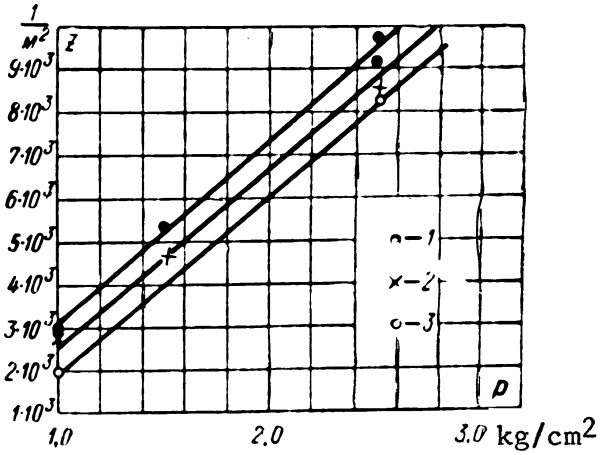

Fig. 1. Variation of the number of vaporization centers in boiling water with pressure for various heat thermal loads. 1) $q = 62{,}000$ kg-cal/m^2·h; 2) $q = 40{,}000$ kg-cal/m^2·h; 3) $q = 30{,}000$ kg-cal/m^2·h.

The number of centers of vapor formation $\underline{n}$ is plotted in Fig. 2 as a function of the density of thermal flow for water and for aqueous solutions of sodium chloride and glycerol. We see from the graph that the

number n differs considerably for the solution and for pure water. The practical coincidence of the experimental points for the two solutions is apparently accidental. In general, the number n for solutions is a function of the concentration, on which the overheating of the liquid above the vapor temperature t" depends. Another important factor controlling the number of active vaporization centers is the state of the heating surface. In order to shed light on this effect we undertook several investigations using surfaces of different degrees of roughness and made of different materials. The number of vaporization centers is plotted in Fig. 3 as a function of the thermal load for the boiling of water on a steel plate. The corresponding curve for a brass plate is plotted in the same graph for the sake of comparison. The experiments using the steel plate were run as follows: To begin with a plate made of so-called "black" iron was mounted. The surface of the plate was extremely uneven and highly porous. During the initial period the number of vaporization centers on this plate was extremely high. Subsequently, as the air adsorbed on the surface "boiled away," apparently, the number of centers gradually diminished, finally reaching some end value n and remaining constant. These values of n are plotted in the graph of Fig. 3 as circles.

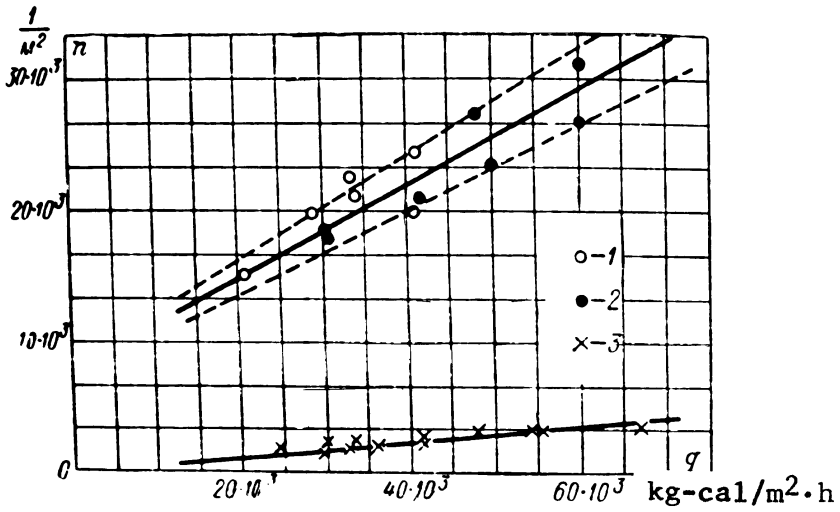

Fig. 2. Number of vaporization centers in the boiling of water and of aqueous solutions as a function of the thermal load on the heating surface.
1 - 40% aqueous solution of glycerol; 2 - 15% NaCl solution; 3 - water.

After completing a series of tests on an unfinished surface, we tested a polished iron plate. During the first day of tests the number of vaporization centers on this plate was extremely high (higher than with the clean brass plate), but then, however, it diminished gradually. The flaky rust that formed on the plate was washed off daily with a jet of water. The number of vaporization centers remained constant once a stable oxide film had formed on the surface. These values of n are denoted by inverted triangles and crosses in Fig. 3.

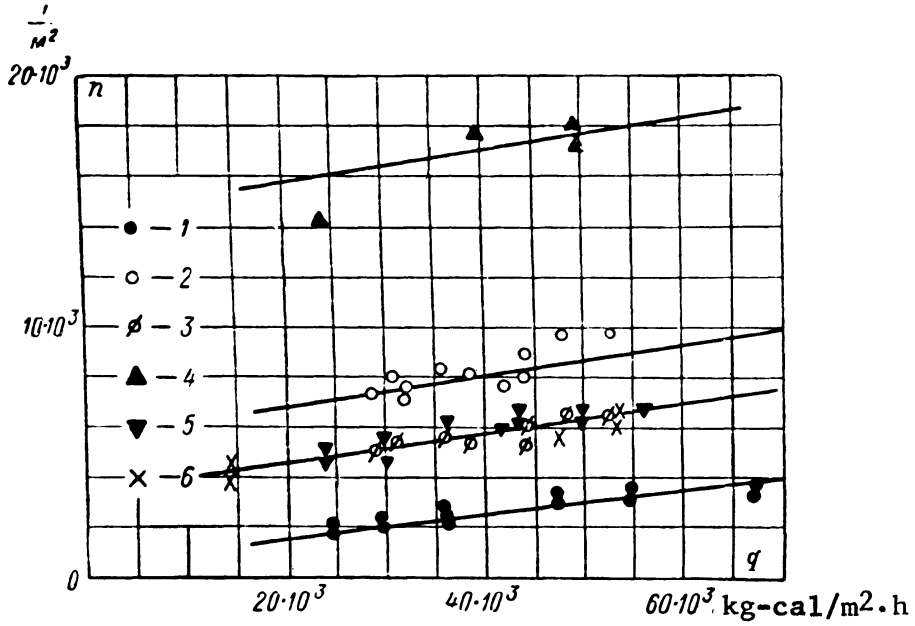

Fig. 3. Number of vaporization centers in the boiling of water as a function of the thermal load and of the condition of the heating surface.
1 - Ordinary brass surface; 2 - unfinished iron surface; 3 - unfinished iron surface, corrected for the surface dimensions; 4 - polished iron surface after 10 hours of operation; 5 - polished iron surface after 26 hours of operation and 100 hours of immersion in water; 6 - polished iron surface after 42 hours of operation and 200 hours of immersion in water.

Inasmuch as the unfinished surface was very rough, its actual area was greater than the area of the smooth surface. This increase in surface area was of the order of 30%, so that the values of n for the unfinished plate had to be reduced by about 30% for comparison with the corresponding values for the polished plate. These corrected values of n are denoted in Fig. 3 by circles with lines drawn through them. As we see the limiting value of n was the same for both iron plates.

The same phenomenon was observed with the brass plate. The limiting curve for the brass plate is likewise plotted in Fig. 3.

For the sake of comparison let us examine the data plotted in Fig. 4 for the values of coefficients of heat transfer on brass and iron heating surfaces as functions of time. As we see, the rate of heat exchange exhibits the same trend as the number of vaporization centers: approaching some limiting minimum value as the heating surface is "worn away."

Jakob's experimental data /Ref. 2/ for the rates of heat exchange on surfaces of differing roughness are plotted in Fig. 5. Surfaces of the same material were considered: 1) sand blasted; 2) grooved.

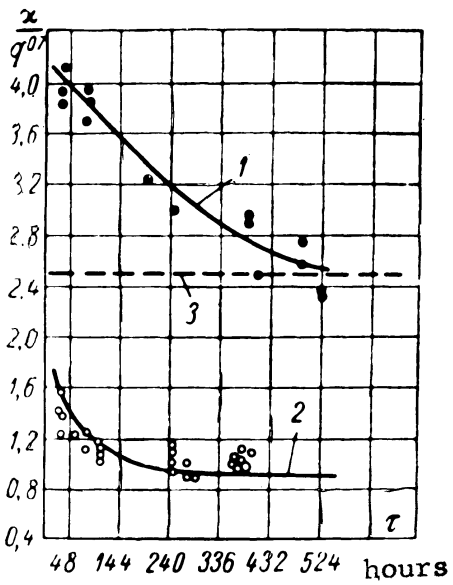

Fig. 4. Rate of heat exchange between the heating surface and a boiling liquid as a function of the period of operation.
1 - Kornilovich's experiments, brass tube; 2 - the author's experiments, steel tube; 3 - curve for the steady state according to Jakob's experiments with a brass plate.

Comparing the values of the coefficient of heat transfer α for these two types of rough surface, we see that although the values of for these two surfaces were quite different at the beginning of the test (Curves 1 and 5), the rates of heat exchange for both approached very close together (Curves 4 and 7) as the surface was "worn away."

Thus, here too we find a certain degree of similarity with the corresponding curves for the number of vaporization centers.

The fact that the limiting values of α and n in Jakob's experimens and in ours approach the same limit for surfaces made of the same material, independently of the methods used to roughen the surface initially, justifies the assumption that the source of vaporization centers is microroughness related to the structure of the surface material, rather than to the external macroroughness of the heating surface.

Examination of Fig. 3 indicates that the limiting value of n for an iron plate is higher than that for a brass plate. At first glance this appears unexpected, since the heat transfer coefficients for the iron plate are much lower than for the brass one, as shown in Fig. 4. Experimental data on the evolution of film boiling indicates, however, that the value of Δt_{kp} for a chrome-plated iron plate is much lower than the corresponding figure for polished brass. Evidently, the factor controlling the numerical value of α in ordinary heating surfaces is the thermal conductivity of the oxide plate, which makes it impossible to determine the true value of α and, as we know, results in a change in the degree to which the coefficient of heat transfer varies with the thermal load, in addition to the overall change in the coefficient.

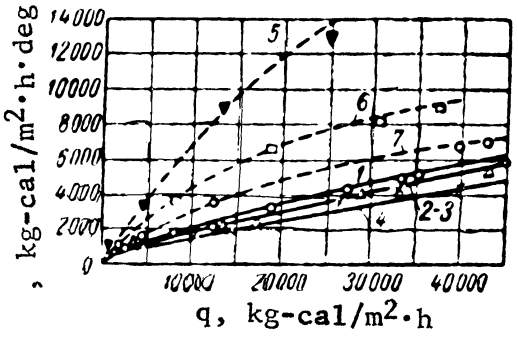

Fig. 5. Rate of heat exchange as a function of the thermal load for rough heating surfaces, according to Jakob's experiments.

1 - Heating surface freshly covered with sand; 2 - the same surface oxidized as a result of prolonged operation; 3 - the same surface again covered with sand; 4 - the same surface after prolonged operation; 5 - surface covered with freshly scraped out grooved; 6 - the same surface after 4 hours of operation and 24 hours of immersion in water; 7 - the same surface after 12 hours of operation and 48 hours of immersion in water.

LITERATURE CITED

1. L. M. Zysina-Molozhen, S. S. Kutateladze, J. Tech. Phys. 20, No. 1, 1950.

2. M. Jakob and V. Linke, Phys. Z., No. 8, 1936.

INFLUENCE OF THE HEATING-SURFACE MATERIAL ON HEAT EXCHANGE IN NUCLEAR BOILING IN A LARGE SPACE WITH FORCED MOVEMENT OF THE LIQUID

N. G. Styushin, Candidate of Engineering Sciences

The I. I. Polzunov Central Scientific Research Institute for Boilers and Turbines

It is known that the material of the heating surface affects the value of the coefficient of heat transfer in the region of nuclear boiling. Some experiments on boiling at different heating surfaces in a large space with forced circulation of the liquid are set forth below.

The experimental setup has been described in detail by us earlier /Ref. 1/.

The liquid tested (distilled water) was poured into the chamber. The bottom of the chamber, henceforth called the experimental plate, was heated by slightly superheated 2-3 °C) steam, supplied by a small electric boiler. A stirrer run by an electric motor was installed in the chamber. Ten copper-constantan thermocouples were inserted in the experimental plate to measure the temperature of the heating surface. After the latter had been embedded the surface of the plate was cleaned and polished. The amount of heat transmitted to the boiling liquid was measured by the weight of the condensate accumulated in the inner container of the heater.

The distinguishing feature of this procedure was the fact that the influence of all other factors was excluded in the investigation of the influence of the heating surface material on heat exchange during boiling.

This was attained by galvanizing the experimental plate to cover it with some metal or other. At first, we deposited a layer of nickel (20 microns); after the experiment with the nickel surface had been completed, the latter was covered with silver (24 microns). After the deposition of each layer the plate was polished with a felt buffing wheel.

Thus experiments with two different heating surfaces were run under completely identical conditions (the same initial mechanical processing of the plate, the same thermocouples, the same effect of external factors, etc.).

All the tests were run at atmospheric pressure.

Experimental data were secured for each of the heating surfaces during boiling with natural convection (without stirring), as well as with forced movement of the liquid, produced by the stirrer.

The variation of the heat transfer coefficients with the specific thermal flow for the nickel and silver heating surfaces during boiling with natural convection is shown in Fig. 1, where we have also plotted the data (Curve 3) secured by us previously with the same apparatus, boiling water on a chrome-plated surface /Ref. 1/.

In view of the fact that the experimental conditions were the same it is possible to compare the data secured with all three heating surfaces. We see in Fig. 1 that for identical densities of thermal flow all the tested heating surfaces yield different values of the coefficient α of heat transfer in boiling water. The values of α for the chrome-plated surface are, moreover, 25-28% lower than for the nickeled surface throughout the range of specific loads investigated.*

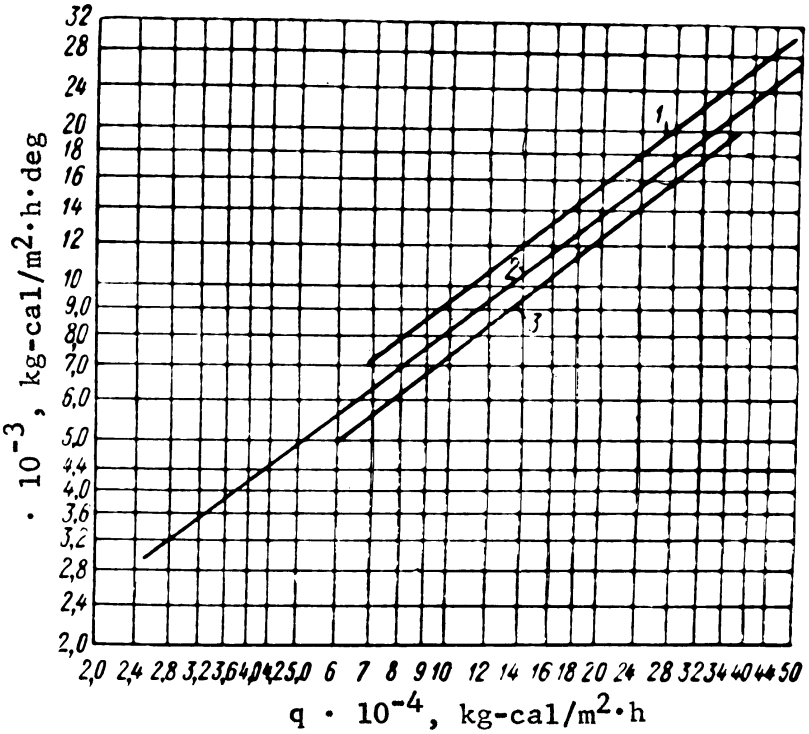

Fig. 1. Comparison of the coefficients of heat transfer to boiling water secured with different heating surfaces and natural convection.
1 - Nickel surface; 2 - silver surface; 3 - chrome-plated surface.

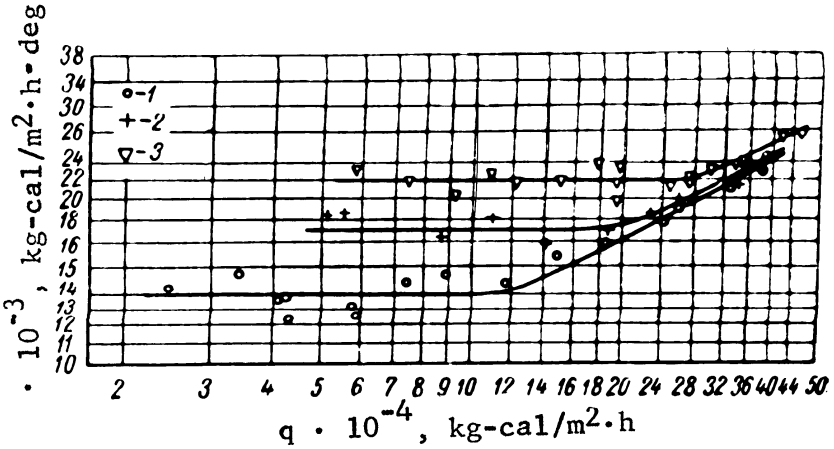

Fig. 2. Coefficient of heat transfer α as a function of the specific thermal flow q **with stirring** (nickel surface).
1) n = 290 rpm; 2) n = 500 rpm; 3) n = 750 rpm.

* It is important to bear in mind that the experiments revealed a discrepancy only in the absolute values of α at various surfaces. The nature of the relationship between α and q is the same for all the surfaces. - Editor.

TABLE 1

Coefficients of Heat Transfer for Different Velocities w and Specific Thermal Flows q, Secured with a Nickel Heating Surface

n* = 0 w** = 0		n = 290 w = 1.85		n = 500 w = 2.3		n = 750 w = 3.0	
q	α	q	α	q	α	q	α
kg-cal/m^2·h	kg-cal/m^2·h·deg	kg-cal/m^2·h	kg-cal/m^2·h·deg	kg-cal/m^2·h	kg-cal/m^{2}h deg	kg-cal/m^2·h	kg-cal/m^2·h·deg
97,000	9,050	24,500	14,400	51,750	20,400	58,300	25,300
101,400	9,230	34,000	15,450	55,700	20,600	74,200	23,900
131,000	11,100	40,800	13,600	87,800	18,500	92,300	22,500
138,300	12,350	41,200	13,970	110,000	20,000	108,500	84,900
169,000	14,200	43,400	12,400	141,000	17,630	121,400	23,800
199,300	16,340	57,500	13,050	188,000	19,000	150,400	24,270
236,000	17,400	58,500	12,450	230,600	20,800	177,000	26,050
312,000	22,450	74,100	14,800	262,000	21,800	195,000	21.900
336,000	24,000	89,000	15,350	324,000	23,850	195,500	23,800
403,000	26,550	117,700	14,900	344,000	23,700	198,500	25,600
476,500	30,500	149,000	16,930	355,000	25,750	251,000	23,250
--	--	186,300	17,600	375,000	25,700	271,000	23,750
--	--	244,000	19,850	--	--	272,000	24,500
--	--	263,000	21,070	--	--	301,000	25,100
--	--	268,500	21,600	--	--	342,000	26,100
--	--	329,000	23,200	--	--	350,500	26,350
--	--	383,000	24,900	--	--	421,000	29,800
--	--	411,000	27,300	--	--	457,000	30,100

* Stirrer rpm.

** Velocity of the liquid, measured at a distance of 1.5 mm from the heating surface, in m/sec.

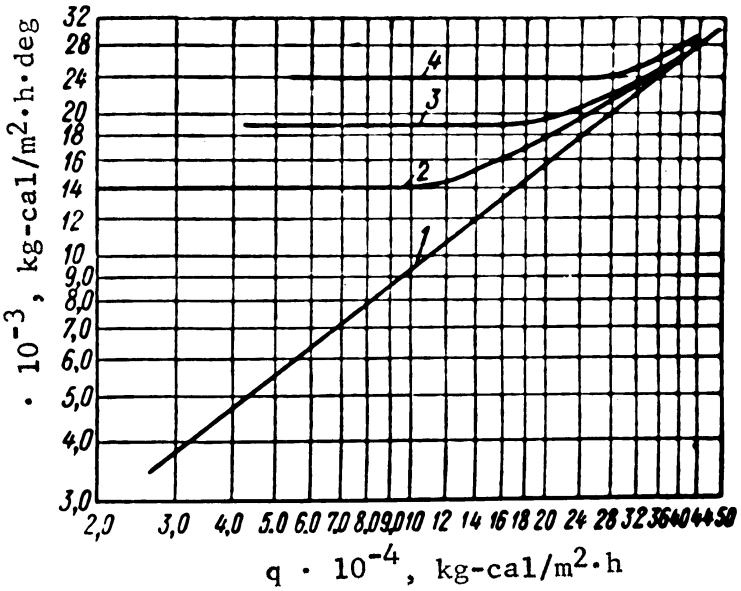

Fig. 3. Comparison of coefficients of heat transfer in the boiling of water at a nickel surface.

1) n = 0; 2) n = 290 rpm; 3) n = 500 rpm; 4) n = 750 rpm.

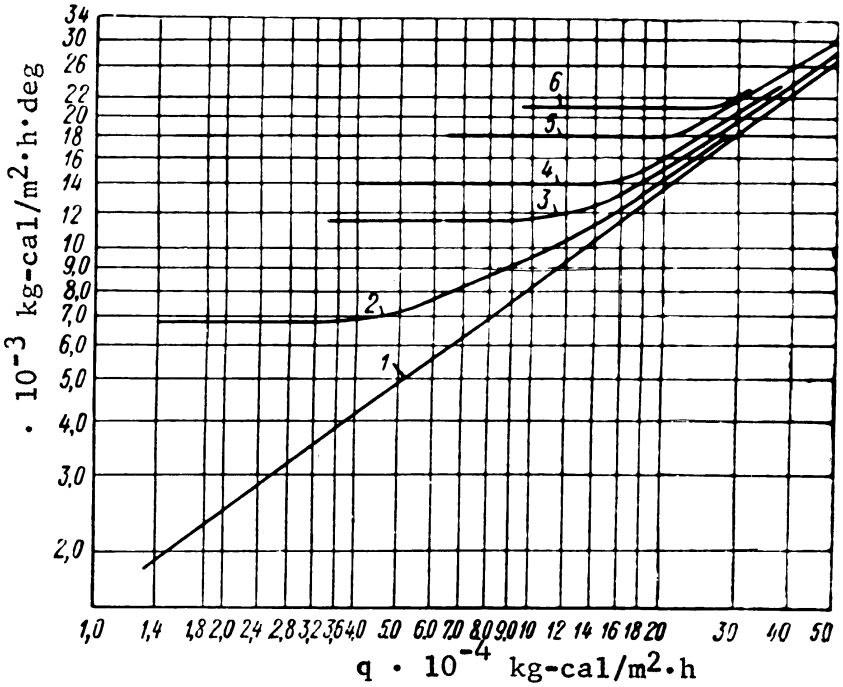

Fig. 4. Comparison of coefficients of heat transfer in the boiling of water at a silver surface.

1) n = 0; 2) n = 100 rpm; 3) n = 160 rpm; 4) n = = 290 rpm; 5) n = 500 rpm; 6) n = 750 rpm.

TABLE

Coefficients of Heat Transfer for Different Velocities w and

n* = 0 w = 0		n = 100 w = 0.6		n = 160 w = 0.95	
q kg-cal/m².h	α kg-cal/m².h.deg	q kg-cal/m².h	α kg-cal/m².h.deg	q kg-cal/m².h	α kg-cal/m².h.deg
6,300	1,450	17,400	6,700	35,200	12,130
12,000	1,935	22,900	7,160	57,800	11,120
25,100	3,025	30,100	6,400	73,800	11,350
45,000	4,670	38,700	6,570	94,500	12,260
63,300	6,400	53,800	8,280	104,000	11,000
76,300	6,950	54,000	7,830	134,300	12,050
105,300	8,390	62,900	7,270	187,000	14,600
110,500	9,280	79,850	8,365	211,000	15,560
116,500	9,320	116,000	10,540	215,500	15,900
119,300	9,110	130,000	10,740	265,000	18,030
140,500	10,340	177,000	13,300	297,000	19,900
150,000	10,730	178,500	13,740	312,500	20,300
185,000	13,020	201,000	14,260	318,000	20,800
190,000	13,290	239,000	16,050	337,000	20,800
200,800	13,650	244,000	15,650	371,000	23,300
249,000	16,180	258,000	16,800	454,000	26,000
267,000	16,530	--	--	476,000	28,000
477,000	26,800	--	--	--	--
--	--	--	--	--	--
--	--	--	--	--	--
--	--	--	--	--	--
--	--	--	--	--	--
--	--	--	--	--	--
--	--	--	--	--	--
--	--	--	--	--	--

* See footnote to Table 1.

Specific Thermal Flows q Secured With a Silver Heating Surface

n = 290 w = 1.85		n = 500 w = 2.3		n = 750 w = 3.0	
q $\frac{\text{kg-cal}}{\text{m}^2\cdot\text{h}}$	α $\frac{\text{kg-cal}}{\text{m}^2\cdot\text{h}\cdot\text{deg}}$	q $\frac{\text{kg-cal}}{\text{m}^2\cdot\text{h}}$	α $\frac{\text{kg-cal}}{\text{m}^2\cdot\text{h}\cdot\text{deg}}$	q $\frac{\text{kg-cal}}{\text{m}^2\cdot\text{h}}$	α $\frac{\text{kg-cal}}{\text{m}^2\cdot\text{h}\cdot\text{deg}}$
47,750	15,650	65,700	19,050	89,700	21,400
59,400	12,370	87,700	18,300	113,000	20,500
78,300	13,500	99,300	16,550	137,000	20,300
117,500	14,150	111,500	17,150	164,000	21,550
131,500	14,140	133,000	18,470	179,000	19,660
135,600	13,560	149,600	16,650	196,000	21,200
144,000	14,000	163,000	16,300	212,000	19,400
152,500	14,650	183,000	17,400	239,500	20,300
158,000	14,430	186,000	17,850	291,000	21,600
195,000	16,530	200,000	18,000	313,000	22,800
220,000	16,430	213,400	18,370	--	--
237,000	18,400	237,500	19,300	--	--
291,000	19,420	247,000	19,000	--	--
301,500	21,300	263,000	20,000	--	--
333,500	21,700	297,000	21,340	--	--
466,000	26,800	305,000	21,940	--	--
--	--	324,000	23,500	--	--
--	--	333,000	23,450	--	--
--	--	340,000	23,280	--	--
--	--	368,000	25,500	--	--
--	--	390,000	26,500	--	--
--	--	391,000	26,400	--	--
--	--	435,000	28,500	--	--
--	--	515,000	30,000	--	--
--	--	527,000	31,000	--	--

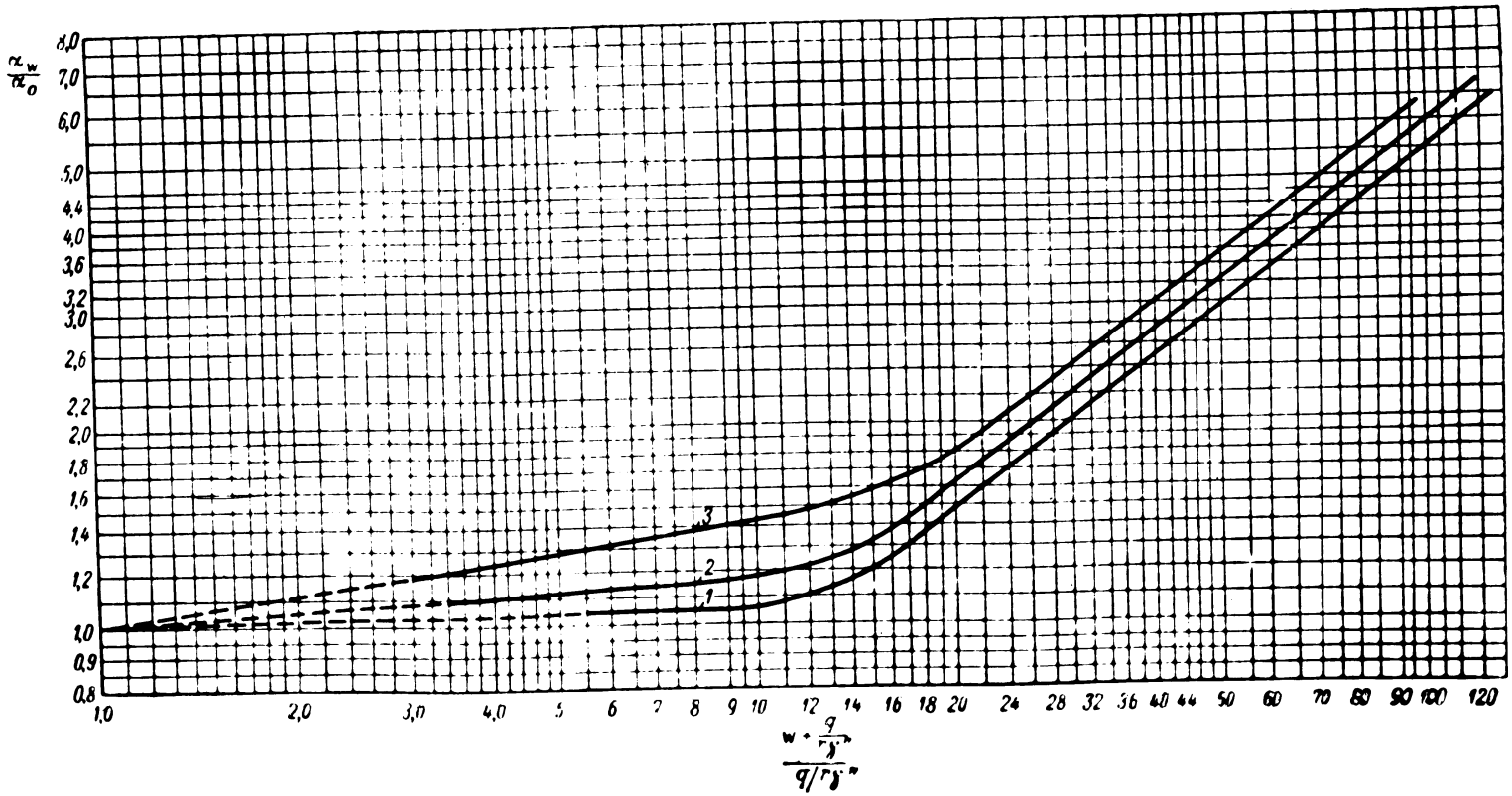

Fig. 5. Comparison of the experimental data secured with all the heating surfaces in dimensionless coordinates

1 - Nickel surface; 2 - silver surface; 3 - chrome-plated surface.

The coefficients of heat transfer secured experimentally with a nickeled heating surface and forced movement of the liquid are shown in Fig. 2.

A comparison of all the experimental data for the two heating surfaces is given in Figs. 3 and 4 and Tables 1 and 2.

As we see the nature of the curves secured for the nickel and silver heating surfaces is the same as in the experiments previously performed with chrome-plated surface.

It is evident that at low thermal loads the latter have no appreciable influence on the magnitude of the coefficient of heat transfer when the liquid is in forced movement, heat exchange in this case being controlled solely by the velocity of the liquid. At high specific thermal loads depends both on the velocity of the liquid and on q. The influence of velocity is, of courese, greater at low values of q.

Comparison of the coefficients of heat transfer secured for different heating surfaces at the same stirrer rpm indicates that in the region where α is determined by the velocity of the liquid, the material of the heating surface does not affect the heat exchange during boiling. It is understandable that this region of thermal flows is smaller at a given velocity for the heating surface whose coefficients of heat transfer are higher during natural convection (without stirring).

To secure an approximate estimate of the velocity of the liquid with respect to the heating surface we measured the dynamic heads in the space between the edge of the stirrer blade and the heating surface at a distance of 1.5 mm from the latter (with a pneumometric tube)*.

The results of our measurements of heat transfer coefficients and liquid velocities for both heating surfaces at different stirrer rpm are given in Tables 1 and 2.

The experimental data secured previously with the chrome-plated surface for the region where heat exchange is controlled by the overall action of velocity and thermal load were processed /Ref. 1/ in the form of the equation:

$$\frac{\alpha_w}{\alpha_0} = \left(\frac{w + \frac{q}{r\gamma''}}{\frac{q}{r\gamma''}} \right)^m , \qquad (1)$$

where α_w = coefficient of heat transfer to the boiling liquid at the given velocity and thermal flow, kg-cal/m^2·h·deg.

α_0 = coefficient of heat transfer for boiling without stirring, kg-cal/m^2·h·deg.

w = liquid velocity at a distance of 1.5 mm from the heating surface, m/h.

$\frac{q}{r\gamma''}$ = vaporization rate, m^3/m^2·h.

* The distance between the edge of the stirrer blade and the heating surface was 8 mm in the experiments on the silver and nickel heating surface. This distance was 10 mm in the experiments on the chrome-plated surface.

The exponent m was found to be about 0.18.

We processed the experimental data secured for the nickel and silver heating surfaces, using the same dimensionless coordinates,* this time covering the entire range of thermal load. This was also done for the chrome-plated surface. Comparison of the experimental data secured with the various heating surfaces is shown in Fig. 5 in dimensionless coordinates.

We see in Fig. 5 that the exponent m in Eq. (1) is about 0.8 for all the heating surfaces in the region where the coefficients of heat transfer are controlled solely by the velocity of the liquid, i.e. it corresponds to the velocity exponent for ordinary convective heat exchange. Thus, the ordinary equations for convective heat exchange can be used for calculation in this region of heat transfer to the boiling liquid. This also agrees with the experimental data obtained when water was boiled in a vertical pipe /Ref. 1/.

The exponent m is different for all the heating surfaces tested in the region where heat exchange is governed by the combined action of velocity and heat flow. We obtained m= 0.03 for the nickel surface, m = 0.07 for the silver surface, and m = 0.16 for the chrome-plated surface.** This rise in the value of the exponent m as we proceed from the nickel to the chrome-plated surface is understandable, for this exponent reflects the influence of velocity. All the curves are extrapolated to unity at the velocity w = 0, when $\alpha_w = \alpha_0$.

The variation of the coefficient of heat transfer with the specific thermal flow and with speed secured by us is of a qualitative nature because of the conditional nature of the latter and cannot be employed for a quantitative determination of α during boiling with forced movement of the liquid.

LITERATURE CITED

1. L. S. Sterman and N. G. Styushin, "Heat transfer and aerohydrodynamics," Trans. Cent. Sci. Res. Inst. Boil. Turb. 21, No. 5, 1951

* This treatment is valid only for a single pressure. - Editor.

** This value of m for the chrome-plated surface is apparently more accurate.

PART THREE

HEAT EXCHANGE IN THE FREEZING AND MELTING OF ICE

EXPERIMENTAL INVESTIGATION OF HEAT EXCHANGE IN MELTING

A. G. Tkachev, Candidate of Engineering Sciences
The Leningrad Institute of the Refrigeration and Dairy Industries

1. INTRODUCTION

The problem of heat exchange in melting is of practical importance in refrigeration engineering when ice or solid eutectic solutions are used as cooling media. The problems related to the melting of solids may be encountered in metallurgy, hydraulic engineering, and meteorology. Practically no research has been done along these lines, however. There is a short discussion of this problem in the monograph by S. S. Kutateladze /Ref. 1/, dealing principally with the establishment of the similitude criteria that may be used to describe the process. S. S. Kutateladze ran a few experiments on the melting of ice to confirm the general mechanisms suggested. The limited extent of these experiments did not enable him to secure functional relations that are required for practical calculation. In that monograph the author asserts that we must expect the coefficient of heat transfer to be independent of the change of state, as a first approximation, in fusion. This required experimental verification.

2. DESCRIPTION OF THE EXPERIMENTAL SETUP

In our experiments we melted spheres and cylinders (in the horizontal and vertical positions).

The specimens were prepared by slowly freezing the liquid; as this was done gas was removed from the liquid, and the specimens were secured in a homogeneous state. Experiments were run with ice, containing a fairly high percentage of air, to ascertain the effect of gases. Comparison of these experiments with those on specimens containing no air indicated that there was no perceptible difference in the results.

The specimens were melted with free movement of the liquid in vessels with a capacity of 20 and 1000 liters, depending upon the dimensions of the specimen. Before immersion in the liquid the specimen was kept for a fairly long time in the bath at the melting point to insure that the temperature of the melting point was reached throughout the specimen. The liquid in the vessel was at a temperature equal to the temperature of the surrounding air, which eliminated heat exchange with the ambient surroundings. For low-temperature tests the vessel (20-liter capacity) was placed in a second vessel in which the water temperature was kept constant by adding ice. Experiments were run at various liquid temperatures, ranging from 0 to 30° C. Threads were frozen into the specimen for attachment to a frame, which was immersed in the vessel together with the sample.

The following measurements were made during the experiment: melting time, liquid temperature at some distance from the specimen, and specimen dimensions during melting. To increase the precision of measurements the specimen was projected on a screen where its dimensions were noted at definite instants of time during the melting process. Figure 1 shows how this projection was done

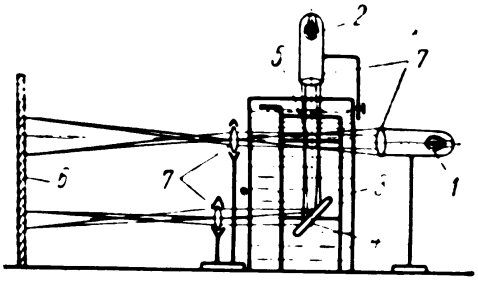

Fig. 1. Diagram of specimen projection
1 - Light source for vertical projection; 2 - light source for horizontal projection; 3 - frame; 4 - mirror; 5 - specimen; 6 - screen; 7 - lenses.

Lens 7 was made moveable for the vertical cylinder so that measurement could be made along the cylinder's height. Measurements were made in two projections for the sphere and the horizontal cylinder, inasmuch as the change in dimensions during the melting process was not uniform over the surface, the geometrical form of the melting body changing. In our investigation of heat exchange only 2 or 3 of the first few measurements, when the form of the body had not yet changed, were used for calculation.

3. METHOD USED IN WORKING UP THE EXPERIMENTS

The Fourier number, which includes the melting time, was determined for a sphere and a cylinder of infinite length, for which the effect of a change in some geometrical dimensions is eliminated, from the following function:

$$\mathrm{Fo} = f_1\left(\mathrm{Gr};\ \mathrm{Pr};\ K;\ \frac{\gamma'}{\gamma}\right), \tag{1}$$

where

$$\mathrm{Fo} = \frac{a\tau}{D^2};$$

$$\mathrm{Gr} = \frac{gD^3\beta\Delta t}{\nu^2};$$

$$\mathrm{Pr} = \frac{\nu}{a};$$

$K = \frac{r'}{c\,\Delta t}$ is the criterion that characterizes change of state.

Here:

a = coefficient of thermal conductivity of the liquid, m^2/h.

c = specific heat of the liquid, kg-cal/kg·degree.

D = diameter, meters.
g = acceleration of gravity, m/sec^2.
Δt = temperature difference between that of the liquid (t) and that of the surface, assumed equal to the melting point, t_o.
β = coefficient of volumetric expansion of the liquid, $\frac{1}{degree}$.
γ' = density of ice, kg/m^3
γ = density of liquid, kg/m^3.
r' = heat of fusion, kg-cal/kg.
ν = coefficient of kinematic viscosity of the liquid, m^2/sec.
τ = time, hours.

The dimensionless coefficient of heat transfer was determined from the condition that a change of state has no effect on heat exchange between the surface of the melting body and the liquid:

$$Nu = f_2(Gr;\ Pr),$$

where $Nu = \frac{\alpha D}{\lambda}$;

α = coefficient of heat transfer, kg-cal/m^2·degree·h.
λ = coefficient of thermal conductivity of water, kg-cal/m·degree·h.

In computing the similitude criteria the physical constants were based on the mean temperature of the liquid and of the surface (latter being taken as equal to the melting point). The coefficients of volumetric expansion were computed as the mean figures for the range from the melting point to the temperature of the liquid. The liquids employed in the experiments (benzene and ethylene glycol) were not chemically pure so that their viscosity and coefficient of thermal conductivity were determined experimentally. This work was done by G. N. Danilova, candidate of engineering sciences. The experiments showed that the liquids at our disposal possessed properties that did not differ from those cited in the literature.

The outer surface of the body receives from the liquid in an infinitesimal interval of time a quantity of heat:

$$dQ = \alpha \Delta t F d\tau, \tag{3}$$

where F is the surface of fusion in m^2.

A layer of ice whose thickness is dR melts in the same interval of time $d\tau$. On the assumption that the temperature of the entire body is equal to that of the melting point, we can set the quantity of heat used for fusion at:

$$dQ = r'\gamma' F dR, \tag{4}$$

where R is the radius in meters.

From Eqs. (3) and (4) we get:

$$\alpha = \frac{r'\gamma'}{\Delta t}\frac{dR}{d\tau}. \tag{5}$$

Equation (5) indicates that the coefficient of heat transfer can be determined for a given change of the radius of the sphere or the cylinder with time.

Our measurements enables us to determine $\frac{\Delta R}{\Delta \tau}$, thus utilizing Eq. (5). The Nusselt number was computed from the resultant coefficient of heat transfer.

The condition that Equations (5) are identical for two phenomena is satisfied if the similitude factors are related as follows

$$\frac{i_a i_t i_\tau}{i_r i_\gamma i_l} = 1.$$

If the numerator and denominator on the left-hand side of this equation are multiplied by $i_l i_\lambda i_c i_\gamma$, we secure after transformation:

$$\frac{\mathrm{Fo}}{K \frac{\gamma'}{\gamma}} \mathrm{Nu} = \text{idem.} \qquad (6)$$

Experiments have confirmed the correctness of Eq. (6). The product:

$$\frac{\mathrm{Fo}}{K \frac{\gamma'}{\gamma}} \mathrm{Nu}.$$

remains constant as well as invariant over a fairly wide range of changes of all the variables that characterize the phenomenon.

In light of the foregoing the experiments were processed using the following equations:

$$\mathrm{Nu} = c\,(\mathrm{GrPr})^m, \qquad (7)$$

$$\frac{\mathrm{Fo}}{K} = c_1\,(\mathrm{GrPr})^{-m}. \qquad (8)$$

We have omitted the criterion $\frac{\gamma'}{\gamma}$ from Eq. (8), inasmuch as this criterion changes no more than 4% when the water temperature is varied from 0 to 100° C.

4. EXPERIMENTAL RESULTS

a) Change in the Dimensions of Ice Cylinders During Melting

Curves showing the change in the radius of a melting horizontal cylinder as a function of time are shown in Fig. 2. Inspection of the curves yields the conclusion that the coefficient of heat transfer changes during the melting process, inasmuch as $\frac{\Delta R}{\Delta \tau}$ changes /see Eq. (5)/.

In laminar flow the change in the coefficient of heat transfer may be produced by the influence of the cylinder diameter and by the change of shape during the melting process. The shape changes because of the nonuniform conditions of heat exchange over the surface as a result of which

melting is uneven over the surface. We see from the vurves that the coefficient of heat transfer rises as the radius decreases.

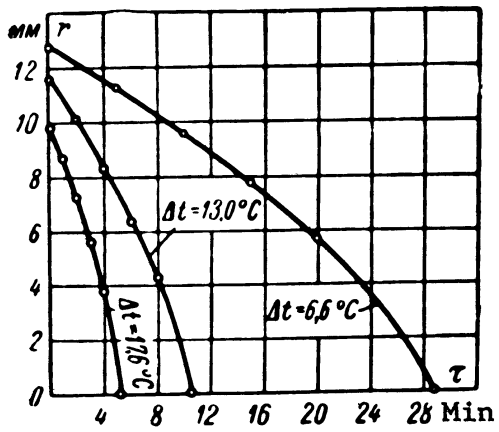

Fig. 2. Curves showing the change in the radius of horizontal cylinders with time.

b) Influence of the Anomaly in the Density of Water Upon the Heat-Exchange Conditions

It is known that the density of water is a maximum at + 4° C. As a result the mean coefficient of volumetric expansion changes sign, becoming negative, at a temperature of approximately + 8°C. As a result of this anomaly the direction of motion of the water changes with respect to the floating specimen, whose surface temperature is 0° C, depending upon temperature. When the water temperature is below 4° C, the water moves upward around the specimen, since the temperature is below 4° C in the boundary layer and hence the water density is lower. When the water temperature exceeds 4° C, the motion becomes more complicated, since two directions may be present, as shown in Fig. 3.

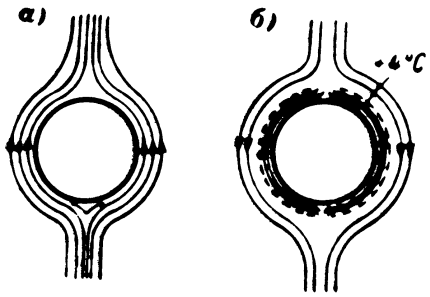

Fig. 3. Nature of water motion: a - water temperature $\leq$ 4° C; б - water temperature $>$ 4° C.

To ascertain the influence of the water temperature we ran experiments in which the initial diameter of the cylinder remained the same. It was found that the coefficient of heat transfer is lowest for a water

temperature of some 5.5°C. It must be assumed that in this case the velocity of water movement will be a minimum, inasmuch as the forces setting up two opposite motions will be approximately equal. Observations of the nature of melting indicate that under these conditions the coefficient of heat transfer changes along the length of a horizontal cylinder as well as about its perimeter (Fig. 4). This nature of melting was not observed under other conditions.

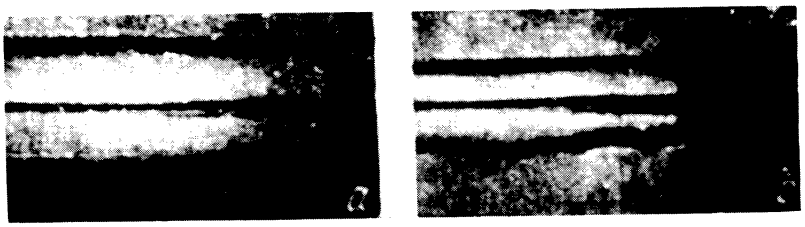

Fig. 4. Melting of a horizontal cylinder at a water temperature of + 5.1° C:
a - before beginning of melting; б - during melting.

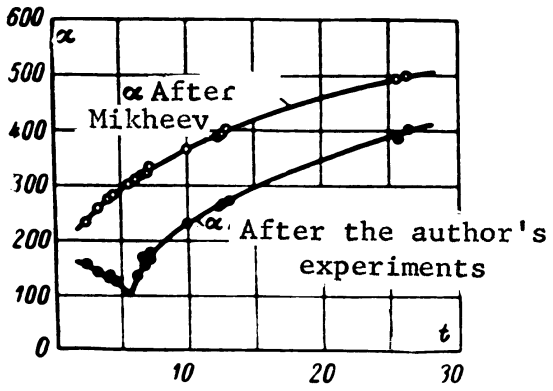

Fig. 5. Coefficient of heat transfer as a function of water temperature.

The experimental coefficients of heat transfer for different water temperatures are shown in Fig. 5. The influence of the water anomaly on heat exchange will be manifested not only during a change of state, so that the sharp drop in the coefficient of heat transfer must be borne in mind for heat exchange both with water moving freely and at temperatures close to 0° C. The values of the coefficients of heat exchange calculated from Mikheev's equation /Ref. 2/ for free motion without a change of state are plotted in Fig. 5 to provide an approximate estimate of this decrease. As a result of the anomalous behavior of the coefficient of volumetric expansion for water, we get a substantial scattering of points for the water temperature range of 0-15° C when our data are processed with the similitude criteria. For this reason only the experiments with water made at a temperature higher than 15° C were considered in comparing the results for different liquids.

c) Processing the Experiments, Using Criteria of Similitude

The results of experiments made on horizontal cylinders of ice, benzene, and ethylene glycol are plotted in Fig. 6 in the coordinates log Nu_{md}; log $(GrPr)_{md}$. For the sake of comparison the experimental points of Belter /Ref. 3/ and of Ackerman /Ref. 4/, as well as the equations suggested by M. A. Mikheev /Ref. 2/ are also plotted in Fig. 6. The experiments were made over a range of values of Gr Pr extending from 10^5 to 10^8, where laminar motion turns into turbulent motion. According to our experiments this transition occurs for a Gr Pr of about 10^7, which agrees with the data of M. A. Mikheev. Belter's experiments, in the region of laminar motion, and Ackerman's experiments, in the region of turbulent motion, agree fairly well with our experiments. The substantial difference between our results and the function given by M. A. Mikheev for heat exchange in free motion without a change of state should be borne in mind. This discrepancy is 35% for laminar motion and 30% for turbulent motion. After a detailed analysis of the experimental data secured by several research workers who performed their experiments on gases, we are inclined to believe that the discrepancy is due to an insufficiently accurate allowance for that part of the heat transmitted by radiation. This assertion requires checking, however, since our experiments were performed with the thermal flow directed from the liquid to the solid, whereas the comparable experiments were run in the opposite direction of thermal flow.

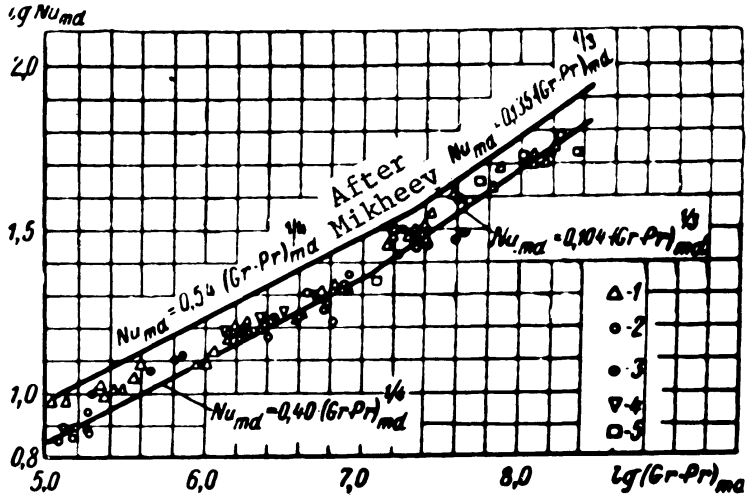

Fig. 6. Results of experiments with horizontal cylinders.
1 - Author's experiments with water; 2 - the same with benzene; 3 - the same with ethylene glycol; 4 - Belter's experiments with water; 5 - Ackerman's experiments with water.

The experimental results secured by melting vertical cylinders of ice up to 0.5 m high are plotted in Fig. 7 in the following coordinates: log Nu_{md}; log $(GrPr)_{md}$. We see from the figure that the transition from laminar to turbulent motion occurs when GrPr equals 10^6. In this case, the experimental points are likewise lower than Eigenson's experimental curve /5/, plotted in Fig. 7. But when the height of the cylinder is taken as the controlling dimension we get satisfactory agreement with the experiments made by Eigenson, Carnes /Ref. 6/, and Jakob /Ref. 7/, as is seen in Fig. 8. When the results of experiments on vertical cylin-

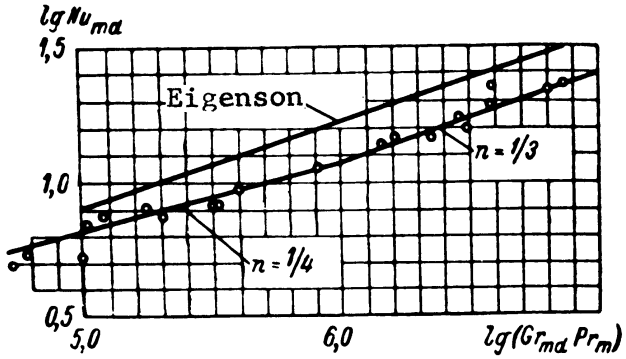

Fig. 7. Results of experiments with vertical cylinders.

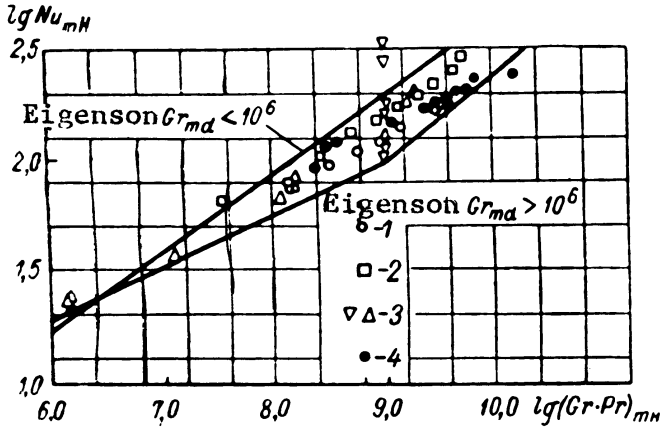

Fig. 8. Results of experiments with vertical cylinders (with respect to their height).
1 - Author's experiment No. 5; 2 - author's experiment No. 14a; 3 - Carnes' experiments; 4 - Jakob's experiments.

ders are plotted according to diameter in Fig. 6, we find that the difference is negligible; we therefore can recommend the following general relationship for cylinders:

for

$$10^3 < (\mathrm{GrPr})_{md} < 10^7$$

$$\mathrm{Nu}_{md} = 0{,}40 \cdot (\mathrm{GrPr})_{md}^{1/4}; \tag{9}$$

for

$$(\mathrm{GrPr})_{md} > 10^7$$

$$\mathrm{Nu}_{md} = 0{,}104\,(\mathrm{GrPr})_{md}^{1/3}. \tag{10}$$

The results of experiments on the melting of ice spheres are given in Fig. 9. When we compare them with Mikheev's equation we find that the agreement is quite satisfactory. This is likewise borne out by the paper by Kudryavtsev /Ref. 8/, in which he gives the modeling of natural convection in water. Kudryavtsev's experiments, made with heating of the liquid, justify the assumption that the influence of the direction of thermal flow is slight.

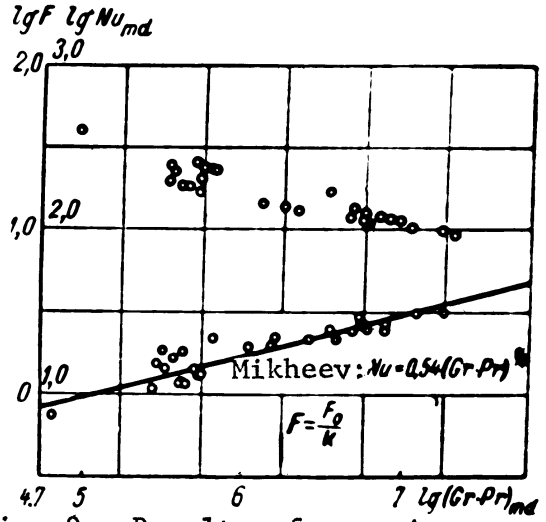

Fig. 9. Results of experiments with spheres.

Thus, the coefficient of heat transfer in the melting of the sphere can be determined for laminar flow $[10^3 < (GrPr)_{md} < 10^7]$ from the equation:

$$Nu_{md} = 0{,}54\,(GrPr)_{md}^{1/4}; \tag{11}$$

and for turbulent motion $[(GrPr)_{md} > 10^7]$ from the equation:

$$Nu_{md} = 0{,}135\,(GrPr)_{md}^{1/3}. \tag{12}$$

Working up the experiments on spheres and cylinders in conformity with Eq. (6) enables us to derive a function for determining the time required for complete melting as follows:

$$\frac{Fo_{md}}{K}\,Nu_{md} = 0{,}305. \tag{13}$$

Thus, once we know the value of the Nusselt number we can readily determine the time of melting from Eq. (13).

5. CONCLUSIONS

This paper describes experiments to determine melting times and coefficients of heat transfer between a freely moving liquid and the surface of a melting body (sphere, horizontal cylinder, and vertical cylin-

der). In the experiments the effect of the anomaly in the density of water on the conditions of heat exchange was determined. The results of the investigations were worked up in criterial forms; the melting time and the coefficients of heat transfer can be determined from the equations obtained.

LITERATURE CITED

1. S. S. Kutateladze. Heat Transfer in a Change of State (Principles of the Theory). State Scientific and Technical Publishing House of Literature on Machinery, 1939.

2. M. A. Mikheev, Principles of Heat Transfer. State Power Press, 1949.

3. R. Martinelli and L. Belter, Heating, Piping, and Air Conditioning, August, 1939.

4. G. Ackerman, Forschung 3, No. 1, 1932.

5. M. V. Kirpichev, M. A. Mikheev, and L. S. Eigenson. Heat Transfer. State Publishing House for Technical and Theoretical Literature, 1940.

6. I. Carnes, Philosophical Magazine 24, No. 162.

7. I. Tulukian, G. Hawkins, and M. Jakob, Trans. ASME 70, No. 1, Jan. 1948.

8. E. V. Kudryavtsev, "Modeling of natural convection at large controlling dimensions," Bull. USSR Acad. Sci., Dept. Tech. Sci., No. 1, 1948.

HEAT EXCHANGE IN THE FREEZING OF ICE

A. G. Tkachev, Candidate of Engineering Sciences, and G. N. Danilova, Candidate of Engineering Sciences

The Leningrad Institute of the Refrigeration and Dairy Industries

1. INTRODUCTION

Crystallization processes are widely employed in various branches of engineering (in the metallurgical industry: in the solidification of castings; in the chemical and allied industries: in the crystallization of salts from solutions; in the food industry: in manufacturing ice and in the heat treatment of various food products containing moisture, etc.). Nonetheless, not enough research has been done as yet on the thermal processes that accompany and bring about the processes of crystallization, although there is no doubt that knowledge of these conditions is of essential importance to the establishment of the scientific principles of organization of processes of this sort and to the rationalization of various branches of production.

The present paper deals with the problem of investigating heat exchange during the formation of ice, the problem being posed and solved for definite limited conditions.

In S. S. Kutateladze's monograph* the author analyzed the differential equations that describe the process of heat exchange during the solidification of a liquid around certain centers of crystallization, and secured criteria that described this process. He also furnishes an analytical solution of some special problems involved in the formation of ice in reservoirs.

The papers by A. A. Gukhman and Veinik /Ref. 1/, A. K. Skryabin /Ref. 2/, and A. London and R. Seban /Ref. 5/ are likewise well known.

A. K. Skryabin considers the process of crystallization from melts or from solutions and poses the problem in its general form. The solution obtained is too general and complicated and hence not very well adapted to practical use.

London and Seban employed an approximation method of analyzing the processes of ice formation in liquids for various forms of the bounding surfaces. They secured equations for the time required for ice formation on plane, cylindrical, and spherical surfaces. The solutions are given in dimensionless quantities. The form of the equations secured is not very convenient for practical use, however, and moreover, it does not disclose the criteria that describe the process. It should also be noted that London and Seban ignore the thermal supercooling of the ice layer formed, considering the role of this heat as negligible in general. This limits the application of their equations to cases where the specific heat is low compared to the heat of fusion, as is the case with ice.

The solution of the problem based on the assumption that the heat travels in one direction is likewise inexact, since in actuality freez-

* See /Ref. 1/ in the preceding paper.

ing never takes place at infinite cylindrical or plane surfaces. On the contrary, in practice the temperature field is far from one-dimensional when water is frozen in molds. It should be borne in mind, however, that the complication of the problem involved in introducing even a two-dimensional field results in reducing the practical value of the solution because of its complexity.

The most generalized and theoretically substantiated research of the thermal processes involved in crystallization has been made by A. A. Gukhman and A. I. Veinik /Ref. 1/. They have provided methods for calculating the crystallization processes during casting.

The authors divide the entire process into two stages of time: cooling the liquid metal from the temperature at which it is poured into the mold to the temperature of crystallization and solidification of the casting at the crystallization temperature. The thermal phenomena characterizing the processes of the solidification of molten metal and the freezing of water are the same if we consider the stage in which the temperature of the liquid is at the crystallization temperature. Basing their analysis on the same considerations as those employed by London and Seban, the authors also make allowance for the change of temperature in the solid layer that is formed as a function of time. To simplify the problem they considered the simple law of temperature distribution within the casting: a straight-line change of temperature through the thickness of the layer formed. No change of temperature in other directions was considered. The solutions are given for plane cylindrical, and spherical surface forms. Their mathematical analysis yielded general criterial equations that describe the process.

We also have some experimental data on crystallization. Thus, in the paper by A. A. Gukhman and A. I. Veinik referred to above the results of two experiments on the solidification of a metallic casting are reported. P. F. Konoplev ran experiments on the formation of ice in molds, and A. P. Dobrovolsky ran experiments on the freezing of ice on a cylindrical pipe. Brine was used for cooling in both cases. Long and Seban ran experiments on the formation of ice inside and outside a cylindrical mold when the latter was cooled by a current of air /Ref. 5/.

We made an experimental investigation on the freezing of ice inside and outside vertical cylinders with free movement of the water. Our experimental results are given below together with a comparison of these results with the figures secured by other researchers.

2. EXPERIMENTS ON THE FREEZING OF ICE IN CYLINDERS

a) Experimental Procedure

In these experiments ice was frozen in steel cylinders 94 mm in diameter and 410 and 200 mm high.

The cylinders were filled with water and placed in a freezing chamber where the required air temperature was kept constant. Constancy of temperature throughout each experiment and the temperature required for the different experiments were secured by appropriate operation of the refrigerating plant.

In the experiments that were used for plotting the difference between the air temperature within the chamber and the mean value throughout the experiment was 0.5° C on the average. Its maximum deviation from the mean was 1-3° C at individual instants of time and then only in some experiments.

Experiments at low air temperatures were performed in a freezing cabinet equipped with automatic temperature regulation. The experiments were run with free and forced movement of the air. Forced movement was provided by a powerful fan installed in the chamber for this purpose. The cylinders were placed at some distance from the inlet of the fan, with their entire surface exposed to a strong current of air.

The following measurements were made during the experiments: time, thickness of layer of frozen ice, temperature of the water in the cylinder, and temperature of the air in the chamber. When forced air circulation was employed we also measured the air velocity. The water and air temperatures were measured with standard thermometers graduated to 0.1°C. No special observation of the cooling of the water was made; the only variable recorded was the temperature at which ice formation set in. We either poured water at a temperature of 1.5-2° C into the cylinders, after which they were placed in the chamber for observation, or observation of freezing was begun when the temperature of the water in the cylinder placed in the chamber approached 2° C. The thickness of ice was measured with an inside micrometer at the mean cross section of the cylinder; the amount of solution was measured with a slide gage to within 0.05 mm.

At the beginning of the process, when the temperature of the water in the cylinder was close to the temperature at which freezing set in, observations of the cylinder in the chamber were made at 5-minute intervals. Subsequently, after we had determined the instant of time corresponding to the onset of freezing, measurements were made at larger intervals of time (10-15 min) and later on every 0.5-1 hour.

The velocity of the air flowing around the cylinder was measured by means of a cup anemometer at twelve points on the surface: at four points around the cross section of the cylinder and at three sections with respect to height.

A total of ten experiments were made. The principal data characterizing the experiments performed on the freezing of ice in cylinders are given in Table 1.

b) Processing the Experimental Data and the Experimental Results

The processing of the experimental data was based on the theory of similitude. S. S. Kutateladze, analyzing a system of differential equations that describe the process of solidification of a liquid, obtained the following type of criterial equation for such a process:

$$\mathrm{Fo} = f\left(\mathrm{Pr}, K', \mathrm{Re}, \frac{\gamma'}{\gamma}, \mathrm{Bi}, \frac{l}{l_0}; \frac{l_-}{l_0}\right), \tag{1}$$

where

$$\mathrm{Fo} = \frac{a'\tau}{l_0^2};$$

$$\mathrm{Pr} = \frac{\nu}{a};$$

TABLE 1

Kind of motion	Air velocity, m/sec	Air temperature, °C	Magnitude of criteria Bi	K'
Free	--	-16.1	0.318	9.55
"	--	-16.4	0.318	9.4
"	--	-30.0	0.318	5.34
"	--	-13.6	0.310	11.0
"	--	-16.0	0.318	9.4
"	--	-16.6	0.318	5.34
Forced	13.8	-10.0	2.12	15.3
"	12.8	-9.9	2.04	15.3
"	12.8	-14.0	2.2	11.0
"	10.9	-13.4	1.82	11.6

$K' = \frac{r'}{c' \Delta t'}$ is a criterion characterizing the change of state;

$$Re = \frac{w l_0}{\nu};$$

$\frac{\gamma'}{\gamma}$ = criterion characterizing the transposition of volume due to the difference in the densities of the liquid and solid phases:

$$Bi = \frac{\alpha l_0}{\lambda'};$$

l_0 = characteristic linear dimension at the initial instant of time.
l = linear dimension at the moment time is read.
a = liquid's coefficient of temperature conductivity, m^2/h.
c = liquid's specific heat, kg-cal/kg·degree.
D_0, R_0 = initial diameter and radius, respectively, meters.
t = water temperature, °C.
t_0 = freezing temperature, °C.
t_f = temperature of the cooling medium, °C.
Δt = difference between freezing temperature and temperature of the cooling medium, °C.
α = coefficient of heat transfer, kg-cal/m^2·degree·h.
β = liquid's coefficient of volumetric expansion, $\frac{1}{\text{degree}}$.
γ = liquid density, kg/m^3.
δ = ice thickness, meters.
r' = heat of fusion of ice, kg-cal/kg.
λ = liquid's coefficient of thermal conductivity, kg-cal/m·deg·h.
ν = liquid's coefficient of kinematic viscosity, m^2/h.
τ = time, hours.*

When freezing takes place in the still water the Reynolds Re may be ignored, using the Grashof number $Gr = Ga \beta \Delta t$, instead, $Ga = \frac{g l_0^3}{\nu^2}$ where

The physical constants of water may be considered constant for the

* The physical constants of the solid phase are designated by the same letters as the constants for the liquid, but with a "prime" (').

formation of ice in still water at a water temperature equal to or close to the freezing point, as was the case in our experiments. The specific gravity of ice may likewise be considered constant within the narrow temperature range in which the experiments were performed. Under these conditions the following criteria may be ignored: Pr, Re, Gr, $\frac{\gamma'}{\gamma}$.

Equation (1) then takes on this form:

$$\mathrm{Fo} = f\left(K',\ \mathrm{Bi}\frac{l_\tau}{l_0}\right). \tag{2}$$

In processing our experimental results we took D_0, the diameter of the cylinder, as the characteristic dimension l_0 that enters into the Biot and Fourier criteria, while the thickness of ice at every given instant of time, δ, was taken as l_τ.

The ice thicknesses δ for different instants of time were taken from the experiment. The physical constants of ice, a', λ', and c', were chosen for the mean temperature:

$$t_m = \frac{t_0 + t_f}{2}.$$

The coefficient of heat transfer of the air was determined as the sum of the coefficients of convective and radiative heat transfer:

$$\alpha = \alpha_к + \alpha_p. \tag{3}$$

The coefficients of convective heat transfer for free motion were found from M. A. Mikheev's equation /Ref. 3/:

$$\mathrm{Nu}_m = A_1(\mathrm{GrPr})_m^n. \tag{4}$$

The outer diameter of the cylinder was taken as the controlling dimension in Eq. (4). The constants were taken for the mean temperature of the surface of the cylinder and the air. The surface of the temperature was taken as equal to the freezing point.

The coefficient of convective heat transfer for forced motion was found from the equation:

$$\mathrm{Nu}_f = A_2\mathrm{Re}_f^n. \tag{5}$$

All the physical constants in Eq. (5) were chosen for the mean air temperature.

The air velocity was found as the mean of the velocities at twelve points around the surface of the cylinder.

The coefficient of radiative heat transfer was calculated from the equation:

$$\alpha_p = \frac{c_p}{T_{cm} - T_f}\left[\left(\frac{T_{cm}}{100}\right)^4 - \left(\frac{T_f}{100}\right)^4\right], \tag{6}$$

where c_p = coefficient of radiation.

T_{cm} = absolute temperature of the cylinder wall.

T_f = absolute temperature of the air.

The criterial equation taken as the starting point in working up the experiments is as follows:

$$\mathrm{Fo} = CK'\left(\frac{\delta}{D_0}\right)^n\left(\frac{1}{\mathrm{Bi}}\right)^m. \tag{7}$$

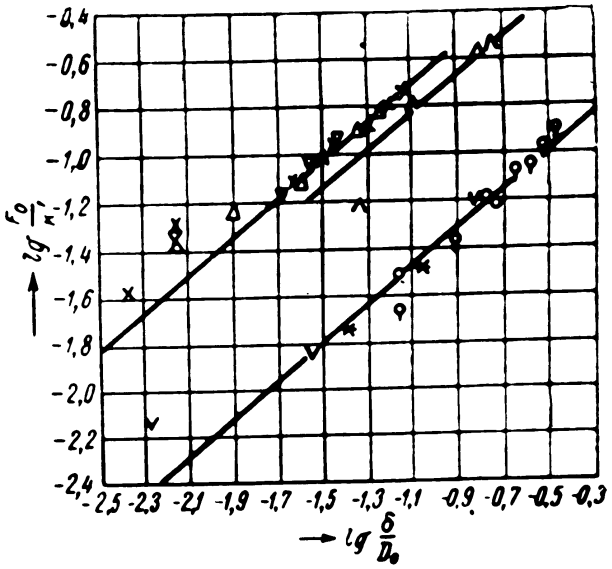

Fig. 1. Results of tests on the freezing of ice in cylinders at various air temperatures.

The test results are plotted in Fig. 1 in the following coordinates:

$$\lg\frac{\mathrm{Fo}}{K'};\ \lg\frac{\delta}{D_0}.$$

The exponent n for $\frac{\delta}{D_0}$, was found to be 0.8 from the graph in Fig. 1.

The same experiments are plotted in Fig. 2 in the following coordinates.

$$\lg\frac{\mathrm{Fo}}{K'}\left(\frac{D_0}{\delta}\right)^{0.8};\ \lg\frac{1}{\mathrm{Bi}}.$$

Inspection of the results plotted in this figure indicated that C = 0.5 and m = 1 in Eq. (7). Thus, Eq. (7) may be written as follows:

$$\mathrm{Fo} = 0{,}5K'\left(\frac{\delta}{D_0}\right)^{0.8}\frac{1}{\mathrm{Bi}}. \tag{8}$$

It follows from Fig. 1 that there is a great discrepancy at the initial instant between the experimental data and the assumed law governing the change in the rate of freezing with time. This may be due to the fact that other behavior patterns are present at the beginning of the process as well as to the fact that at the beginning of the process the

relative precision of measurement of the thickness of ice is lower and the possible experimental error higher. The mean departure of the individual experiments from the straight line in Fig. 2 is ± 10%.

The three experiments by London and Seban /Ref. 4/ worked up by us satisfactorily lie on the assumed curve (Figs. 1 and 2). In these experiments ice was formed in cylinders with a diameter of 14.1 mm, at a temperature difference $\Delta t = 17.4^{\circ}$ C, and at an air velocity w = 4-11 m/sec.

A formula was derived from Eq. (8) for calculating the freezing time:

$$\tau = 0{,}5 \frac{r'\gamma'}{\alpha \Delta t} D_0 \left(\frac{\delta}{D_0}\right)^{0{,}8}. \tag{9}$$

For ice, on the assumption that r' and γ' are constant and have the following values, respectively: r' = 80 kg-cal/kg, and γ' = 920 kg/m in the temperature range in which freezing takes place under actual conditions, we can derive the following formula from Eq. (9):

$$\tau = 36{,}8 \cdot 10^3 \frac{D_0^{0.2}}{\alpha \Delta t} \delta^{0.8}. \tag{10}$$

The following equation was derived for determining the thickness of the ice formed during freezing:

$$\delta \approx 2 \cdot 10^{6} \frac{(\alpha \Delta t)^{1.25}}{D_0^{0.25}} \tau^{1.25}. \tag{11}$$

c) Comparison of Experimental Results With Theoretical Equations

Formula (9) can be transformed somewhat by substituting the radius R_0 for the diameter. The freezing time will then be:

$$\tau = 0{,}575 \frac{r'\gamma' R_0}{\alpha \Delta t} \left(\frac{\delta}{R_0}\right)^{0{,}8}. \tag{12}$$

Let us introduce:

$$A = \frac{r'\gamma' R_0}{\alpha \Delta t}.$$

Equation (12) then becomes:

$$\tau = 0{,}575 A \left(\frac{\delta}{R_0}\right)^{0.8}. \tag{13}$$

We compared the freezing time calculated from Eq. (13) with the figures obtained from the theoretical formulas of A. A. Gukhman and A. I.Veinik. The relationships secured by these authors for the solidification of cylindrical castings are as follows:

1) for $1 < \mathrm{Bi} < 50$

$$M = c_1 \vartheta_r + c_2 \vartheta_r^2 + c_3 \vartheta_r^3 + c_4 \ln(1 + \mathrm{Bi}\vartheta_r); \tag{14}$$

2) for $0.1 < \mathrm{Bi} < 1$

$$M = \vartheta_r (1 + c_2' \vartheta_r + c_3' \vartheta_r^2), \tag{15}$$

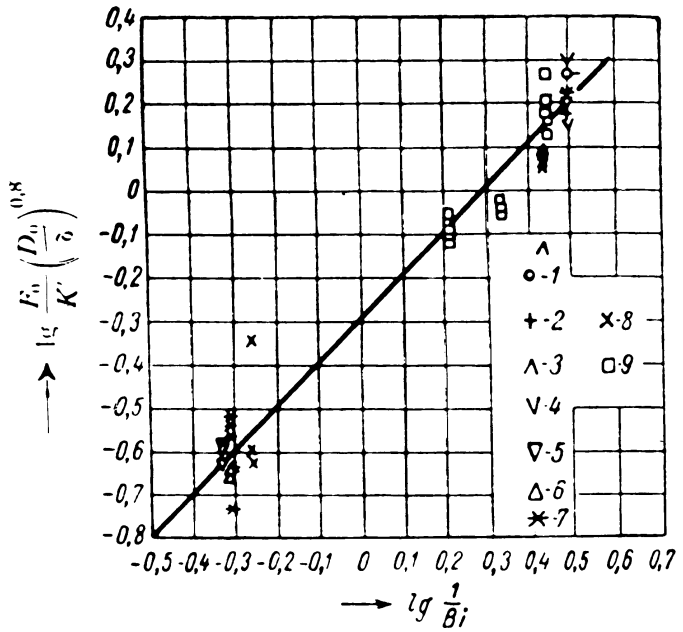

Fig. 2. Results of tests on the freezing of ice in a cylinder, plotted in the following coordinates.

1 - Author's experiment	No. 1	6 - Author's experiment	No. 7
2 - " "	No. 2	7 - " "	No. 8
3 - " "	No. 3	8 - " "	No. 10
4 - " "	No. 9	9 - London's experiment	
5 - " "	No. 6		

3) for Bi $<$ 0.1

$$M = \delta_r \left(1 - \frac{1}{2}\delta_r\right). \tag{16}$$

The terms entering Eqs. (14), (15), and (16) have the following significance:

$$M = \frac{\alpha (t_0 - t_f)\tau}{r\gamma' R_0}; \quad \mathrm{Bi} = \frac{\alpha R_0}{\lambda'}; \quad \delta_r = \frac{\delta}{R_0};$$

$$\mathrm{N} = \frac{c'(t_0 - t_f)}{r} = \frac{1}{K'};$$

$$c_1 = 1 + \frac{1}{2}\mathrm{N} + \frac{1}{6}\frac{\mathrm{N}}{\mathrm{Bi}}; \quad c_2 = \frac{1}{2}\mathrm{Bi}\left(1 + \frac{1}{2}\mathrm{N}\right) - \frac{1}{2}\left(1 + \frac{1}{6}\mathrm{N}\right);$$

$$c_3 = -\frac{1}{3}\mathrm{Bi}\left(1 + \frac{1}{3}\mathrm{N}\right); \quad c_4 = -\frac{1}{2}\frac{\mathrm{N}}{\mathrm{Bi}}\left(1 + \frac{1}{3\mathrm{Bi}}\right);$$

$$c_2' = \frac{1}{2}[\mathrm{Bi}(1 + \mathrm{N}) - 1]; \quad c_3' = -\frac{1}{3}\mathrm{Bi}\left(1 + \frac{1}{2}\mathrm{N}\right).$$

The conditions under which our experiments were run corresponded to the following values of the criteria:

$$\mathrm{Bi} = \frac{\alpha R_0}{\lambda'} = 0{,}16 \div 1{,}1;\ \mathrm{N} = 0{,}1 \div 0{,}2.$$

Under these conditions the formulas (14), (15), and (16) can be simplified.

1) $1 < \mathrm{Bi} < 50$.

If we set Bi = 1 and N = 0.15 in Formula (14), corresponding to the experimental conditions, and substitute the ratio of ice thickness to the initial radius for δ_r, this formula becomes:

$$M = \frac{\delta}{R_0}\left[1{,}067 + 0{,}04\,\frac{\delta}{R_0} - 0{,}34\left(\frac{\delta}{R_0}\right)^2\right] - 0{,}368\ln\left(1 + \frac{\delta}{R_0}\right).$$

Bearing in mind the expression for $\underline{M}$, we get:

$$\tau_r = \frac{\gamma' r'}{\alpha \Delta t} R_0\,\frac{\delta}{R_0}\left[1{,}067 - 0{,}04\,\frac{\delta}{R_0} - 0{,}34\left(\frac{\delta}{R_0}\right)^2\right] - 0{,}368\ln\left(1 + \frac{\delta}{R_0}\right),$$

or

$$\tau_r = A\,\frac{\delta}{R_0}\left[1{,}067 + 0{,}04\,\frac{\delta}{R_0} - 0{,}34\left(\frac{\delta}{R_0}\right)^2\right] - 0{,}368\ln\left(1 + \frac{\delta}{R_0}\right). \qquad (17)$$

The results of our calculations of freezing time from Formulas (13) and (17) are given in Table 2. The maximum discrepancy between the time calculated from the Gukhman and Veinik equation (τ_r) and from our formula is 26%.

TABLE 2

$\frac{\delta}{R_0}$	1	0,9	0,7	0,5	0,3	0,1
$\frac{\tau_r}{\tau}$	1,14	1,04	1,11	1,26	1,24	1,01

2) $0.1 < \mathrm{Bi} < 1$.

We set Bi = 0.1 and N = 0.15 in Formula (15), substitute τ and $\underline{A}$ for $\underline{M}$, and substitute the corresponding expression for δ_r. Formula (15) is then transformed as follows:

$$\tau_r = A\left[\frac{\delta}{R_0} - 0{,}44\left(\frac{\delta}{R_0}\right)^2 - 0{,}035\left(\frac{\delta}{R_0}\right)^3\right]. \qquad (18)$$

Calculations of the freezing time from Formulas (13) and (18) are given in Table 3. The maximum discrepancy is 19%.

TABLE 3

$\frac{\delta}{R_0}$	1	0.9	0,7	0,5	0,3	0,1
$\frac{\tau_r}{\tau}$	0,904	0,973	1,09	1,18	1,19	1,09

3) $Bi < 0.1$

In this case, the time is independent of the magnitude of the Biot number, according to Gukhman and Veinik. Formula (16) is transformed into the following expression:

$$\tau_r = A \frac{\delta}{R_0}\left(1 - \frac{1}{2}\frac{\delta}{R_0}\right). \tag{19}$$

The comparison of the times secured from Formulas (19) and (13) is listed in Table 4. The maximum discrepancy is 17%.

Table 4

$\frac{\delta}{R_0}$	1	0,9	0,7	0,5	0,3	0,1
$\frac{\tau_r}{\tau}$	0,87	0,93	1,05	1,14	1,17	1,04

At low freezing thicknesses the theoretical equation characterizing the process is as follows:

$$M = \delta_r \quad \text{or} \quad \tau_r = A \frac{\delta}{R_0}. \tag{20}$$

When $\frac{\delta}{R_0} = 0{,}1$, we get: $\frac{\tau_r}{\tau} = 1{,}1$, , i.e., the theoretical time is 10% higher than that calculated from Formula (13).

The comparison indicates that Formula (13) yields a satisfactory agreement with the theoretical data. The simpler formula (13) may be recommended for practical calculations of ice-formation time in the region of Biot number values that corresponds to the conditions under which the experiments were run.

3. EXPERIMENTS ON FREEZING UPON THE OUTER SURFACE OF A CYLINDER

a) Experimental Procedure

The apparatus employed in the experiments on the freezing of ice upon the outer surface of a cylinder is shown schematically in Fig. 3.

The experimental pipe was 520 mm high and had an outer diameter of 56 mm. The brine from the evaporator of the refrigerating machine was fed by a pump to the annular space around the pipe and was then returned to the evaporator via the inner pipe. The brine temperatures at the pipe inlet and outlet were measured by thermometers graduated to 0.1° C. The brine temperature within the tube was kept constant during the experiment by regulating the operation of the refrigerating machine and the current in the heating coil mounted on the brine pipe. The brine, whose temperature was negative, chilled the outer surface of the tube, which was submerged in water. Ice froze on the tube surface.

The experiment consisted of measuring the thickness of frozen ice, the time, the brine temperature at the inlet and outlet, and the water temperature. The water temperature was measured by a thermometer graduated to 0.1° C located at the center of the tank in which the experimental pipe was mounted. The thickness of ice was measured by projecting an image of the pipe on a screen. Owing to the large size of the tank (its capacity was 1 m^3), the water temperature within the tank did not vary by more than 0.1° C during the course of the experiment. In each experiment we likewise measured the flow velocity of the brine by measuring the time required to fill a calibrated vessel with the brine forced through the system by the pump. Four experiments were performed in all.

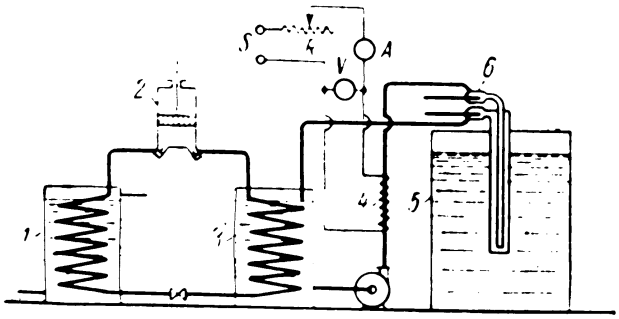

Fig. 3. Diagrammatic sketch of the experimental apparatus for freezing ice on a vertical cylinder.
1 - Condenser; 2 - compressor; 3 - evaporator; 4 - heater; 5 - water tank; 6 - experimental pipe.

The principal data characterizing the conditions under which the experiments were run are listed in Table 5.

b) Processing the experimental Data and the Experimental Results

The experimental results were worked up, using Eq. (7). The outer diameter of the pipe was taken as the characteristic dimension. The ice thickness , entering into Eq. (7) was calculated as the average value along the height of the pipe immersed in water. This height was 0.38 meters.

In Fig. 4 we have plotted the function:

$$\frac{Fo}{K'} = f\left(\frac{\delta}{D_0}\right). \tag{21}$$

Besides our four experiments, we have plotted on the graph the results of our processing of the experiments made by A. P. Dobrovolsky on the freezing of ice in a vertical pipe.

Analysis of the graphs indicated that the entire freezing period can be divided into three stages. At the beginning of the process the change in the time required for freezing is proportional to the thickness of the ice:

$$\tau \sim \frac{\delta}{D_0}. \tag{22}$$

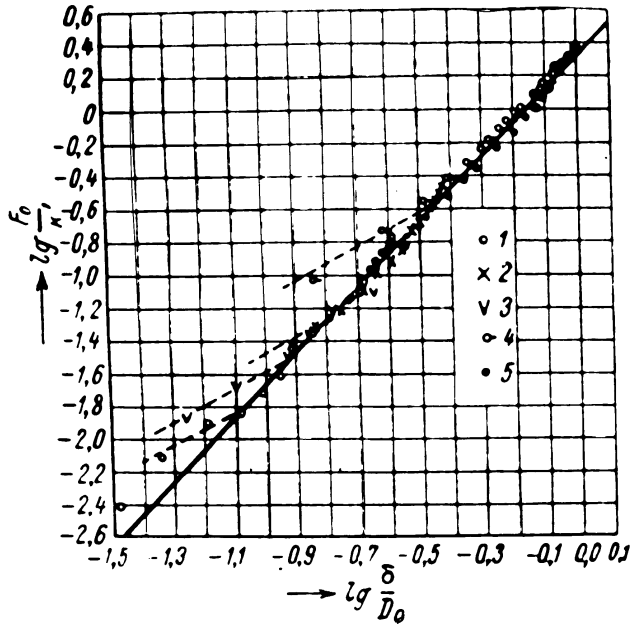

Fig. 4. Results of experiments on the freezing of ice upon a vertical cylinder.

1 - Author's experiment No. 1
2 - " " No. 2
3 - " " No. 3
4 - Dobrovolsky's experiment No. 1
5 - " " No. 2

Furthermore, at a certain thickness of the freezing ice there appears a second stage in which the process is characterized by a new relationship between the time and the thickness, with other conditions remaining constant. This relationship has the following form:

$$\tau \sim \left(\frac{\delta}{D_0}\right)^2. \tag{23}$$

And finally, there comes the moment when freezing ceases. This corresponds to a stationary process, i.e. to conditions under which the amount of heat taken from the brine equals the amount of heat used to cool the water. During a period close to this instant freezing slows down. This period is described mathematically by the equation:

$$n \to \infty; \quad \frac{\delta}{D_0} = \text{const.} \tag{24}$$

The rate of freezing varies with the height of the tube: in its lower section it is much faster than in the upper one, especially during the initial period. This is attributable to the chilling of the water as it moves along the cold surface of the pipe from top to bottom. In two experiments we worked up the results for the upper section of the pipe. These results are shown in Fig. 5. The curves shown in this figure indicate that the behavior patterns are different in different stages of the process.

The change in time with thickness is shown by the graph plotted in Fig. 6 for the bottom of the tube, where the thickness of the freezing ice is such that we approach a stationary regime. The second and third stages of the process, corresponding to Eqs. (23) and (24), are clearly shown in the graph.

The two different laws for the two stages of the process may be replaced by a single law with a sufficient degree of accuracy if we take the exponent of $\frac{\delta}{D_0}$ as equal to 1.9. Then,

$$\tau \sim \left(\frac{\delta}{D_0}\right)^{1.9}. \tag{25}$$

This relationship is due to the fact that the initial stage of the process, when the exponent $\underline{n} = 1$, is much shorter than the subsequent stages where the exponent $\underline{n} = 2$.

The experiments described above were performed at a low velocity of the brine, and hence at Biot numbers that were very close together. That is why we could not establish numerical values for $\underline{C}$ and $\underline{m}$ in Eq. (7). Similarly, we did not establish the influence of the criterion

$$K = \frac{r'}{c(t - t_0)}.$$

Elucidation of these problems should constitute the topic of further investigation of heat exchange in freezing on the outside surface of a cylinder.

4. CONCLUSIONS

An experimental investigation has been made of the processes of heat exchange occurring in the freezing of ice inside and outside a cylindrical surface. The experimental results have been processed, using similitude criteria.

A simple formula that is convenient for practical calculation has been secured for calculating the time required for ice to freeze inside

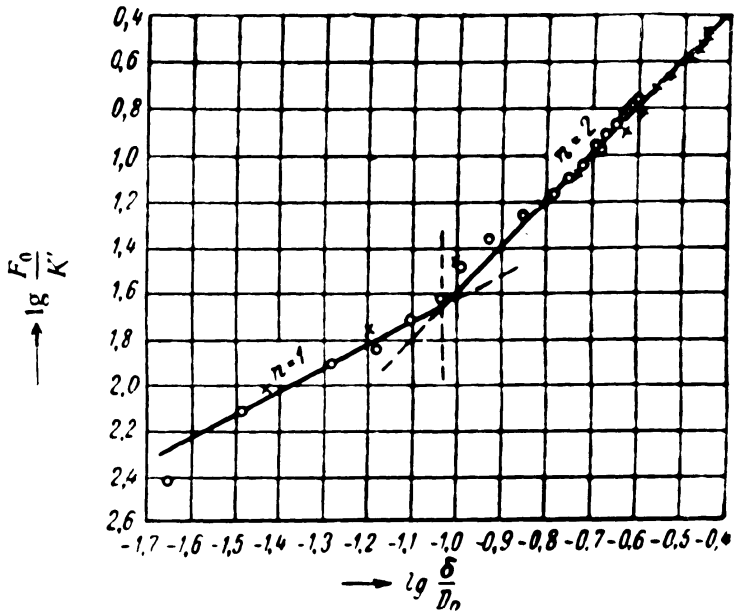

Fig. 5. Experiments on the freezing of ice upon a vertical cylinder (at the top of the cylinder).

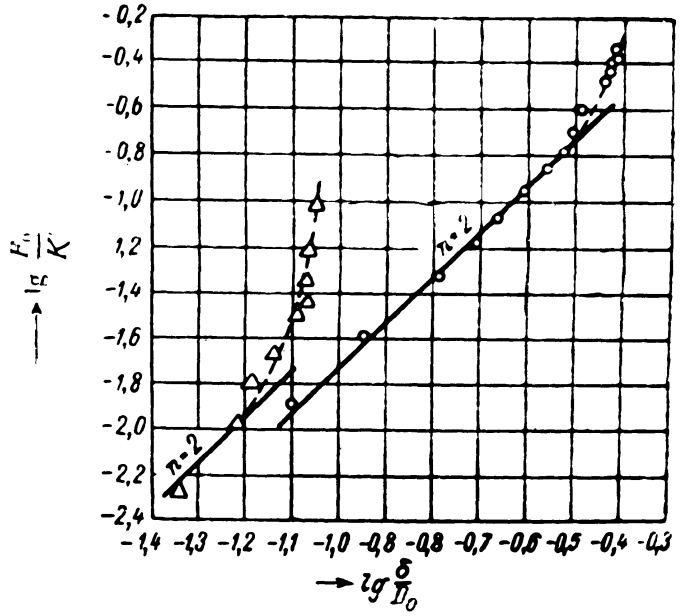

Fig. 6. Experiments on the freezing of ice upon a vertical cylinder (at the bottom of the cylinder).

the cylinder as a function of the conditions under which it occurs and of the thickness of the ice. The function found agrees satisfactorily with the theoretical equations proposed by A. A. Gukhman and A. I. Veinik for the crystallization of a metallic casting.

The existence of different behavior patterns during different time stages of the process has been established for the case of freezing on the outer surface of a vertical cylinder. A mathematical expression has been found expressing the relationship between the freezing time and the thickness of the freezing ice.

LITERATURE CITED

1. A. A. Gukhman and A. I. Veinik, Jour Tech. Phys., 21, No. 1, 1951.

2. A. K. Skryabin. Kinetics of crystallization with allowance for a change of the basic surface; Scientific Research Institute of Chemical Machinery. Calculation, design, and investigation of chemical equipment and machinery. State Scientific and Technical Publishing House of Literature on Machinery, 1950.

3. M. A. Mikheev, Principles of Heat Transfer. State Power Engineering Press, 1949.

4. A. London and R. Seban, Trans. ASME 65, No. 7, 1943.

5. R. Seban and A. London, Trans. ASME, No. 1, Jan. 1945.